

Switchable ETFE façades:
A study on the thermo-optical, daylighting and energy performance of climate adaptive building envelopes

by

Jan-Frederik Flor

Thesis submitted to the University of Nottingham
for the degree of Doctor of Philosophy, June 2020

Acknowledgements

It has been an exciting and challenging academic journey. I received much support and guidance from many of whom I am now expressing my gratitude for:

Faculty of Engineering in the University of Nottingham - for awarding the PhD studentship and for funding living expenses throughout all three-year study duration in the U.K.

Architen Landrell - The collaborative industry partnership with Christopher Rowell, its Managing Director. Highest appreciation for lending the expertise of his company and team. Without the generous provision of material samples and a full-size mock-up, my experiments would not have been possible.

My team of supervisors - Assoc. Prof. Dr Yupeng Wu 'Jack', Ass. Prof. Dr Paolo Beccarelli, Research Fellow Dr Yanyi Sun and Emeritus Professor Dr John Chilton- to whom have all guided this academic journey with their collective expertise and knowledge. I am deeply grateful for them in supporting me at all stages of this PhD. To Jack: thank you for entrusting me with the freedom of doing independent experimentation work, yet still challenge the quality and depth of my results. For creating research opportunities and relationships into the deeper networks of science. Paolo: the man responsible for my recruitment and initiation into the research team at UoN, also a personal advisor for academic life while navigating the PhD. Yanyi: post-doc and "big sister" with very insightful technical advice, guidance on simulations and lab work which resulted in several fruitful publishing collaborations. One to organise epic research group barbecues as well as that conference in Chengdu, these times will always be remembered. Last but not least, to John: for the many hours of inspiring lunchtime conversations. These were precious and treasured times. John kept me focussed and relaxed even when things got complicated or fuzzy, whose wisdom channelled and shaped towards my scientific writing style. His rigorous checking of my English is impeccable and much needed- Thank you so much.

To technical personnel and managers of the ETB on Jubilee Campus: a special shoutout to Karl, Mick and Andy, for keeping the safety of the research work in the labs.

The great friendships and collaborations with my colleagues; Xiao and Xiu, for the times in the labs until late. Dingming and Haomin for excellent co-authored papers. VR project with Fedaa and Marina, as well as for hosting our conference in Adelaide. Also big thank you, participants, collaborators and volunteers, who made it possible to conduct all my experiments.

I am most grateful to my loving parents Bernd and Brigitte, brother and sister, Philli and Zissi: for supporting my adventures and endeavours, always. The visits, the messages and memories from home, an open ear in times of happiness or trouble were strong anchors to keep me grounded. To my love, my grumpy wife, Najah. Without her pulling me out of the lab, feeding me homecooked meals, and seeing over our life-social-work balance, my PhD experience and life would not be as exciting and colourful. Thank you for being a supportive partner, lighting my travel motivations and for all the pep-talks when things were slow. Most importantly, for making me feel at home, with you. Thank you.

Abstract

The development of transparent, light, flexible, and resistant materials like ethylene tetrafluoroethylene (ETFE) foil allows rethinking the function of the building envelope as an interactive and moderating membrane between the internal and external environment. Air inflated ETFE foil constructions, forming pneumatic cushions, are structurally efficient and have increasingly been used in state-of-the-art architecture. However, the prediction of the thermo-optical behaviour of ETFE structures in building façades is a challenge for designers and manufacturers. The proposal of adaptive or switchable systems, which can be modified on demand to respond to changing climate conditions, is a recent technological answer to that challenge. Nevertheless, the understanding of the impact of switchable ETFE façades on the energy and daylighting performance of buildings, as well as on comfort and user experience, is still limited and represents a barrier to large scale implementation. In this research switchable multi-layer ETFE cushions were investigated through a series of independent but interrelated studies, using ray-tracing, energy simulations and virtual reality, to assess daylighting qualities, energy performance and view perception of spaces enclosed with switchable ETFE façades. The main findings of the conducted studies revealed the superior energy and daylighting performance of spaces enclosed by switchable ETFE cushions. In comparison to static ETFE cushions and standard double glazing, climate adaptive switchable systems actively reduce solar gains and improve the environmental performance of the building envelope. Implications on energy consumption and natural daylighting of the enclosed spaces are of relevance for future applications in building façades: Glare reductions of 59% and an increase of useful daylight illuminance of 58%, with annual energy savings of up to 56% were predicted in this thesis. However, the study revealed that view clarity of foils, print inks, and patterns of current switchable ETFE cushions is not yet satisfactory and remains a challenge for future research and development. It is expected that the outcomes of this research will contribute to advancements in ETFE-foil façade technology, that may lead to energy savings in the building sector and support the agenda against climate change.

Preamble

The present thesis collects the work of three years of research conducted during a PhD program in the laboratories of the Department of Architecture and the Built Environment at the University of Nottingham. This thesis is not a single, monolithic research project. Instead, it contains most of the diverse research projects aiming to answer a set of questions surrounding the environmental performance of switchable ETFE cushions in climate adaptive building façades. Inasmuch as this dissertation has a central theme, each of the projects presented in the individual chapters has its own aims and objectives. It is through the findings of each study that establishes the connections between the chapters and lead naturally towards an expansion of knowledge on the topic.

Large parts of the work presented in this thesis have been published in scientific conference papers and journal articles during the PhD program. These publications are based upon original research projects undertaken by the thesis author between 2016 and 2019. Parts of text, graphs and images from these publications were adapted to fit the structure and format of this thesis. On all, but one publication the thesis author was the first and leading author. In all cases, the thesis author was in large parts responsible for the idea, initiation, design, conduct and direction of the projects and the consequently published work. The thesis author has contributed substantially to the co-authored publications, which build up mainly on the previous work of the applicant. Collaboration with and from other PhD candidates, researchers and industry partners has been the norm for all the here presented work, leading with the contribution of different skillsets and resources to research outcomes which are more than the sum of the individual parts.

Permission has been pursued and granted from the co-authors to use the content of the publications for this thesis. Declarations about the contributions of the author and co-authors to the individual papers are attached in the appendix of this thesis. It is hereby declared that the works submitted for this Doctor of Philosophy have not previously been submitted for any other qualification at a tertiary institution of higher education.

Table of Contents

Acknowledgements i

Abstract iii

Preamble iv

Table of Contents 5

List of Publications 14

List of Figures 16

List of Tables 32

Glossary 37

Nomenclature 40

Chapter 1: Introduction 42

1.1. Introduction to chapter one 42

1.1.1. Environmental adaptation of building envelopes and the role of ETFE 43

1.1.2. Building envelopes of ETFE 45

1.1.3. Responsiveness in textile building envelopes 47

1.2. Motivation and Justification for the study 50

1.3. Aims of the thesis 51

1.4. Objective and sub-objectives of the thesis 52

1.5. Research questions 53

1.6. Structure of the thesis 54

1.6.1. Chapter one outline 55

1.6.2. Chapter two outline 55

1.6.3. Chapter three outline 55

1.6.4. Chapter four outline 56

1.6.5. Chapter five outline 56

1.6.6. Chapter six outline 57

1.6.7. Chapter seven outline 57

1.6.8. Chapter eight outline 57

1.6.9. Chapter nine outline 58

Chapter 2: Literature Review 59

2.1. Introduction to chapter two 59

2.2. Adaptive and energy-efficient building envelopes with ETFE 60

2.3. Material properties of ETFE 63

2.4. Characteristics of pneumatic ETFE foil construction: static and switchable 64

2.5. The thermal and optical behaviour of membrane and foil constructions 72

2.6. Chapter summary 82

Chapter 3: General Methods 84

3.1. Introduction to chapter three 84

3.2. Methods outline 84

3.3. Methods for the optical characterization of ETFE foil constructions 85
3.4. Methods for the thermal characterization of ETFE foil constructions 87
3.5. Methods for the daylighting performance prediction of ETFE foil constructions 90
3.6. Methods for the energy performance prediction of ETFE foil constructions 92
3.7. Methods for the evaluation of the view qualities of ETFE double-skin façades 96
3.8. Chapter summary 99

Chapter 4: Optical Characterisation 100
4.1. Introduction to chapter four 100
4.2. Optical aspects of switchable ETFE cushions 101
4.3. Methods and parameters 103
4.3.1. Geometry and frit pattern design 103
4.3.2. Optical model for ETFE 106
4.4. Results and discussion 109
4.4.1. The effects of sag and frit pattern on the optical performance 110
4.4.2. Optical performance with variations of frit print properties and different incidence angles 113
4.5. Chapter summary 121

Chapter 5: Thermal Characterisation 123

5.1. Introduction to chapter five 123

5.2. Background on the thermal performance of building envelopes with ETFE 124

5.3. Methods, equipment and samples 126

5.3.1. Climate Chamber 127

5.3.2. ETFE cushion samples 128

5.3.3. Experimental set-up 130

5.3.4. Dynamic air-supply 132

5.3.5. Sensor types and position 134

5.3.6. Testing scenarios 135

5.3.7. Experimental measurements 136

5.3.8. Standard calculation method 137

5.4. Results and discussion 139

5.4.1. Thermal performance at standard condition 139

5.4.2. Air supply and pressure loss 145

5.4.3. Thermal performance of switchable ETFE cushion 146

5.4.4. Thermal performance with dynamic air-supply 149

5.4.5. Comparison of experimental and calculated results 153

5.5. Chapter summary 155

Chapter 6: Daylighting Performance 156

6.1. Introduction to chapter six 156

6.2. Retrofitting Office Façades: Improving daylighting performance with ETFE 157

6.3. Methods 163

6.3.1. Measurement of optical properties of switchable ETFE foil 165

6.3.2. Modelling of ETFE Cushion and Material 167

6.3.3. Bidirectional-scattering-distribution-function (BSDF) 170

6.3.4. Simulation scenarios 173

6.3.5. Geographic Location and weather data 176

6.3.6. Sky model and matrixes 179

6.3.7. Simulation Parameters 180

6.3.8. Dynamic daylight performance metrics 182

6.3.8.1. Daylight glare probability metrics 182

6.3.8.2. Daylight illuminance uniformity metrics 184

6.3.8.3. Useful daylight illuminance metrics 185

6.4. Results and Discussion 186

6.4.1. Results of Spectroscopy and optical characterization 187

6.4.2. Model calibration and partial validation 195

6.4.3. Spatial light distribution and luminance of surfaces 199

6.4.4. Daylight Glare Probability results 202

6.4.5. Daylight illuminance uniformity 208

6.4.6. Useful daylight illuminance results 214

6.5. Chapter summary 224

Chapter 7: Energy Performance 226

7.1. Introduction to chapter seven 226

7.2. Energy performance of building enclosed with ETFE 227

7.3. Methods 232

7.3.1. Workflow and Software tools 232

7.3.2. Location and climate data 233

7.3.3. Building model and zone configuration 235

7.3.4. Model and zone parameters 237

7.3.5. Simulated parameters and scenarios 241

7.4. Results and discussion 242

7.4.1. Results for the London climate scenario 243

7.4.2. Results for the Barcelona climate scenario 245

7.4.3. Results for the Shanghai climate scenario 247

7.4.4. Energy gains and losses 249

7.4.5. Energy savings 256

7.5. Energy and daylighting performance 260

7.6. Chapter summary 264

Chapter 8: View Perception 267

8.1. Introduction to chapter eight 267

8.2. View qualities and user acceptance of ETFE double-skin façades 268

8.3. Experimental methods 271
8.3.1. Test facility 271
8.3.2. Experimental equipment 272
8.3.3. Generation of the virtual environment 273
8.3.4. Material definitions and view scenarios 276
8.3.5. Design of the experiment 278
8.3.6. Experimental procedure 279
8.3.7. Studied parameters 281
8.3.8. Sample population of participants 282
8.4. Results and discussion 283
8.4.1. Sample Rankings 283
8.4.2. Statistical data 287
8.4.3. Limitations 291
8.5. Chapter summary 292

Chapter 9: Conclusions 294
9.1. Conclusions 294
9.2. Limitations 298
9.2. Future work 298

References 300

Appendix A: Annual solar radiation graph showing average diffuse horizontal and direct normal radiation for London, Barcelona and Shanghai 328

(graphs by the thesis author, unpublished) 328

Appendix B: Annual solar radiation graphs showing the hourly global horizontal radiation for London, Barcelona and Shanghai 329

(graphs by the thesis author, unpublished) 329

Appendix C: UDI bins London.....330

(graphs by the thesis author, unpublished) 330

Appendix D: UDI bins Barcelona.....331

(graphs by the thesis author, unpublished) 331

Appendix E: UDI bins Shanghai.....332

(graphs by the thesis author, unpublished) 332

Appendix F: Virtual reality experiment questionnaire 333

(form by the thesis author, unpublished) 333

Appendix G: Virtual reality experiment ethics approval.....334

Appendix H: Virtual Reality consent form sample 341

Appendix I: Title page of published paper (1).....343

Appendix J: Co-authors contribution declaration (paper 1) 344

Appendix K: Title page of published paper (2) 345

Appendix L: Co-authors contribution declaration (paper 2) 346

Appendix M: Title page of published paper (3) 347

Appendix N: Co-authors contribution declaration (paper 3) 348

Appendix O: Title page of published paper (4) 349

Appendix P: Co-authors contribution declaration (paper 4) 350

Appendix Q: Title page of published paper (5) 351

Appendix R: Co-authors contribution declaration (paper 5) 352

Appendix S: Title page of published paper (paper 6).....353

353

Appendix T: Co-authors contribution declaration (paper 6).....354

354

List of Publications

The following list includes all topic related articles published by the applicant during the three-year PhD program at The University of Nottingham. The articles are academic papers, peer-reviewed and presented at international conferences or published in recognized indexed journals. The work published in the articles is based on collaborative efforts between the applicant, supervisors, industry partners and fellow PhD colleagues. The applicant was in five out of six listed publications, the first author, responsible for organizing and leading the execution of the works, as well as writing and editing the manuscripts and coordinating the publishing process. Article titles are listed below in chronologic order with an indication of publishing category of journal or conference publication. The title page of each paper is included in Appendix I, K, M, O, Q and S.

1. Flor, J.-F., Sun, Y., Beccarelli, P., Wu, Y., Chilton, J., Switchable ETFE cushion: designing and building a model for experimental testing, 2019. In Proceedings of the IASS Annual Symposium 2019 – Structural Membranes 2019, C. Lázaro, K.-U. Bletzinger, and E. Oñate, Editors. 2019: Barcelona, Spain. *(conference paper)*

2. Flor, J.-F., Sun, Y., Beccarelli, P., Rowell, C., Chilton, J., Wu, Y., Experimental study on the thermal performance of ethylenetetrafluoroethylene (ETFE) foil cushions. 2019. IOP Conf. Ser.: Mater. Sci. Eng. 556 012004. *(conference paper)*

3. Wang, H., Flor, J.-F., Sun, Y., Wu, Y., Numerical investigations on the thermal performance of adaptive ETFE foil cushions. Energy Procedia, 2019. 158: p. 3191-3195. *(conference paper)*

4. Flor, J.-F., Liu, D., Sun, Y., Beccarelli, P., Chilton, J., Wu, Y., Optical aspects and energy performance of switchable ethylene-tetrafluoroethylene (ETFE) foil cushions. Applied Energy, 2018. 229: p. 335-351. *(journal paper)*

5. Flor, J.-F., Wu, Y., Beccarelli, P., Chilton, J., Dynamic environmental control mechanisms for pneumatic foil constructions. E3S Web Conf., 2017. 22. *(conference paper)*

6. Flor, J.-F., Aburas, M., Abd-AlHamid, F., & Wu, Y. (2021). Virtual reality as a tool for evaluating user acceptance of view clarity through ETFE double-skin façades. Energy and Buildings, 231, 110554. *(journal paper)*

List of Figures .

Figure 1. 1. Dynamic shading mechanisms for the environmental control of multi-layer ETFE cushions in building envelopes (top right diagram abbreviations read as follows: SI – Solar Irradiation, OL, ML, IL – Outer, Middle and Inner Layer, P 1 – Pressure) 44

Figure 1. 2. Eden Project, St. Austell, United Kingdom, 2000 45

Figure 1. 3. Schematic section of a responsive building envelope incorporating a dynamic shading mechanism within a multi-layer ETFE cushion 49

Figure 1. 4. Flow-chart of the thesis structure, showing the interrelationship between the chapters main topics and methods 54

Figure 2. 5. Environmental control mechanisms for multi-layer foil construction 65

Figure 2. 6. Dynamic triple-layer shading mechanism for pneumatic foil constructions, functional diagram and rendering of a section in perspective view 66

Figure 2. 7. System overview of a pneumatic multi-layer foil construction (switchable) 67

Figure 2. 8. (A, B) Diagrams showing two alternative air-supply and control schemes for the switching mechanism of the pneumatic foil cushion 68

Figure 2. 9. Function flow chart of pneumatic switchable triple-layer foil cushion 68

Figure 2. 10. Project Images: A) Duales System World Exposition Pavilion, Hannover Germany; B) Festo, Paris, France; B) Kingsdale School, London, United Kingdom, (photos © Vector Foiltec, retrieved from: http://www.vector-foiltec.com, accessed 30th April 2017, published with permission in: Flor et al., 2017) 69

Figure 2. 11. Ray reflection for different orientation angles of switchable multi-layer ETFE cushions in the open and closed position 75

Figure 2. 12. Building physics of a pneumatic cushion structure 76

Figure 2. 13. Measured spectral data for ETFE foils 79

Figure 4. 14. Switchable foil cushion in the open (A) and closed mode (B) 101

Figure 4. 15. Transmitted and reflected light beams on a switchable foil cushion in open (A) and closed mode (B)..... 102

Figure 4. 16. Cushion geometry (A) and variable sag to span ratio (2.5% to 15%) of the centre section (B) 104

Figure 4. 17. Material application on cushion model (A) and generated cushion samples (B) 105

Figure 4. 18. Ray-tracing 3D model (A) and ETFE cushion section with traced rays (B) 107

Figure 4. 19. Incidence angles of rays on cushion geometry, hemispheric (A), section (B) 109

Figure 4. 20. Optical performance of switchable triple-layer cushion (50 x 50 mm frit layout) with varying sag geometry – angle dependent transmittance in open (A) and closed mode (B) 111

Figure 4. 21. Optical performance of switchable triple-layer cushion (10% sag with varying frit layout) – transmittance at 90° incidence angle in open and closed mode (A – F)..... 112

Figure 4. 22. 2D Plots (A - H) - Optical performance of switchable triple-layer cushion (10% Sag, 50 x 50 mm frit layout, varying optical frit properties) - Angle dependent transmittance in open and closed mode 115

Figure 4. 23. 3D plot (A – P) - optical performance of switchable triple-layer cushion (10% sag, 50 x 50 mm frit layout, varying optical frit properties) – angle dependent transmittance in open and closed mode 119

Figure 4. 24. Optical performance of switchable ETFE cushions with different frit print properties..... 121

Figure 5. 25. Switching sequence of switchable ETFE cushion (experimental mock-up) from open to closed mode (time frames per minute)..... 125

Figure 5. 26. St. Bartholomew's Hospital, London, UK, courtyard cover with switchable ETFE foil cushions 126

Figure 5. 27. RCS Pavilion EXPO2015, Milan, Italy, roof with switchable ETFE cushions..... 126

Figure 5. 28. ISS Building Lancaster University, Lancaster, UK, skylights with switchable ETFE foil cushions 126

Figure 5. 29. Climate Chamber in open position..... 127

Figure 5. 30. A) Isometric view of the test frame and ETFE cushion, B) exploded view of the test frame showing main system components..... 128

Figure 5. 31. Section views of the sample dimension and layer compositions A) double layer clear ETFE; B) double layer clear and fritted ETFE; C) triple layer switchable ETFE..... 129

Figure 5. 32. ETFE Cushion samples, A) two layers clear ETFE, B) two layers, fritted ETFE, C) three layers, switchable ETFE frit 130

Figure 5. 33. ETFE foil types, A) clear, B) hexagon frit, C) square frit, switchable 130

Figure 5. 34. Overview Section of the experimental set-up in the climate chamber 131

Figure 5. 35. Apparatus set-up for dynamic air-supply 132

Figure 5. 36. Position of air-valves on cushion sample 133

Figure 5. 37. Equipment set-up for dynamic air-supply, A) air-supply with air-con unit, baffle tank and air-pump, B) Flow-meter and adjustable air-valve 134

Figure 5 38. Sensor types and position on ETFE cushion sample 135

Figure 5. 39. Instrumentation of ETFE cushion sample 135

Figure 5. 40. Thermal model for an ETFE cushion showing the main parameters which affect the overall thermal resistance 139

Figure 5. 41. Example data set of measurements taken of surface temperatures and heat-flux on a clear ETFE cushion sample 1 during standard temperature condition 140

Figure 5. 42. Measured Values on the clear ETFE cushion at standard condition (S3). 141

Figure 5. 43. Horizontal Heat Flux through ETFE cushion Samples at Standard Condition (S3) 145

Figure 5. 44. Pressure drop of ETFE cushion, Sample No. 1 (double-layer, clear ETFE) 145

Figure 5. 45. Position of heat flux meter at different frit print locations on the cushion surface 147

Figure 5. 46. Heat flux at different positions on cushion surface during the switching process 147

Figure 5. 47. Thermal exchange mechanisms at different frit print locations (Sensor Position HF3 and HF4) on the switchable cushion for open and closed mode 148

Figure 5. 48. Total Transversal Heat Flux through ETFE cushion (Sample 1, clear)... 149

Figure 5. 49. Air-supply induced heat-flux through ETFE cushion for different flow rates, Sample 1 (clear)..... 149

Figure 5. 50. Air-supply induced heat flux relative to the transversal heat flux for the winter scenario (A) and the summer scenario (B) 151

Figure 5. 51. Heat Flux through clear double layer ETFE cushion, sample No.1 (Temperature Difference 15°C) 154

Figure 5. 52. Heat Flux through clear double layer ETFE cushion, sample No.1 (Mean Temperature 10°C)..... 154

Figure 5. 53: R-Value for a clear double layer ETFE cushion, sample No.1 (Temperature Difference 15°C)..... 154

Figure 5. 54: R-Value for a clear double layer ETFE cushion, sample No.1 (Mean Temperature 10°C)..... 154

Figure 6. 55. A) Photography of a south-east facing façade of an office building, at the University of Nottingham, UK. Image B) shows an artistic rendering of a switchable ETFE double-skin façade added to the original building as a measure of retrofitting 158

Figure 6. 56. A) Visualization of a structure of a typical low-rise office building with a double-kin façade with different ETFE foil types. B) Section of a typical single-unit office room with an ETFE double-skin façade showing the reflected and transmitted rays of solar radiation at the different layers of the building envelope..... 160

Figure 6. 57. Double-skin façades with ETFE A) Unilever Headquarter in Hamburg, with single-layer clear ETFE foil; B) Tic-Media Building in Barcelona with double layer ETFE foil cushion, switchable with nitrogen gas injection; C) Canary Wharf Crossrail Station in London with fritted double-layer ETFE foil cushion..... 161

Figure 6. 58: Light transmission and reflection of a switchable ETFE cushion in the open (A) and closed mode (B)..... 163

Figure 6. 59: Specular (A) and diffuse light transmission and reflection on a translucent material section 163

Figure 6. 60. Workflow diagram for daylight simulation, showing interconnectivity and data stream between software programs and plug-ins 164

Figure 6. 61. Screenshot showing the office model generated in Rhinoceros with projected daylight simulation results and Grasshopper/Honeybee simulation definition (screenshot by the thesis author, unpublished)..... 164

Figure 6. 62. Two layers of switchable ETFE foil samples *A)*, spectral analysis of ETFE standard light source and spectral sensor B)..... 166

Figure 6. 63. Modelled cushion geometry with different mesh densities A), B), C), D), E) 167

Figure 6. 64. Cushion geometry (perspective, section and plan view) with assigned materials 170

Figure 6. 65. Radiance custom ETFE material definitions 170

Figure 6. 66. A) Schematic diagram showing principle of BSDF generation. B) depicts a plan view of the Klems hemispheres with 145 subdivided patches of ray incidence angles 172

Figure 6. 67. A) Mock-up of switchable ETFE cushion with a solar shielded black box; B) Illuminance meter with extended luminance sensor that was introduced to the box; C) analogue digital model with assigned material data and black box with test points 173

Figure 6. 68. Schematic diagram of the simulation model 174

Figure 6. 69. Simplified DSF Model for Radiance including BSDF 174

Figure 6. 70. Window to wall ratios of façade scenarios for daylighting simulation, A) 30% / 70%, B) 45% / 55%, C) 60% / 40%, D) 75% / 25%, E) 90% / 10% 175

Figure 6. 71. World map showing the geographic location of cities used for the climate-based Radiance simulation 177

Figure 6. 72. Stereographic projection on discretized three-dimensional sky model for Barcelona showing the annual Total Radiation (A), Diffuse Radiation (B) and Direct Radiation (C) 180

Figure 6. 73. Plan views of the room model showing the sensor grid distribution for the Radiance simulation of the Useful daylight illuminance (A), Illuminance (B),

Simplified Daylight Glare Probability (C) and Daylight illuminance uniformity ratio (D) 182

Figure 6. 74. General optical properties (A), global, specular and diffuse transmittance (B), global, specular and diffuse reflectance of three ETFE foil types (clear, fritted and dense fritted) taken from a switchable ETFE foil sample 189

Figure 6. 75. Spectral distribution of visual light transmittance, reflectance and absorbance of three ETFE foil types taken from a switchable ETFE foil sample, A) clear, B) fritted and C) dense fritted 189

Figure 6. 76. Spectral distribution of specular transmittance (A), diffuse transmittance (B), specular reflectance (C) and diffuse reflectance (D) of three ETFE foil types (clear, fritted and dense fritted) taken from a switchable ETFE foil sample 190

Figure 6. 77. Switchable ETFE cushion mock-up (photo by the thesis author, unpublished) 192

Figure 6. 78. Switchable ETFE cushion, in open (A) and closed mode (B), rendered in Radiance with material data from spectral analysis of material sample assigned .. 192

Figure 6. 79: Transmission on the frontside of the switchable ETFE cushion in (A) open mode (B) closed mode for a incidence angle perpendicular to the horizontal plane (images by the thesis author, unpublished) 194

Figure 6. 80. Reflection on the frontside of the switchable ETFE cushion in (A) open mode (B) closed mode for an incidence angle perpendicular to the horizontal plane 194

Figure 6. 81. Illuminance across the section in black test box for different ETFE BSDF models 196

Figure 6. 82. Comparison of measured and simulated illuminance across the section in mock-up and virtual black box with ETFE switchable ETFE cushion in open mode 196

Figure 6. 83. Annual, hourly switching schedule for Barcelona climate with a luminance threshold of 0 lux set for the sensor 197

Figure 6. 84. Annual, hourly switching schedule for Barcelona climate with a luminance threshold of 500 lux set for the sensor 198

Figure 6. 85. Annual, hourly switching schedule for Barcelona climate with a luminance threshold of 1000 lux set for the sensor 198

Figure 6. 86. Illuminance simulated over 24 hours with a Barcelona climate file at a centred sensor point in the generic test-box with switchable the ETFE cushion in the south face. A) shows the illuminance at the solstice of summer for the open and closed mode. B) shows the illuminance at the solstice of winter for the open and closed mode (graphs by the thesis author, unpublished) 199

Figure 6. 87. Fish eye view realistic renderings and false colour illuminance renderings of south facing room for 12:00 am summer solstice in Barcelona, showing in A 1,2) double glazing with 100% WWR, B 1,2) double glazing + clear ETFE cushion with 100% WWR, C 1,2) double glazing + switchable ETFE cushion in open mode with 100% WWR, D1,2) double glazing + switchable ETFE cushion in closed mode with

100% WWR, E 1,2) double glazing + clear ETFE cushion with 30% WWR, F 1,2) double glazing + clear ETFE cushion with 90% WWR 201

Figure 6. 88. Fisheye view realistic renderings and false colour illuminance renderings of south-facing room for 12 am summer solstice in Barcelona, showing in A 1 and A2 double glazing with 30% WWR 202

Figure 6. 89. Simplified Daylight Glare Probability (DGPs) at the viewpoint for south-facing office in London with different ETFE double-skin façades and varying window to wall ratio, A) 30%, B) 45%, C) 60%, D) 75%, E) 90%,..... 204

Figure 6. 90. Simplified Daylight Glare Probability (DGPs) at viewpoint for south facing office in Barcelona with different ETFE double-skin façades and varying window to wall ratio, A) 30%, B) 45%, C) 60%, D) 75%, E) 90%,..... 205

Figure 6. 91. Simplified Daylight Glare Probability (DGPs) at the viewpoint for south-facing office in Shanghai with different ETFE double-skin façades and varying window to wall ratio, A) 30%, B) 45%, C) 60%, D) 75%, E) 90%,..... 206

Figure 6. 92. Daylight illuminance uniformity ratio (UR) at task area for south-facing office in London with different ETFE double-skin façades and varying window to wall ratio, A) 30%, B) 45%, C) 60%, D) 75%, E) 90%..... 210

Figure 6. 93. Daylight illuminance uniformity ratio (UR) at task area for south-facing office in Barcelona with different ETFE double-skin façades and varying window to wall ratio, A) 30%, B) 45%, C) 60%, D) 75%, E) 90%..... 211

Figure 6. 94. Daylight illuminance uniformity ratio (UR) at task area for south-facing office in Barcelona with different ETFE double-skin façades and varying window to wall ratio, A) 30%, B) 45%, C) 60%, D) 75%, E) 90%..... 212

Figure 6. 95. UDI (1) and Illuminance (2) across the section of a south-facing office in London with different ETFE double-skin façades and varying window to wall ratio, A) 30%, B) 45%, C) 60%, D) 75%, E) 90%..... 217

Figure 6. 96. UDI (1) and Illuminance (2) across the section of a south-facing office in Barcelona with different ETFE double-skin façades and varying window to wall ratio, A) 30%, B) 45%, C) 60%, D) 75%, E) 90% 218

Figure 6. 97. UDI (1) and Illuminance (2) across the section of a south-facing office in Shanghai with different ETFE double-skin façades and varying window to wall ratio, A) 30%, B) 45%, C) 60%, D) 75%, E) 90% 219

Figure 6. 98. UDI 500-2000lux bin at 0.75 m height horizontal plan for a 5-day working hours schedule of a south-facing office in London with double-skin façades comprising DG (1), DG+fritted ETFE cushion (2) and DG + switchable ETFE cushion (3) for different WWR ratios A) 30%, B) 45%, C) 60%, D) 75%, E) 90% 220

Figure 6. 99. UDI 500-2000lux bin at 0.75 m height horizontal plan for a 5-day working hours schedule of a south-facing office in Barcelona with double-skin façades comprising DG (1), DG+fritted ETFE cushion (2) and DG + switchable ETFE cushion (3) for different WWR ratios A) 30%, B) 45%, C) 60%, D) 75%, E) 90%, ... 221

Figure 6. 100. UDI 500-2000lux bin at 0.75 m height horizontal plan for a 5-day working hours schedule of a south-facing office in Shanghai with double-skin façades comprising DG (1), DG+fritted ETFE cushion (2) and DG + switchable ETFE cushion (3) for different WWR ratios A) 30%, B) 45%, C) 60%, D) 75%, E) 90% 222

Figure 6. 101. UDI Performance trends at the centre of the room for different double-skin façades with varying window to wall ratio across different climates, A) London, B)Barcelona, C) Shanghai..... 223

Figure 7. 102. TicMedia building in Barcelona, Spain, A) street view of the building with switchable ETFE double-skin façade, B) close-up view of the switchable ETFE cushion façade, C) backside view of the switchable ETFE cushion seen from the space between primary and secondary façade 230

Figure 7. 103. Heat transfer mechanisms through double-skin façades with ETFE cushion 231

Figure 7. 104. Workflow diagram of energy simulation showing data stream between programs and plug-ins..... 233

Figure 7. 105. Plan view of building model with indicated test office 235

Figure 7. 106. Isometric view of building model and zones (A) and test office room (B) 236

Figure 7. 107. Office test room with incremental window to wall ratios ranging from 30% to 90% in steps of 15%..... 237

Figure 7. 108. Schematic diagram showing the layer composition of the double-skin façade with ETFE 240

Figure 6. 109. Annual lighting, heating and cooling electric energy consumption of an office room in London, with different façades and window to wall ratio 244

Figure 7. 110. Annual lighting, heating and cooling electric energy consumption of an office room in Barcelona, with different façades and window-to-wall ratio 245

Figure 7. 111. Annual lighting, heating and cooling electric energy consumption of an office room in Shanghai, with different façades and window-to-wall ratio 248

Figure 7. 112. Annual energy balance on a monthly basis - London climate, double Glazing, 90% WWR 250

Figure 7. 113. Annual energy balance on a monthly basis - London climate, switchable ETFE double-skin façade, 90% WWR 250

Figure 7. 114. Annual energy balance on a monthly basis - Barcelona climate, double Glazing, 90% WWR 251

Figure 7. 115. Annual energy balance on a monthly basis - Barcelona climate, switchable ETFE double-skin façade, 90% WWR 251

Figure 7. 116. Proportional annual heat gains and losses through the main building components of an office room with double glazing under Barcelona climate conditions 253

Figure 7. 117. Proportional annual heat gains and losses through the main building components of an office room with a double-skin façade with switchable ETFE cushions, under Barcelona climate conditions 253

Figure 7. 118. Energy gains and losses by heat conduction and solar radiation for a DSF with a WWR of 90% in different climates, from 22nd of Mar. to 21st of Sept. 255

Figure 7. 119. Energy gains and losses by heat conduction and solar radiation for a DSF with a WWR ratio of 90% in different climates, from the 22nd of Sep. to 21st of Mar. 255

Figure 7. 120. Percentage of annual energy savings with DSF relative to the reference case with Double Glazing – London 257

Figure 7. 121. Percentage of annual energy savings with DSF relative to the reference case with Double Glazing – Barcelona 258

Figure 6. 122. Percentage of annual energy savings with DSF relative to the reference case with Double Glazing – Shanghai 259

Figure 7. 123. Correlation of the annual energy and daylighting performance for a façade with double-glazing compared to a double-skin façade with switchable ETFE cushions, with different window-to-wall-ratios under London climate conditions 262

Figure 7. 124. Correlation of the annual energy and daylighting performance for a façade with double-glazing compared to a double-skin façade with switchable ETFE cushions, with different window-to-wall-ratios under Barcelona climate conditions 262

Figure 7. 125. Correlation of the annual energy and daylighting performance for a façade with double-glazing compared to a double-skin façade with switchable ETFE cushions, with different window-to-wall-ratios under Shanghai climate conditions 263

Figure 7. 126. Schematic section showing double-skin façade with switchable ETFE cushion in open mode (A) and closed mode (B) shading the primary building façade 264

Figure 8. 127. Energy Technology Building at The University of Nottingham Jubilee Campus. Image A) original building office building. Image B) artistic rendering showing the same building with an ETFE double-skin façade 269

Figure 7. 128: Dimension and spatial configuration of the test room, showing in A) a transversal section, in B) a plan view, and in C) an isometric view 272

Figure 7. 129. A) External view of the building façade showing the installed ETFE cushion mock-up. B) Inside view showing the camera in the view position for the 360-degree stereographic imaging 274

Figure 8. 130. Process of VR image generation, 1. stereographic HDRI photography of test room, 2. stitching of images, 3. Post-processing and 3D projection of images to spherical geometry, 4. projection of imagery to VR headset 275

Figure 8. 131. A) Participant equipped with the virtual reality headset as used during the experimental sessions. B) Close-up view of the virtual reality mask from the participant's perspective, showing the two Fresnel lenses through which, the stereoscopic images of the room are projected 276

Figure 8. 132. An example of the stereographic images projected through the lenses of the virtual reality headset 276

Figure 8. 133. Views through DSF material samples, A) REF double glazing, B) DSF 1, double glazing + clear ETFE, C) DSF 2, double glazing + fritted ETFE, D) DSF 3, double glazing + switchable ETFE 278

Figure 7. 134. Flowchart of the experimental procedure 280

Figure 7. 135: Results of the questionnaire showing average ratings of samples..... 284

Figure 8. 136: Ranking charts of mean values corresponding to the view clarity parameters of the different view samples, A) View clarity (Question No. 1), B) View satisfaction (Question No. 2), C) View amount (Question No. 3), D) View appearance (Question No. 4), E) View perception (Question No. 5) , F) View vividness (Question No. 6)..... 286

Figure 8. 137: Ranking charts of mean values for those parameters corresponding to the emotional response on the different view samples, A) Spatial pleasure (Question No. 7), B) Spatial arousal (Question No. 8), C) Spatial dominance (Question No. 7) .. 287

List of Tables .

Table 2. 1

List of projects incorporating multi-layer foil constructions with integrated dynamic environmental control mechanisms 70

Table 2. 2

Thermo-optical properties of ETFE foil constructions from different literature sources 81

Table 4. 3

Optical properties of frit prints and material for ray-tracing simulation input 107

Table 4. 4

Starting conditions for the ray-tracing simulations 108

Table 4. 5

Optical performance of switchable triple-layer ETFE cushions with different frit print properties in open and closed mode 120

Table 5. 6

Temperature *testing scenarios* 136

Table 5. 7

Sample No. 1 (2 layers, clear ETFE), measured values 142

Table 5. 8

Sample No. 2 (2 layers, fritted ETFE), measured values 142

Table 5. 9

Sample No. 3, Open Mode (3 layers, fritted ETFE), measured values 143

Table 5. 10

Sample No. 3, Closed Mode (3 layers, fritted ETFE), measured values 143

Table 5. 11

Transversal-Horizontal heat-flux through ETFE cushion, sample 1 (2 layers, clear), (table by the thesis author, unpublished) 152

Table 5. 12

Calculated results for heat flux and R-value of a clear double layer ETFE cushion for different climate scenarios 153

Table 6. 13

Double skin façade buildings with ETFE 161

Table 6. 14

Grasshopper/Honeybee Input parameters for Radiance 'trans' material generator 170

Table 6. 15

Material combinations for double skin façade simulation 176

Table 6. 16

Summary of the input data for the model wall material 176

Table 6. 17

Simulation Parameters for Radiance daylighting simulation set-up 181

Table 6. 18

Optical characteristics of visible light transmittance, reflectance and absorbance of three ETFE foil types (clear, fritted and dense fritted)..... 188

Table 6. 19

*Diffuse reflectance values of red, blue and green channels (RGB) according to different colour models for three ETFE foil types (clear, fritted and dense fritted)*191

Table 6. 20

BSDF samples direct hemispherical visible transmittance and reflectance on front and backside for a perpendicular incidence angle 192

Table 6. 21

Simplified Daylight Glare Probability (DGPs): numerical data summary for London 207

Table 6. 22

Simplified Daylight Glare Probability (DGPs): numerical data summary for Barcelona 207

Table 6. 23

Simplified Daylight Glare Probability (DGPs): numerical data summary for Shanghai 208

Table 6. 24

Daylight illuminance uniformity ratio (UR): numerical data summary for London 213

Table 6. 25

Daylight illuminance uniformity ratio (UR): numerical data summary for Barcelona 213

Table 6. 26

Daylight illuminance uniformity ratio (UR): numerical data summary for Shanghai 214

Table 6. 27

Climate classification of simulated locations 234

Table 6. 28

Meteorological data for London, Barcelona and Shanghai 234

Table 7. 29

Input data for the material definition of the glazing and ETFE (source: Knippers et al. 2011; Flor et al., 2018, experimental data chapter 5 and 6)..... 238

Table 6. 30.

Comparison between measured and calculated U-values of ETFE cushions 239

Table 7. 31

Construction components and materials' thermal resistance 240

Table 7. 32

Zone parameters 241

Table 7. 33

Applicability of ETFE double-skin façade design options for different climate scenarios and window-to-wall ratios..... 260

Table 8. 34

Material description and layer composition of ETFE double-skin façades used in the experiment 278

Table 8. 35

Evaluated Parameters in the questionnaire 282

Table 7. 36

Overview of descriptive statistical data of the experimental sample rating results 290

Glossary .

Abbreviations:

ACPH	Air Change Rate per Hour
ANSI	American National Standards Institute
ASTM	American Society for Testing and Materials
ASHRAE	American Society of Heating, Refrigerating and Air-Conditioning Engineers
BRDF	Bidirectional Reflectance Distribution Function
BSDF	Bidirectional Scattering Distribution Function
BS	British Standard
CABS	Climate Adaptive Building Shells
CEN	Comité Européen de Normalisation (engl. transl.: European Committee for Standardization
CFS	Complex Fenestration System
CIE	Commission internationale de l'éclairage (engl. transl.: International Commission on Illumination)
C	Chamber (Air Chamber of ETFE Cushion)
CFD	Computational Fluid Dynamics
CO_2	Carbon Dioxide
CPU	Central Processing Unit
DIN	Deutsches Institut für Normung e.V. (engl. transl.: German Institute for Standardization)
DITF	Deutsche Institute für Textil- und Faserforschung (engl. transl.: Institute of Textile Technology and Process Engineering)
DSF	Double-Skin Façade
DGP	Daylight Glare Probability

DGPs	Simplified Daylight Glare Probability
DG	Double Glazing
EN	European Norm
EIA	Energy Information Administration (U.S.)
ETFE	Ethylene Tetrafluoroethylene
EPW	Energy Plus Weather
GHI	Global Horizontal Irradiation
HDRI	High Dynamic Range Image
HPC	High-Performance Computer
HVAC	Heating, Ventilation and Air-Conditioning
IDF	Input Data File
IEA	International Energy Agency
IL	Inner Layer
ISO	International Standard Organisation
IWEC	International Weather for Energy Calculations
LBNL	Lawrence Berkeley National Laboratory
LED	Light Emitting Diode
LPD	Lighting Power Density
ML	Middle Layer
nZEB	nearly Zero Energy Building
OECD	Organisation for Economic Co-operation and Development
OL	Outer Layer
OLED	Organic Light-Emitting Diode
PEB	Plus Energy Building
PV	Photovoltaics
REF	Reference
RGB	Red, Green, Blue Channels
S	Surface
SHGC	Solar Heat Gain Coefficient

SLPM	Standard Litre Per Minute
UDI	Useful Daylight Illuminance
UV	Ultraviolet (Radiation)
UR	Daylight Illuminance Uniformity Ratio
URS	Update Reference Strategy
VR	Virtual Reality
VCI	View Clarity Index
WWR	Window to Wall Ratio
3D	Three-Dimensional

Nomenclature .

Symbols:

A	Optical Absorbance	%
C_p	Specific Heat Capacity	J/(K·kg)
$D\lambda$	Relative Spectral Distribution	-
E	Thermal Emittance	-
E_e	Irradiance	W/m^2
E_v	Illuminance	$cd \cdot sr \cdot m^{-2}$
ε	Emissivity	-
h	Convective Heat Transfer Coefficient	$W/m^2 \cdot K$
IR	Infrared Radiation	cm^{-1}
k	Thermal conductivity	W/m·K
λ	Wavelength of Visible Light	nm
m	Mass Flow	kg/s / slpm
n	Refractive Index	-
p	Pressure	Pa / mbar
Q	Energy	W/m^2
R	Thermal Resistance	$m^2 \cdot K/W$
R	Optical Reflectance	%
Si	Radiation	W/m^2
T	Optical Transmittance	%
T	Temperature	K / °C
U	Thermal Transmittance	$W/m^2 \cdot K$
Ra	Surface Roughness	mm

Subscripts:

c	convective
e	external
es	external surface
ext	external
g	gas
i	internal
int	internal
is	internal surface
ref	reflected
sol	solar
trans	transmitted
vis	visible

Chapter 1: Introduction

1.1. Introduction to chapter one

Membrane and foil structures have become over the last decades an attractive alternative to conventional materials and building systems with increasing implementation in different typologies and scale. The development of transparent, light, flexible and resistant materials like Ethylene Tetrafluoroethylene (ETFE) has triggered a rethinking of the building envelope in the building industry towards lightweight systems. ETFE foil cushions have proven to fulfil the design requirements in terms of structural efficiency and aesthetic values. However, the strategies to satisfy the increasing demands of energy efficiency and comfort conditions are still under development. The prediction and manipulation of the thermo-optical behaviour of ETFE foil cushion structures currently remain as one of the main challenges for designers and manufacturers. This chapter reviews ongoing research regarding the control of the thermo-optical performance of ETFE cushion structures and highlights challenges and possible improvements. An overview of different dynamic and responsive environmental control mechanisms for multi-layer foil constructions is provided and state of the art in building application outlined by the discussion of case studies.

This chapter section further outlines the state of the art of the theories and technical aspects of adaptive environmental control mechanism for multi-layer foil constructions by an extensive literature review and sets the theoretic background knowledge for the further investigation. Research aims, objectives of the thesis are stated in this chapter, and an overview of the thesis structure and methodical approach is provided. Parts of the content of this chapter is based on a paper published by the applicant during his PhD course. The title page and authors contribution declaration can be found in the appendices Q and R:

> *Flor, J.-F., Wu, Y., Beccarelli, P., Chilton, J., Dynamic environmental control mechanisms for pneumatic foil constructions. E3S Web Conf., 2017. 22.*

1.1.1. Environmental adaptation of building envelopes and the role of ETFE

The energy performance of the building envelope is becoming increasingly important since the building sector is held responsible for more than one-third of the worldwide energy consumption, according to the International Energy Agency [2019]. Dynamic environmental control mechanisms in building envelopes are a common strategy to balance the reduction of solar heat gains and achieving satisfactory natural daylighting while reducing energy consumption for cooling and artificial lighting at the same time. The integration and automatization of these mechanisms into complex fenestration systems and high-tech building façades have become a reality and opens possibilities for further optimisation of the energy performance and improvement of comfort conditions in the built environment. Responsive building envelopes can adapt to changing environmental conditions, or user demanded requirements and enhance the performance of the building. The developments in mechatronics, sensors and computer technology during the last decades, have made possible miniaturisation, mass production and successive cost reduction, which have allowed designers to integrate sensors and actuators into building elements making them truly responsive to the environment and occupant needs.

Pressurised multi-layered cushions of thin Ethylene Tetrafluoroethylene (ETFE) foil are increasingly applied in building envelopes and are now considered state of the art since the contributions of Frei Otto initiated the evolution of lightweight building over sixty years ago [Otto, 1954; Otto et al., 1973]. Lightweight and transparent materials play an essential role in this development, and ETFE is probably one of the most outstanding. ETFE has become an effective alternative to glass and other transparent materials mainly because of its excellent material characteristics like low weight, flexibility, high translucency, tensile strength and excellent weathering performance. However, the thermal and optical behaviour of ETFE multi-layer cushions is somehow still a topic of ongoing research, and the difficulty of predicting their energy performance has led in the past to reported problems of overheating of indoor spaces during summertime (Afrin, 2016). Dynamic environmental control systems, including responsive shading mechanisms, could be a possible solution for the adverse effects of overheating and glare. However, despite

their broad application in complex fenestration systems, they have not yet arrived at the same level of development in membrane and foil constructions. Advances in controlling the optical and thermal properties of the cushion system through, mainly, static adaptation measures are now standard practice in the industry. Currently, the most widely used techniques are frit prints of reflective inks and combinations of different layer type compositions. However, these techniques are often not sufficient under changing climate conditions, and the integration of dynamic environmental control mechanisms into multi-layer ETFE cushions remains a design objective alongside multiple approaches from the past. In the search for technical solutions to respond to pressing environmental issues, new building techniques and materials are under constant development for more efficient and better-performing building envelopes [Hausladen, 2007; Monticelli et al.; 2015; Shahin, 2019]. A conceptual drawing showing an adaptive ETFE façade is shown in Figure 1.1.

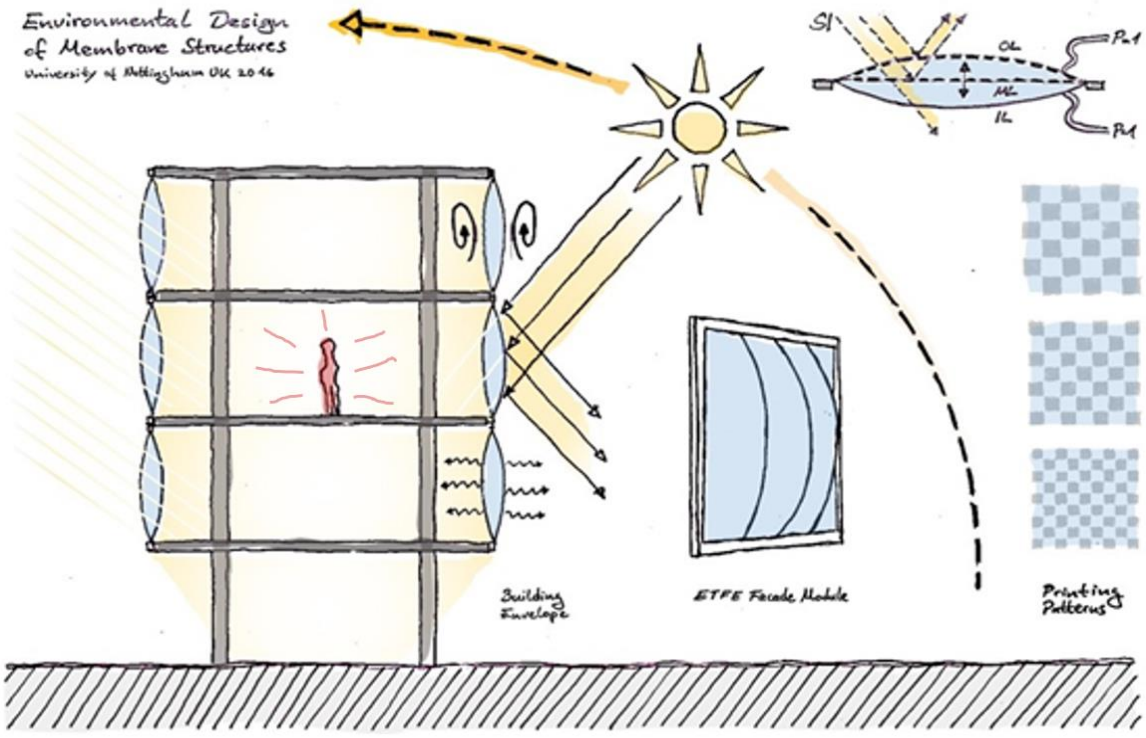


Figure 1. 1. Dynamic shading mechanisms for the environmental control of multi-layer ETFE cushions in building envelopes (top right diagram abbreviations read as follows: SI – Solar Irradiation, OL, ML, IL – Outer, Middle and Inner Layer, P 1 – Pressure) (image by the thesis author, unpublished)

1.1.2. Building envelopes of ETFE

ETFE foil has been increasingly employed as a building material for building envelopes over the past decades [Gómez-González et al., 2011]. Although used initially because of its high transparency only for temporary agricultural coverings and greenhouses, ETFE is now a recognised alternative for conventional transparent building materials such as glass [Hanke, 2013]. The acceptance of the material among designers and the building industry can be attributed mainly to its excellent properties like transparency, flexibility, tensile strength and robustness towards weathering [Tanno, 1997]. Since the first application of ETFE foil in a permanent building for the Mangrove Hall project in Burgers' Zoo, Arnheim, the Netherlands in 1982 [Robinson-Gayle, 2001], substantial technological advances have been made. New form-finding methods and simulation software, as well as automated production and manufacturing processes together with a highly specialised design industry, have contributed to its widespread use in building envelopes. The absence of homogenised design codes and standardised testing methods remain as an obstacle, but ETFE coverings are now considered to be a reliable and safe solution for performance-orientated building envelopes [Hu et al., 2017]. Iconic building projects like the Eden Project in St. Austell, UK (2000) shown in Figure 1.2, the Allianz Arena in Munich Germany (2005) and the Water Cube swimming pool in Beijing China (2008) exemplify the outstanding performance and architectural attractiveness of ETFE as a building material [LeCuyer, 2008; Chilton, 2013].



Figure 1. 2. Eden Project, St. Austell, United Kingdom, 2000
(photo by the thesis author, published in: Flor et al., 2017)

ETFE as a material for building envelopes is typically employed as an extruded thin foil in multi-layer cushions which are pneumatically stabilised structural systems. The cushions can be composed of various layers of foil with air chambers in between. These foils are cut and welded together according to pre-calculated optimal shapes of equilibrium state. The foil cushion is clamped into a rigid frame system, typically of extruded aluminium profiles, inflated with air and maintained by means of a blower system at a predetermined pressure which enables the system to withstand external loads and maintain geometric stiffness. The number of layers of the cushion can vary in order to improve the structural or thermal resistance of the system. The foil thicknesses may also vary, according to the expected loads. Different tints or printed patterns can be applied, in response to the thermal and optical requirements [Knippers, 2011].

Different building systems for ETFE foil are currently in use, but according to a case study from Moritz in 2007 [Moritz, 2007], ETFE is most commonly employed in pressurised multi-layer cushions systems (87%) and significantly less in mechanically pre-stressed single layer systems (10%), which however are getting used more often in recent years. According to the study, ETFE is generally used in buildings related to occupancy for offices and housing (28%), swimming pools (18%), exhibition spaces and pavilions (15%). The building elements usually covered by ETFE are atria (35%), hall roofs (33%), canopies (14%) and building façades (8%) among others, ranging in a covered area between 100 and 10000 m². The predominant cushion geometry found in the analysed projects was reported as rectangular (60%) within a range of other hexagonal, triangular, circular or rhombic geometries. A comprehensive study by Schiemann [2009] about the structural behaviour of ETFE foils proposed a classification of cushion systems according to the layer number and configuration which also is of interest to the understanding of the building physics regarding optical and thermal performance when applied as a second building skin, as proposed by Grunwald [2007] in an extensive study on mechanically prestressed ETFE foil façades. Several experimental designs with different layer build-ups and combinations of materials have been carried out so far [Karwath, 2011; Maxa et al. 2012], including novel double-layer ETFE panels which are pre-tensioned by heat

shrinking and do not require an internal air pressure [Martin et al. 2015]. Nevertheless, few of these novel systems have been tested in any commercial construction so far.

Even though the majority of studies on ETFE have focused in the past on the structural efficiency of the building system, recently the interest in current research has been shifted increasingly towards the energy performance of ETFE envelopes.

1.1.3. Responsiveness in textile building envelopes

Active or responsive building envelopes are commonly referred to as shelter systems which can adapt autonomously, using sensors and actuators, to changing environmental conditions, or user and activity demanded requirements [Wyckmans, 2005]. While the concept is not entirely new, as can be learned from several historical examples, like the Roman velarium or Venetian blinds, the idea of autonomously self-adapting buildings has emerged only recently [Barozzi et al., 2016], fulfilling the technological innovations envisioned by modernist scholars like Sigfried Ebeling almost a century ago [Ebeling, 2016/1926]. The development of environment responsive membrane structures with automated mechanisms is indeed very recent and although several projects are reported in the literature most of them are prototypes or of an experimental nature [Cardoso et al., 2007].

Mainini et al. [2016] showed with the experimental design of an ETFE panel with two parallel ETFE layers and integrated water spray nozzles that the application of a water film on the internal ETFE surfaces enhances the thermal performance by reducing solar gains and surface temperatures. Preliminary experimental results of this study showed a reduction of solar gains of up to 10% while simultaneously reducing the ETFE surface temperature by 10°C. In both effects potential was seen to enhance comfort conditions in indoor spaces during summer time. In another study it has been demonstrated with a experimental prototype and computer simulations that circulating tinted fluids in a 3D formed channelled ETFE layer enhances the thermal and solar performance of a triple layer ETFE cushion [Hanke, 2016]. The circulating fluid in the middle layer was reversibly tinted on demand with dark pigments to shade interior building spaces, absorb solar

radiation and remove the solar gains with a pump from the ETFE cushion unit for solar thermal applications such as the support of the heating system or warm water generation using a heat exchanger. The conducted experiments with a solar simulator and a 1 m x 1 m demonstrator unit showed that the solar heat gain coefficient (SHGC) of ETFE cushions could be reduced from 0.67 to 0.56 when switching the fluid from clear to black tinted. The fluid temperature correspondingly increased from 37°C to 56°allowing to extract heat gains of 45 W and 200 W , respectively, of an total incident radiation of 900 W/m^2.

More conventional applications of integrated shading lamellas and retractable textile schading screens inside the ETFE cushions had been proposed previously [Höpfner, 2002; Sinnesbichler, 2015] for practical applications in the building industry. Although limited information on the thermo-optical performance of these systems in combination with ETFE is available, extensive research has been conducted for integrated solar lamella, parallel shading slats and translucent insulation material in double glazed windows showing enhanced performance for daylight and insulation properties [Sun et al., 2016; Sun et al., 2017; Sun et al., 2018]

All of the studies reviewed here support the hypothesis that the thermal and optical performance of a building envelope can be reversibly adapted to reach climate comfort conditions and reduce energy consumption in a responsive way, hence modifying with actuators the structure or material properties with the real-time input of environmental sensors. As an illustration, for the above-described principle, a schematic building section of the functional relations of a responsive building envelope incorporating a dynamic shading mechanism within a multi-layer ETFE cushion is shown in Figure 1.3. A floor to ceiling façade is replaced with a triple-layer ETFE foil cushion, inflated with air by an air blower unit. All ETFE layers are transparent with reflective frit print applied to the middle and outer layer. The middle layer can be moved back and forth by air pressure, shading the internal space, light-sensor controlled.

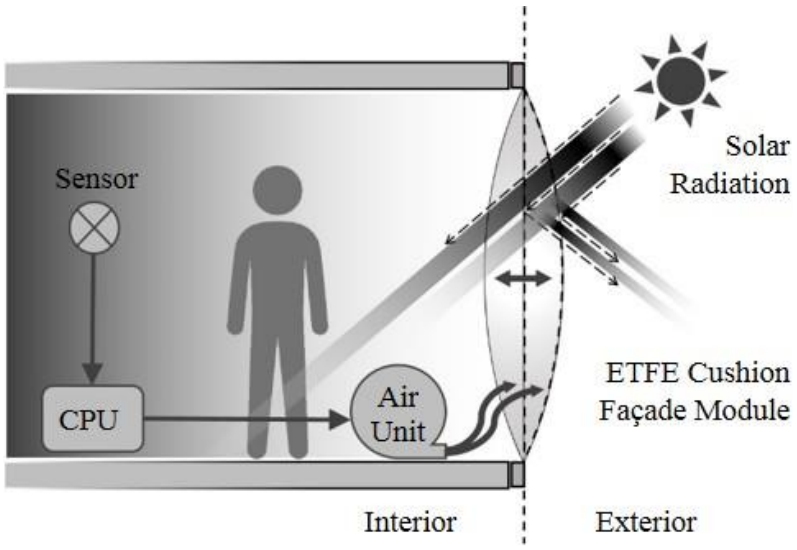


Figure 1. 3. Schematic section of a responsive building envelope incorporating a dynamic shading mechanism within a multi-layer ETFE cushion
(image by the thesis author, published in: Flor et al., 2017)

The principle of a switchable ETFE façade, as described in the previous section and depicted in Figure 1.3 corresponds to the category of Climate Adaptive Building Shells (CABS) which have evolved as flexible and lightweight building enclosures aiming to respond dynamically to changing weather conditions to improve building performance, rather than withstanding environmental pressures with static robustness of building mass [Loonen, 2013]. A multitude of materials and mechanisms have been explored based on different principles of physics, applied at different scales, such as thermo- or electrochromic windows, phase-changing insulation materials, kinetic origami-inspired shadings and flexible form changing façade elements among others. The common feature of CABS is the ability to change reversibly from one state to the other, with an electrical, chemical or kinetic mechanism which is triggered either passively by environmental vectors or actively through environmental sensing with an operator or automated actuator. Meaning, the light transmittance, thermal conductivity or shading angle of a façade element can be changed actively according to indoor comfort requirements or varying outdoor climate conditions. The adaptive capacity of a building envelope provides theoretically a large potential for saving energy in lighting, heating and cooling appliances in buildings

allowing to improve the indoor comfort conditions at the same time. However, despite the variety and advanced stage of product developments, few buildings exist were CABS have been applied, and their superior performance has been proven. An early example is the Arab World Institute, by architect Jean Nouvel, built in Paris, France in 1988, incorporating mechanical mechanisms in the façade, similar to a camera lens shutter, being able to moderate the incoming light. One of the most recent examples CABS application is the Ed Kaplan Family Institute for Innovation and Tech Entrepreneurship at the Illinois Institute of Technology in Chicago, USA, designed by John Ronan Architects, finalized in 2018, which incorporates a switchable ETFE cushion system similar to the diagram presented in Figure 1.3. Other examples emploring different mechanisms and materials have been documented in the literature and are discussed in the following chapter 2. The interrogative that remains is the quantification of the enhanced building performance that CABS promise and the search for tools that provide answers to that question [Kunwar & Bhandari, 2020].

1.2. Motivation and Justification for the study

A variety of environmental control mechanisms for multi-layer foil constructions has been outlined, and their function and application in building envelopes have been discussed through a range of case studies. From this first overview of the state-of-the-art, it can be concluded that besides the perceived fascination in the public opinion about adaptive building envelopes and energy-saving façade systems the topic of the dynamic shading mechanisms for multi-layer cushions appears to be neglected in the literature opening a gap for research. Even though mentioned in several studies, the building physic aspects of dynamic foil constructions have not been addressed thoroughly. Nevertheless, they continue to be applied in new construction despite the vagueness of understanding of their influence on the energy performance of buildings. There have been remarkably few published reports directly addressing the problem of the thermal and optical behaviour of these systems. Only 10 out of over 120 reviewed scientific articles on ETFE reported useful information on the thermo-optical properties, as will be discussed in detail in the literature review presented in chapter 2. Currently, the thermo-optical effects of ETFE building

envelopes on the energy and daylighting performance of buildings remains an uncertainty in the building industry and a research question in science. This represents a risk and opportunity at the same time, which needs to be addressed and which bears great potential for improving the system performance of both building and envelope. It is believed that a thorough understanding of the systems' optical and thermal behaviour is indispensable to predict and assess their effectiveness in controlling the climatic factors, enhancing occupant comfort conditions, and improving the energy performance of the building. Literature provides only limited information on the effectiveness of the reviewed systems. An explicit description of their optical and thermal properties and the complex physical mechanisms of light and heat transfer are available only to a limited extent. This initial review can only be the first step towards a broader understanding of dynamic environmental control mechanisms for multi-layer ETFE cushions. More data from the monitoring of operating buildings is required as well as new approaches towards the simulation of their dynamic behaviour with simplified numerical calculation methods and advanced computer simulation. Development of adapted testing methods to determine the thermo-optical properties of multilayer ETFE cushions and further validation of computational methods is perceived as a necessity to advance the understanding of the effects on building performance. Great potential is seen in these tasks proposed for this thesis from a scientific point of view but also from an industry perspective.

1.3. Aims of the thesis

In congruence with the identified knowledge gap in the preliminary literature review the overall aim of this thesis is to investigate the new developments in the environmental design of building envelopes incorporating structural membranes, focusing primarily on the thermo-optical, energy and daylighting performance of switchable multi-layer ETFE foil cushions. The thesis further aims to:

- Gain more insights into the building physics of switchable ETFE façades, understanding dominating principles and identifying primary performance parameters.
- Contribute to the unlocking of potential for energy-efficient buildings, providing knowledge on the characteristics and performance of switchable ETFe cushions.
- Develop a methodology which aligns a set of tools and methods in a workflow able to analyze, predict and improve the environmental performance of dynamic membrane envelopes and their influence on the whole building.

1.4. Objective and sub-objectives of the thesis

More specifically the overall objective of this thesis is to investigate the building physics of switchable ETFE cushions concerning multiple aspects of design and environmental parameters in order to improve the system performance and evaluate if their application could significantly improve the energy performance of buildings in comparison to conventional static cushion systems.

Furthermore, specific sub-objectives were derived from the overall objective:

1. Review the current state of the art of environmental control mechanism for ETFE foil building envelopes.
2. Investigate the physical processes involved in the environmental behaviour of ETFE foil building envelopes and identify the principal optical and thermal transmittance mechanisms in multi-layer ETFE cushions which have a significant impact on the energy performance of buildings.
3. Compare and evaluate the energy performance of dynamic shading mechanisms for multi-layer ETFE cushions in comparison to conventional systems, including the influence of design parameters like frit pattern, cushion geometry and solar orientation.

4. Develop a workflow scheme with a set of tools which allow to evaluate, predict and optimize the environmental behaviour dynamic multi-layer ETFE cushions and the influence on the whole building performance.
5. Analyze the strengths and weaknesses of current switchable ETFE cushions, identify the potential for optimization and propose novel concepts for advanced environmental control systems.

1.5. Research questions

This section outlines the research questions of this thesis. The research questions emerge as interrogative, along with the aims and objectives, from the preliminary literature review and challenge the idea of a climate adaptive building envelope as a per se high-performing technology, like commonly portrayed. This thesis asks critically:

- To which level can adaptive multilayer ETFE foil cushions improve the environmental performance of façades and buildings in terms of energy and daylighting, and how effectively, in comparison to conventional, static systems?

Furthermore:

- Would it be viable to apply adaptive ETFE structures as a second building skin and measure of retrofit to reduce the energy consumption and improve the daylighting performance of outdated multi-story buildings?
- What are the influencing parameters on performance, and in which climates integration of adaptive ETFE systems into building envelopes would generate the most significant benefits?
- Which are the effects of an ETFE double-skin that are to be expected to affect the user experience and acceptance of building occupants?

To provide answers to these questions, a set of research campaigns were designed to investigate with simulations and experimental methods, different aspects of ETFE building envelopes connected to the interrogative formulated in this thesis. On continuation, the individual study outlines and proposed methods presented within the thesis chapters will be laid out and discussed. Conclusive remarks providing answers to the here formulated questions are summarized in the final chapter nine.

1.6. Structure of the thesis

This section outlines the structure of the thesis. The thesis is composed of nine chapters, several of which incorporate work reported in published articles or submitted manuscripts. Therefore, the work contained in the main body of the thesis is presented in a classical paper style structure with sections divided into introduction, methods, results and discussion, and conclusions. The seven chapters of the main body are bound by an introductory chapter and a conclusion chapter, as shown in flow-chart in Figure 1.4. It must be disclaimed that even though the chapters are structured and aligned logically and constructively to form a unified piece of work, they can be considered as individual pieces of work, making it possible to be read on its own without further introduction. On continuation, the content of each chapter is summarised, and the interrelation between each of them highlighted and linked to the overall thesis topic:

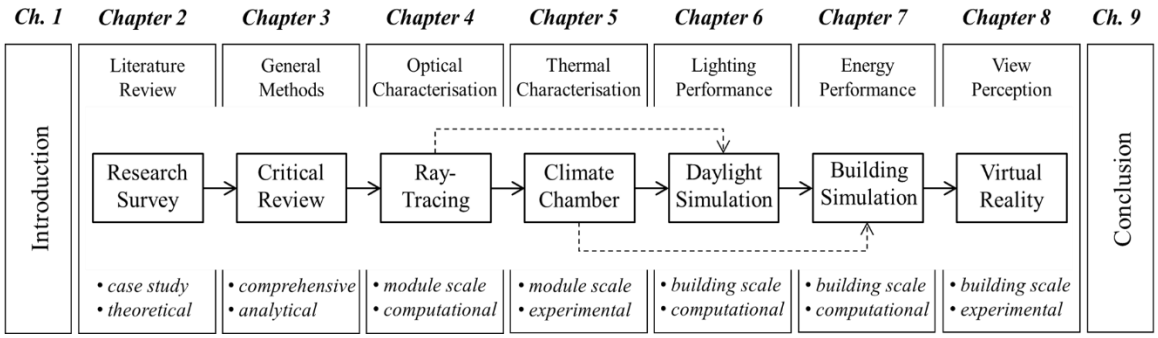


Figure 1. 4. Flow-chart of the thesis structure, showing the interrelationship between the chapters main topics and methods
(flow-chart by the thesis author, unpublished)

1.6.1. Chapter one outline

Chapter one constitutes the introduction to the thesis, covering with a classic structure the general background of switchable ETFE façades. The brief introduction to the topic is followed by an outline of the current state of knowledge and highlight problems and challenges related to the technology of switchable multi-layer foil constructions, including the state of the art of the technology, including a broad overview of historical developments, materials, mechanisms and building applications. The introduction further sets the main focus of the proposed research and justifies the need to investigate the performance of these structures from a building physics perspective, followed by the current research in ETFE and research gaps, leading to the original research topics of the thesis, aims, objectives and an outline of the methodology.

1.6.2. Chapter two outline

This chapter outlines the current body of knowledge of the building physic aspects of membrane building envelopes with ETFE. Information from the literature regarding material properties, optical performance, in terms of the transmittance, reflectance, absorptance of ETFE foil with different surface treatments (inks, frits, prints, coatings) are discussed as well as the overall transmittance, reflectance of the ETFE structure. Also, the thermal performance, in terms of the U-value, indoor-outdoor temperature impact are addressed, concluding with a critical analysis of recent technological advances in the context of previous development for ETFE constructions and tensioned membrane structures in general.

1.6.3. Chapter three outline

In chapter three a general methods review is carried out based on literature findings providing a comprehensive overview of methods used in research on the thermo-optical, energy and daylighting performance of tensioned membrane structures and in particular

ETFE foil. The chapter critically reviews methods relevant to the topics of each chapter and links to the specific method selected for the research work presented in the individual chapters. The applied methods are detailed and specified in each particular study.

1.6.4. Chapter four outline

This chapter explores the optical performance of switchable multi-layer foil constructions and evaluates the influencing parameters of design and environment. The overall transmittance and reflectance of the ETFE cushion are simulated using ray-tracing techniques. Different parameters affecting the performance, like the structure's geometry, orientation, solar incidence angles, frit patterns and also materials variations are analyzed. The outcomes of this chapter are linked to the daylighting study carried out in chapter six, providing input for the simulations and informing the result interpretation.

1.6.5. Chapter five outline

Chapter five reports on the thermal performance of ETFE cushions in general and provides insight into the unique characteristics of switchable cushions. In a series of comparative performance tests different cushion samples with design variations, including switchable cushions, are exposed to different climate scenarios in a climate chamber. Different parameters, like the heat-flux, ambient air- and surface-temperature, are measured, and the thermal resistance determined for different temperature conditions. The influence of airflow on the cushion's thermal performance is tested in a second experimental setting, controlling the air pressure and temperature. All results from this series of tests are used to feed into the energy simulation in chapter seven and provide, as a transferrable useful outcome, a thermal characterization profile for switchable ETFE cushions.

1.6.6. Chapter six outline

This chapter addresses the natural daylighting qualities of spaces enclosed by multi-layer foil constructions with ETFE and focuses on the effects the adaptive mechanism has on the performance in terms of useful daylight, visual comfort and lighting quality. The study builds on the analysis of the optical performance from chapter 3 and introduces the obtained results into daylighting simulation software (Radiance). BSDF data of different cushion designs are derived and support the parametric simulation process of different building and climate scenarios. Results of the simulations inform about the daylight performance of office spaces retrofitted with a double skin façade of ETFE, delivering values of the daylight factor and dynamic daylight metrics, like, useful daylight illuminance (UDI), daylight illuminance uniformity ratio (UR) and daylight glare probability (DGP).

1.6.7. Chapter seven outline

Based on the experimental work in the previous chapters, a calibrated energy simulation, using EnergyPlus, is conducted in chapter seven to determine the influence of switchable multi-layer foil constructions on the energy performance of buildings. The outcomes of the simulation are further compared and validated with the results from the experimental work and set in the context of the built environment with a series of case studies where switchable ETFE cushions have been incorporated.

1.6.8. Chapter eight outline

Chapter eight investigates the user perception of ETFE cushions in double-skin building façades. The view clarity and emotional response to window views through ETFE façade systems were evaluated within immersive environments, using virtual reality equipment and a developed questionnaire applied to a sample of volunteering participants. Chapter eight discusses and summarizes the research results.

1.6.9. Chapter nine outline

Chapter nine, summarizes the main research findings, draws the conclusion of the thesis as a whole, discusses limitations and drafts an outlook on the future developments of switchable ETFE cushions and the application in the built environment. The chapter further highlights linked topics of interest which have not been covered in the thesis, poses some unanswered questions and provides suggestions for future research projects.

Chapter 2: Literature Review

2.1. Introduction to chapter two

This chapter presents systematic literature review covering the role of ETFE in context of the built environment, general material characteristics of ETFE, and the application as a building material in pneumatic multi-layer constructions, structural principles and components, and mechanisms and strategies to enhance the environmental performance in building envelope applications. The chapter further covers the system components of switchable ETFE cushion, explaining in detail the relevant functions, emphasizing on structure and controls needed to transform the system into a climate adaptive building envelope. Several case studies of built examples incorporating switchable ETFE cushions are presented throughout the chapter. The chapter concludes with an overview of the thermal and optical performance of ETFE foil construction, and a detailed discussion on the investigative methods used based on the current knowledge retrieved from the literature. The chapter is based on extensive and systematic literature research carried out at different stages of the research study, covering the state-of-the-art research carried out on an international level on the topic. Additional information on material and system characteristics are included from published conference papers by the applicant listed below. The title pages and an author's declaration detailing the contributions to the papers is attached in the appendices I, J, Q and R.

Flor, J.-F., Sun, Y., Beccarelli, P., Wu, Y., Chilton, J., Switchable ETFE cushion: designing and building a model for experimental testing, 2019. In Proceedings of the IASS Annual Symposium 2019 – Structural Membranes 2019, C. Lázaro, K.-U. Bletzinger, and E. Oñate, Editors. 2019: Barcelona, Spain.

Flor, J.-F., Wu, Y., Beccarelli, P., Chilton, J., Dynamic environmental control mechanisms for pneumatic foil constructions. E3S Web Conf., 2017. 22.

2.2. Adaptive and energy-efficient building envelopes with ETFE

The building sector currently consumes one-third of the global final energy [UN Environment and International Energy Agency, 2017; Singh, 2016; Zhang et al., 2016; Berger & Mendes, 2017]. Increasing energy demands for commercial and residential buildings with an expected growth of up to 1.9%/year [US Energy Information Administration, 2017], raises the concern for the improvement of the energy performance of buildings. Buildings also contribute significantly to the global CO2 emissions responsible for climate change. According to the World Energy Outlook, 2019 by the International Energy Agency buildings account for one-quarter of the total CO2 emissions and consume one half of the globally consumed electric energy [IEA, 2019]. While the goal of the Paris agreement of 2015 is to limit global temperature rise below an average of 1.5 - 2ºC [United Nations, 2016] the latest International Energy Outlook by the U.S. Energy Information Administration [EIA, 2019] shows that energy consumption in the building sector is rising by a rate of 1.3% per year, a trend moving in the opposite direction of what is needed to reach the global climate goals. Building energy consumption in developing non-OECD countries is projected to grow even faster, with a two per cent annual increase due to economic growth and changing lifestyles.

Most of the energy consumed in buildings during the operation and maintenance period is for space conditioning (approx. 50%) and lighting (approx. 25%) [Perez-Lombard et al., 2008]. The building envelope, which is the interface between the external and internal environment, is, therefore, a crucial element of the building unit [Lin et al., 2016; Lei et al. 2016; Peng et al., 2016]. It has enormous potential to impact the indoor comfort conditions and to improve the overall energy performance of the building by up to 40%, considering only savings in heating and cooling [International Energy Agency, 2013; Peng et al., 2013; Wang et al., 2017; Peng & Yang, 2013]. Much attention has been paid, over recent decades, to passive strategies, which aim to maximize the thermal damping effects of the building mass, while increasing insulation of walls and windows, and reducing thermal bridging of building elements [Pacheco et al., 2012; Chen & Yang, 2017; Wang et al., 2016]. However,

the general tendency in architectural design moves towards light and transparent structures, such as membrane and foil structures, which offer high flexibility in form and function [Robinson-Gayle et al., 2001]. Although challenging in terms of energy-efficient design, this solution is often adopted for widespan canopies because of its reduced weight and resulting cost-effectiveness [Jones, 2000]. A case study on the "Gardens by the Bay" project in Singapore evaluated the influence of the dynamic operation of shading screens on the hygro-thermal performance of a dome structure covering a botanical garden. It was found that the retractable textile membranes are able to control the incident solar irradiation on the glass envelope, lower the risks of overheating and reduce cooling loads while maintaining stable natural lighting conditions for the plants throughout the year [Davey et al. 2010].

Although these results are promising for the development of more energy-efficient building envelopes with woven textile membrane materials, few studies have evaluated the potential of adaptable multi-layer ETFE (ethylene tetrafluoroethylene) foil constructions. Modifying the properties of surface coatings and print inks rather than changing the ETFE material or structure has been in the focus of recent research. Energy savings for cooling demands using a novel ETFE foil with infra-red absorbing coatings were calculated to range between, 5 - 8% for double and triple-layer cushions [Cremers & Marx, 2016]. Innovative 3D printing techniques applied to the middle layer of triple-layer ETFE foil construction were predicted to reduce the solar gains and achieve even higher energy savings for cooling load of 69% to 87%, compared to conventional ETFE cushions [Cremers & Marx, 2017]. While these techniques are mainly passive, the technological trend in the development of building envelopes is moving towards adaptive solutions which respond dynamically to the changing weather conditions, effectively control daylighting and reduce energy demands for cooling [Boer et al., 2011; Wang et al., 2012; Loonen et al., 2013; Perino & Serra, 2015; Attia et al., 2015; Konstantoglou & Tsangrassoulis, 2016, Sun et al., 2017; Sun et al., 2018]. The most widely reported strategy for the active control of ETFE foil constructions is the switchable multi-layer shading mechanism [Forster & Moellert, 2004; LeCuyer, 2008; Jeska, 2008; Knippers et al., 2011; Huntington, 2013].

Recent technological advances in control systems, and miniaturization of sensors and actuators, have made the development of actively adaptable building envelopes possible [Vlasceanu et al., 2013]. Moveable parts and transforming elements are fully integrated into the building system and are able to react instantly to changes in the environment or the user demands [Biloria & Sumini, 2009]. These technologies create great opportunities for the optimization of the thermal and optical performance of the building envelope and improve the energy efficiency of membrane structures [Goia et al. 2010]. While adaptable shading mechanisms for textile membranes rely mainly on mechanically retractable systems, which have been applied in many stadia and amphitheatres, the pneumatically controlled mechanisms for inflated foil construction is relatively new. The concept was first introduced by Robbin in 1996 [Robbin, 1996], based on a design concept study by David Geiger from 1977, and more recently, literature has emerged that offers specific project applications incorporating switchable ETFE cushions [Knippers et al., 2011; Poirazis, 2009; Schmid, 2009; Gomez-Gonzalez et al., 2011; Chilton, 2013; Maywald & Riesser, 2016]. Studies suggest that integrating such elements into double-skin building façades may reduce heating and cooling loads and improve the indoor lighting conditions [Shameri et al., 2011]. A theoretical study calculated the energy consumption for a building with a transformable membrane DSF façade in comparison to a standard glass façade finding an overall reduction in energy consumption between 7% and 18% across different climates [Chiu, 2015], while another project related report predicted a 55% reduction of CO2 emissions for a building with switchable ETFE DSF façade [cited in Juaristi and Monge-Barrio, 2016]. ETFE foil, a transparent, light and resistant material have been used increasingly over the past decade as a cladding material in building envelopes [Monticelli, 2015; Houtman, 2015], either as a single, double or triple layer construction [Paech, 2016; Srisuwan, 2017]. Inflated with air ETFE foil cushions provide structural integrity, excellent thermal and lighting performance and are yet very lightweight [Chilton, 2013].

2.3. Material properties of ETFE

ETFE or ethylene tetrafluoroethylene is a mineral-based polymeric material consisting of carbon, fluorine and hydrogen. It has a high tensile strength; it is a chemically inert and resistant to UV radiation, with a very high translucency comparable to glass. [Beccarelli, 2015; Wypych, 2016]. The main application of ETFE is as an insulation material in the electrical and aerospace industry, but also as a cladding and roofing material in building envelopes. This high performing material can be extruded into foils, of typically 250 μm thickness. ETFE foils are at the same time very thin, with a resulting very low thermal mass, and highly translucent to a wide range of radiation wavelength, diverging largely in their thermo-optical behaviour from traditional building materials [Chilton & Lau, 2015]. The most relevant energy exchange mechanisms for membrane structures are convection and thermal radiation. Due to the transparency and thinness of the material, radiation is the climatic element which is highly relevant to their energy performance of ETFE as a building material [Cremers & Marx, 2016]. Due to this unique condition and the complex three-dimensional geometries of standard performance evaluation methods, like for example, U-value calculation, apply only to a limited extent [Devulder et al., 2007]. Environmental adaptation mechanisms, in consequence, cannot be simply transferred from other building systems and materials but must be customized accordingly to the individual requirements. It can be summarized that ETFE can be considered as a versatile and highly performative material for many building envelope applications regardless of the specific structural system in use. However, the main benefits may relate to the following material characteristics [AGC, 2016]:

- Lightweight
- High transparency to a wide spectrum
- UV Resistant and long life-cycle
- Dirt repellent and good ageing and soiling performance
- Outstanding mechanical performance

- Weldable
- Printable
- Flexible

2.4. Characteristics of pneumatic ETFE foil construction: static and switchable

This section provides a general description of pneumatic ETFE foil construction, covering its main components and structural principle. Technical justification is outlined for the use of foil construction in double-skin façades, focusing on environmental aspects and its potential for enhancing daylighting and energy performance when equipped with reflective prints and switchable mechanisms. The switching mechanisms of adaptive, or switchable, ETFE cushions are described briefly with a focus on the controls, air supply and switching process.

ETFE cushions function as a pneumatic system and are structurally stabilized by air pressure which is provided by an external air blower unit. The air-pressure (in the range of 300-600 Pa) keeps the foil tensioned and allows to withstand external forces, like wind and snow. The ETFE cushions are connected thru a piping system to an air blower which provides a constant low-pressure airflow. True adaptability and responsiveness of building envelopes to indoor requirements and outdoor climate conditions represent a relatively new approach for ETFE cushion systems, considering the advances which have been made with other materials or building systems like, for example, retractable textile membrane structures, glass and complex fenestration systems. This could be owing to the fact that ETFE has been in use for only a relatively short period as a construction material, but it is also related to its very distinctive physical characteristics which are still in the process of being investigated. A variety of different environmental control strategies have been developed for multi-layer foil constructions as can be seen in Figure 2.5. All these strategies look at different ways on how to modify the solar and thermal transmission of the ETFE cushion in a reversibly way, using different mechanisms including injection of soap bubbles, or nitrogen gas, circulating tinted fluids, internal water spray, rotating lamellas and retractable screens. Some of these mechanisms have been described in great

detail in the literature; however, very few systems have passed beyond the experimental prototype phase, and even less have been tested so far in a commercial building application. The most relevant systems are discussed later in this section.

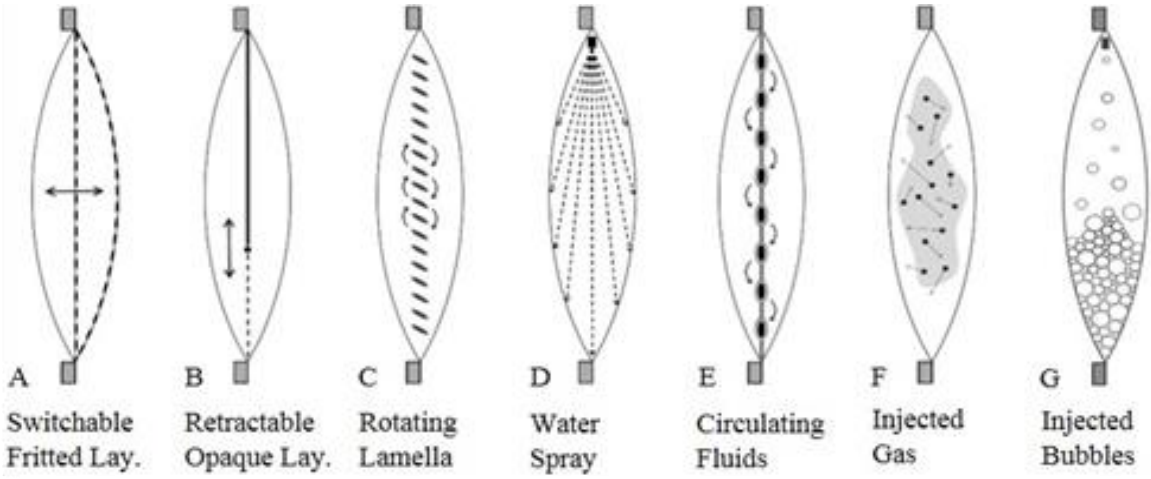


Figure 2. 5. Environmental control mechanisms for multi-layer foil construction (images by the thesis author, published in: Flor et al., 2017)

The currently most widely used active mechanism for ETFE cushions is a triple layer system which employs positive and negative, reflective printing patterns on the middle layer and the inner or outer layer. These printed patterns fit exactly when overlapped, covering 100% of the cushion surface. The middle layer position can be moved by the control of the air pressure within the cushion chambers, making it geometrically overlap, either with the inner or outer layer. This allows adjustment to achieve a partial percentage of light translucence or total coverage, depending on the layer position, as can be seen in the diagrams and schematic sections of Figure 2.6.

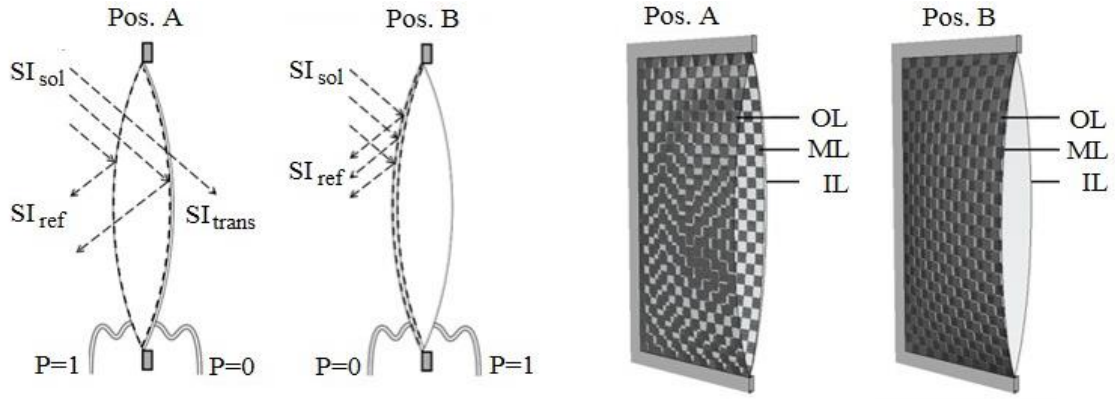


Figure 2. 6. Dynamic triple-layer shading mechanism for pneumatic foil constructions, functional diagram and rendering of a section in perspective view
(image by the thesis author, published in: Flor et al., 2017)

The ETFE cushion assembly comprises three foil layers, inner-, middle- and outer -layer (IL, ML, OL), which are welded air-tight and clamped to a structural frame on the perimeter edge, forming the shape of a rectangular cushion, when fully inflated with air. The cushion becomes a pre-tensioned structural system through the air pressure inside the cushion, able to carry external loads. The middle layer divides the cushion into two air chambers, C1 (between the ML and OL) and C2 (between the ML and IL), with individual air-valves. All three layers have the same but symmetrically mirrored, three-dimensional synclastic geometry. The position of the middle layer within the boundaries of the cushion can be changed by inflating one chamber and deflating the other. The middle layer overlaps geometrically either on the inside of the inner or the outer layer. The middle layer and the outer layer are printed with a reflective frit ink. The pattern of the frit is a geometry which covers approximately 50% of the surface area of the middle and outer layer. The pattern is shifted in a way that when the foils overlap, the unprinted areas of the inner foil are covered with the printed areas of the outer foil and vice versa, arriving at a 100% covered or "closed" position. When chamber C1 is inflated, while C2 is deflated, the middle layer changes its position and moves from the geometric position of the outer layer to the inner layer. While it does so, the geometry of the middle layer flips over from a convex to a concave shape. When the external air chamber C1 arrives at the maximum pressure and all air is evacuated from the inner chamber C2 the middle layer is geometrically overlapping

with the inner layer and has arrived at the "open" position. A system overview with all functional components is shown in Figure 2.7.

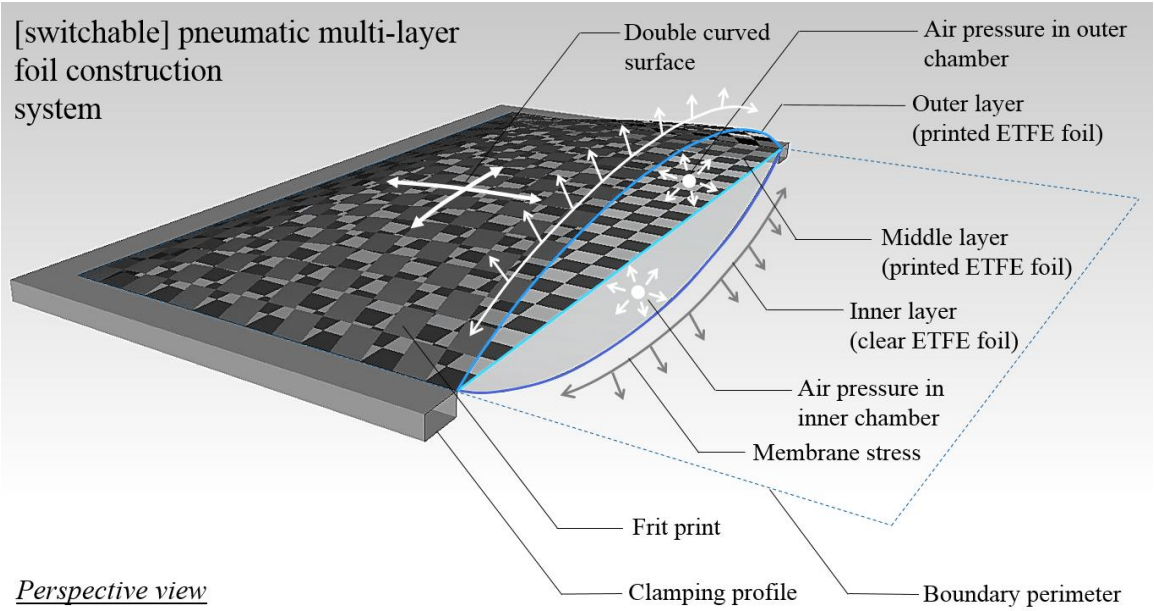


Figure 2. 7. System overview of a pneumatic multi-layer foil construction (switchable) (image by the thesis author, unpublished)

The light transmittance of the foil cushion changes when the fritted middle layer is moved from one position (open/closed) to the other. This movement is achieved by redirecting the air supply and changing the internal pressure of chamber C1 and C2. The air supply for the foil cushion is generated by an air blower which connects to valves at chamber C1 and C2 of the foil cushion. The air blower operates with a high air volume but at low pressure. Based on a case study building application, two different schemes for the airflow control of the shading mechanism of triple-layer ETFE cushions were identified and explored. The diagrams in Figure 2.8 A and B show the two alternative air supply system and the switching process as a step by step working flow scheme in Figure 2.9.

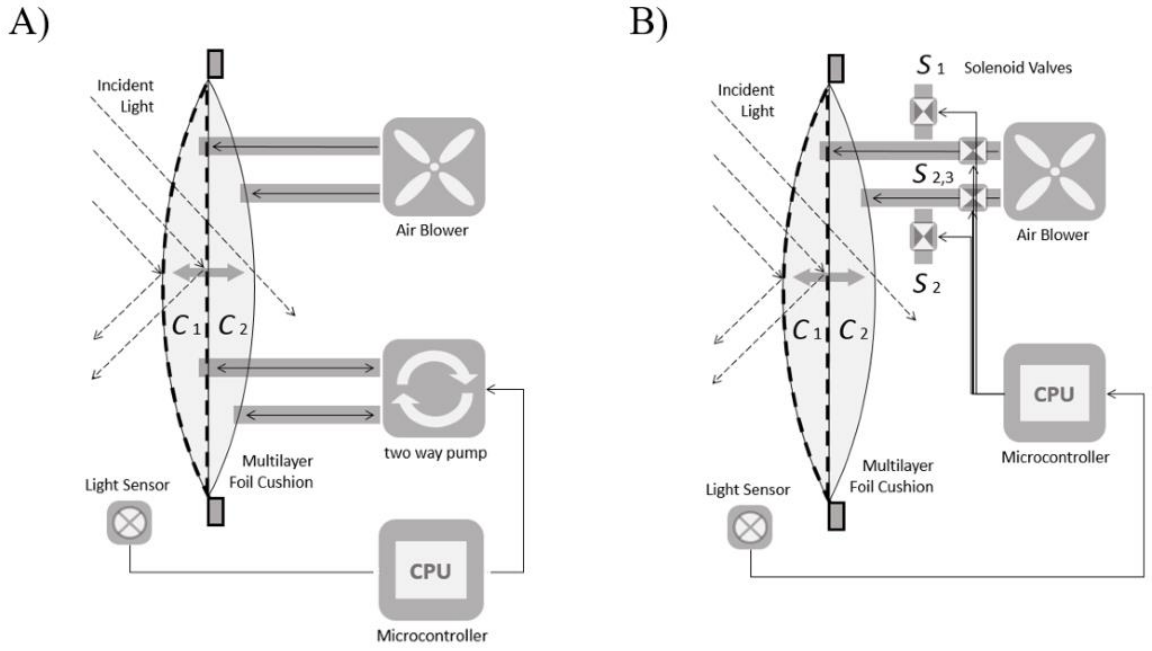


Figure 2. 8. (A, B) Diagrams showing two alternative air-supply and control schemes for the switching mechanism of the pneumatic foil cushion
(image by the thesis author, published in: Flor et al., 2019)

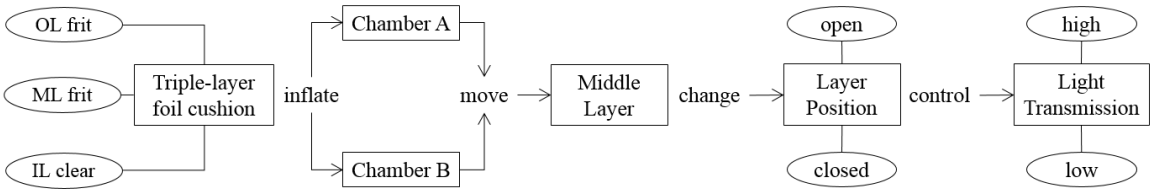


Figure 2. 9. Function flow chart of pneumatic switchable triple-layer foil cushion
(image by the thesis author, published in: Flor et al., 2019)

This mechanism has been reported in several studies [Poirazis, 2009; Gómez-González et al., 2011; Knippers et al., 2011, Xie, 2011; Chilton, 2013; Juaristi & Monge-Barrio, 2016; Shahin, 2019] and was first employed in a building for the World Exposition pavilion "Duales System Deutschland (DSD) Cycle Bowl" in Hannover, Germany in 2000 [Forster & Mollaert, 2004; LeCuyer, 2008]. The project comprised an 1800 m² active shading façade composed of a triple layer system with positive/negative frit patterns. In the same year another innovative building complex, the "Festo Technology Center", an office

building with a 2655 m² roof structure of triple-layer ETFE cushions was constructed in Germany, and later in a scaled version for a branch project in France. A similar system as in the DSD project was employed, with the same mechanism of a switchable middle layer, but with a different frit pattern. In this case, the frit pattern was laid out as a squared checkerboard pattern. This project was followed by the "Kingsdale School" project in the UK in 2004, where a courtyard was covered with a dynamic ETFE roof which employed a rectangular frit pattern, as can be seen in the images of Figure 2.10.



Figure 2. 10. Project Images: A) Duales System World Exposition Pavilion, Hannover Germany; B) Festo, Paris, France; B) Kingsdale School, London, United Kingdom, (photos © Vector Foiltec, retrieved from: http://www.vector-foiltec.com, accessed 30th April 2017, published with permission in: Flor et al., 2017)

Several other projects incorporated the same or a similar mechanism in recent years and are listed below in Table 2.1. In addition to the mechanism mentioned above, very few alternative systems have been applied in commercial buildings. Retractable opaque middle layers have been employed in a 56 m² ETFE skylight of a gas-station in Munich, Germany, in 2004 [Moritz et al., 2005]. Venetian blinds have been incorporated into membrane envelopes only in a few built projects. One case is the Association for Medical Information (GFI) in Munich-Riem, Germany, built in 2003, which incorporates solar shading lamellas inside the air chamber of a triple layer cushion covering an area of 120 m² [Köster, 2003]. The Media-Tic building in Barcelona, Spain built in 2009 is an experimental building which integrated the above discussed dynamic triple-layer shading mechanisms into the façade. In the same building, a novel shading mechanism based on gas injection was used for the first time, where the solar transmittance of the cushion was modified by pumping

nitrogen into the air chambers of the ETFE cushions [Chilton, 2013; Juaristi & Monge-Barrio, 2016].

Table 2. 1
List of projects incorporating multi-layer foil constructions with integrated dynamic environmental control mechanisms
(table by the thesis author, published in: Flor et al., 2017)

Project Name	Building	Application	Mechanism	Area m²	Year
Duales System World Exposition	Pavillion	Façade	A	1800	2000
Festo Technology Center	Office	Roof	A	2655	2000
Society for Medical Information (GFI)	Office	Roof	C	120	2003
Kingsdale School	School	Roof	A	5000	2004
Pasadena Art Center	Cultural	Skylight	A	690	2004
Allguth GmbH Service Center	Gasstation	Skylight	B	56	2004
The Mall Athens	Mall	Roof	A	-	2005
Archibald Vivian Hill Building	Research	Roof	A	547	2007
ZEP Leisure Park	Multiuse	Skylight	A	-	2009
JinSo Pavilion	Restaurant	Roof	A	600	2009
Lancaster University, ISS Building	University	Skylight	A	-	2009
Media-TIC Building	Office	Façade	A,F	2500	2010
University of Adelaide Learning Hub	University	Roof	A	9000	2011
St. Bartholomew's Hospital	Hospital	Roof	A	405	2013
RCS Pavilion EXPO2015	Pavillion	Skylight	A	72	2015
Urban Algae Folly EXPO2015	Canopy	Roof	A	-	2015
IIT Innovation Center	University	Façade	A	1280	2018
Adelaide Botanic High School	School	Skylight	A	-	2018

Mechanism Type: A - Switchable fritted Layer, B - Retractable Opaque Layer, C - Rotating Lamella, F - Injected Gas

Recently, there has been a spate of interest in the more unconventional mechanism, incorporating spray, liquids and bubbles as a strategy for dynamic environmental control mechanisms at an experimental stage. Mainini et al. [2016] investigated the influence of water spray on the thermal performance of a mechanically pre-stressed double-layer ETFE panel as a strategy for reducing solar heat gains on building façades during summer climate conditions. The effectiveness of different spray nozzles in relation to the thermal performance of the ETFE panel was tested. However, it was found that the system performance improvement was somewhat limited, as the water spray, while effectively

reducing the surface temperature of the foil, had only a small influence on the mean radiant temperature. This was mainly attributed to the fact that water is a weak absorber of solar radiation. The effectiveness of the system was therefore strongly reliant on the volume of water sprayed on to the foil. Previously a study with a similar approach had been carried out [Xie, 2011]. The evaporative cooling effect of water on the middle layer of a triple-layer foil construction was investigated. This study found great potential in improving the thermal behaviour of foil constructions with water. Numerical calculations and experiments under laboratory conditions showed a reduction of the inner layer surface temperature of up to 5°C. Other research projects have explored the possibility of achieving environmental control of multi-layer foil constructions with tinted fluids [Hanke et al., 2016]. The fluids are circulated in pre-formed channels, in-between the foil layers of the cushion. The system is made switchable from a transparent to a translucent state by changing the tint concentration of the circulating fluid. The system is able to modify the light transmission but also has the capacity to absorb and remove heat from the cushion. A general U-value of 0.64 W/(m²K) was calculated for the system. The optical performance was tested according to DIN EN 410 and showed absorption of 95.7%, a reflection of 4.3% and a solar transmission of nearly 0.0% using a 7.5% black-tinted fluid. A similar system was used for a showcase pavilion construction at the Milan EXPO 2015 [Poletto & Pasquero, 2019]. But instead of tinted fluids, an algae substrate was pumped through the ETFE panels. The algae substrate would filter the solar radiation eventually and absorb part of it and provoke photosynthesis of the algae. The growth of algae enhances a biological self-regulating effect on the shading performance of the canopy structure. Another highly experimental mechanism was tested for double layer foil constructions in greenhouses where for thermal and solar control soap bubbles where injected into the air chamber [Rayner, 2020]. This allowed the system to be switched from the initial transparent condition to a highly insulated and light scattering state. Prototypes have been built, and the thermal performance of the system was investigated. The results of CFD simulations showed that liquid bubbles could improve the performance of greenhouses. The temporary increase of the thermal insulation with liquid bubbles reduces the energy

demand for heating in winter and the risk of overheating during the summer season [Gan, 2009].

2.5. The thermal and optical behaviour of membrane and foil constructions

The complexity of the building physics of membrane and foil constructions raises questions of considerable interest for our understanding of the affecting parameters. Various investigations have mentioned that the difficulty of describing the building physics of membrane and foil constructions is mainly related to their unique optical characteristics, low mass and geometric complexity. This section reviews the most recent studies reported in the literature in an attempt to provide an overview of the state-of-the-art of the understanding of the thermo-optical properties of membrane and foil constructions.

Fabric membranes are currently widely used, but the off-trade of single-layer systems is the reduced thermal resistance and their limited visual translucency. Therefore, they are mostly employed in open or semi-open structures, like canopies and walkways, where no special measures for thermal insulation are required, and shading is more a need then natural lighting. The building physics of spaces enclosed by single layer fabric membranes have been comprehensively covered by Harvie and later by Devulder who developed a thermal model, calculated the energy performance and validated their results with monitoring data from multiple case studies [Harvie, 1996, 2015; Devulder, 2004, 2007]. Attempts have been made to improve the thermal performance of single-layer foil and membrane constructions by combining them with other functional layers. A study reported on a system where ETFE foil was combined with layers of thermal insulation, PVC/Polyester fabrics and silicon glass fabrics in order to create an energy harvesting multi-layer system for a tensile building envelope, which resulted consequently in an opaque system with little possibilities for creating working conditions with natural lighting [Karwath, 2011]. Similar studies had been previously carried out investigating multi-layer textile membrane constructions for inflated air halls where multiple layers of fabric textiles were combined with insulation materials in order to improve the thermal performance. The studies reported similarly on a significant reduction of the light transmittance up to the total

opaqueness of the envelope which resulted in higher energy demand on artificial lighting counterbalancing the savings for the better thermal performance [Lombardi & Canobbio, 2016]. Advanced Air halls with multi-layer membranes were also covered by Suo et al. [2015] and Cremers et al. [2016] who reported on the design and construction of a transparent multi-layer membrane roof with improved thermal performance.

Multi-layer constructions, especially foil cushions, have been reported to have a much better thermo-optical performance. However, a general building physics model has only partially been established what can be accounted to the multiple system configurations and the lack of material and monitoring data. Also, the integration of optical and thermal calculations has been a reported problem in literature which has been studied by many authors and is currently the concern of ongoing research projects. The following review discusses the multiple studies related to the description of the thermo-optical behaviour of transparent foil, and especially multi-layer foil constructions to outline the state-of-the-art regarding the general understanding of their building physics:

Robinson-Gayle [2003] investigated the environmental impact of transparent building envelopes and measured the solar and visual light transmittance and reflectance (Tsol 92%, Rsol 7%) of clear ETFE foils as well as the U-value according to BS 874 horizontal (2.7 W/m²K) for a triple-layer cushion construction for different radiation incidence angles and observed better thermal performance in vertical than in horizontal position. Another study by Antretter [2008] calculated the heat transfer through double-layer ETFE cushions using computational fluid dynamics (CFD) and compared the results with experimental measurements of temperature distribution and heat flux taken from a real scale mock-up under realistic condition. The experimental climate data, heat flux and internal and external air temperatures were used to set up the boundary conditions of a CFD model with similar dimensions to the mock-up. The CFD simulation was carried out using the software Ansys Fluent. The characteristic behaviour of the cushion in each scenario was outlined, and the comparison showed good consistency what allowed for an extrapolation with new boundary conditions, including different temperature scenarios and angle orientation. The CFD simulations revealed the air temperature distribution and air

velocities within the cushion chamber as well as the flow patterns in horizontal, vertical and 45-degree angle position. The study concluded that without considering solar radiation, the total heat flux is by 30% caused by convection and 70% by surface radiation. The radiative heat transfer increases with the temperature differences between the internal and external side of the cushion surfaces independent from the inclination angle, while the convective heat transfer increases with the inclination of the cushion. Parameters like direct solar radiation, thermal bridging of the clamping system and the constant airflow of the pressure system were not taken into account, which may limit the general applicability of the results [Antretter, 2008]. Poirazis [2009] discussed thermal and solar transmittance for glazing units and ETFE cushions with a general approach and presented relative U-values from a previous report [Salz & Schepers 2006] for double, triple and quadruple layer cushions, with values of 2.9, 1.9 and 1.4 W/m²K, respectively. Ward et al. [2010] measured and calculated transmittance and U-value for different frit pattern prints on ETFE finding for a clear foil, with a thickness of 200 μm and a frit coverage of approx. 65% transmittance of Tsol 47%. Printing of the foils with reflective inks is currently the most used technique in the industry to mitigate the thermal and optical downside effects of ETFE [Hu et al., 2017; Mikkonen et al., 2018; Lamnatou et al., 2018]. These so-called frit patterns are designed in a way that their geometry density per area reflects the required amount of solar irradiation and reduce the solar gains in order to keep the indoor environment at peak periods at an acceptable thermal comfort level while ensuring sufficient natural lighting [Ward et al., 2010]. Recently a novel workflow methodology for qualitative and quantitative analysis of daylight performance of pneumatic ETFE foil cushions with printed frit patterns was proposed by Roudsari and Waelkens [2015]. The complexity of mapping frit patterns onto a double-curved surface was addressed using parametric open-source software applications. The study aimed with the newly developed workflow to automate the daylighting analysed with Radiance for a range of frit print variations with different pattern sizes for a ETFE cushion project. Given the flexibility of ETFE for the application in complex building geometries, the number of individual cushion modules , with a particular shape and orientation, rises according to the division ratio of a

multifaceted building envelope and increments the number of cases to be considered for design variations and daylighting scenarios. The schematic study shown below in Figure 2.11 demonstrates the complexity of different reflection patterns of solar rays for different orientation angles of printed multi-layer cushions with a switchable middle layer. The interaction between solar angles, curved geometry, cushion orientation and the printing pattern is intricate, and it is thus of interest to learn how the different parameters are related to one another and affect the thermo-optical performance. Opportunity for future research addressing the building physics of shading mechanisms in an integrated way is evident—the proposed solution resides within parametric and automated design and analysis tools.

Knippers et al. [2011] measured and calculated transmittance and U-value for different foil thicknesses, frit coverage and cushions with different layer combinations and presented a thorough description of the building physics of multi-layer ETFE cushion constructions. Cremers [2011] discussed the energy-saving design of membrane building envelopes and reviewed several ETFE projects which employ energy-saving or producing strategies. He compared the optical behaviour of different membrane and foil materials and reviewed an energy model for multi-layer foil construction which was earlier presented by Knippers et al. [2011]. A reproduction of the energy model is shown in Figure 2.12.

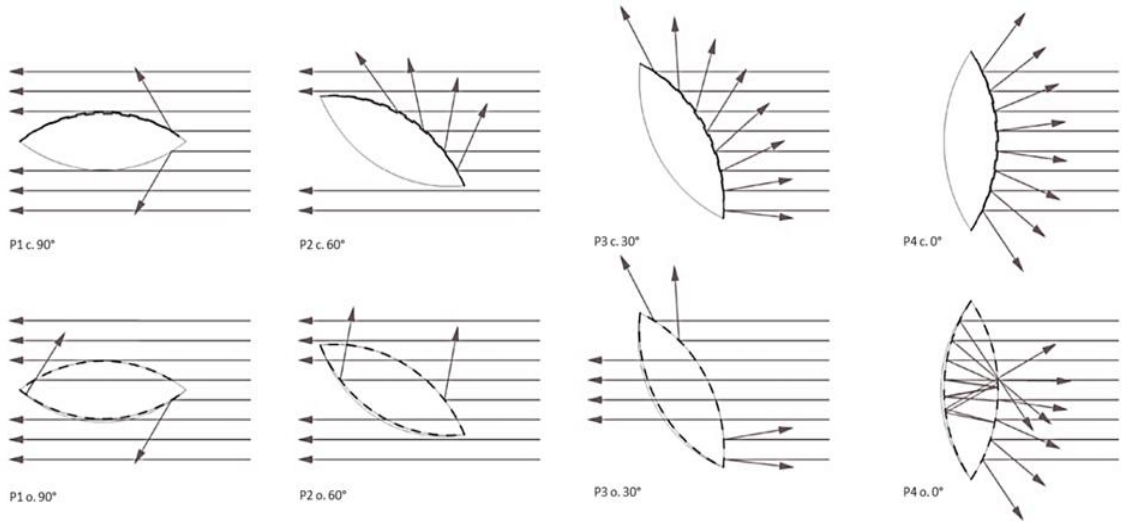


Figure 2. 11. Ray reflection for different orientation angles of switchable multi-layer ETFE cushions in the open and closed position
(image by the thesis author, unpublished)

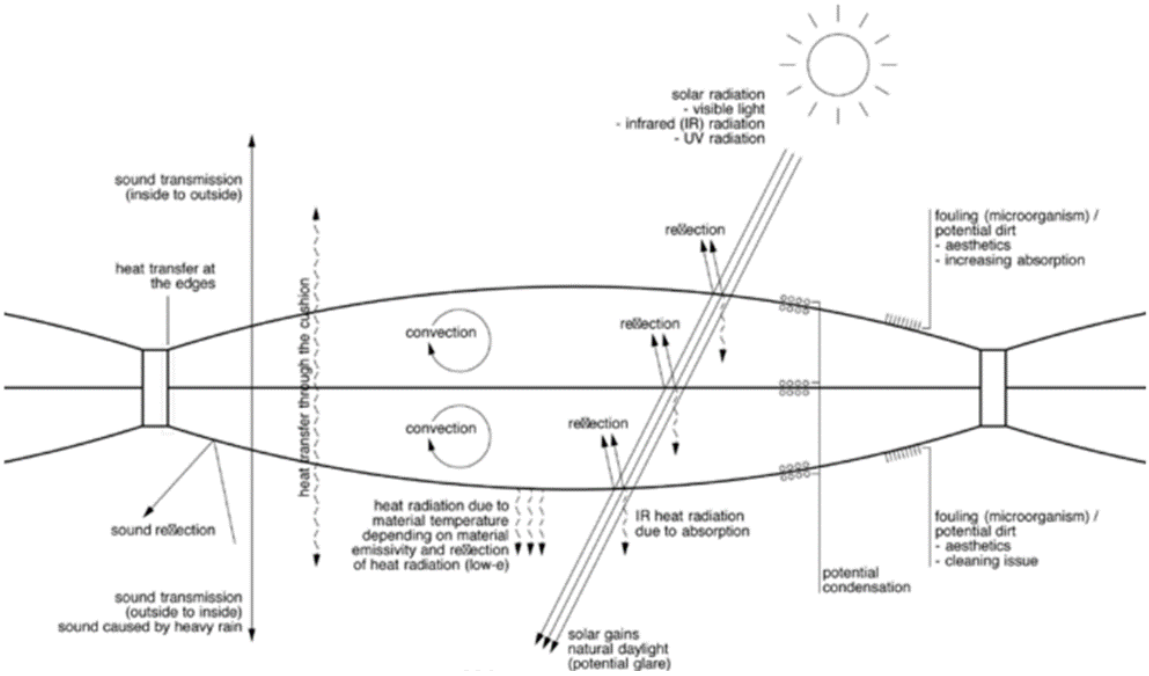


Figure 2. 12. Building physics of a pneumatic cushion structure
(image published in: Cremers, 2011)

Improvement of the energy performance of foil constructions was also investigated by Maxa et al. [2012], who presented an experimental design where ETFE foil and float-glass were combined into a novel system. The light transmittance of the multi-layer system was measured for different spectral ranges and incidence angles in a field experiment with hot boxes. Dimitriadou [2013] calculated the transmittance (Tsol 91%) and U-Value (2.9 W/m²K) for a double layer cushion of clear ETFE foil and a double layer with frit on the inner layer (Tsol 54%) making use of IES simulation software. The results were validated with an experimental test [Dimitriadou & Shea, 2015 Dimitriadou 2015]. Two experimental set-ups using hot boxes under real sky conditions evaluated the thermal and energy performance of unprinted and printed single and double layer ETFE foil panels compared to double glazing. The comparison of the measurements with the simulation results showed good consistency with a satisfactory level of correlation with a bivariate correlation coefficient of 0.98 and an error of 0.001 kWh for the energy consumption of, both, the double-glazing and ETFE sample. Based on the results of the study it was

estimated that a building with a fritted ETFE cushion roof would consume 4.9% less energy for space conditioning, compared to double glazing, and a roof with clear ETFE cushions would consume 3.5% more energy. Mainini et al. [2014] investigated the influence of soiling effects on the thermal and optical transmittance of double-layer panels of ETFE. The visual transmittance was measured for different incidence angles and the thermal heat flux measured horizontally by exposing the sample single-sided to a guarded hot box with a controlled temperature scenario. The U-value was determined with measurements obtained before and after the soiling had happened (EN673 HF horizontal, 3.0 W/m²K). Martin et al. [2015] tested thin double-skinned framed panels with different ETFE foil thickness in a climate chamber measuring the thermal flux through the panel in a vertical position and calculated the U-value (3.0 W/m²K) using results from the test. Buchner [2015] calculated the annual light transmission and U-value for a double layer ETFE cushion using newly developed software. Opposed to the steady-state approach of the DIN normative (DIN 6946, DIN 673), Buchner calculated a variable monthly U-value according to the fluctuating temperatures of the annual seasons. The values ranged from 0.04 W/m²K in July to 1.43 W/m²K in December. This seems to be a more realistic approach but lacks the back up of any normative. A similar approach had previously been presented by Kaufmann [2013] in a study where the U-value was calculated from the dynamic heat flow measured on an ETFE cushion.

Another widely adopted strategy to improve the thermal performance is to simply increase the number of cushion layers in order to increase the thermal performance of the façade module by adding with each air chamber and ETFE foil to the overall thermal resistance. U-values comparable with double pane standard glass windows can be achieved, making use of this strategy. With each additional layer of ETFE foil, which subdivides the cushion inner chamber volume, and adds two additional surface resistances (between air and membrane on both sides of the foil layer), contributing to the overall thermal resistance. While thermal conduction through the very thin ETFE foil is not significant for the overall thermal transfer, convection on foil surfaces and in the inner air chamber are of great importance for the thermal insulation properties of the cushion unit.

Thus, U-values significantly decrease with the number of layers as has been shown by Lippke [2009] and Knippers et al. [2011], calculating the U-value according to the standard DIN 673 and DIN 6946 for ETFE cushions with different layer numbers and cushion orientations. While it was found that the air chamber width had only a limited influence on the overall heat transfer, the orientation and heat transfer direction through the cushion had a more significant impact. However, radiative heat transfer caused by solar radiation is the most import aspect of the thermal performance, as mentioned in the previous section and shown in Figure 2.12. Unconsidered in this study but of the utmost importance in practice, is the avoidance of thermal bridging at the aluminium clamping profiles of the cushion, avoiding undesired heat gains and losses as well as internal condensation. Key results of the above-mentioned studies are summarized in Table 2.2 at the end of this chapter.

In building practice, a combination of passive strategies, such as previously discussed reflective frit prints and multiple foil layers, is commonly applied and has been reported for several commercial projects, for example on the roof structure of Canary Wharf Crossrail station and on an elliptical-shaped envelope for a winter garden project in Verona, Italy [Monticelli et al., 2013]. In both cases, the orientation of the cushion towards the solar angle and resultant incident solar radiation was taken into account as a criterion to design the frit patterns and decide on the layer application and percentage of coverage density. The evident downside of these passive techniques is that the design is static and is usually calculated to respond only to the requirements of peak situations or average condition scenarios. This contains the risk for overheating during summer or the lack of natural light during the winter period.

A similar approach to the printing of the foil with reflective ink is the application of Low-E coatings to the film, reducing the emission of longwave radiation. This technique is mainly used by ETFE foil manufacturers who offer Low-E coated foils as standard products of their catalogue. Cremers and Marx [2016] measured and compared the transmittance and U-value of clear ETFE foil and a new ETFE foil with infrared light-absorbing properties. The study included simulations on the effect of the building envelope on the environmental performance of buildings in different climate regions. The

performance of the foil was compared to conventional clear and printed ETFE foils by computational dynamic simulations using climate data sets. Optical measurements were conducted on the new foil, conventional clear and silver printed ETFE foil in order to derive by spectral analysis the coefficients for transmittance, reflectance and absorbance on a different wavelength. A reproduction of the results is shown in the graph of Figure 2.13. The measured data was imported into the raytracing programs Optics 6 and Window 7.4 in order to generate angle dependence data which was required for further energy and comfort calculations in the program TRNSYS. The main parameters for the performance evaluation of the foils were considered to be the operative temperature and surface temperature, which allowed the calculation of the heating and cooling demand during a period of time. The results showed generally good performance for the tested systems, but the novel low e-foil would most likely outperform conventional ETFE foils in some climatic regions [Cremers & Marx, 2016].

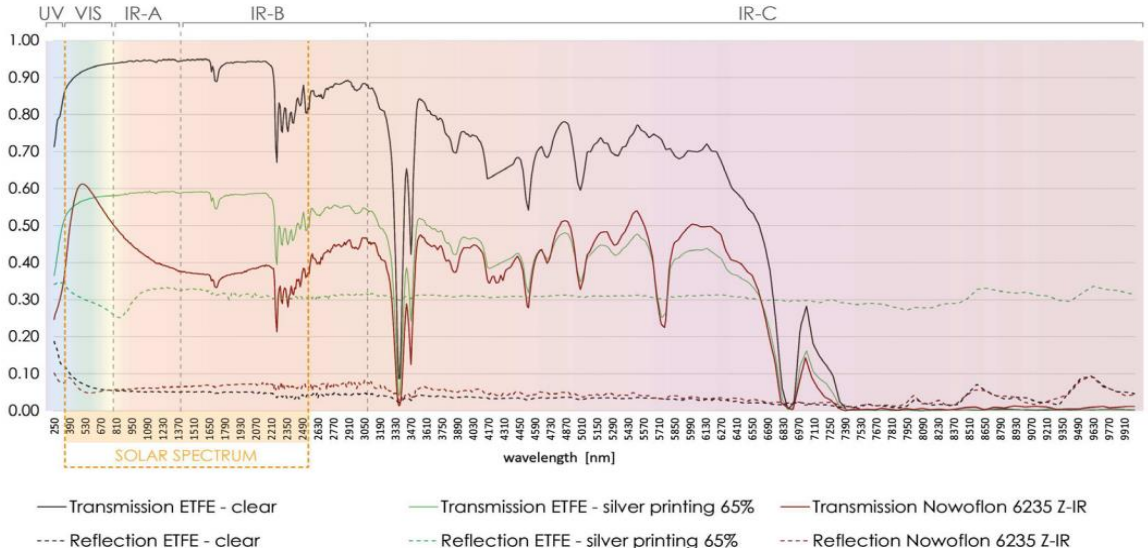


Figure 2. 13. Measured spectral data for ETFE foils
(image published in: Cremers & Marx, 2016)

A recent study [Liu et al., 2016] about the solar radiation properties of common membrane materials used in roof structures was carried out to determine the effect of the solar load/heat gain to the supporting steel structures underneath. The solar radiation

coefficients of common membrane roof materials were obtained from systematic specimen tests. One of the evaluated materials was ETFE foil with different print and ink variations. While the solar radiation coefficients of transmission and reflectance of the material samples were obtained experimentally, the solar absorbance was derived numerically using the equilibrium formula of Kirchhoff's law. Further Numerical calculation methods were applied to determine the solar radiation transmittance of ETFE foils with different printing dot ratios and different layer numbers. It was found that the printed frit patterns have a low solar transmittance and a high solar reflectance and absorbance coefficient, which consequently modifies the overall solar performance of the foil according to the ratio of the printed area.

Integration of energy-producing elements into the building envelope is a relatively new trend in the building industry and has been investigated broadly. PV cells are now being integrated into membrane and foil cushion systems. The iterative thermal exchange between the foil cushions and the PV cells is of much interest because of the thermal sensitivity of the PV cells, which influences on their efficiency. Hu et al. [2015] investigated the thermal performance of triple-layer ETFE cushions with integrated, flexible photovoltaic cells. The study focused on the temperature distribution within the cushion, the role the photovoltaic cells may play in the thermodynamic processes and the influence on the thermal performance which may affect the overall building performance . This topic is not directly related to the focus of this study but gives an outlook to the broad interest of understanding the environmental behaviour of membrane and foil constructions and the applicability for future developments.

It can be concluded that the thermal and optical performance of kinetic multi-layer ETFE systems has been described in the literature only to a limited extent making reference merely to the potential benefits, with scarce or no evidence at all on simulated or monitored data on the performance in building applications. Documentation of the few built projects, which employ this technology, is limited to photographs and schematic diagrams of the mechanism's principle but no data on energy performance has been published so far.

Table 2. 2
Thermo-optical properties of ETFE foil constructions from different literature sources
(table by the thesis author, unpublished)

Layer & Material Combinations	U-value [W/m² K]	Transmittance T_{sol} [%]	Reflectance R_{sol} [%]	Literature Reference
Single layer, ETFE Foil, 100 µm, clear	-	90	9	[6]
	-	86	-	[5]
	-	Tvis 93	-	[8]
Single layer, ETFE Foil, 150 µm, clear	-	92	7	[7]
Single layer, ETFE Foil, 150 µm, clear, 5 mm dots frit	-	60	25	[2]
Single layer, ETFE Foil, 200 µm, clear	5.8 (DIN 6946 HF hori.)	93	6	[2]
	6.8	93	6	[3]
	-	91	8	[7]
Single layer, ETFE Foil, 200 µm, clear, approx. 65 % frit	-	47	-	[1]
	-	57	30	[2]
	-	57	30	[3]
Single layer, ETFE Foil, 250 µm, clear	-	80	8	[4]
Single layer, ETFE Foil, 250 µm, clear, approx. 63 % frit	-	32	37	[4]
Single layer, ETFE Foil, 250 µm, clear, approx. 80 % frit	-	16	52	[4]
Double layer, ETFE Foil, 100 µm, clear	3.0 (EN673 hori.)	81	-	[6]
	3.1	-	-	[9]
Double layer, ETFE Foil, 200 µm, clear	3.0	84	-	[2]
	3.3 / 3.0 DIN673 DIN6946	-	-	[10]
	2.9	91	-	[5]
Double layer, ETFE Foil, 250 µm, clear	2.8 (DIN 6946 HF hori.)	-	-	[2]
	-	69	15	[4]
	3.0	-	-	[9]
Triple layer, ETFE Foil, 250 µm, clear, 63/63/0 % frit	-	10	50	[4]
Triple layer, ETFE Foil, 150/50/150 µm, clear	2.7 (BS 874 horiz.)	-	-	[7]
Triple layer, ETFE Foil, 200 µm, clear	2.0	77	-	[2]
Triple layer, ETFE Foil, 250 µm, clear	-	57	23	[4]

References: [1] Ward, 2010; [2] Knippers, 2011; [3] Cremers and Marx, 2016; [4] Liu et al., 2016; [5] Dimitriadou, 2013, 2015; [6] Mainini et al., 2014; [7] Robinson-Gayle, 2003; [8] Johannes F.J. Maxa, 2012; [9] Martin, 2015; Lippke, 2009 [10]

The direct comparability of the measured and calculated values from the reviewed studies is somewhat difficult due to the great variety of measurement methodologies and tools. Additionally, the specification details of the tested materials are not always clear. The calculation methods and software used are also varying from study to study. A lack of information regarding details on simulation parameters assumed model simplifications and geometry definitions for the simulated cushion systems could be noticed in most of the reviewed studies. A selection of the most complete and well-defined values, calculated or measured, for optical transmittance, reflectance and u-values found in the literature is summarized in a comparative Table 2.2 on the previous page.

2.6. Chapter summary

This chapter investigated the material characteristics of ETFE foils and outlined the working principles of pneumatic foil constructions. Additionally, an overview of the main applications in building envelopes was provided, including a general description of the thermal and optical behaviour. The main goals of this chapter were to provide a theoretical base for the investigations carried out in the following chapters, providing a comprehensive overview of ETFE as a building material and recording benchmark values for the comparison of its thermal and optical behaviour in alternative scenarios.

The method used for the study was based on a comprehensive literature review which collected systematically material and system performance data from different sources. Additionally, state-of-the-art projects were visited on-site in the United Kingdom, Germany and Spain were applications of static and switchable ETFE cushions in building envelopes were reviewed and documented.

The results from the literature review revealed that even though ETFE as a building material has been investigated extensively, most of the studies focus on the structural and form-finding aspects and considerably less on the thermal and optical performance. However, it was found that recently there had been a widespread interest, from both industry and science, on the environmental performance of buildings incorporating ETFE. It was found that this spate of interest was due to the fact that ETFE was being applied

more frequently in building envelopes, leading to a recent increase in research studies related to the energy and daylighting performance of ETFE. Moreover, it was found that the knowledge on the thermal and optical performance of ETFE multi-layer foil constructions was scattered and, in some cases, inconsistent among different sources, with specific information on switchable ETFE cushions completely lacking. It was therefore decided that a comprehensive approach towards evaluating ETFE as a building material was required to gain a fundamental understanding of the thermal and optical characteristics which would enable further investigations on the effects of ETFE on the building energy performance.

Corresponding to the identified knowledge gap in the literature review, the aim of this thesis, as stated in detail in section 1.3, is to obtain a better understanding of the climate adaptive behaviour of switchable ETFE façades to enable the prediction of the environmental performance in building envelopes and estimate potential energy savings and daylighting performance. Herein, the main objective is, as stated in section 1.4, to identify the multiple aspects of system design, control and material parameters that affect the climate-adaptive behaviour of switchable ETFE cushions in order to evaluate and quantify if their application could significantly improve the environmental performance of buildings in comparison to conventional building façades or other types of static ETFE double-skin façades. The research studies carried out to fill the knowledge gap on the thermal and optical characteristics of switchable ETFE cushions will be covered in the following two chapters, three and four. Further studies on investigating the effects on the daylighting and energy performance of buildings will be addressed in chapter five and six.

Chapter 3: General Methods

3.1. Introduction to chapter three

This chapter outlines the methodological approach to the proposed research project and links a review of appropriate methods to the specific methods adapted in the individual studies reported in chapter four to eight. Due to the diversity of the different methodological and technical requirements for each of the individual research studies presented in this thesis, the specific methods applied to test and analyse influencing environmental parameters, and system-specific aspects of building physics are discussed in individual project related methods sections throughout the chapters of the main body of the thesis. Here in chapter three, an overview is provided, summarizing the principal research methods and techniques used in each of the chapters of the main body of the thesis, followed by a critical review and discussion of alternatives that let to the guided selection of the chosen methods.

3.2. Methods outline

This section briefly outlines the methods used in each of the chapters as a mode of introduction for the following detailed review and discussion. With the aim to identify research gaps the method used in chapter one is based on a preliminary literature review, scanning and outlining the current state-of-the-art on research and technology regarding switchable ETFE facades and linked aspects of energy efficiency of buildings. Chapter two reports on the thermo-optical material properties and general system characteristics of switchable ETFE facades and uses a systematic literature review as well as specific case studies as the primary method of research. This chapter three critically reviews appropriate methods employed in science and industry to study and characterize the thermo-optical properties and predict the energy and daylighting performance. Chapter four employs forward ray-tracing techniques to evaluate the effects of coatings, shape, and solar angles

on the overall transmittance and reflectance on the optical performance of switchable ETFE cushions. Chapter five investigates the thermal performance of ETFE cushions using experimental methods and standard calculations to determine heat flux and thermal resistance of a real-size mock-up sample under different climate scenarios. A large climate chamber and multiple measurement devices were used as the primary research tools. Chapter six investigates the natural daylighting qualities of spaces enclosed by ETFE foil cushions, with a focus on the effects of the adaptive mechanism using 5-phase parametric simulation techniques. Radiance ray-tracing software with BSDF data, derived from spectral analysis of ETFE material samples was used. Chapter seven uses weather-data based whole-building energy simulation techniques within EnergyPlus software to investigate the energy performance of buildings incorporating switchable multilayer ETFE cushions. The eighth and last chapter of the main body of the thesis investigates the user perception of ETFE cushions in double skin building façades. The view clarity and emotional response to window views through ETFE façade systems were evaluated within immersive environments, using virtual reality equipment and a developed questionnaire applied to a sample of volunteering participants. Chapter nine summarizes the findings of the previous chapters and states the conclusions of the thesis.

3.3. Methods for the optical characterization of ETFE foil constructions

Characterising the optical properties of translucent materials and building components is well understood and based on methods developed around classical and physical optics. However, complex fenestration systems with novel materials and complex geometries, such as pneumatic multi-layer ETFE foil cushions, require a combination of specialized methods to approximate a full description of there characteristics. Research has focussed, in the past, mainly on the structural aspects of foil constructions, being the most common type a pneumatic structure in the shape of a cushion, which consists of at least two foil layers and is pressurized with air for structural stability. Only recently has the optical performance of ETFE envelopes been addressed in depth in the literature [Pohl, 2010; Knippers et al., 2011; Llorens, 2015; Liu et al. 2016]. This development, along with

the increasing number of built ETFE structures, has opened questions about the need for climate-adaptive foil systems [Lippke, 2009; Ward et al., 2010; Haase et al.; 2011; Kaufmann et al. 2013; Mainini et al., 2014; Lau et al., 2016; Hu et al., 2017; Lamnatou et al., 2018]. Although extensive research has been carried out, validation of predictive analysis results with specialist software packages and monitoring data remains a challenge for designers and researchers. The experimental determination of the optical properties of a full size inflated ETFE cushion is impractical and current instruments for physically deriving detailed information about reflection, transmission and scattering effect on both sides of the sample for multiple solar incidence angles, described by the bi-directional scattering distribution function (BSDF) could only be achieved with a large goniophotometer. While studies had shown a high degree of accordance between computed and the measured BSDF [Andersen et al., 2005; Grobe et al., 2015], common goniophotometry techniques only allow for relatively small samples, and speciality equipment is costly and rare. Classical spectral analysis provides here a generally more accessible route of optical analysis and is widely available. Outputs of spectral analysis are also commonly used as input data for simulation programs to calculate the performance of an optical system.

Ray- tracing is a computational method used to calculate the trajectory of light and the refraction, reflection, and scattering effects through optical systems by the representation of beams and is evaluated for this study as an alternative for experimental characterisation of optical properties of ETFE cushions. The theoretical base for ray-tracing was initially developed by Spencer and Murty [Spencer & Murty, 1962] and is now a widely accepted technique to aid the design of solar energy systems and solar façades [Kämpf & Scartezzini, 2011; Sun et al., 2017; Eltaweel & Su, 2017; Connelly, 2017]. The use of ray-tracing for the analysis of the optical behaviour of the multi-layer cushion system seemed, therefore, appropriate in this study. Ray-tracing has been used previously to examine the optical performance of CFS (Complex Fenestration Systems) [Andersen et al., 2005; Chan & Tzempelikos, 2012; Sun et al., 2016; Sun et al., 2016; Wu et al., 2016; Capperucci et al., 2019] and offers a practical method to virtually trace solar beams through

geometrically complex components such as pneumatic foil constructions. The results of the reviewed optical simulations showed a distinctive optical profile for the switching modes of the cushion and provided insights into the angle-dependent behaviour of the different designs. Since the study proposed in this thesis aims to investigate the optical performance of switchable ETFE cushions in the open and closed mode under different solar angles and carry out a 360-degree analysis, this was another in favour of the evaluated method. Software packages such as SolTrace and TracePro, able to handle radiometric and photometric physical light models, were considered during the evaluation process as suitable tools for the intended task [Cruz et al., 2017]. Details on the software and specific details on the simulation set-up will be provided in the relevant chapters four and six.

3.4. Methods for the thermal characterization of ETFE foil constructions

Characterising the thermal properties of translucent materials and components used in building envelopes is an essential step on the path towards the energy efficiency and sustainability of buildings and the built environment. Therefore, this section provides an overview of the multiple methods and techniques which have been reported in the literature to investigate the thermal performance of transparent ETFE foil constructions.

Studies from the literature frequently report on the potential of adaptive building envelopes to substantially improve the energy performance of buildings. However, due to the geometrical complexity of pneumatic structures and the specific material characteristics of ETFE, switchable foil constructions are hard to characterize with standard calculations and state of the art simulation software. Multiple evaluation criteria for solar control systems in building envelopes, such as switchable ETFE cushions, have been elaborated [Kuhn, 2017]. For the evaluation of the thermal performance with simulation software, the R-value is commonly required as an input to specify the thermal resistance of a building component. International building codes and standards have adopted the U-value, as a coefficient, which allows the building industry to quantify and compare the thermal transmittance of building components in order to evaluate the overall heat transfer of the building envelope. The U-value for different ETFE foil structures is frequently cited in the

literature and compared to the common clear double-pane or reflective glazing [Chilton, 2013]. Numerical calculations based on available standards suggest ETFE cushions appear to have a comparative or even better thermal performance than common glazing [Lippke, 2009]. However, questions about the accuracy of the calculated values arise due to difficulties resulting from the three-dimensional geometry and sensitivity to solar radiation of the ETFE cushions. The complexity of the heat exchange mechanisms in ETFE cushions may be represented only to a limited extent by standard calculation methods [Afrin, 2016]. A more realistic approach for investigating the thermal performance of the ETFE cushions, deriving U- and R-value and validating numerical models, might be through experimental testing, as the literature suggests:

For the Eden Project (2000, St. Austell, UK), a large biome greenhouse assembly of geodesic domes, thermal performance tests of a triple layer cushion with 200 µm thick foil ETFE, were conducted using a combined method of theoretical analysis with computational fluid dynamics and finite element analysis, and experimental testing using the hot-box method. The tests were done during the planning phase to ensure that the thermal performance of the building envelope would create and maintain the required climate for the tropical biomes to grow inside. A U-value of 2.7 W/m^2K was reported [Whalley, 2000].

Robinson-Gayle investigated the environmental performance of transparent building envelopes and carried out a number of thermal performance tests following the British Standard BS874 using a guarded hot-box. A small triple-layer ETFE cushion (150 µm - 50 µm - 100 µm) with a surface area of 1964 mm2 was tested in a vertical, inclined and horizontal position. The U-value calculated from the experimental measurements found to range from 2.59 to 2.73 W/m^2K, for the different positions, respectively [Robinson-Gayle, 2003].

In an investigation on the soiling effects on ETFE transmittance, Mainini et al. [Mainini et al., 2014] also used the hotbox method following, but following ISO 9869, to determine the thermal performance of a clear ETFE double-layer cushion experimentally, measuring 1050 x 1140 mm, with a foil thickness of 100 µm. An approximate thermal

transmittance value of 2.75 W/m^{2}K in a vertical sample position was derived from the experimental measurements which agreed well with the simulation results. In another thermal transmittance assessment, a climatic chamber was used to test a double layer flat ETFE panel, measuring 1200 x 1200 mm, with clear parallel foils of different thickness (100 μm, and 250 μm) and an air gap of 30 mm [Martin et al. 2015]. The reported U-values ranged from 3.00 to 3.06W/m2K.

In a more recent study, which aimed for the thermal characterisation of a double layer ETFE foil cushions, in-situ long term measurements using a set of insulated boxes was used [Dimitriadou, 2015]. The cushion measured 900 x 900 mm, with a foil thickness of 200 μm, of clear ETFE with silver reflective dotted frit applied to the inner layer. Following numerical calculations of BS EN 6946 the derived U-value, using mean values from the experimental measurements was reported as 3.2 W/m2K for a horizontal position. Variations in the U-value of ETFE cushions not only depend on the number of layers, foil thickness, air chamber volume and frit prints, but also on the spatial orientation and direction of heat flux. The U-value of an ETFE cushion in a horizontal installation situation, as for example in a canopy of a roof structure, has an approximately 30 to 50% higher U-value, depending on the number of layers, for an up-wards orientated heat flow, in wintertime, opposed to a down-ward heat flow during summertime. The U-value variations using different calculation methods (DIN EN ISO 6946 and DIN EN 673) are only minor in comparison to the differences caused by the cushion orientation and heat flow direction [Knippers et al., 2011]. The difference of thermal transmittance between an ETFE cushion in horizontal or vertical orientation is largely affected by the convective cells that form inside the air chambers of the cushion [Antretter et al., 2008; Lippke, 2009; Knippers et al., 2011]. Experimental measurements conducted using a hot-box had shown for a triple-layer ETFE cushion a lower U-value in vertical position of 2.59 W/m2K in comparison to 2.73 W/m2K in horizontal orientation [Robinson-Gayle, 2003]. These observations are of importance for this study when considering the thermal characterisation for switchable ETFE cushions applied to building facades where the main geometric orientation of the cushion unit would be vertical. Overall, these studies provide evidence

that the hot-box method is the most commonly used method for testing the thermal performance of large-scale samples with complex geometries, as ETFE cushions. However, up to date, this method has not been used to investigate the thermal performance of ETFE cushions with switchable shading mechanisms. For the studies carried out in this thesis project, an adapted, simplified version of the hot box method has been used. The detailed description of the applied methods is provided in the methods section of chapter five.

3.5. Methods for the daylighting performance prediction of ETFE foil constructions

Simulating the daylighting performance of adaptive building components in glazing and façade systems is a complex matter. Various modelling and simulation methods have been proposed in the literature and are currently still under evaluation [Wienold, 2007; Do & Chan, 2018; Giovannini et al., 2018]. The methods evaluated to be used in this study to investigate the natural lighting qualities of semitransparent ETFE double-skin façades (DSF) are centred around climate data based daylighting simulations with radiosity-based tools and matrix-based methods that rely on raytracing. The validated programme package Radiance (by Greg Ward at Lawrence Berkeley National Laboratory (LBNL) a part of the U.S. Department of Energy (DOE)) had been used in earlier studies to calculate the annual daylighting performance of office spaces with south-oriented DSF with different material combinations, an approach previously reported [Bueno et al., 2015]. Dynamic metrics, such as useful daylight illuminance (UDI), daylight glare probability (DGPs) and daylight illuminance uniformity ratio (UR) developed to describe the daylight performance comprehensively, with the illuminance-based results that Radiance can generate, were evaluated for this study. Those metrics had been used in previous simulation studies as an alternative to the traditionally used, but insufficient, dayligfht factor to evaluate other transparent building materials [Nabil et al., 2006; Santos et al., Fang et al., 2019; Sun et al., 2020]

The current state of the art method for the daylighting simulations is considered to be the validated five-phase method [Geisler-Moroder et al., 2018], based on the previously

developed and validated three-phase method [McNeil & Lee, 2013] which has been extensively discussed in the literature [Santos et al., 2018]. Within the three-phase method, the process of light transmission and reflection between the external environment and internal space is subdivided into three phases. In the first phase, the flux between the sky, dominated sky matrix, and the external surface of the window, named daylight matrix, is calculated. The second phase consists of the flux passing through the window, from there external surface or daylight matrix to the internal surface, referred to as the transmission matrix. The third phase accounts for the flux from the inner side of the window, i.e. transmission matrix to the interior analysis space, referred to as view matrix. The five-phase method can be understood as a more sophisticated, advanced version of the three-phase method, where the weather-data based sky matrix is subdivided into the direct solar and diffuse sky component. The solar component is replaced with a more precise solar model making the overall daylighting simulation results more accurate and realistic in appearance [McNeil, 2013]. Both methods make it computationally feasible to simulate the daylight performance of complex fenestration systems using bidirectional scattering distribution functions [Ward et al., 2011; Ward, 2011]. BSDF data is used within the calculation process of the five-phase method as the proxy representation of a complex fenestration system (CFS) such as a DSF with ETFE cushions. The specular and diffuse transmission and reflection of a CFS must be precalculated for 145 patches of light ray incident angles on a Klems hemisphere on both sides of the CFS using the genBSDF program, part of Radiance software [Molina et al., 2015]. A simplified proxy geometry with the assigned BSDF material matrix of the CFS can then be used within the simulation process thus reducing the time and computational power required to calculate the annual daylight performance based on hourly weather data [Brembilla et al., 2019]. The light transmittance and reflectance of the ETFE material needed for generating the BSDF data can be determined experimentally using common spectral analysis and calculation methods following international standards ASTM D1003 and BS EN 410 [ASTM 2013; BS/EN, 2011]. In the industry, the leading ETFE foil manufacturers (ASAHI GLASS Co., LTD., NOWOFOL ® Kunststoffprodukte GmbH & Co. KG,) currently use these methods to

specify their products. The virtual generation of BSDF data with ray-tracing methods had been validated previously with a study on complex solar screens [Andersen et al., 2005].

The combination of different BSDF material matrixes allows to test hypothetical complex fenestration systems (CFS) and compare them to standard double-glazing solutions under different climate conditions. In order to obtain a comprehensive overview of the daylighting performance with sufficient data resolution, the use of annual weather data with hourly values was considered for the research of this study. Opposed to point-in-time analysis, used previously to look at the performance at specific days and hours of the day, novel analysis approaches consider simulating every hour of the year, resulting in 8760 sub-set for each simulation scenario [Brembilla et al., 2019]. This approach is made possible with more efficient simulation methods, using automation routines and BSDF data, and the availability of hourly weather data in online databases [EnergyPlus, 2018]. Comprehensive meteorological data compiled into ready to use weather files is available at effectively no cost for a wide range of places and cities around the globe [Deng et al., 2016; Fela et al. 2019]. The great advantage of this method is the comprehensive analysis of daylighting conditions for virtually any place on earth, which makes it feasible to evaluate the suitability of different glazing systems in different environments and climates.

For the simulation procedures in this study, a new integrated parametric control approach was adapted [Do et al., 2018], coupling several of the above-described methods and software, enabling efficient control of the simulation parameters and processes [Qingsong et al., 2015; Ghobad, 2018; Toutou, 2018]. The advantage of this approach is the ease of control and visualization of dataflows and the possibility for the automatization for simulation routines. A detailed description of the applied methods is provided in the methods section of chapter six.

3.6. Methods for the energy performance prediction of ETFE foil constructions

Over the last decades, ETFE has been used extensively in the building industry as an extruded thin foil in mechanically or pneumatically prestressed building envelopes, due to its lightness, transparency and resistance [Hu, 2020]. However, in the literature, only a

few studies have reported on the energy performance of buildings with ETFE enclosures [Hu et al., 2016; Harder et al., 2019] and even less have demonstrated an attempt to analyze the effect of ETFE in a double-skin façade. A possible reason for this gap in research may reside in the complexity of simulating ETFE foil construction with current energy simulation software and the unavailability of detailed data for the optical and thermal material characteristics required for the simulation input. This is a challenge for whole building energy simulation to be carried out and limits the understanding of the energy performance of ETFE double-skin façades. Therefore, this section reviews some of the most recent studies reported in the literature in order to evaluate the applicability and limitations of the used methods to achieve the goals of this thesis, which aims to assess the energy performance of buildings with ETFE double-skin façades.

Due to double-skin façades' inherent complexity, reported examples of simulation studies are rare in the literature. One of the most recent studies which investigated the effect of ventilated DSF designs including a transparent and white single-layer ETFE foil on the lighting, heating and cooling energy consumption for a winter and summer condition in a hot Mediterranean climate (Naples, Italy) using a combination of WINDOW, Radiance and TRNSYS software for the modelling and simulation procedures [Scorpio et al., 2020]. The model for the energy simulation mirrored a single room test cell facility with a south-facing façade. The findings showed, for both the clear and white ETFE DSF, an improved energy performance with a reduction of 9.4% for the heating demand during winter and 34.9% for cooling demand during the summer scenario. However, the assumptions made for the material modelling of the ETFE revealed limitations as they were based entirely on theoretical values. The DSF geometry was modelled as a flat single-layered unit which hardly can represent a realistic application of ETFE in the building constructions, were double-curved single layer and inflated double-layer cushions usually are the norm of common building practice. Besides these limitations, a single climate study may not be sufficient for a general statement about the validity of the results as it is the only representative for the specific case of Naples and does not offer any differentiated view on the performance in other climate zones.

Significant analysis and discussion on the application of different methods for modelling the thermal behaviour of ETFE cushions was carried out by Cremers et al., [2019] investigating the influence of novel ETFE surface treatments with enhanced optical and thermal properties on the heating and cooling load of buildings in different climates. The study used different numerical models and commercial simulation software TRNSYS for a whole building energy simulation of a multi-zone atrium building. Different ETFE triple-layer ETFE cushion configurations were modelled and applied to the façade and atrium cover of the building model. The studied showed an improved energy performance for all ETFE fenestration designs; however, the most substantial energy savings for heating and cooling were achieved with an ETFE cushion design with a low emissivity coating followed conventional frit printed designs. Under the cool climate conditions of Munich, Germany, a maximum relative energy-saving potential of 29% for heating and 30% for the cooling demand was predicted. In contrast, in the hot climate of Riad, Saudia Arabia, a potential energy saving of 60% for the cooling demand was achieved with a design which employed the low-emissivity coating on the outer layer. A proposed theoretical design with electrochromic switchable shading mechanisms on PET was forecasted to deliver energy savings of up 22%. While this is an interesting result and provides theoretical ground for further discussion, the study came short of delivering more details and material characteristics of the system as well as a systematic description of the model set-up and the influencing parameters, which might have affected the results, besides the climate and the ETFE material itself.

Another relevant study investigated textile double-skin façades using a software combination of IES, Ecotect and Radiance for a whole building energy simulation and daylighting analysis [Chiu & Lin, 2015]. The study analyzed the energy performance of a multi-story atrium building under different climate conditions replacing the façade with different membrane material options, including dynamic, responsive systems. The largest annual energy savings were achieved with an operated shading screen of perforated PVC polyester reducing the energy demand by 18%, 1%, and 12%, for the climate of Los Angeles, Chicago and Abu Dhabi, respectively. Unfortunately, the study considered the

ETFE façade only for the daylighting analysis and did not deliver any detailed analysis of the parameters responsible for the improved energy performance achieved with the other textile membrane materials. This methodological inconsistency made it difficult to evaluate the performance of ETFE in comparison to other DSF designs. The lack of methodological rigour, more in-depth analysis of the results and development of a hypothesis for the improvement of the modelling of commonly used membrane façades components is a shortcoming reflected in all the reviewed studies. Therefore, it is a crucial point to be considered in the methodological approach of the present study to reflect the interplay of the façade with the internal space realistically within the energy simulation, using validated simulation tools and material data to evaluate existing construction components for novel strategies in energy retrofitting of buildings.

The literature review revealed several limitations of current software compatibilities to fully integrate thermo-optical data of ETFE with the bandwidth resolution of spectral analysis into whole building energy simulations. Up to the moment of this thesis being edited, it was not possible to incorporate BSDF data generated by Radiance into the EnergyPlus simulation due to the currently limited implementations of Honeybee to read and process BSDF files as IDF files. However, it is expected that the modelling of the DSF materials as reported in the following chapters, provide sufficient data resolution to obtain results which indicate a distinctive performance ranking of the tested materials in the given scenarios. The limitations of the façade modelling are taken into account in the results and discussion section in the relevant chapters to factor in any implicit bias due to modelling discrepancies. The study was also limited by the current capabilities of EnergyPlus to model complex fenestration systems such as switchable ETFE cushions. Simplifications and assumptions had to be made to model a climate adaptive building façade which in reality exhibits a complex geometry with unique optical characteristics. Modelling semi-transparent, multilayered double-skin façades is currently a challenge, and more flexibility would be a requirement for future building simulation program version to respond to the increasing complexity of state-of-the-art building envelopes. In addition, the control of the switching mechanism of the adaptive ETFE

cushion is currently limited to a single factor, which is the illuminance, due to software capabilities. For future studies, it would be highly recommended to incorporate multi-objective control logics which allow mediating between the requirements of energy and daylighting performance. However, up to the finalization of the current literature review, no software capable of simulating these features and meeting the compatibility criteria with validated energy simulation software was identified. The adaptations made to the simulation methods to fulfil the requirements set by the objectives of this study are outlined in detail in the methods section of chapter seven.

3.7. Methods for the evaluation of the view qualities of ETFE double-skin façades

Conducting representative view experiments in a realistic setting to determine the ideal material for a façade project with specific requirements for natural daylighting and view clarity is difficult. Changing lighting conditions in realistic settings and the cost of fitting out a mock-up with interchangeable glazing materials represents a real challenge to repeatability and predictability of performance. Conventional glazing materials such as glass are well investigated, and view perception is assumed to be a common experience of daily life. However, the same assumption cannot be made for novel building materials such as ETFE. Especially when combined in multilayered façade assemblies with other glazing materials, view and lighting performance might have unexpected effects on space illumination and emotional response of the users. Therefore, this thesis aims in addition to determining the energy and daylighting benefits to investigate the user acceptance of ETFE foil façades with the objective to deepen the understanding of view perception and the associated emotional states in relation to design parameters for enhancement of future applications in building envelopes.

In the building industry, it is customary to evaluate the visual qualities of a finished building surface comparing hand-samples from the production line to the final building application, as for example a façade or a window. It is common practice in the construction business, the sample is held against the finished surface and visually compared from a defined distance by professional representatives of the construction company, architect or

designer and the client, which agree or disagree in consensus on the quality of the finished product. For the case of transparent building components such as ETFE cushions, this method is useful to determine the quality of the product; however, it does not provide enough criteria to make a judgement on the view experience building occupants will have in the finished building. Haze is the material property describing the wide-angle range of light scattering, while clarity provides information about the narrow-angle (<2,5°) light scattering behaviour. Light scattering of transparent material can be caused by imperfections of the material, such as surface roughness, air or material enclosures in the material. The effect can be an unclear or distorted view through the material, undesired for applications in building fenestration. A method used in the material manufacturing industry as well as in the car industry to determine the see-through-qualities of transparent materials uses a hazemeter to measure the percentage of light transmission, haze and clarity. A hazemeter comprises a collimated beam light source and a reflective sphere photodetector. Light is sent through the sample reflected in the sphere, and the amount of reflected light is measured following international testing standards ASTM D1003 and BS EN ISO 13468. ETFE manufactures provide numerical data for the light transmittance level and haze in the datasheets of their foil products. Numerical data on haze and transmittance is a good indicator for the material performance, but still provides little information on the actual experience viewing a scenery through the material, or a complete fenestration system, which would be impossible to test with a small-scale hazemeter.

The development of a view clarity index (VCI), which provides a combined evaluation of objective and subjective measurements offers a more differentiated criterion on the view clarity of transparent building envelopes, such as ETFE foil cushions. A simplified model for view clarity index was developed by Konstantzos et al. [2015], looking at metrics of openness factors and normal visible transmittance of textile shading material, and validating the relation of both factors with experimental data obtained from questionnaires. This approach seemed more appropriate for the evaluation of novel complex fenestration systems and was therefore evaluated for the work presented in this

thesis, though, still challenging in terms of construction and logistics considering the experimental test of several real size samples.

Creating large mock-ups and walk-in experimenters room to test the view through novel fenestration systems is expensive. It has been speculated that the experimentation with a realistic, physics-based virtual representation of complex façade and glazing system, such as ETFE foil cushions, might lead to a reduction in costs for physical prototyping as has been suggested previously [Kim, 2019]. Facilitating pre-build testing of innovative building solutions with virtual mock-ups might also allow for more flexibility and risk-taking in the decision making of the design process, leading to higher productivity, enhanced user experience and ultimately a better building performance [Heydarian et al., 2015]. Immersive virtual reality tools have not been used previously for evaluating different ETFE foil constructions. However, VR has been used in recent studies as a novel and validated methodical approach to complement the otherwise difficult task of obtaining feedback from participants on experimental (luminous) viewing conditions of different window views [Heydarian et al., 2015; Abd-Alhamid et al., 2019; Subramaniam, S. et al., 2020].

Virtual reality equipment is a powerful tool to create an immersive environment for testing alternative designs within the same space and lighting conditions, thus bearing the potential for a better understanding of the impact of light and view on the space conditions and user experience [Heydarian et al., 2015]. Using virtual environments for visualization of products and spaces has been a reality for nearly fifty years, with well-established technologies and procedures allowing virtual scenarios in which users perceive and behave as in reality to be created [Naz et al., 2017; Gonzalez-Franco & Lanier, 2017]. In the automotive, aeronautic, medical and, recently, in the building industry as well, immersive environments are a practical tool for design reviews before prototyping and production [Dunston 2010; Leicht et al., 2015; Zaker & Coloma, 2018]. While previously this technology was very costly and the viewing experience through virtual reality googles limited by optical resolution and computing power [Heydarian et al., 2014], nowadays virtual reality equipment has become economically accessible and technically

sophisticated enough to provide realistic simulations of reality for architectural purposes [Majumdar et al., 2006; Portman et al., 2015].

The detailed methodology description and with some of the optimisations and adaptions made to fit the purpose of this study is fully covered in the methods section of chapter eight.

3.8. Chapter summary

This chapter gave an overview of the methods considered to fulfil the objectives of this thesis. A Substantial review of methods considered suitable for the experimental tasks conducted in the main body of the thesis was presented. Previous studies using some of the proposed methods were analysed and evaluated. While far from covering comprehensively all possible methods to investigate the core topics of the thesis, the chapter instead focused on tracing the trail of methodological decisions that let to the development of specific methods, adapted and optimized to achieve the research goals of the studies proposed in each of the individual chapters. In the chapters, four, five, six, seven and eight detailed descriptions of the applied methods are provided based on the review presented in this chapter.

Chapter 4: Optical Characterisation

4.1. Introduction to chapter four

This chapter reports on the attempt of an optical characterization of switchable ETFE cushion based on the findings from the previous chapter two. A parametric study was carried out with the purpose of investigating the optical performance of the switchable ETFE cushion in order to generate the base data for further studies to be carried out in this thesis focusing on adaptive building envelopes and its impact on building energy performance regarding heating, cooling and lighting. Ray-tracing techniques were used to investigate the effects of surface curvature, frit layout and frit properties, on the optical performance of the cushion in open and closed mode. A range of incidence angles for solar radiation were simulated with the purpose of deepening the understanding of the angle-dependent optical behaviour for both switching states of the cushion. As such, this study provides additional insight into the optical behaviour of multi-layer foil constructions and the factors of design and environment that potentially have a major impact on buildings energy performance.

Research reported in this chapter was published in 2018 in a paper co-authored by the applicant, supervisors and fellow PhD colleagues to contribute to the optical characterization of switchable ETFE foil cushions. Parts of the article which overlap with the content of other chapters have been omitted or modified to fit the structure of this thesis. The full reference of the article is given below, with the title page and authors declaration on individual contributions to the paper detailed in appendices O and P:

> *Flor, J.-F., Liu, D., Sun, Y., Beccarelli, P., Chilton, J., Wu, Y., Optical aspects and energy performance of switchable ethylene-tetrafluoroethylene (ETFE) foil cushions. Applied Energy, 2018. 229: p. 335-351.*

4.2. Optical aspects of switchable ETFE cushions

The optical performance of ETFE material, and ETFE foil constructions is an important aspect for predicting the daylighting and energy performance of buildings. Due to their material thinness (t = 12–300 μm), low weight (density = 1.75 g/cm^3) and high light transmittance over a wide spectrum (solar = 93%, visible = 90 - 97%), [Knippers et al., 2011; Wypych, 2016], ETFE foils present both risks and opportunities for their use in building envelopes. ETFE allows one to build lighter while offering better light transmittance than glass, but uncomfortable conditions such as glare and overheating during the summer season have been reported as potential problems of spaces enclosed by ETFE foil constructions [Ward et al., 2010; Cremers & Marx, 2017]. Added functionalities with printing techniques, inks and material additives with high reflection, absorption and low emittance properties are some of the developments of recent years that can be used to improve the optical and thermal performance of ETFE foils and mitigate overheating and glare. Actively changing the optical properties to adapt to changing solar radiation is the strategy proposed in this thesis. The pictures in Figure 4.14 show a demonstrator model of a switchable triple-layer ETFE cushion with reflective frit print in open and closed mode, which has been created at the laboratories of Nottingham University, UK.

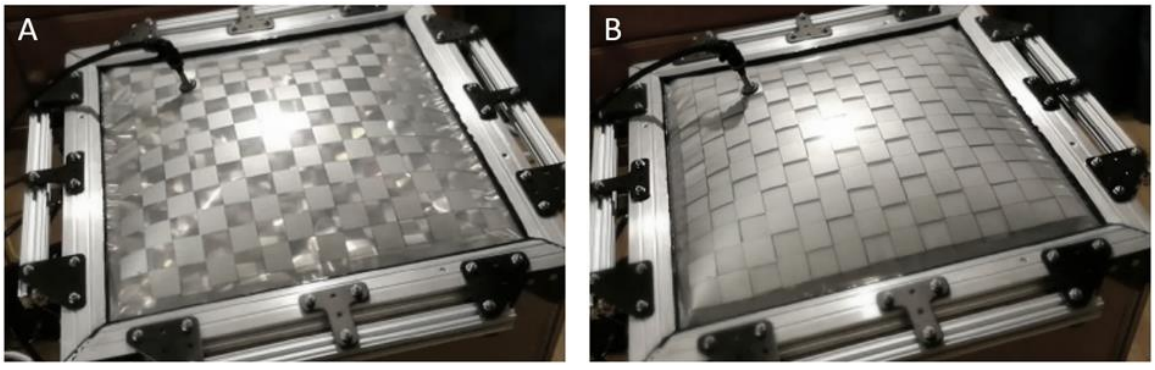


Figure 4. 14. Switchable foil cushion in the open (A) and closed mode (B)
(photos by the thesis author, published in: Flor et al., 2018)

The principle of the switchable shading mechanism is based on changing the overall solar transmittance of the cushion unit by controlling the air pressure in the two cavities between the three ETFE layers to adjust the position of the moveable middle layer, thus switching between open and closed mode as shown in Figure 4.15.

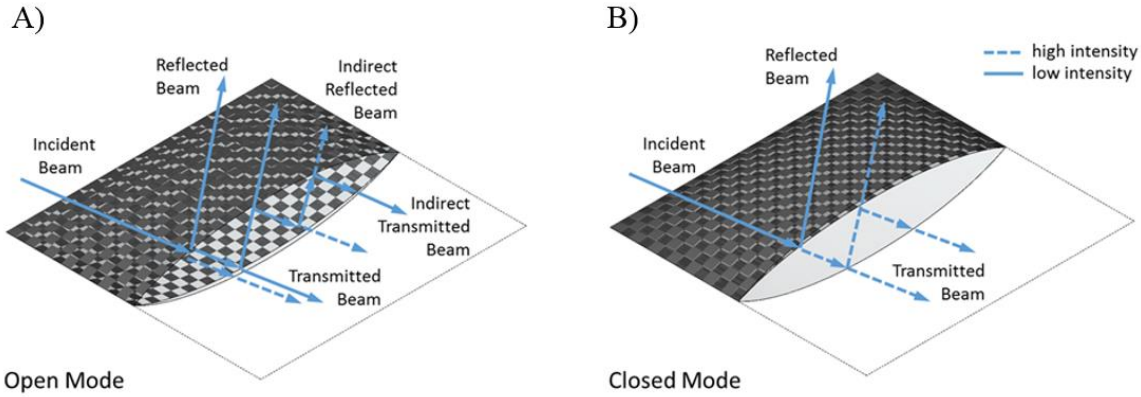


Figure 4. 15. Transmitted and reflected light beams on a switchable foil cushion in open (A) and closed mode (B)
(images by the thesis author, published in: Flor et al., 2018)

Despite having been applied and tested in several buildings ("Duales System World Exposition Pavilion" 2000 [Morris, 2000], "Festo Technology Center" 2000 [Jeska, 2008], "Kingsdale School" 2004 [LeCuyer, 2008], "Media-TIC Building" 2010 [Juaristi & Monge-Barrio, 2016]), very little information has been disclosed on the building physics of this adaptable mechanism, and it is still unclear to what degree the dynamic performance of the foil cushion is contributing to the overall performance of buildings. This gap in knowledge is related to the fact that the relevant material properties data are only partly available in the public domain, resulting in limited implementation in daylighting and energy performance simulations. The same applies to data collection of long-term performance and post-occupancy studies, which have been carried out only to a limited extent, as in the case of the "Media-Tic Building" where user acceptance and comfort was evaluated [Juaristi & Monge-Barrio, 2016] but a clear link to the envelope performance could not be established. Therefore the main purpose of this chapter is to expand the body of knowledge of the environmental behaviour of adaptive foil constructions, aiming

specifically to investigate the optical performance of switchable triple-layer ETFE cushion with a dynamic shading mechanism. A series of design parameters for ETFE cushions, including geometry curvature and frit prints, were simulated under different solar angles using ray-tracing methods with the goal to characterize the optical performance of switchable ETFE. In the following section, the employed methods and investigated parameters of the optical characterization are presented and discussed.

4.3. Methods and parameters

This section, and subsections, firstly describe the geometry generation process of the pneumatic ETFE cushion and the modelling of the ETFE material and frit patterns. The following part covers in detail the ray-tracing simulation methods and model settings, concluding with a description of the simulation scenarios for the optical model.

4.3.1. Geometry and frit pattern design

As the first step in this study of optical ray-tracing analysis, the cushion geometry of an inflated triple-layer cushion was generated. This was done using a combination of 3D modelling software (Rhinoceros - 5 SR7 64-bit 5.7.31213.18395 Educational Version Release 2013-12-13, by Robert McNeel & Associates), a series of plugins (RhinoMembrane V2.0 64 Bit - 2.05 Release 2016-05-26, by ixRay ltd) and in-house developed software components. The form-finding procedure is based on the Updated Reference Strategy (URS). This method generates the equilibrium shape and principal stresses for tensioned membrane structures [Bletzinger & Ramm, 1999]. The specific method of modelling pneumatic multi-layer cushions has been described extensively [Ströbel et al., 2013]. The synclastic form of all three layers of the cushion is identical and mirrored to form a symmetric geometry where the middle layer offsets the inner or outer layer. The generated three-dimensional cushion geometry is illustrated in Figure 4.16 A.

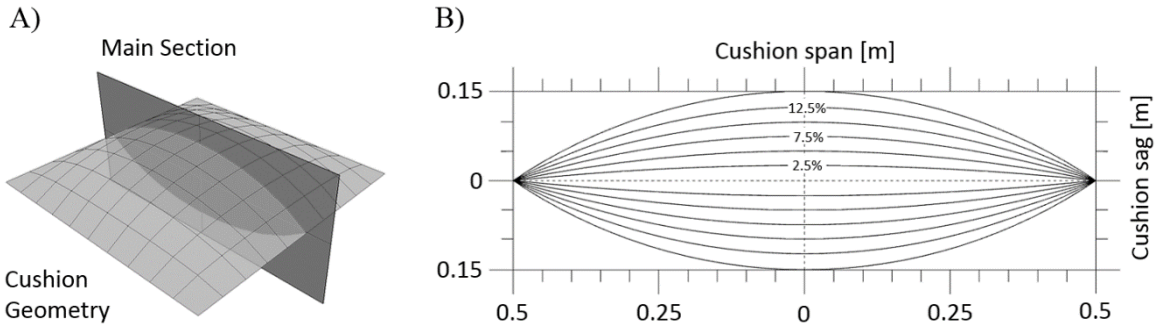


Figure 4. 16. Cushion geometry (A) and variable sag to span ratio (2.5% to 15%) of the centre section (B)
(images by the thesis author, published in: Flor et al., 2018)

For this study, the cushion geometry is limited to a 1 metre by 1 metre planar boundary frame. While these dimensions are relatively small, compared to typical ETFE cushions [Knippers et al., 2011], they provide ease for the control and analysis of the ray-tracing simulation. The shape of the cushion geometry was controlled within a range of boundary conditions, where the main parameters are the span, which is the width of the main section, and the sag, which is the maximum displacement of the layer curvature at the centre of the main section relative to the span width, given commonly in percentage. The cushion sag for the centre section was selected based on evidence from the literature [Jones, 2000; LeCuyer, 2008; Jeska, 2008; Li & Yang, 2013], ranging in 6 steps from a minimum of 2.5% to a maximum of 15% sag, symmetrically on both sides of the horizontal boundary frame. The geometry of the cushion was controlled during the form-finding process by the parameters of surface pre-stress and the inner pressure. The centre section geometry of each of the cushion samples is shown in Figure 4.16 B.

Printed frit patterns on the clear ETFE foil are an essential design aspect for controlling the optical performance of multi-layer foil constructions. The silver ink, which is used normally for the frit, is highly reflective and printed onto the foil surface in patterns which are designed to cover a specific area ratio in order to reflect a defined percentage of incident light and energy. A variety of transmittance gradients can be achieved when the frit ink is printed in different densities on the ETFE foil. The total transmittance of the foil and cushion is also dependent on the frit print coverage per area [Ward et al., 2010].

Normally, common dot or hexagon frit pattern cover 20% to 75% of the foil surface area and thus result in an overall transmittance ranging between 39% and 74%, however, in this study, for the kinetic system a pattern is required that covers nearly 100% of the surface area when the positive and negative print, of both, the outer and middle layer, are overlapped (Figure 4.17 A). The inner layer is of clear material without any frit. Design variations of this layout, including different geometries and grades of print densities, are available in the building industry. However, the most commonly used design for this shading system is a chequerboard pattern covering 50% of each layer. This layout, based on a commercial ETFE frit print design developed by the industry , was adopted for this study and applied onto the generated meshes with three different grid sizes (100mm, 50mm, 33mm), which correspond to a variation of common commercial frit design developed by the industry partner of the thesis author. The projection of the frit pattern to the cushion geometry was inspired by the method proposed by Roudsari and Waelkens [2015]. However, the method was modified according to the model requirements of the ray-tracing simulation. Therefore, the geometric deformation of the frit pattern layout caused by the double-curved surface had to be neglected for this study, since the software allowed only for planar mesh faces. The full array of design samples selected for the ray-tracing simulation can be seen in Figure 4.17 B.

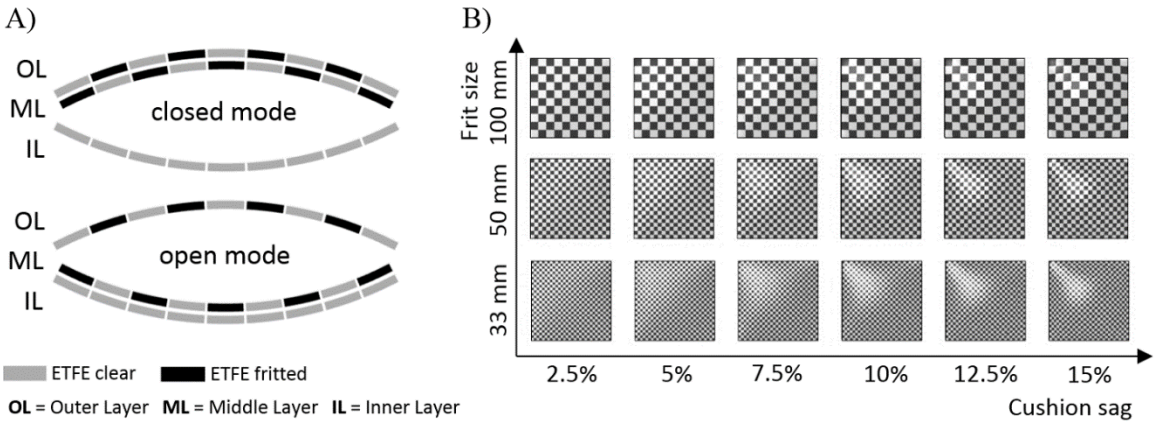


Figure 4. 17. Material application on cushion model (A) and generated cushion samples (B)
(images by the thesis author, published in: Flor et al., 2018)

4.3.2. Optical model for ETFE

The optical model created for this study considered design variations, like the sag and frit pattern, of the ETFE cushion. The effect of the optical properties of printed frit ink on the optical performance of the cushion was investigated in depth. Based on a comprehensive literature review in chapter two, the absorptance and reflectance for ETFE and frit print were assigned to the cushion geometries [Robinson Gayle, 2003; Ward et al., 2010; Knippers et al., 2011; Dimitriadou, 2013; Liu et al., 2016; Connelly et al., 2016, Maywald, 2019]. While precise optical data for clear ETFE is widely available, information on the properties of printed ETFE is somewhat limited. In order to further deepen the understanding about the impact of frit ink on the overall optical performance of the ETFE cushion, theoretical variations of frit transmittance and reflectance were added as a parameter to the study. Additionally, to the collected data from the literature for printed [Goia et al., 2010] and clear [Davey et al., 2010] ETFE foil, the transmittance of a notional frit ink was modified gradually from 5% to 95% with an interval of 15%, while the reflectance was correspondingly reduced from 95% to 5%. The selected optical property variations for the clear and printed ETFE foil are shown in Table 4.3. For the ray-tracing simulation TracePro software (7.7 Release 2016-01-25, by Lambda Research Corporation) was use. A homogeneous radiation source with a known intensity was assumed, incident to the surface of the ETFE system, with each ray carrying the same amount of energy. After the initial process of ray independence testing, 1,000,000 rays were applied on the square frame aperture containing the ETFE cushion. The beams were emitted from a one metre square grid with one metre distance to the horizontal centre section of the cushion. The dimensions of the radiation source were corrected to adjust for the changing incidence angle, thus projecting beams only onto the surface, while maintaining the same flux ratio. Figure 4.18 A, B illustrates the ray-tracing simulation set-up for the proposed ETFE cushion at a solar incidence angle of 90°. The beams were traced, allowing up to 10 multiple reflections. The flux of the transmitted and reflected light-beams was collected with virtual absorber surfaces and quantified while calculating the total absorbed energy

according to the law of conservation of energy. An overview of the starting conditions for the ray-tracing simulation is shown in Table 4.4.

Table 4. 3
Optical properties of frit prints and material for ray-tracing simulation input (table by the thesis author, published in: Flor et al., 2018)

Data Source	Material Code	Transmittance [%]	Reflectance [%]	Absorptance [%]
Theoretical Variations	Frit Print 1	5	95	0
	Frit Print 2	20	80	0
	Frit Print 3	35	65	0
	Frit Print 4	50	50	0
	Frit Print 5	65	35	0
	Frit Print 6	80	20	0
	Frit Print 7	95	5	0
Literature	Frit Print 8*	5	61	34
	ETFE clear**	93	6	1

*[Liu et al., 2016], **[Knippers et al., 2011]

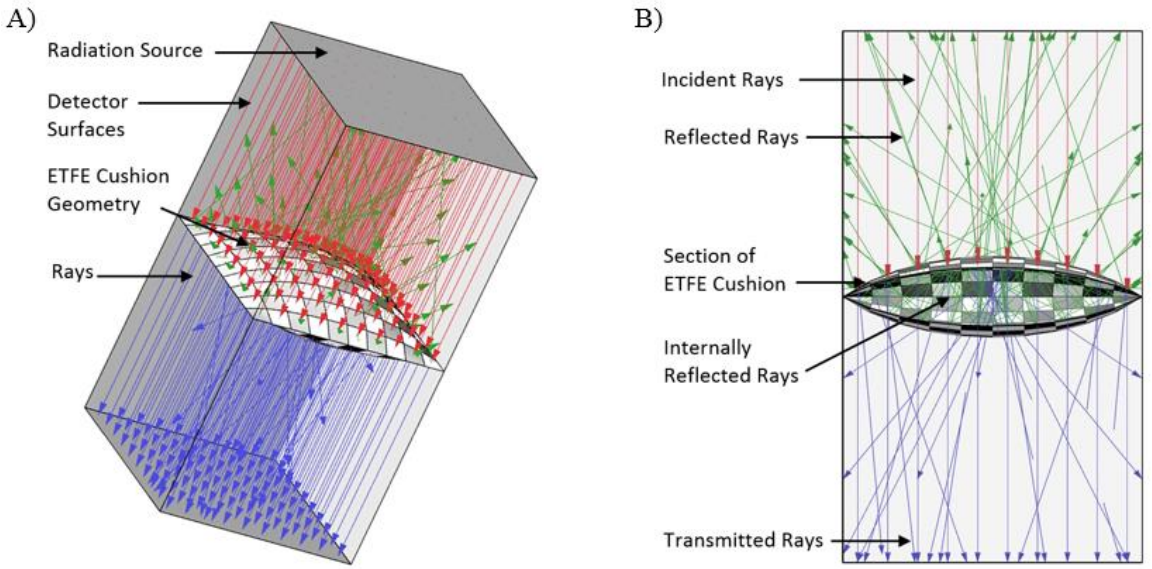


Figure 4. 18. Ray-tracing 3D model (A) and ETFE cushion section with traced rays (B) (images by the thesis author, published in: Flor et al., 2018)

Table 4. 4
Starting conditions for the ray-tracing simulations
(table by the thesis author, unpublished)

Polarization Max. *[n]*	Ray Splitting Max. *[n]*	Reflections Max. *[n]*	Emitted Irradiance *[W/m²]*	Emitter Surface *[mm²]*	Absorber Surface *[mm²]*	Number of Rays *[n]*	Grid Source (Emitter) *[type]*
1	1	10	1000	1000	1000	1000000	rectangular

The initial sample group consisted of 36 different cushion models in open and in closed mode, corresponding to the three different frit grid sizes and six sag variations. The performance of all cushion samples was compared for the open and closed position while only three sag ratios (5%, 10%, 15%) were selected for further scenario simulations. During the following simulation round, the optical properties and the grid geometry of the frit print was kept constant, simulating the transmittance of the cushion at different incident angles. The rays were traced at incident angles ranging from 10° to 90°, in steps of 20°, on a vertical plane, parallel to the rectangular boundary frame of the cushion. In a further step the effect of the frit print grid size variation in combination with different sag ratios was evaluated under a single incident angle. A grid size of 33 mm, 50 mm and 100 mm was tested on six different cushion geometries with a sag of 2.5%, 5.0%, 7.5%, 10.0%, 12.5% and 15.0% under a 90° incidence angle, perpendicular to the horizontal plane of the cushions. For both scenarios only the optical properties gathered from the literature were considered in the simulation. In order to evaluate, as well, the three-dimensional performance, multi-angle scenarios including polar ranges, were set up. For all further simulations within these 3D scenarios, a single model with a sag of 10% and a frit grid size of 50 mm was selected. This selection was considered appropriate to limit the influence of other parameters such as the mesh smoothness and overall accuracy of the model while reducing the sample size and simulation time. The previously performed mesh independence test had shown that the accuracy of the model would not further improve beyond 1 million rays, however, the calculation time for each individual model was increasing heavily with higher mesh grid densities. Convergence for both factors was

achieved with a 50mm grid density, as a reasonable compromise between model accuracy and computation time.

On continuation, the optical properties of the theoretical frit print variations were assigned to the cushion and the optical performance compared with the material data selection from the literature. The incidence angle scenarios ranged in steps of 15° from an azimuth angle of 0° to 45° and a solar altitude of 15° to 90°, perpendicular to the horizontal plane of the cushion. The symmetry of the model geometry allowed extrapolation all other hemispheric angles as can be observed in Figure 4.19 A and B.

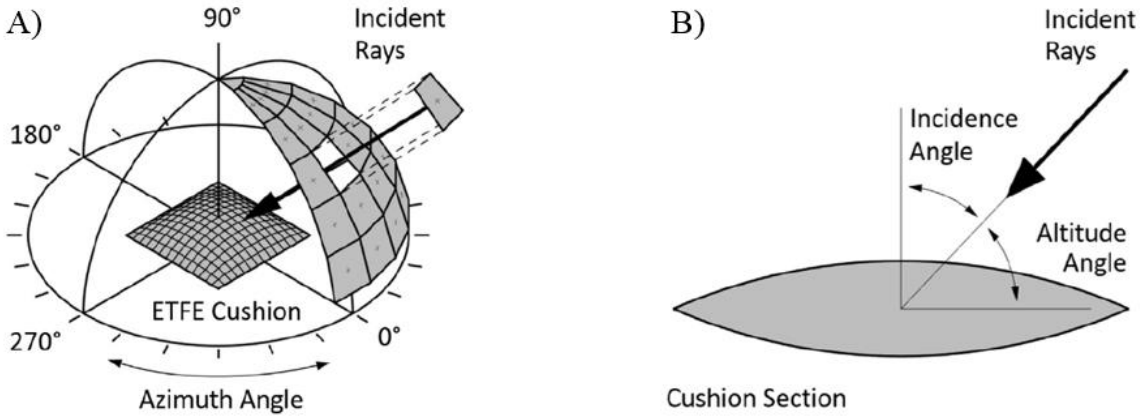


Figure 4. 19. Incidence angles of rays on cushion geometry, hemispheric (A), section (B) (images by the thesis author, published in: Flor et al., 2018)

The analysis of the optical performance of different cushion designs over a wide range of solar angles provided the basis to conduct a comprehensive energy simulation of a whole building incorporating switchable ETFE glazing systems. This predictive performance simulation with selected material scenarios is described in the following section.

4.4. Results and discussion

The following section covers in detail the ray-tracing simulation methods and model settings, concluding with a description of the simulation scenarios for the optical

model. The present study was designed to determine the effect of design parameters, like geometry and frit print, on the optical performance of a multi-layer ETFE cushion with a kinetic shading mechanism. It was further hypothesized that such switchable glazing system may improve the overall energy performance of buildings and enhance comfortable lighting conditions. In the following sections, the results of the ray-tracing and energy simulations relating to these questions are presented, and the performance of the ETFE cushion under different environmental scenarios is discussed.

4.4.1. The effects of sag and frit pattern on the optical performance

The effects of sag and frit pattern on the optical performance of an ETFE foil cushion with switchable mechanism are discussed in the following section. At first, three different cushion geometries with a sag ratio of 5%, 10% and 15% were simulated in open and closed mode with material and frit print properties collected from the literature [Liu et al., 2016; Knippers et al., 2011], (scenario of frit print 8). Solar incidence angles ranging in steps of 20° from a nearly horizontal angle of 10° to 90°, perpendicular to the horizontal cushion plane, were simulated using ray-tracing. Figure 4.19 (A and B) shows the total transmittance of the ETFE cushions in the open and closed mode. As can be seen, the optical performance of the cushion in open and closed mode showed a clearly distinctive behaviour with a characteristic higher transmittance in open mode. In the open mode transmittance values from a minimum of 2.8% to a maximum of 24.0% were obtained, while in the closed mode the transmittance ranged between a minimum of 0.1% to a maximum of 7.0%. While the sag proportions have only minor effects on the optical performance of the cushion it can be seen from the results that the optical behaviour is strongly dependent on the incident angle, an observation which had also been noted for single-layer structures in previous studies [Kaufmann et al., 2013; Robinson-Gayle, 2003; Good et al., 2016]. The results in Figure 4.20 A and B show a general trend of decreasing transmittance and increasing reflectance for an ascending incidence angle. A higher number of Internal reflections due to overlaps between the two fritted layers caused by the surface curvature of the cushion are the factors which generate the above-described optical

effect for the ascending incidence angles. Higher transmittance values at lower incident angles can be explained by higher optical permeability of the cushion, allowing for unobstructed, direct solar ray paths through the reflective frit patterns of the printed layers.

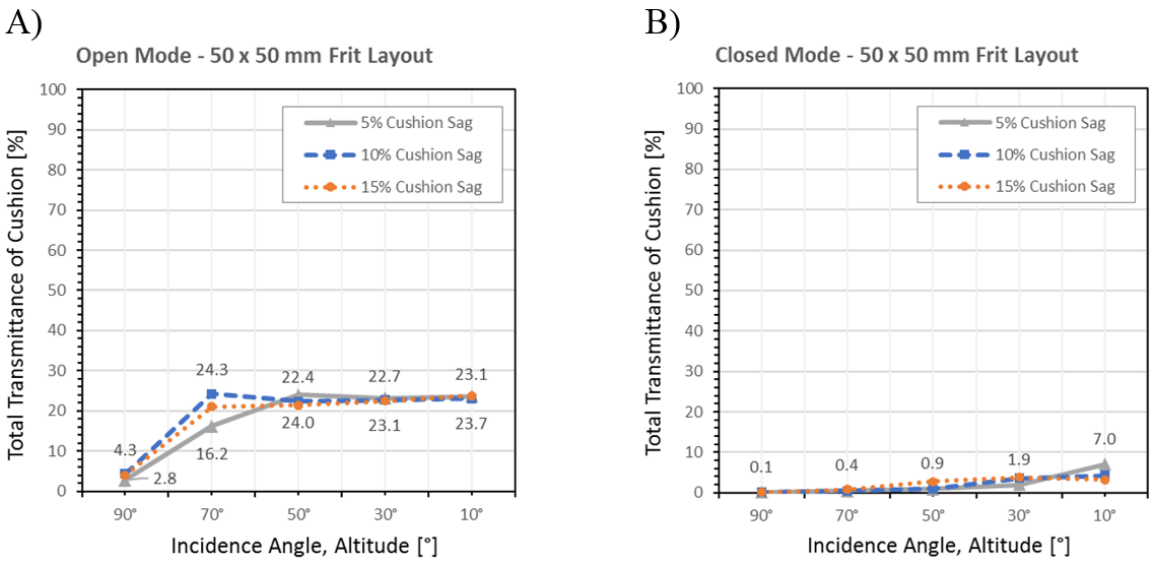


Figure 4. 20. Optical performance of switchable triple-layer cushion (50 x 50 mm frit layout) with varying sag geometry – angle dependent transmittance in open (A) and closed mode (B)
(graphs by the thesis author, published in: Flor et al., 2018)

In the next step, the combined effect of the frit print grid size with variations of the cushion geometry was evaluated at a perpendicular 90° incidence angle. From the graphs in Figure 4.21, it can be seen that the general tendency in open mode is of lower transmittance for smaller sag ratios (0.6%) and higher transmittance for larger sag ratios (4.3%). The effect of the grid size was minimal, showing only a small increase of transmittance for bigger frit grid-sizes (0.8%). For the closed mode under the same 90° incidence angle, a constant transmittance close to zero and a reflectance of 60% was found with little variance for all simulated models, as shown in Figure 4.21 A to F.

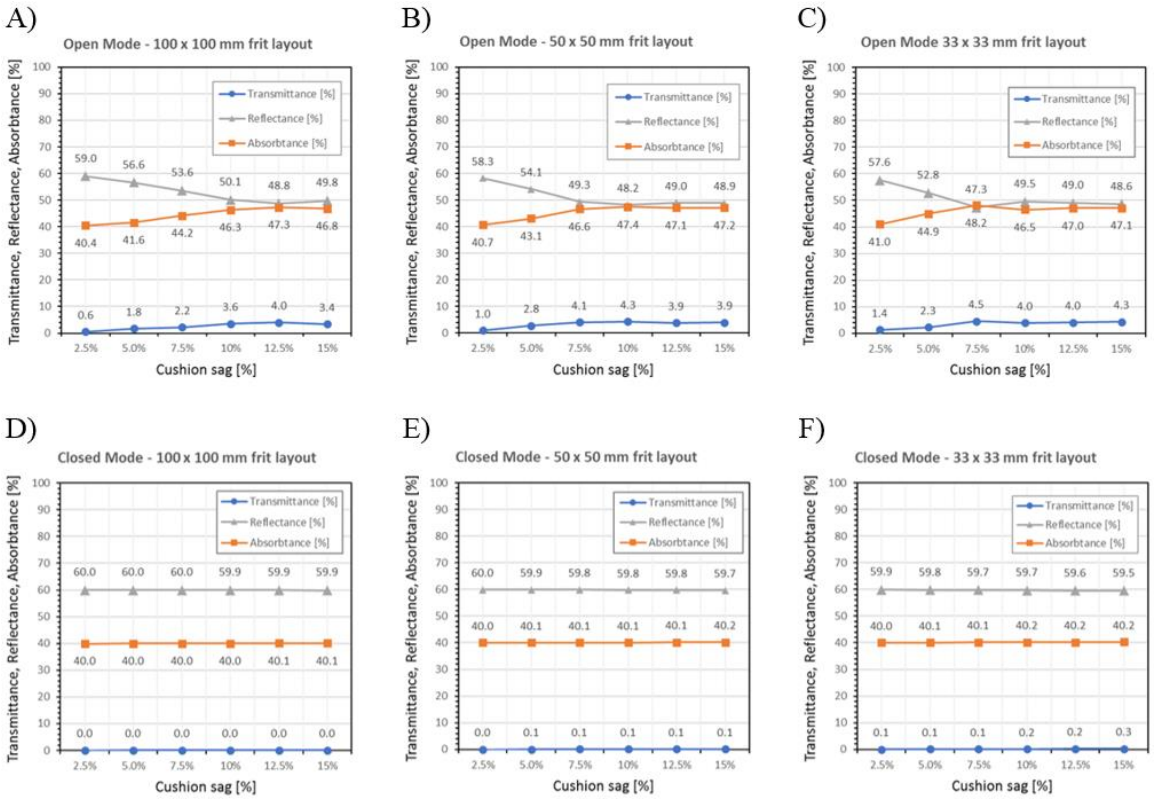


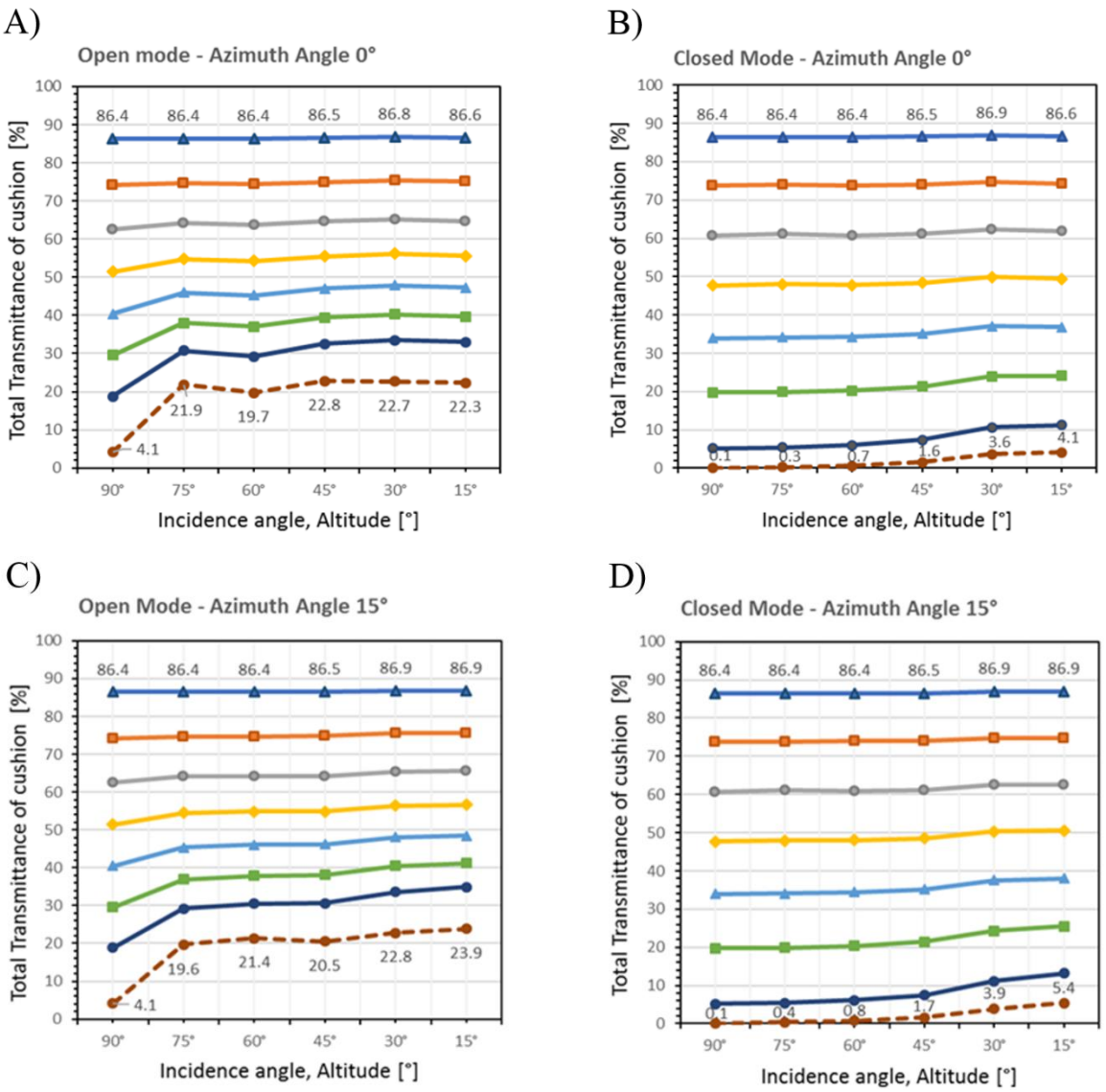
Figure 4. 21. Optical performance of switchable triple-layer cushion (10% sag with varying frit layout) – transmittance at 90° incidence angle in open and closed mode (A – F)
(graphs by the thesis author, published in: Flor et al., 2018)

In general, the obtained transmittance values for the perpendicular angle were significantly lower compared to those all other incident angles. However, these results only represent an extreme case; in real roofs, the solar incidence will typically be less than 90°, except for regions close to the equator. The transmittance of a switchable cushion in open mode ranges typically between 20% to 25%, as can be seen from the previous Figure 4.19. The relatively small difference of energy flux, of less than 4%, for all the combinations of cushion geometries and frit pattern (Figure 4.21), led to the conclusion that the grid size has only little influence on the performance. Therefore, the grid size parameter was not considered for further analysis. Nevertheless, from a perspective of lighting comfort, it might be beneficial to opt for a smaller grid size as the light will be transmitted in a more homogenous distribution.

4.4.2. Optical performance with variations of frit print properties and different incidence angles

From the discussion in the previous section, it can be seen that design parameters, like sag and frit pattern size, have only a relatively small influence on the optical performance of the ETFE cushion, while the incidence angle of solar radiation has a higher impact on the transmittance. In addition to these preliminary results, it is essential to ask if other factors like the optical frit print properties can contribute to improved performance of the switchable cushion. What follows is a description of the results obtained from an amplified study on multiple cushion models with gradually modified optical frit print properties. The simulations were conducted under a range of three-dimensional ray-tracing scenarios that produced hemispherical mean transmittance values for the cushions with different frit print types applied. Seven virtual frit print types were generated, each with a gradually increasing transmittance and simultaneously decreasing reflectance. The absorptance was neglected in this specific test case scenario and kept at a constant value of zero. This was believed feasible firstly because the absorptance of theoretically assumed ideal frit prints is, contrary to commercially available inks, simply unknown, and secondly because limiting the number of variables allowed to conduct the simulation routine more effectively. The optical properties from Liu's [2016] and Knipper's [2011] work (frit print type 8) were included in the study as a reference for comparison. The testing scenarios comprised a range of incidence angles in steps of 15° from 15° to 90° in a vertical plane and from 15° to 45° in a horizontal plane. The predicted optical performance of the cushion with 10% sag, 50 x 50 mm frit layout with various frit print is illustrated in the graphs of Figure 4.22 A to H. As expected, the cushions with an assigned frit print with a high transmittance also displayed a high overall light transmittance, and the inverse behaviour for high reflective frit prints was the case. It can also be seen from the graphs of Figure 4.22 that the angle-dependent optical behaviour is characteristic in all models. Similar trends to the simulation scenarios from the previous section can be observed. However, a

more pronounced decrease of the overall transmittance rate at higher incidence angles (60° to 90°) is evident in cushions with frit prints with higher reflectance and lower transmittance. A significant increase in overall transmittance was observed at low incidence angles, with almost 10% at 45° azimuth angle in the closed mode. The effect seems to increase with a changing azimuth angle, reaching a maximum optical permeability at an azimuth angle of 45°, where the direction of incident rays is diagonal, relative to the rectangular frit pattern.



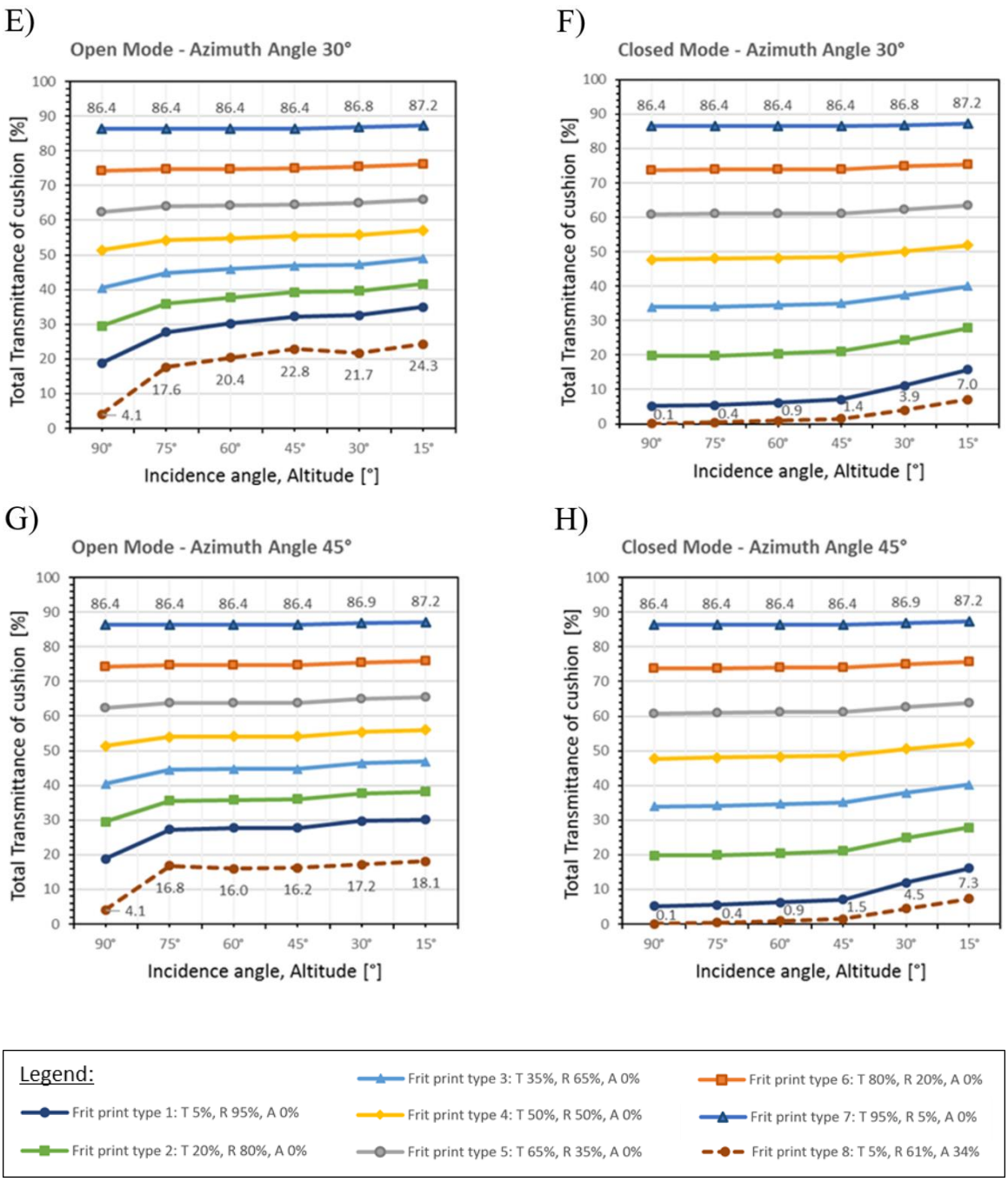
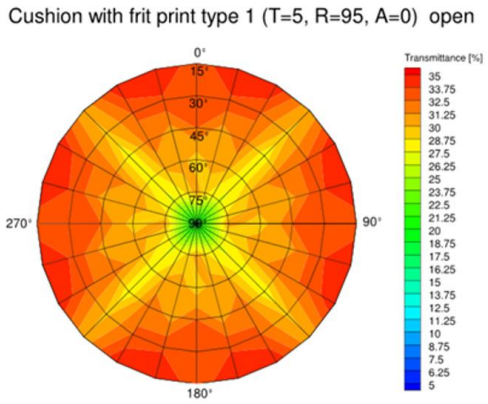


Figure 4. 22. 2D Plots (A - H) - Optical performance of switchable triple-layer cushion (10% Sag, 50 x 50 mm frit layout, varying optical frit properties) - Angle dependent transmittance in open and closed mode

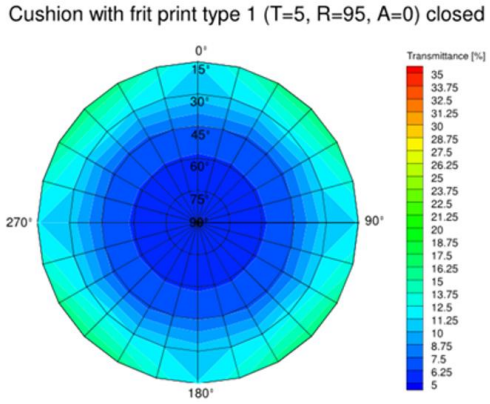
(graphs by the thesis author, published in: Flor et al., 2018)

For better visualization of the three-dimensional data, radial contour plots were generated, shown in Figure 4.23 A to P. From the summary data plots in Figure 4.23 again, the distinct optical behaviour of the switchable cushions in open and closed mode can be observed. In open mode, all cushion specimens show in comparison to diagonal incident angles (azimuth 45°) a higher mean transmittance when the rays are incident perpendicular to the cushion edge (azimuth 0°), with a difference ranging from 0.1% to 4.2%, for high and low transmittance frit prints, respectively. Analysis showed that effect results from the square boundary geometry but also from the frit grid layout, which has a higher percentage of optical overlap in diagonal ray direction. However, from Figure 4.23 it also can be seen that the opposite optical behaviour is the case for the closed mode, but with a much smaller effect. For the closed mode azimuth angles at 45°, perpendicular to the cushion, result in marginally higher mean flux rates, with a comparative difference to perpendicular azimuth angles (0°), ranging from 0.1% to 0.7% for high and low transmittance frit prints, respectively. In both operational modes, the transmittance of all cushion samples is higher at low altitude angles (15°) than close to the zenith, 90° angle, with a mean difference ranging from 0.6% to 18.1% at open and from 0.6% to 5.9% at closed mode, for high and low transmittance frit prints, respectively. In case of the open mode, this observation can clearly bet attributed to the near-perfect alignment of the frit pattern of both, middle and outer layer, in the optical view angle direction of the zenith. Even though the layers are physically separated, solar rays are effectively blocked out in this precise position and orientation. Only a small proportion of the light flux is transmitted through the frit print itself and re-reflected internally by the concave curvature of the cushion layer, and eventually, some percentage is internally reflected and transmitted as secondary radiation. Comparing the different frit prints with varying parameters of transmittance and reflectance showed that the mean degree of influence on the cushion performance is related to the optical properties of the frit and the incidence angle of radiation. From the contour plots of Figure 4.23, it can be noted that in all eight cases of this study, the angular hemispheric transmittance shows similar patterns, but at different flux rates.

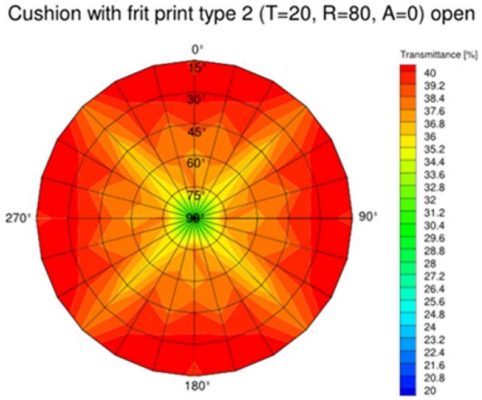
A)


Cushion with frit print type 1 (T=5, R=95, A=0) open
Transmittance [%]
35
33.75
32.5
31.25
30
28.75
27.5
26.25
25
23.75
22.5
21.25
20
18.75
17.5
16.25
15
13.75
12.5
11.25
10
8.75
7.5
6.25
5
0°
15°
30°
45°
60°
75°
90°
270°
90°
180°

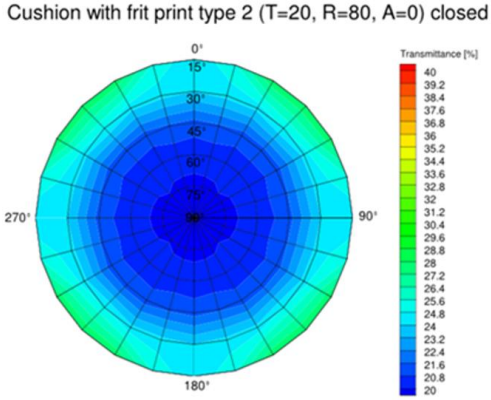
B)


Cushion with frit print type 1 (T=5, R=95, A=0) closed
Transmittance [%]
35
33.75
32.5
31.25
30
28.75
27.5
26.25
25
23.75
22.5
21.25
20
18.75
17.5
16.25
15
13.75
12.5
11.25
10
8.75
7.5
6.25
5
0°
15°
30°
45°
60°
75°
90°
270°
90°
180°

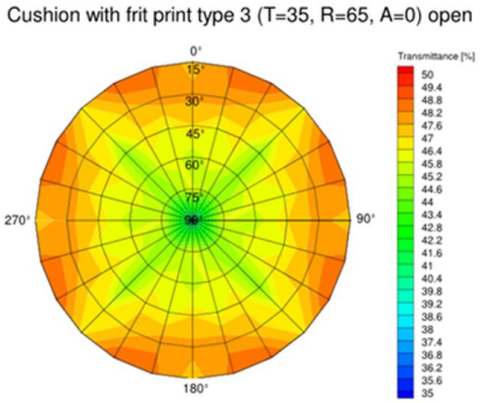
C)


Cushion with frit print type 2 (T=20, R=80, A=0) open
Transmittance [%]
40
39.2
38.4
37.6
36.8
36
35.2
34.4
33.6
32.8
32
31.2
30.4
29.6
28.8
28
27.2
26.4
25.6
24.8
24
23.2
22.4
21.6
20.8
20
0°
15°
30°
45°
60°
75°
90°
270°
90°
180°

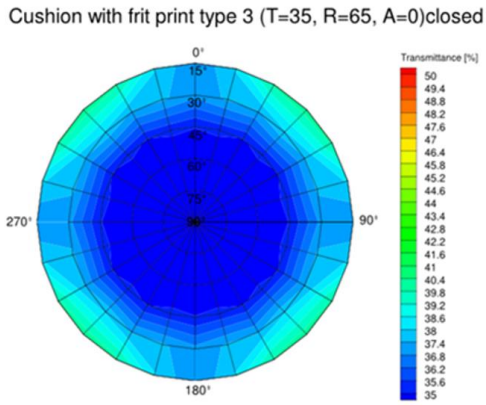
D)


Cushion with frit print type 2 (T=20, R=80, A=0) closed
Transmittance [%]
40
39.2
38.4
37.6
36.8
36
35.2
34.4
33.6
32.8
32
31.2
30.4
29.6
28.8
28
27.2
26.4
25.6
24.8
24
23.2
22.4
21.6
20.8
20
0°
15°
30°
45°
60°
75°
90°
270°
90°
180°

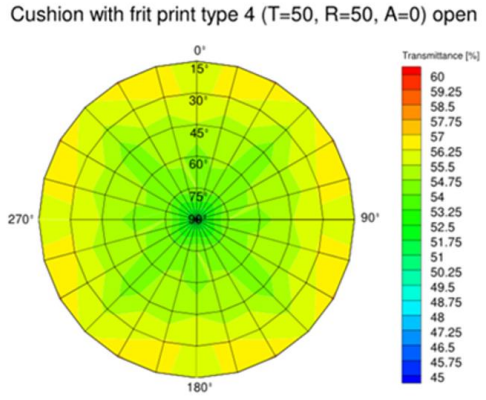
E)


Cushion with frit print type 3 (T=35, R=65, A=0) open
Transmittance [%]
50
49.4
48.8
48.2
47.6
47
46.4
45.8
45.2
44.6
44
43.4
42.8
42.2
41.6
41
40.4
39.8
39.2
38.6
38
37.4
36.8
36.2
35.6
35
0°
15°
30°
45°
60°
75°
90°
270°
90°
180°

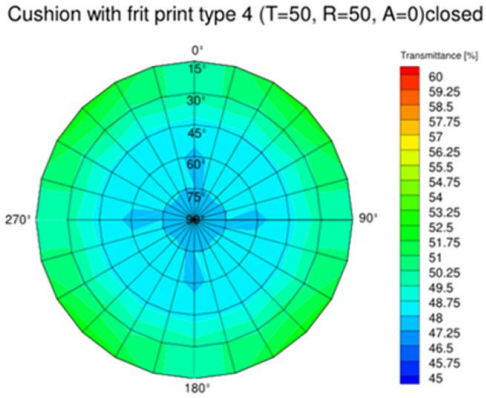
F)


Cushion with frit print type 3 (T=35, R=65, A=0)closed
Transmittance [%]
50
49.4
48.8
48.2
47.6
47
46.4
45.8
45.2
44.6
44
43.4
42.8
42.2
41.6
41
40.4
39.8
39.2
38.6
38
37.4
36.8
36.2
35.6
35
0°
15°
30°
45°
60°
75°
90°
270°
90°
180°

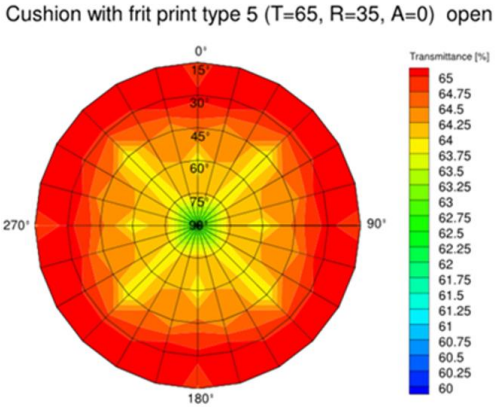
G)


Cushion with frit print type 4 (T=50, R=50, A=0) open
Transmittance [%]
60
59.25
58.5
57.75
57
56.25
55.5
54.75
54
53.25
52.5
51.75
51
50.25
49.5
48.75
48
47.25
46.5
45.75
45
0°
15°
30°
45°
60°
75°
90°
270°
180°

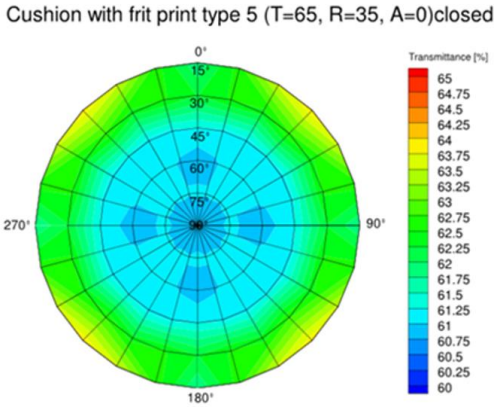
H)


Cushion with frit print type 4 (T=50, R=50, A=0)closed
Transmittance [%]
60
59.25
58.5
57.75
57
56.25
55.5
54.75
54
53.25
52.5
51.75
51
50.25
49.5
48.75
48
47.25
46.5
45.75
45
0°
15°
30°
45°
60°
75°
90°
270°
180°

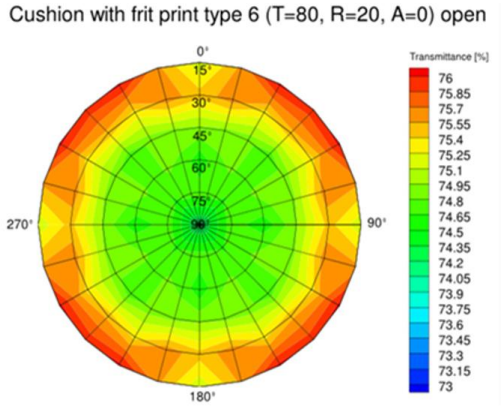
I)


Cushion with frit print type 5 (T=65, R=35, A=0) open
Transmittance [%]
65
64.75
64.5
64.25
64
63.75
63.5
63.25
63
62.75
62.5
62.25
62
61.75
61.5
61.25
61
60.75
60.5
60.25
60
0°
15°
30°
45°
60°
75°
90°
270°
180°

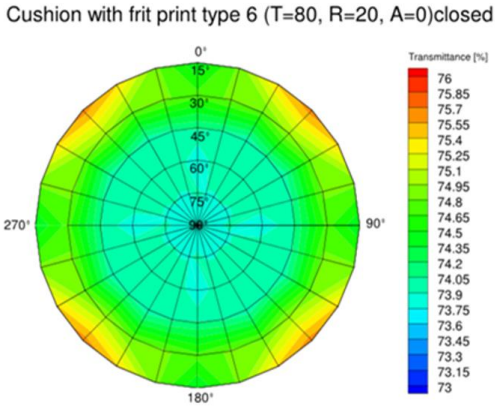
J)


Cushion with frit print type 5 (T=65, R=35, A=0)closed
Transmittance [%]
65
64.75
64.5
64.25
64
63.75
63.5
63.25
63
62.75
62.5
62.25
62
61.75
61.5
61.25
61
60.75
60.5
60.25
60
0°
15°
30°
45°
60°
75°
90°
270°
180°

K)


Cushion with frit print type 6 (T=80, R=20, A=0) open
Transmittance [%]
76
75.85
75.7
75.55
75.4
75.25
75.1
74.95
74.8
74.65
74.5
74.35
74.2
74.05
73.9
73.75
73.6
73.45
73.3
73.15
73
0°
15°
30°
45°
60°
75°
90°
270°
180°

L)


Cushion with frit print type 6 (T=80, R=20, A=0)closed
Transmittance [%]
76
75.85
75.7
75.55
75.4
75.25
75.1
74.95
74.8
74.65
74.5
74.35
74.2
74.05
73.9
73.75
73.6
73.45
73.3
73.15
73
0°
15°
30°
45°
60°
75°
90°
270°
180°

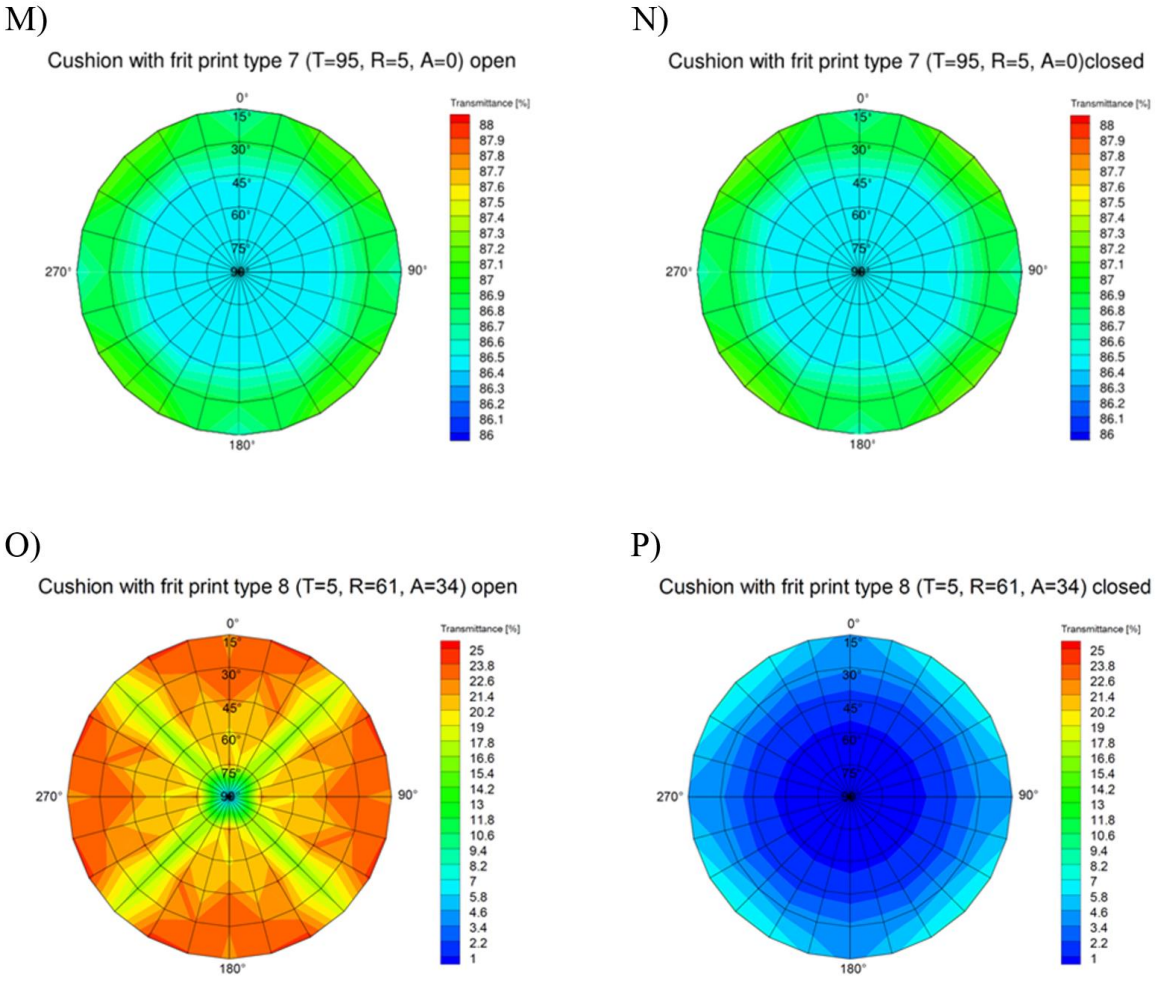


Figure 4. 23. 3D plot (A – P) - optical performance of switchable triple-layer cushion (10% sag, 50 x 50 mm frit layout, varying optical frit properties) – angle dependent transmittance in open and closed mode
(plots by the thesis author, published in: Flor et al., 2018)

Based on the ray-tracing results, hemispheric mean transmittance values were calculated for each of the cushion samples with a different frit print, in the open and closed mode shown in Table 4.5. The comparative graph of Figure 4.24 shows that the calculated mean transmittance follows a general trend towards a more distinctive optical behaviour between the two operational modes the lower the transmittance and higher the reflectance of the frit ink are. The cushion with a low transmittance (5%) and high reflectance (95%)

frit print (Frit Print 1) achieves the lowest overall mean transmittance of all analysed samples, with 31.1% in the open and 8.8% in closed mode, respectively. Nevertheless, the mean difference in transmittance between the open and closed mode is representing with 22.3% the highest difference of transmittance of all simulated frit prints. From a design perspective, this finding might suggest that highly reflective and opaque frit inks could be more effective compared to frit inks with an inverse ratio, meaning, low reflectance and high transmittance. The summary results in Figure 4.24 suggest that a distinctive optical behaviour of the two modes is advantageous for a switchable building envelope, which is expected, to adapt to a wide range of temporary changes of climate, weather and solar radiation. This combination of findings provides support for the premise that the higher the difference in transmittance between the two modes, the more effective is the radiation control of the switchable ETFE cushion. While a gradual transmittance control of the cushion would be desirable for future developments, only a two-mode switch can be achieved with this system. Therefore, it is important to set the optical properties of the frit print at the best possible thresholds for transmittance and reflectance during the design phase in order to achieve the desired energy performance of the building envelope.

Table 4. 5
Optical performance of switchable triple-layer ETFE cushions with different frit print properties in open and closed mode
(table by the thesis author, published in: Flor et al., 2018)

Test Specimen		Frit Print 1			Frit Print 2			Frit Print 3			Frit Print 4			Frit Print 5			Frit Print 6			Frit Print 7			Frit Print 8		
Value Unit [%]		*T*	*R*	*A*	*T*	*R*	*A*	*T*	*R*	*A*	*T*	*R*	*A*	*T*	*R*	*A*	*T*	*R*	*A*	*T*	*R*	*A*	*T*	*R*	*A*
	Max.	34.9	81.2	0.0	41.6	70.5	0.0	49.0	59.6	0.0	57.1	48.6	0.0	65.9	37.5	0.0	76.1	23.9	0.0	87.2	13.6	0.0	24.3	48.2	47.7
Cushion open	*Mean*	**31.1**	**68.9**	**0.0**	**38.4**	**61.6**	**0.0**	**46.5**	**53.5**	**0.0**	**55.3**	**44.7**	**0.0**	**64.6**	**35.4**	**0.0**	**75.1**	**24.9**	**0.0**	**86.6**	**13.4**	**0.0**	**20.6**	**42.3**	**37.1**
	Min.	18.8	65.1	0.0	29.5	58.4	0.0	40.4	51.0	0.0	51.4	42.9	0.0	62.5	34.1	0.0	74.2	25.8	0.0	86.4	12.8	0.0	4.1	39.8	35.0
	Max.	16.1	94.8	0.0	27.9	80.2	0.0	40.2	66.0	0.0	52.2	52.3	0.0	63.9	39.3	0.0	75.7	26.3	0.0	87.2	13.6	0.0	7.3	59.7	40.2
Cushion closed	*Mean*	**8.8**	**91.2**	**0.0**	**22.4**	**77.6**	**0.0**	**36.0**	**64.0**	**0.0**	**49.2**	**50.8**	**0.0**	**61.7**	**38.3**	**0.0**	**74.3**	**25.7**	**0.0**	**86.6**	**13.4**	**0.0**	**2.5**	**57.5**	**40.0**
	Min.	5.2	83.9	0.0	19.8	72.1	0.0	34.0	59.8	0.0	47.7	47.8	0.0	60.7	36.1	0.0	73.7	24.3	0.0	86.4	12.8	0.0	0.1	52.9	39.8

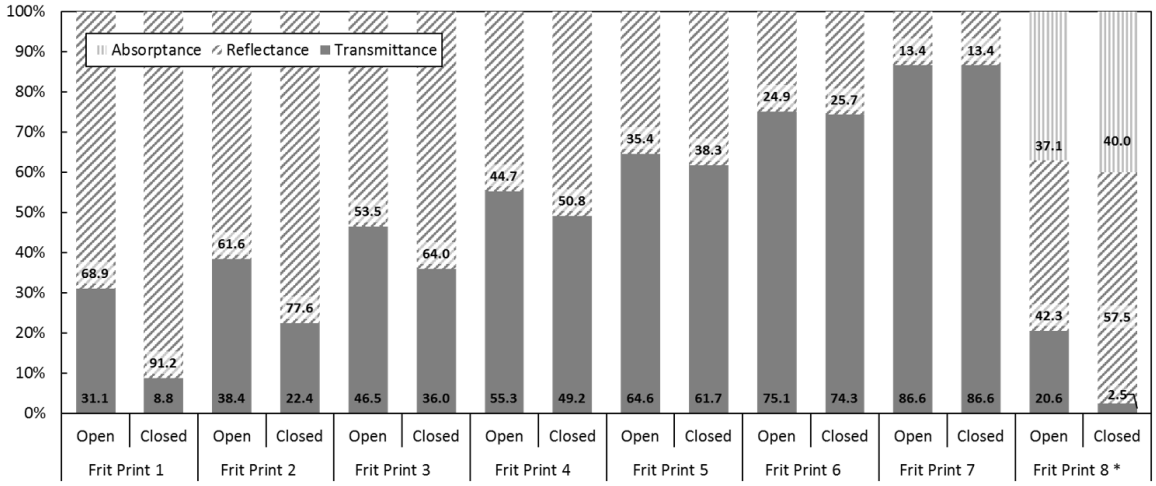


Figure 4. 24. Optical performance of switchable ETFE cushions with different frit print properties
(chart by the thesis author, published in: Flor et al., 2018)

4.5. Chapter summary

In this chapter, the aim was to characterize the optical behaviour of inflated ETFE foil cushions and assess specifically the adaptive performance of switchable multi-layer foil constructions as a base study for investigating the impact on buildings. The results of this investigation suggest that the two modes of the kinetic shading mechanism allow the building envelope to adapt actively to the variant climate conditions and thus may lead to better natural lighting conditions in buildings. This might have positive implications on both the visual comfort of the building's occupiers and the energy performance of the building because less electric lighting is needed, a hypothesis which will be addressed in chapter six and seven. While the analysis showed that the optical performance of switchable ETFE cushions is highly dependent on the solar incidence angle, design parameters like the sag and frit print size seem to have only limited influence. The optical properties of frit prints, however, play a crucial role. Frit prints with a higher reflectance and lower transmittance amplified the distinctive optical behaviour between open and closed mode and thus increased the adaptive performance of switchable ETFE cushions.

Several limitations to this pilot study need to be acknowledged. Firstly, the cushion dimensions might not be representative of the most common building applications of

ETFE, however, they clearly indicate a trend in performance which can be extrapolated to building scales. Secondly, the used material data from Liu and Knippers [2016; 2011] can only serve as a reference that might need to be updated with complete spectral data from material suppliers or direct tests. Notwithstanding these limitations, the study contributes to the understanding of the building physics of adaptable multi-layer foil constructions.

Future work on this topic would benefit from experimental investigation or post-occupancy studies to support the validation of the simulation results. Further potential is also seen in experimentation with foils having modified optical properties, new printing inks and techniques which could possibly lead to a better overall optical performance of multi-layer cushions, and more effective shading mechanism, thus enhancing the energy performance of future buildings. Aspects of these interrogatives are discussed in depth in the following chapters of this thesis.

Chapter 5: Thermal Characterisation

5.1. Introduction to chapter five

The research presented in the previous chapter revealed that the light transmittance of switchable ETFE cushions could effectively be modified, switching reversibly between two modes. Frit pattern design and reflective ink print properties play a crucial role for the effectiveness of the mechanism, under varying incident angles of solar radiation, and may contribute to an enhanced daylighting and energy performance of buildings. Chapter four aimed for an optical characterization of switchable ETFE cushions, yet the thermal performance is an equally important aspect to take into consideration for the comprehensive evaluation of building and energy performance. The thermal characterization of switchable ETFE cushions is, therefore, the aim and topic of the present chapter five.

In this study, an experimental set-up was designed to test the thermal performance of a full-scale triple-layer ETFE cushion with a switchable frit print using a large climate chamber. Two additional samples, with a conventional, static, double-layer design of clear and printed ETFE foil, were used for comparative performance evaluation under different climatic conditions. Data of surface temperatures and heat flux were obtained from the samples by experimental measurements, for a range of climate scenarios with and without dynamic air-supply. Changing volume and temperature of air-supply was further evaluated as a variable for strategically improving the thermal performance during short term extreme weather conditions. The data obtained from the experimental measurements were compared with calculation methods based on international standards, CEN BS EN 673-1998 [CEN, 2011], to pursue the hypothesis that basic predictions over the thermal performance of ETFE cushions can be approximated with simplifying calculation methods. Overall, this study contributes to the general understanding of the thermal performance of multi-layer ETFE foil constructions and offers some important insights into the building physics of switchable frit print mechanisms. Furthermore, the numerical results are

expected to serve as an initial basis for future studies on switchable ETFE building envelopes and provide preliminary input and calibration benchmarks for whole-building energy simulations in chapter seven.

The work presented in this chapter has been carried out during the course of 2018 in the laboratories of the Energy and Technology Building on Jubilee Campus at The University of Nottingham. The ETFE materials and mock-up structures were designed in collaboration with and manufactured by the applicant's industry partner company, Architen Landrell. The results of the experimental work were presented at conferences in Hong Kong and Chengdu, China, and published in peer-reviewed papers in the conference proceedings, co-authored by the applicant, supervisors, industry partner and fellow PhD colleagues. The content of this chapter incorporates research reported in the following publications, with the title pages and authors contribution declaration attached in the appendices K, L, M and N:

Flor, J.-F., Sun, Y., Beccarelli, P., Rowell, C., Chilton, J., Wu, Y., Experimental study on the thermal performance of ethylenetetrafluoroethylene (ETFE) foil cushions. 2019. IOP Conf. Ser.: Mater. Sci. Eng. 556 012004.

Wang, H., Flor, J.-F., Sun, Y., Wu, Y., Numerical investigations on the thermal performance of adaptive ETFE foil cushions. Energy Procedia, 2019. 158: p. 3191-3195.

5.2. Background on the thermal performance of building envelopes with ETFE

Predictability of performance is a key factor for designing buildings which consume less energy. In 2014 it was estimated that the building sector consumes 31% of the total world energy, which is used in large parts to heat, cool and light the built environment [IEA, 2017]. Developing building envelopes which can help to supply these functions with less energy is the goal, to unlock potential for reducing global CO_2 emissions [IPCC, 2018]. Quantifying the savings at an early stage of design to ensure that the aims are met, is the

challenge. This, however, is not easy since technological advancements have driven the development of performance orientated building envelopes at a quick pace, showing in recent times an evolution from static and passive to active and flexible systems, which can adapt and compensate the changes of the environment [Hensel, 2013]. Novel designs for ETFE cushions with the capability of switching between high and low transmittance have been engineered to enhance an adaptive performance of the building envelope. A time step image of the switching process from open to close mode is shown in Figure 5.25 making evident the potential for the employment in climate adaptive building skins. Switchable ETFE cushions have been employed in a number of projects, listed in chapter section 2.4 of chapter two. Illustrations of three examples are shown here in Figure 5.26 to 5.28.

Despite the evident potentials outlined previously, questions arise if switchable ETFE foil cushions have the capacity to improve the energy performance of buildings substantially, in comparison to static building envelopes. Testing the new developments to evaluate the viability of achieving the necessary reduction of energy consumption in buildings, is the focus of this study, laying the basis that is needed to quantify the expected energy savings, which may justify a higher effort for engineering these systems. Therefore, an experimental study is carried out in this chapter to investigate the thermal performance of different ETFE cushion designs, monitoring and comparing the physical behaviour under varying climate conditions, investigating for the first the time, also the thermal performance of switchable ETFE cushions. Outcomes of this study are expected to calibrate and validate numerical models and simulation set-ups to calculate energy savings.

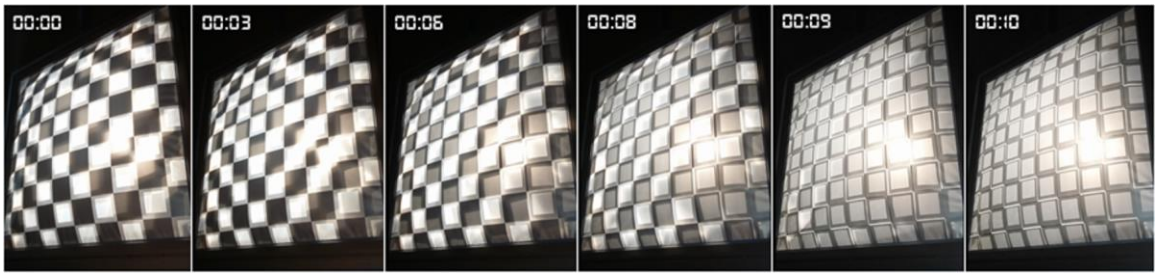


Figure 5. 25. Switching sequence of switchable ETFE cushion (experimental mock-up) from open to closed mode (time frames per minute)
(photos by the thesis author, unpublished)

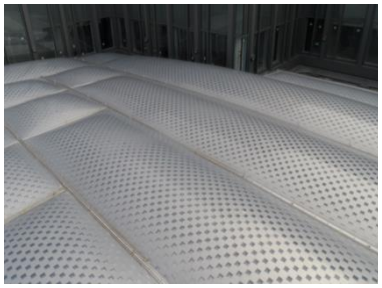


Figure 5. 26. St. Bartholomew's Hospital, London, UK, courtyard cover with switchable ETFE foil cushions (photo by Architen Landrell, retrieved from: https://www.architen.com/)



Figure 5. 27. RCS Pavilion EXPO2015, Milan, Italy, roof with switchable ETFE cushions (photo by Maco Technology srl, retrieved from:https://www.macotechnology.com/)



Figure 5. 28. ISS Building Lancaster University, Lancaster, UK, skylights with switchable ETFE foil cushions (photo by Architen Landrell, retrieved from: https://www.architen.com/))

5.3. Methods, equipment and samples

Based on the conclusion drawn from the literature review in chapter three, this study sets out to investigate in a comparative way the thermal performance of different ETFE foil cushion designs under laboratory conditions, using a large climate chamber and real size, static and switchable, testing samples with different layer compositions and frit print. The specific objective was to determine the heat flux and surface temperatures of a vertical ETFE foil cushions under varying climate scenarios, and different air-supply levels in order to calculate the thermal resistance or R-value which is required to quantify the benefits on the thermal performance of building façades using simulation software. The experimentally and theoretically derived performance data will allow designers to incorporate this information in future prediction studies for energy performance of buildings. The experimental studies reported in this chapter were undertaken at the Laboratories in the Energy Technologies Building at the University of Nottingham. The

experimental set-up, the samples and the testing procedure as well as the data acquisition and analysis is described in the following sections.

5.3.1. Climate Chamber

The thermal performance of the three ETFE cushions was investigated, making measurements of heat flux in an environmental test chamber, type TAS series 2 LTCL600 manufactured by Temperature Applied Sciences Ltd. This apparatus (hereafter denominated climatic chamber) is able to independently control the temperature and humidity of two walk-in-rooms, simulating indoor and outdoor conditions. At the same time, a test sample can be installed in-between, in an insulated surround panel, which separates both rooms. The dimensions of left and right room are similar at 4.0 m x 3.5 m x 2.6 m. The left side room is mounted on wheels and can be moved along rails, allowing access to the separating surround panel for construction and installation works. The temperatures and humidity levels of both rooms are controlled independently with integral air conditioning units allowing for steady-state or cyclic climate conditions in the range of -25°C to +60°C and 10% to 95%, respectively. Various parameters of environmental conditions and thermal performance of the test samples can be measured and monitored during the test cycles with sensors and measurement devices installed inside the chamber. A picture showing the components of the climate chamber is shown below in Figure 5.29.



1. External Room
2. Internal Room
3. Surround Panel
4. Baffle Wall
5. Air Con Unit
6. Control Panel
7. Measurement Logging Station

Figure 5. 29. Climate Chamber in open position
(photo by the thesis author, unpublished)

5.3.2. ETFE cushion samples

Three ETFE cushions were tested in the climate chamber. All samples measured 1000 mm by 1000 mm with a sag/rise of 100 mm of the centre section curvature on each side of the centre plane, in state of full inflation. The air fill volume is 94 litres at a nominal pressure of 300 Pa. Each of the cushions has one air-inlet and one air out-let with removable valves. The cushion edges were clamped into an extruded aluminium profile with a keder system. The clamping profiles were mounted on a structural frame to support the cushion and withstand tension forces when fully inflated. The profile was sealed with a silicone gasket, and aluminium cover plates were screwed on top to close the frame. The whole unit measured 1200 mm x 1200 mm. An overview of the testing module and all its main components can be seen in Figure 5.30, A and B.

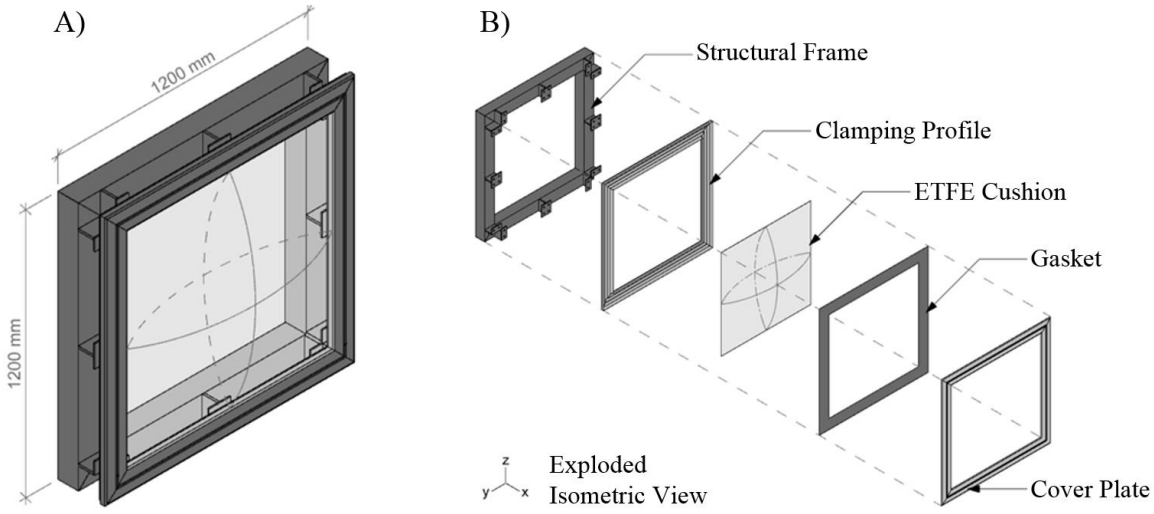


Figure 5. 30. A) Isometric view of the test frame and ETFE cushion, B) exploded view of the test frame showing main system components
(images by the thesis author, unpublished)

All samples are composed of extruded clear ETFE foil with a thickness of 200µm, a weight of 350 g/m^2 (according to manufacturer specification) and thermal conductivity of 0.24 W/m·K [Wypych, 2016]. Different reflective silver frit prints were applied to the

layers of the cushions. An overview of the layer composition of all three cushion samples can be seen in Figure 5.31 A, B and C.

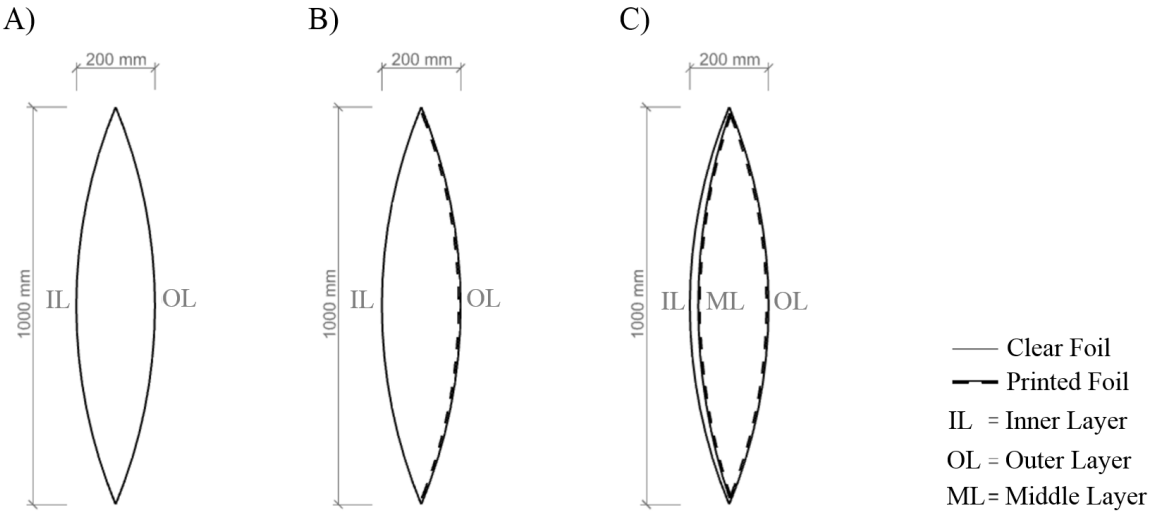


Figure 5. 31. Section views of the sample dimension and layer compositions A) double layer clear ETFE; B) double layer clear and fritted ETFE; C) triple layer switchable ETFE
(images by the thesis author, unpublished)

Sample 1, shown in Figure 5.32 A, is composed of two layers of clear ETFE foil. Both foils are transparent, and the cushion has an overall solar transmittance of approximately 84% [Knippers et al., 2011]. Sample 2 shown in Figure 5.32 B, is composed of two layers, one clear (Figure 5.33 A) and one fritted (Figure 5.33 B), with a hexagon pattern of approximately 71% surface cover with standard silver ink with a print density of 28%. The solar transmittance for the cushion unit is 46% (according to manufacturer data). Sample 3, in Figure 5.32 C, is composed of three layers, one clear (Figure 5.33 A) and two, with a square pattern of approximately 74% surface cover with standard silver ink with a print density of 28% (Figure 5.33 C). The square base-grid of the frit print measures 104 mm x 104 mm. The clear square areas have a dimension of 74 mm x 74 mm. Around the clear area is a printed frame of ca 15 mm width, with a less dense frit ink application. The printed layers are shifted in a way that the printed areas of one layer are overlapping with the clear areas of the second. When one of the two cushion sides are inflated, the printed

middle layer can be moved to overlap or separate from the outer printed layer. This allows the solar transmittance of the cushion to be modified, switching from one state to the other (open / closed).

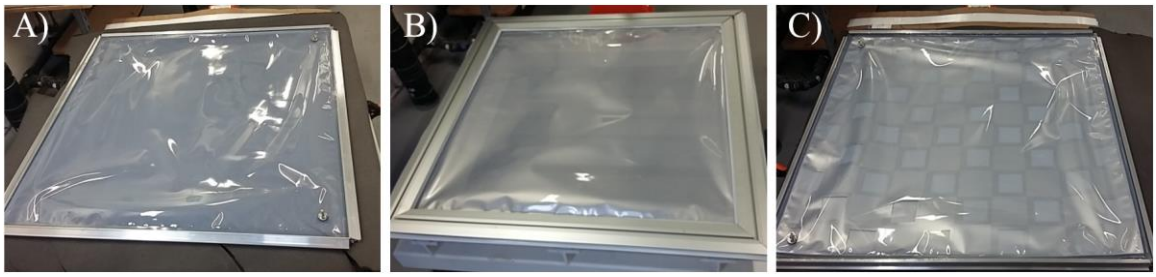


Figure 5. 32. ETFE Cushion samples, A) two layers clear ETFE, B) two layers, fritted ETFE, C) three layers, switchable ETFE frit
(photos by the thesis author, unpublished)

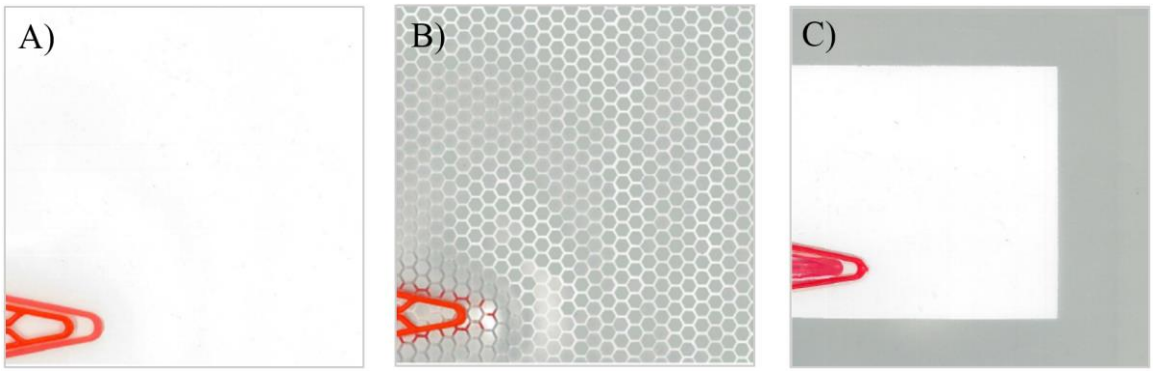


Figure 5. 33. ETFE foil types, A) clear, B) hexagon frit, C) square frit, switchable
(photos by the thesis author, unpublished)

5.3.3. Experimental set-up

The experimental set-up for the measurement was based on the international standard BS EN ISO 12567-1:2010 [ISO, 2010] for the determination of the thermal performance of windows and doors. The chosen measurement method was in close accordance with the international standards BS ISO 9869-1:2014 [ISO, 2014] for in-situ measurements of thermal resistance and thermal transmittance using the heat flow meter

method. Due to the geometry of the ETFE cushion adaptations had to be made to the recommended method in order to carry out the measurements. The Testing frame was fitted in a 1200 mm x 1200 mm frame in the insulated partition wall which separates two rooms for the chamber. The partition wall had a thickness of 300 mm and measured U-value of less than 0.3 W/m^{2}K. The ETFE cushion samples were clamped into the mounted test frame fitting flush with the edges to the outer surface plane of the surround panel. A silicon gasket was mounted on the clamping profile and covered by aluminium plates. Gaps between the test frame and the surround panel were covered from both sides with adhesive tape to avoid air infiltration. The ETFE cushion was inflated with air to a nominal pressure of 100 Pa and the air pressure monitored. In order to reduce forced convection effects, stemming from the air-conditioning to a minimum, thin wooden drywalls were installed on each side of the surround panel, with a separating distance of 500 mm, ensuring convective effect are reduced to a minimum in this baffle zone. Sensors were installed on the cushion surface and the baffled zone on both side of the sample. An overview section of the apparatus set can be seen in Figure 5.34.

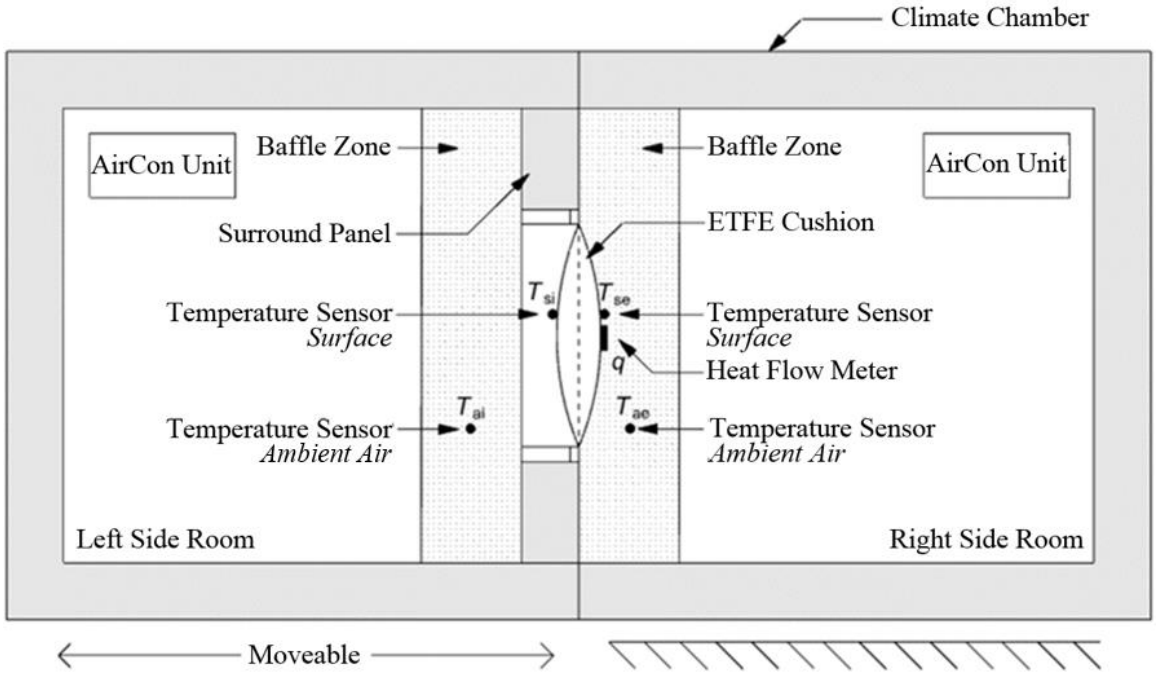


Figure 5. 34. Overview Section of the experimental set-up in the climate chamber (image by the thesis author, unpublished)

5.3.4. Dynamic air-supply

With the aim to investigate the influence of the air supply on the thermal performance of ETFE cushions an experimental set-up was designed, inspired by a study which investigated adaptive thermal mechanisms of ventilated multi-chamber ETFE cushions using computational simulation techniques [Harder et al. 2018]. The experimental set-up for this study was based on the initial thermal performance test described in the previous section. The cushion was mounted in the opening of the surround panel and equipped with thermocouples and heat-flux sensors. Air was injected through an insulated tube to the cushion at an air inlet valve and released through an outlet valve and the air diverted through a second pipe out of the climate chamber. An overview scheme showing all relevant components of the experimental apparatus set-up is shown in Figure 5.35. Specifications of sensor types and position are presented in the following section.

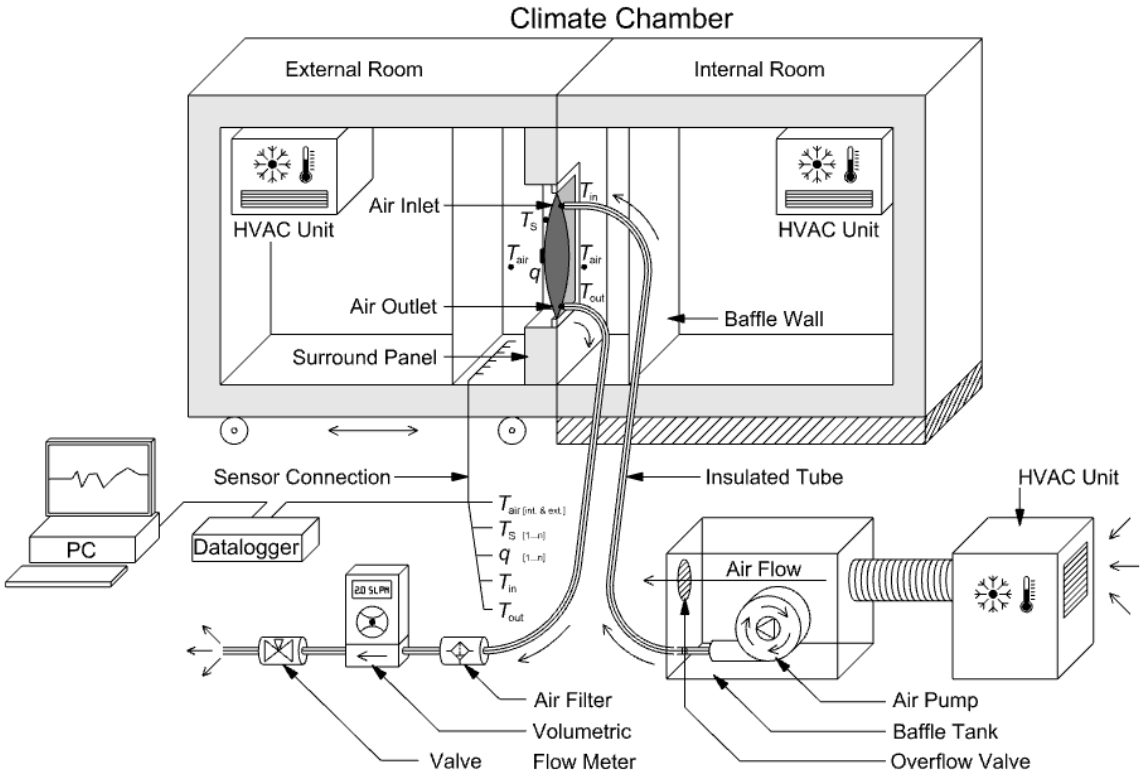


Figure 5. 35. Apparatus set-up for dynamic air-supply
(image by the thesis author, unpublished)

The position of inflow and outflow was varied according to the schemes in Figure 5.36 A to D, with the aim to rule out any influences on the overall thermal performance of the ETFE cushion. The inflow air was provided by equipment located outside the climate chamber. The supply air was preconditioned to a set temperature in a range between 15°C to 30°C, according to the chosen scenarios, by a portable air conditioning unit with a cooling capacity of 2052 Watt, and directed into a baffled tank with a volume capacity of 90 litres, similar to the ETFE cushion. The air was pumped out of a baffled tank with an electric air pump with a maximum capacity of 708 litres per minute and a head pressure of 49 mbar. The temperature of the supply air was monitored at the outflow valve of the baffled tank and the inflow and outflow valve of the ETFE cushion. The flow rate and pressure of the supply air was controlled with adjustable valves at the outflow of the baffled tank and the outflow tube of the ETFE cushion, while measuring pressure and the volumetric mass flow with a calibrated low-pressure drop gas mass flow meter, type FMA-LP1608A-I2, with an accuracy of ±(0.8% of rdg + 0.2% FS), manufactured by Omega Engineering Limited. This allowed maintaining a stable airflow through the ETFE cushion with a constant flow rate, pressure and temperature. The air temperature of the two rooms of the climate chamber was set according to the scenarios outlined in the following sections. With steady-state achieve heat flux and surface temperatures of the cushion layers were measured and recorded at a frequency of 30 seconds for a period of one hour. A picture of the equipment set-up for the dynamic air-supply is shown in Figure 5.37.

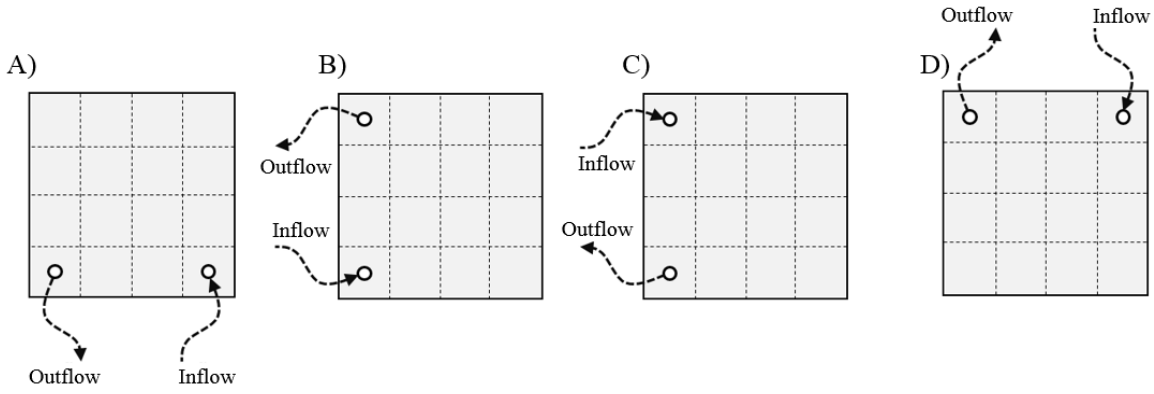


Figure 5. 36. Position of air-valves on cushion sample
(images by the thesis author, unpublished)

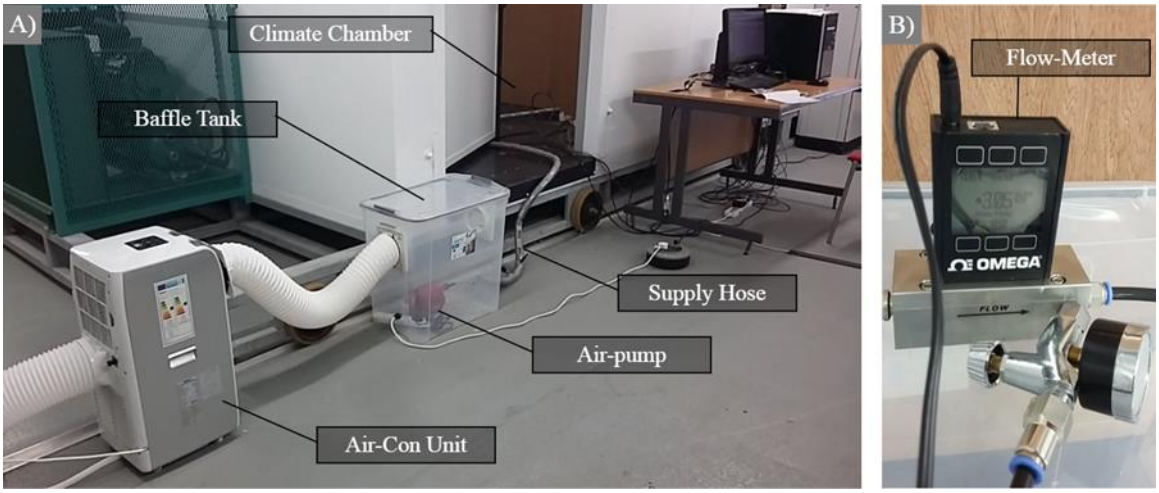


Figure 5. 37. Equipment set-up for dynamic air-supply, A) air-supply with air-con unit, baffle tank and air-pump, B) Flow-meter and adjustable air-valve
(photos by the thesis author, unpublished)

5.3.5. Sensor types and position

The inflated cushions were equipped with calibrated heat flux sensors and T-type thermocouples. For the purpose of measuring the surface temperature of the ETFE cushion, a total of 22 temperature sensors, laboratory fabricated with IEC thermocouple cable type T 1/0.2mm conductors (tested for tolerance class 2 in accordance with IEC 60584:2013 and ASTM E230/E230M-12), were distributed in a square pattern with nine positions, of three by three units, and fixed on the sample. The thermocouples were attached with reflective adhesive-tape to the exterior surface of the inner and outer layer of the cushion. In order to measure the heat flux (W/m^2) through the ETFE cushion sample, three heat flux sensors, type HFP01 Hukseflux thermopiles, calibrated in accordance with ASTM C1130 (uncertainty of calibration: ± 3 % (k = 2), sensor thermal resistance 71 x 10-4 $K/(W/m^2)$ nominal sensitivity: 60 x 10-6 $V/(W/m^2)$ were attached on the central vertical axis over the outer layer of the cushion using a thin layer of silicone heat transfer paste, type RS 217-3835 (thermal conductivity: 2.9 W/m*K) between the sensor and sample surface and adhesive tape on the top side to secure the sensor position. The combined thermal resistance of the heat flux meter and heat transfer paste was low enough in proportion to the overall

heat transfer to not affect the measurements. An additional fourth heat flux meter was attached at the centre of the external side of the inner layer of the sample for measurement control. The homogenous distribution grid of the sensors allowed any variations in heat flux or change of surface temperature over the curved sample surface to be detected. The ambient air temperature was measured stationary with two calibrated temperature probes, Campbell Scientific type CS215 (accuracy ± 0.4°C), within the 500 mm baffle zone on both sides of the sample. An overview of sensor positions is shown in Figure 5.38 and 5.39.

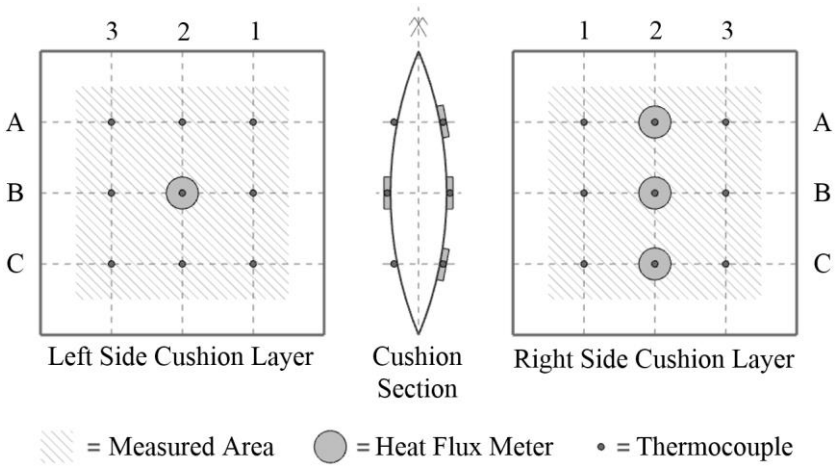


Figure 5 38. Sensor types and position on ETFE cushion sample
(images by the thesis author, unpublished)



Figure 5. 39. Instrumentation of ETFE cushion sample (photo by the thesis author, unpublished)

5.3.6. Testing scenarios

Lightweight structures, such as pneumatic foil constructions, are sensitive to changing outdoor and indoor temperature. In order to characterize the thermal performance of ETFE cushions for different climate conditions, a range of testing scenarios was outlined. Based on the standard boundary conditions of CEN BS EN 673:2011 [CEN, 2011] five scenarios with varying mean surface temperatures and surface temperature differences of the inner and outer cushion layer were established (Table 5.6). Scenario 3 represents the standard condition with a temperature difference of 15°C between the inner

and outer layer surface temperature at a mean temperature of 10°C. Scenario 1,2, 4 and 5 are variations of the standard condition, representing other conditions either for the low or high-temperature environment. In order to achieve the scenario target temperatures, the two rooms of the climate chamber were cooled and heated with built-in air-conditioning units to pre-calculated temperatures. Surface temperatures of the sample and air-temperatures of both rooms were monitored continuously until a steady-state condition was reached. The transversal heat-flux through the samples was then measured at steady state. The measurement procedure is presented in the following section.

Table 5. 6
Temperature *testing scenarios*
(table by the thesis author, unpublished)

Surface Temperatures [°C]	Scenario 1	Scenario 2	Scenario 3	Scenario 4	Scenario 5
Temperature Difference	7.5	10.0	15.0	15.0	15.0
Mean Temperature	10.0	10.0	10.0	15.0	7.5

5.3.7. Experimental measurements

The method for the experimental measurements was designed in close agreement with the recommendations of the standard ISO BS 9869-1-2014 [ISO, 2014]. Following this method, the surface temperatures and the heat flux through the samples is measured as well as the baffled air temperatures on both sides of the sample. The data of these measurements provide the input for the derivation of the thermal resistance and transmittance of the samples and allow for comparison with the results of the numerical calculation for the theoretical U- and R-value. The climate chamber was programmed to the required temperature settings, and the stable surface temperatures of the ETFE cushion sample were achieved after approximately 12 hours. The steady-state condition was monitored for another 24 hours until the measurements of the sensors were logged for the required period of time with a data logger, DataTaker type DT85, with 32 isolated analog

input channels and a resolution of 18 bits at a 30-second logging frequency. The logging procedure was monitored on a live screen with the data display in real-time.

5.3.8. Standard calculation method

A numerical standard method based on CEN BS EN 673-1998 [CEN, 2011], which provides the empirical formulas for calculating a multiple-layer glazing system, was used to calculate the thermal resistance value of a clear ETFE cushion under different thermal conditions, with the purpose to compare the results with the experimental measurement [Wang et al., 2019]. The standard method only considers planar glazing geometries. However, the double-curved geometry of inflated ETFE cushions, as opposed to the two-dimensional straight boundary of glazing, results in different airflow behaviour in the internal air chamber. Therefore, the compromise to this limitation is using an integrated average of the surface distance between the left and right layer to achieve an averaged chamber width of the ETFE double-curved cushion geometry. According to the standard calculation based on CEN BS EN 673 [CEN, 2011], the resistance of the ETFE cushion can be determined by the sum of the resistance of all the materials, which are the ETFE cushion as well as the air inside and outside the surface in this case. The U-Value is then acquired by adding the internal and external surface convection effects. The thermal resistance of ETFE cushion can be calculated through the equation with the ETFE cushion thermal resistance and radiation plus the convection conductance of the air chamber. The experimentally derived thermal resistance R, indirectly obtained from the heat flux measurements, was calculated according to the standard BS ISO 9869-1:2014; dividing the sum of the temperature differences between the internal and external surfaces, T_{si} and T_{se}, across the cushion section by the sum of the measured heat flux q through the sample:

$$R = \frac{\sum_{j=1}^{n}\left(T_{sij} - T_{sej}\right)}{\sum_{j=1}^{n} q_j}$$

Equation 5. 1

An estimate of the thermal transmittance, or U-value here determined *U*, was derived from the experimental measurements by dividing the sum of the heat flux *q* across the ETFE cushion section divided by the sum of the ambient temperature differences, T_{ij} and T_{ej} , measured within the baffle zone on both sides of the ETFE cushion:

$$U = \frac{\sum_{j=1}^{n} q_j}{\sum_{j=1}^{n}\left(T_{ij} - T_{ej}\right)}$$

Equation 5. 2

A graphical representation of the thermal model for a double layer ETFE cushion showing the main parameters which affect the overall thermal resistance is shown in Figure 5.40, where *T* is the internal and external ambient air temperature, *h* the internal and external convective heat transfer coefficient, *IR* the internal and external infrared radiation and *E* the thermal emittance on both sides of the ETFE cushion. The very thin (200 µm), internal and external, cushion layer surfaces S_1 and S_2 are characterised in the below model diagram by the thermal conductivity k_1 and k_2, the surface Temperature T_1 and T_2, surface emissivity $\mathcal{E}_1$ and $\mathcal{E}_1$, and the convective heat transfer coefficient h_g of the internal air-filled chamber.

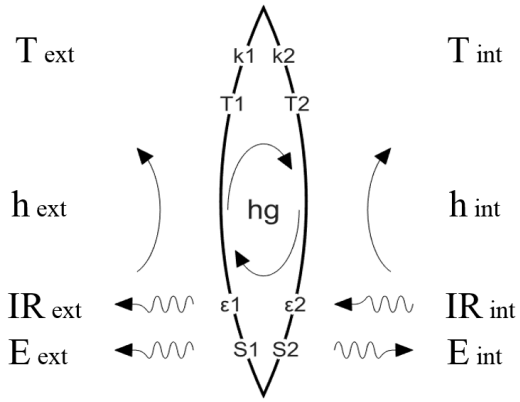


Figure 5. 40. Thermal model for an ETFE cushion showing the main parameters which affect the overall thermal resistance
(image by the thesis author, unpublished)

5.4. Results and discussion

The results obtained from the experimental measurements and numerical calculations are presented and discussed in the following section. Detailed analyses and comparison of the different datasets are provided, highlighting the main findings.

5.4.1. Thermal performance at standard condition

The thermal performance tests were conducted at steady state. In general, the data obtained from the experimental measurements show a similar pattern throughout the climate scenarios for all three ETFE cushion samples. The mean surface target temperatures of the inner and outer layer, aimed for in each scenario was closely achieved with a maximum deviation of less than +/- 1.5°C. The deviation might appear rather high in relation to the given temperature ranges; however, given the difficulty within the experimental procedure to achieve the exact target temperatures, this value is considered relatively acceptable. The difficulty in achieving the exact temperatures resided mainly in the uneven temperature distributions on the double-curved surface geometry and the iterative effects between the left and right-side climate chamber controls, where any change in the temperature settings would immediately affect the surface temperature of both sides

of the ETFE cushion relative to each other due to the low thermal mass of the ETFE cushion and the convective heat exchanges. Therefore, calibration of the system and testing of the climate chamber input control settings were essential previous to the performance tests. A sample data outtake from the obtained measurements can be observed in Figure 5.41, depicting the data set of the first 18 hours of the clear cushion sample in the climate setting of scenario S3, standard condition. The measurement results graphical output shown in Figure 5.41 is characteristic for all three samples.

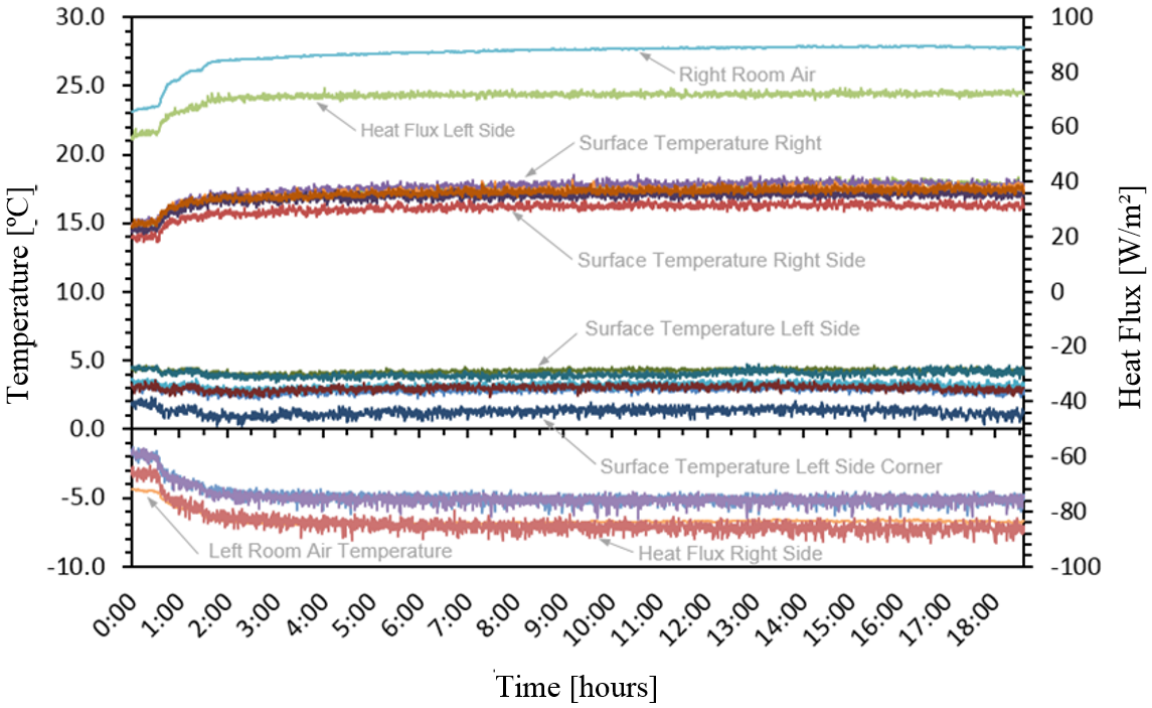


Figure 5. 41. Example data set of measurements taken of surface temperatures and heat-flux on a clear ETFE cushion sample 1 during standard temperature condition (graph by the thesis author, unpublished)

As can be seen from Figure 5.42 the surface temperatures of both layers increase from the lower to the higher part of the cushion section, with a mean difference of approximately 3.5°C on the cold side and 2.5°C on the warm side. Heat flux across the cushion also varies at different points of the section with the highest flow values at the bottom and lowest at the top with an approximate difference of 10%. The values obtained

for the heat flux at different positions of the sample surface showed a variation according to the section height and width of the cushion at the measurement positions. This behaviour was characteristic for all measured samples under the tested scenarios. For the sake of further analysis and comparison with calculation results, these values were averaged and combined into a mean heat flux value for each sample and scenario. A complete overview of all measured values on the three samples for the different climate scenarios can be seen in Table 5.7 to 5.10.

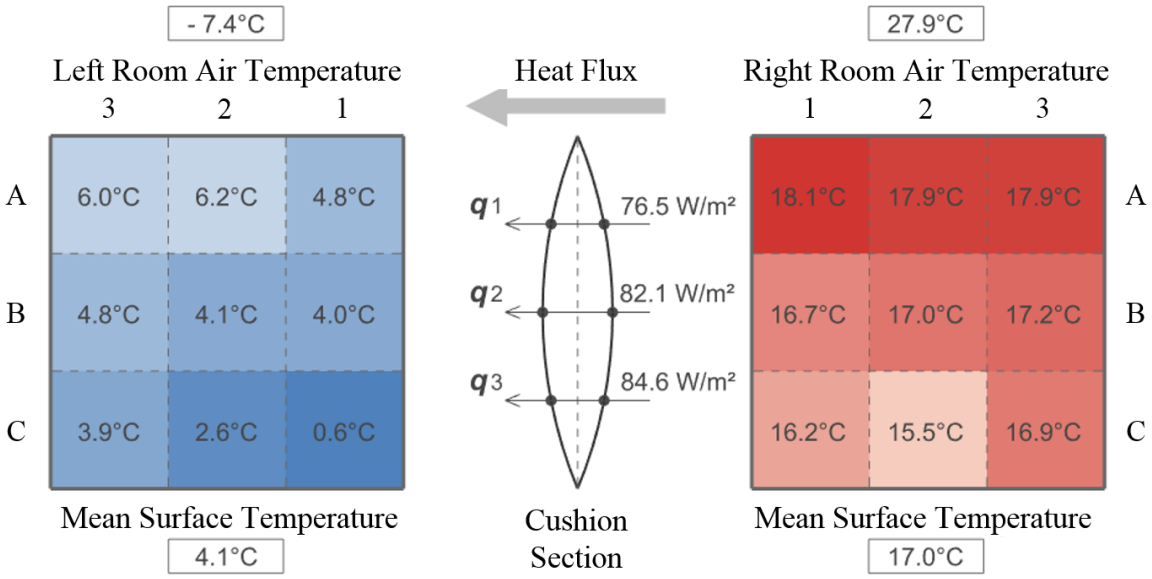


Figure 5. 42. Measured Values on the clear ETFE cushion at standard condition (S3) (images by the thesis author, unpublished)

Regarding the temperature distributions depicted in Figure 5.42 it must be noted that the shown temperature values correspond to the measurements at the sensor positions and vary over the surface between each sensor depending on the section width of the cushion at that point, the surface curvature and orientation, and the internal and external convective dynamics. The measured field represented in Figure 5.42 corresponds approximately to the measured area depicted in the sensor positioning diagram of Figure 5.38 and does not take into account any edge effects related to the clamping profile.

Table 5. 7
Sample No. 1 (2 layers, clear ETFE), measured values
(table by the thesis author, unpublished)

Parameters / Scenarios	Unit	S.1	S.2	S.3	S. 4	S. 5
Left-side ambient temperature	[°C]	-0.4	-3.3	-7.9	-5.5	-12.6
Right-side ambient temperature	[°C]	19.4	23.2	28.2	33.9	26.0
Left-side surface temperature	[°C]	6.5	5.7	4.0	7.7	0.1
Right-side surface temperature	[°C]	13.7	15.4	17.5	22.4	14.6
Surface temperature difference	[°C]	7.2	9.7	13.4	14.7	14.5
Surface mean temperature	[°C]	10.1	10.6	10.8	15.1	7.4
Horizontal heat-flux	[W/m^2]	42.7	59.2	81.1	96.2	87.2
Thermal transmittance	[W/(K·m^2)]	2.2	2.2	2.2	2.4	2.3
Thermal resistance	[(K·m^2)/W]	0.2	0.2	0.2	0.2	0.2

Table 5. 8
Sample No. 2 (2 layers, fritted ETFE), measured values
(table by the thesis author, unpublished)

Parameters / Scenarios	Unit	S.1	S.2	S.3	S. 4	S. 5
Left-side ambient temperature	[°C]	-0.2	-1.8	-7.2	-3.2	-10.6
Right-side ambient temperature	[°C]	20.4	21.8	27.0	33.0	24.8
Left-side surface temperature	[°C]	6	5.3	3	7.6	-0.2
Right-side surface temperature	[°C]	14.8	15.3	17.5	22.7	14.9
Surface temperature difference	[°C]	8.8	9.9	14.5	15.2	15.1
Surface mean temperature	[°C]	10.4	10.3	10.2	15.1	7.4
Horizontal heat-flux	[W/m^2]	40.6	46.8	71	79.1	72.2
Thermal transmittance	[W/(K·m^2)]	2.0	2.0	2.1	2.2	2.0
Thermal resistance	[(K·m^2)/W]	0.2	0.2	0.2	0.2	0.2

Table 5. 9
Sample No. 3, Open Mode (3 layers, fritted ETFE), measured values (table by the thesis author, unpublished)

Parameters / Scenarios	Unit	S. 1	S.2	S.3	S. 4	S. 5
Left-side ambient temperature	[°C]	-	-1.9	-8.8	-	-9.3
Right-side ambient temperature	[°C]	-	20.5	26.5	-	24.1
Left-side surface temperature	[°C]	-	4.9	1.7	-	0.7
Right-side surface temperature	[°C]	-	15.1	17.6	-	15.8
Surface temperature difference	[°C]	-	10.2	15.9	-	15.1
Surface mean temperature	[°C]	-	10.0	9.7	-	8.3
Horizontal heat-flux	[W/m^2]	-	38.4	65.3	-	59.9
Thermal transmittance	[W/(K·m^2)]	-	1.7	1.8	-	1.8
Thermal resistance	[(K·m^2)/W]	-	0.27	0.24	-	0.25

Table 5. 10
Sample No. 3, Closed Mode (3 layers, fritted ETFE), measured values (table by the thesis author, unpublished)

Parameters / Scenarios	Unit	S. 1	S.2	S.3	S. 4	S. 5
Left-side ambient temperature	[°C]	-	-1.9	-8.4	-	-8.4
Right-side ambient temperature	[°C]	-	20.5	26.6	-	26.4
Left-side surface temperature	[°C]	-	4.6	1.6	-	1.1
Right-side surface temperature	[°C]	-	14.8	17.2	-	17.6
Surface temperature difference	[°C]	-	10.2	15.6	-	16.5
Surface mean temperature	[°C]	-	9.7	9.4	-	9.4
Horizontal heat-flux	[W/m^2]	-	47.7	79	-	78.1
Thermal transmittance	[W/(K·m^2)]	-	2.1	2.3	-	2.2
Thermal Resistance	[(K·m^2)/W]	-	0.21	0.20	-	0.21

From the data presented in Table 5.7 to 5.10 it can be seen that all cushion samples showed a similar trend in the magnitude of heat flux throughout all temperature scenarios, ranging from the lowest heat flux of 38.4 W/m^2 to the maximum of 96.2 W/m^2, for sample 3 and 1 respectively. The variation of the temperature difference had a big impact on all

samples, with a significant rise of the heat flux at a higher temperature difference between internal and external air temperature. In terms of total heat flux, however, the results demonstrate a very distinctive behaviour of the three samples, which might be directly linked to the frit print and layer design. Sample 1 presented the highest heat flux rate in all tested scenarios followed by sample 3 in closed mode, then sample 2 and with the lowest heat flux sample 3 in open mode. A comparative graph showing the average heat flux for all three cushion samples at the standard condition (S3) with a surface temperature difference of 15°C at a mean temperature of 10°C, is presented in Figure 5.43. It can be observed that the switchable ETFE cushion performs best under the standard condition with a mean heat flux of 65.3 W/m^2 across the centre cushion section. Sample three is followed by sample two, the fritted ETFE cushion, with a mean heat flux of 71.0 W/m^2. The heat flux through the switchable cushion in closed mode is 79.0 W/m^2. Sample 1, the clear ETFE cushion shows the lowest performance with a mean heat flux of 81.1 W/m^2. It was hypothesized based on the results that the observed thermal behaviour is related to the different emissivity of the printed and unprinted foil surfaces and the number of foil layers, an explanation which had already been presented in previous investigations [Robinson_Gayle, 2003; Lippke, 2009; Knippers et al., 2011]. It was also found that the air pressure inside the inflated cushion, which was measured at different pressure levels, had only a minor influence on the heat flux. It might be worth noting though, that a negative impact on the thermal as much as on the structural performance could be expected when the air pressure is not enough to maintain the shape of the cushion. Figure 5.44 shows a graph of the pressure loss of a sealed cushion sample over time. After an initial drop from 3 to 1 mbar due to air leakage of the sealed ETFE cushion, the pressure level stabilized and was maintained at approximately one millibar, or 100 Pascal, during the measurements, guaranteeing a consistent shape and section width of the cushion during measurements. Air-supply and pressure loss of the ETFE cushion sample is discussed in depth in the following section 5.4.2.

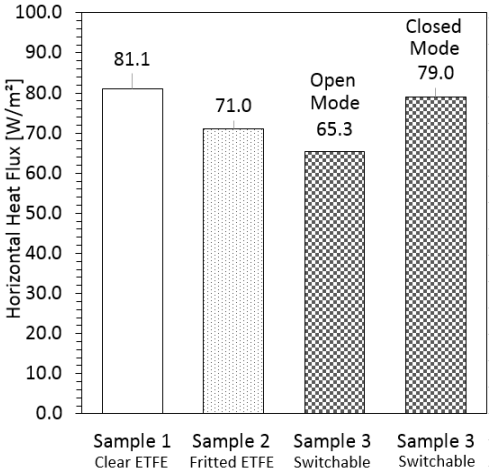


Figure 5. 43. Horizontal Heat Flux through ETFE cushion Samples at Standard Condition (S3)
(graph by the thesis author, unpublished)

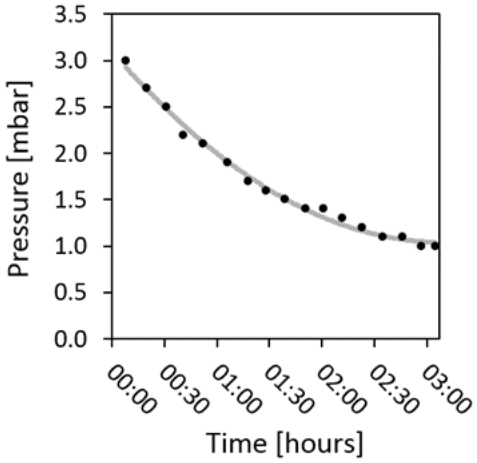


Figure 5. 44. Pressure drop of ETFE cushion, Sample No. 1 (double-layer, clear ETFE)
(graph by the thesis author, unpublished)

5.4.2. Air supply and pressure loss

The relative pressure loss of the cushions was different for all three samples, which could be explained by leakages through welding seals or valve connections that affect the airtightness of the cushions. A certain degree of leakage is desirable in the building application because it removes humidity from the cushions. However, for the experiment, it represents a variable difficult to control, as with the air also heat is escaping from the cushion. Therefore, the pressure loss was monitored during the tests, ensuring a minimum pressure of 1 mbar during the test in the climate chamber. The measurement of the pressure over time for sample number 1, presented in the previous section, 5.4.1, represents the worst case of all three samples. While the tendency of pressure loss for Sample 2 and 3 was similar, the period to reach the same pressure levels of the sample was elongated in comparison to Sample No. 1, hence more airtight. Scenarios with higher air-pressure (1.5, 2.0, 3.0 mbar) were also tested; however, the measurements showed that the air pressure has only a marginal influence on thermal performance compared to parameters of layer

built-up and foil surface treatment and is most likely related to the minimal dimensional change of the cushion due to the pressure loss.

During the dynamic air supply test, the air pressure was monitored continuously using the mass flow meter, ensuring constant air pressure during measurements. Due to tube length, a significant loss of pressure and flow volume came into play which, had been detected in the preparations of the experimental set-up. This effect was mitigated with bigger tube diameters (Inflow tube diameter = Ø 3.5 mm, Outflow tube diameter = Ø 5.0 mm) and choosing the shortest possible route for the tube in order to reduce the total length to a minimum. Additionally, it was opted for a more powerful air-pump. Other parameters of air supply such as the position of air in- and outlet, air volume and temperature are discussed in the following section.

5.4.3. Thermal performance of switchable ETFE cushion

The switchable ETFE cushion has the capacity to be set in two modes, open and closed. The printed middle layer is moved by air pressure from the inner to the outer position, allowing more or less light to be transmitted. The switching mechanism also influences the thermal performance. The horizontal heat flux through the cushion is ca. 15% lower in open mode than in closed mode, across all tested climate scenarios. This variation in thermal performance which appears to be in contradiction to the optical performance can be explained by the different emissivity and position of the printed and unprinted ETFE layers of the switchable cushion. To prove this hypothesis, heat flux sensors were positioned on the printed and unprinted outer surface at two different height levels of the cushion. An overview and a picture of the sensor position is shown in Figure 5.45.

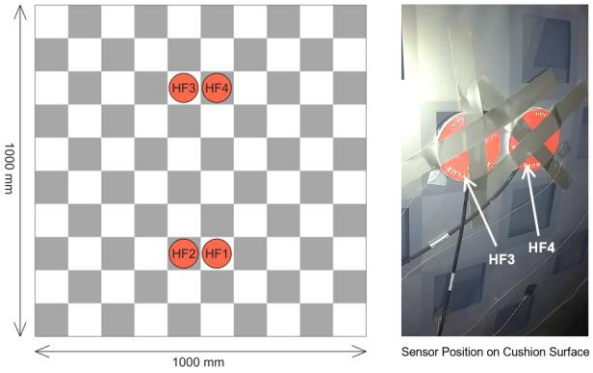


Figure 5. 45. Position of heat flux meter at different frit print locations on the cushion surface
(image and photo by the thesis author, unpublished)

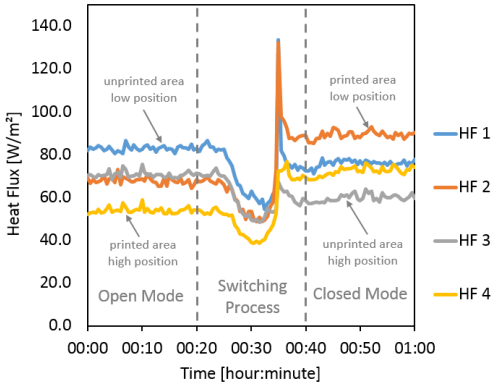


Figure 5. 46. Heat flux at different positions on cushion surface during the switching process
(graph by the thesis author, unpublished)

The heat flux measurements were done before, during, and after the switching process. The measurements shown in the graph of Figure 5.46, reveal that in the open mode the heat-flux of the unprinted high position and the printed low position is almost the same approximately -70 W/m^2. In contrast, at the printed high position only ca. -55 W/m^2 are transmitted in the open mode. The unprinted low position transmits ca. -85 W/m^2. The mean heat-flux in the open mode of all measured positions is ca. -70 W/m^2. When switched to close mode the mean heat-flux increases to ca. -75 W/m^2. In the closed mode the heat-flux through printed low position increases from ca. -70 W/m^2 to ca -90 W/m^2 while the heat-flux decreases at the high unprinted position from ca -70 W/m^2 to ca -60 W/m^2. From the data plot, it can further be seen that heat-flux increases at the printed high position to ca. -75 W/m^2. The heat-flux at the low unprinted increases from ca. -75 to -80 W/m^2. Measurements of the heat flux during the switching process were not evaluated further, due to the unpredictable folding and bending movement of the middle layer inside the cushion during the switching process, which made it difficult to relate the measurements to any meaningful explanation. In summary, the overall results can be interpreted as follows:

In open mode, the light transmittance increases, and the heat flux decreases; In closed mode, the light transmittance decreases, and the heat flux increases. However, this behaviour requires more detailed investigation. It was speculated that it could be explained with the additional thermal resistance created by the second air gap between the middle and outer layers during the switching process, and remaining air pockets after the switching process is completed and full layer contact achieved. Another plausible explanation is related to the different emissivity of the printed and unprinted areas of the layers and the way they overlap in the open and closed mode. To clarify the different heat exchange mechanisms during the switching process, a series of diagrams is sketched in Figure 5.47, showing a printed and unprinted section of the cushion sample in open and closed mode, which exemplify the distinctive thermal performance of the switchable ETFE cushion observed during the experiments. What was surprising to see from the measurements is that the overall heat flux is higher in the closed mode than in the open mode. The remaining question is if this is beneficial or not when the system is employed as a space enclosing building envelope, considering the overall energy performance of a building. Further studies, employing whole building daylighting and energy simulations, reported in chapter seven and eight, provide answers to this question and discuss the conditions under which switchable ETFE cushions enhance the building performance most effectively.

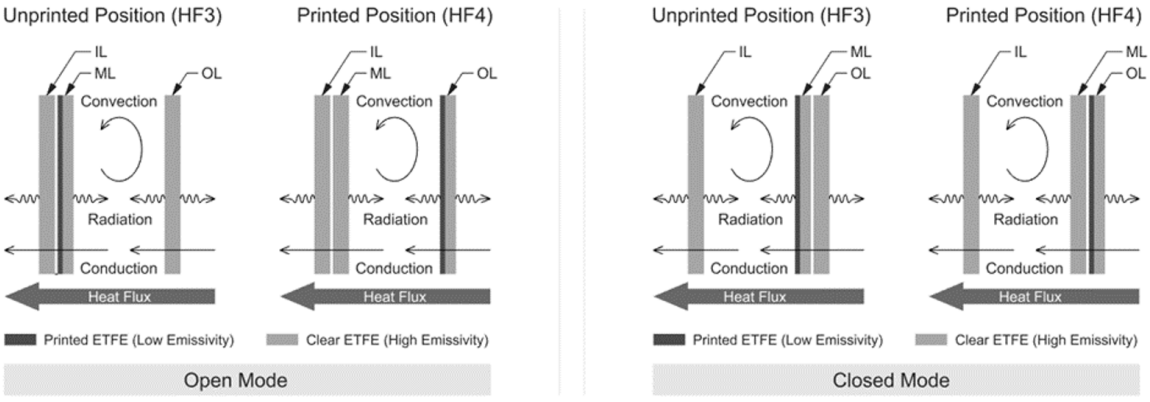


Figure 5. 47. Thermal exchange mechanisms at different frit print locations (Sensor Position HF3 and HF4) on the switchable cushion for open and closed mode (diagrams by the thesis author, unpublished)

5.4.4. Thermal performance with dynamic air-supply

This section reports on the effects of dynamically controlled air supply of a clear double layer ETFE cushion under summer and winter conditions, with varying air temperature and flowrate. The ETFE cushion was inflated with temperature-controlled air (15°C, 20°C, 25°C) provided from a baffle tank at a controlled flow rate of 1, 2, 3 slpm (standard litre per minute), corresponding to an hourly air change rate (ACPH) of 0.7, 1.4, 2.0 ach-1, respectively. While the air-supply-rate of the cushion was effectively controlled with an adjustable valve and the flow meter, it was only possible to keep the air temperature at a constant inflow temperature of -9.2°C during the winter scenario and 28.5° during the summer scenario, which resembles the air temperature of the corresponding climate chamber room. Insulation of the tubes was not sufficient to provide the air at the desired temperatures. Therefore, the different temperature levels of the supply air provided by the baffle tank and HVAC unit was considered only to a limited extent in the following analysis. The graphs in Figure 5.48 and 5.49 show the mean transversal heat flux through the ETFE cushion at different mass flow rates during the summer and winter scenario.

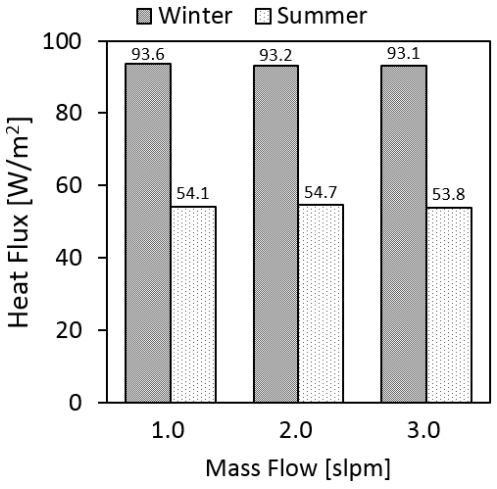


Figure 5. 48. Total Transversal Heat Flux through ETFE cushion (Sample 1, clear) (graph by the thesis author, unpublished)

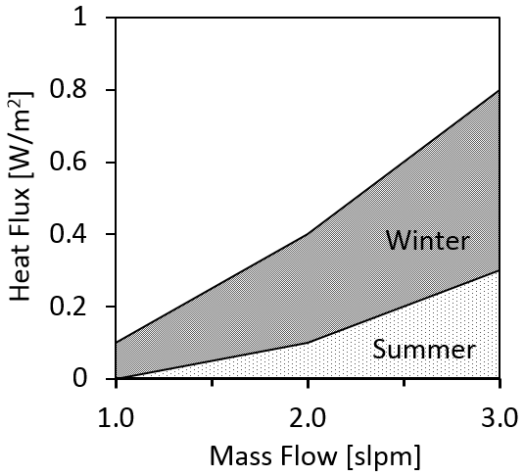


Figure 5. 49. Air-supply induced heat-flux through ETFE cushion for different flow rates, Sample 1 (clear) (graph by the thesis author, unpublished)

The difference of heat flowrate for summer and winter condition might be explained by the different air-temperatures and resulting surface and inner chamber air temperature of the cushion. The difference of the in- and outflow temperature of the air-supply is affected by the temperature of the air volume inside the cushion. The air temperature of the cushion inner air is a resultant of the left and right temperature in the baffle zone of the climate chamber. While the mean temperature of the cushion layer surfaces was monitored extensively it was not possible to measure the inside air temperature of the cushion during this experiment. However, the air temperature of the outflow stream provides an approximate indication of the actual air temperature inside the cushion, considering that the air inside the cushion has not yet mixed thoroughly with the inflowing air during the first seconds after the air pump has started operating.

In order to determine the effect of the air-supply on the thermal performance of the ETFE cushion, Q_1 transversal and Q_2 air-supply was calculated from the test results and compared to each other to obtain a realistic evaluation of the magnitude of the heat flux of both energy exchange mechanisms. For the calculation of Q the following equation 5.3 was used:

$$Q = mc\,\Delta T$$

Equation 5. 3

Where Q is the energy (1 W = 1 J/s) removed or added from/to the ETFE cushion by the air-supply induced mass flow, which is m in kg/s and can be expressed in standard litre per minute (slpm), c is the specific heat capacity of air at 14°C at one bara (C_{pAir}). Q is then given in W/m^2 by dividing Q with the cushion surface area, which allows the transversal heat flux through the cushion to be compared with the air supply induced heat flux. The magnitude and proportion of the air-supply induced heat flux relative to the transversal heat flux can be observed in Figure 5.50 A and B.

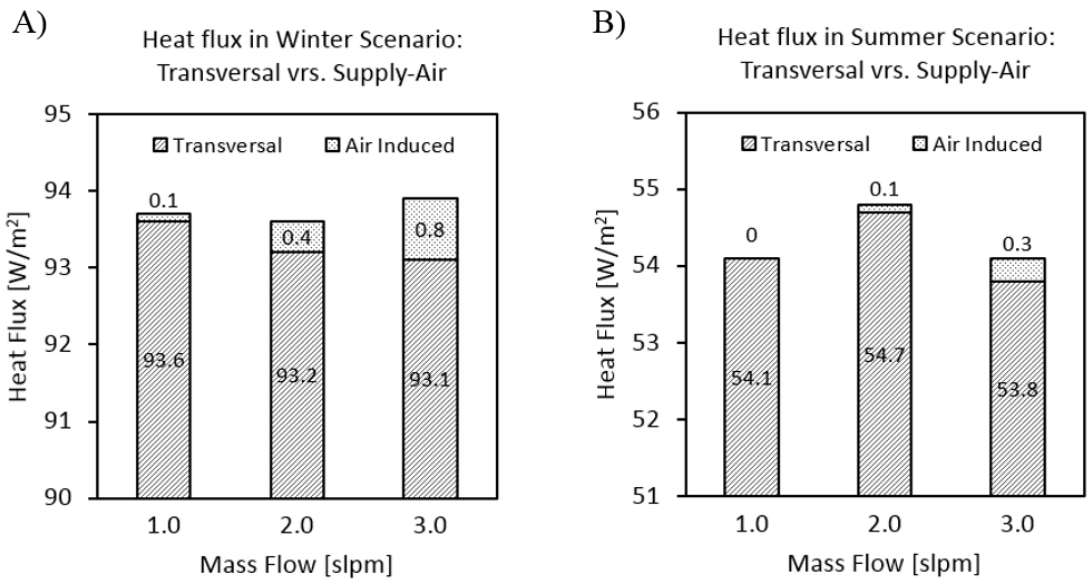


Figure 5. 50. Air-supply induced heat flux relative to the transversal heat flux for the winter scenario (A) and the summer scenario (B)
(graphs by the thesis author, unpublished)

Table 5.11 shows the magnitude of the transversal heat flux through the cushion with the air-supply turned on and off. The cushion was inflated to a minimum pressure of 100 Pa and sealed. When steady-state conditions were achieved, the measurements were taken for an extended period (1 hour). While the cushion was constantly losing pressure any influence on the heat flux measurements, by changes of the geometric shape, was avoided by limiting the time period and pressure level. After the measurement without air-supply, the air pump was switched on, and preconditioned air with a constant temperature was pumped thorough the cushion at different flowrates (1.0 – 3.0 slpm). When a steady-state was achieved the heat flux and surface temperatures were measured at different positions on the cushion. These tests were conducted for a winter and summer scenario.

Table 5. 11
Transversal-Horizontal heat-flux through ETFE cushion, sample 1 (2 layers, clear), (table by the thesis author, unpublished)

Scenarios	Air -supply	1 slpm Mass Flow	2 slpm Mass Flow	3 slpm Mass Flow
Winter	On	93.6 W/m^2	93.2 W/m^2	93.1 W/m^2
Winter	OFF	93.5 W/m^2	93.7 W/m^2	93.5 W/m^2
Summer	On	54.1 W/m^2	54.7 W/m^2	53.8 W/m^2
Summer	OFF	54.0 W/m^2	54.0 W/m^2	54.0 W/m^2

It is clear from the comparison of the magnitude of heat flux between air-supply induced and temperature difference from inside and outside condition that the airflow rate of the air supply has only a minimal influence on the thermal performance of the ETFE cushion. Also, the different positions for inflow and outflow valves had no significant influence on heat transfer of the ETFE cushions. However, it is still unclear if under more realistic testing conditions, including solar radiation gains, the increased air exchange will a have a significant impact on the thermal transmittance of the ETFE cushion by adding or removing temperate air. As a preliminary conclusion, it can be said that the air-supply induced *Q* is too small in comparison to the transversal *Q* in order to have any relevant impact on the thermal performance. Nevertheless, higher flow rates might be still beneficial for the effective removal of moisture from the ETFE cushion if the air is preheated or dried. Also, heating of the circulated air through solar heat gains could increase energy savings when this preconditioned air is looped back into the ventilation system of the building or energy extracted and stored via heat exchangers. This is a technology which had been explored for thermal energy storage in a recent experimental membrane structure project at the Institute of Textile Technology and Process Engineering (DITF) in Denkendorf, Germany [Stegmaier et al., 2018].

5.4.5. Comparison of experimental and calculated results

The results of the numerical calculation method were compared with experimental results at five different scenarios for the clear Sample No.1. Specifically, the scenario 3 is the standard test condition, which specified in CEN BS EN 673-1998 [CEN, 2011] states that the internal and external surface temperature should be set 17.5°C and 2.5°C, respectively. During the experimental procedure, however, the internal free stream surface temperature settled only at 27.9°C and the external surface free stream temperature at 7.4°C with resultant internal and external surface temperatures of 17.0°C and 4.1°C, respectively. In order to match the experimental condition, the surface temperature was set in the calculation to the same values, deviating marginally from the established standard condition. The calculated heat flux and the thermal resistance values of the double layer clear ETFE cushion for the five climate scenarios are shown in Table 5.12.

Table 5. 12
Calculated results for heat flux and R-value of a clear double layer ETFE cushion for different climate scenarios
(table by the thesis author, unpublished)

Parameters / Scenarios	Unit	S. 1	S.2	S.3	S. 4	S. 5
Heat Flux	[W/m^2]	38.2	53.5	74	88.7	82.8
R-Value	[K·m^2/W]	0.1886	0.1812	0.1743	0.1658	0.1752

The comparison between the experimental and calculated values of the heat flux as well as the R-value is shown in Figures 5.51 to 5.54. The calculated values follow a similar trend as the experimentally measured values throughout all climate scenarios. However, the calculated heat flux is, on average, 8.6% lower than the measurements had shown. In contrast, the calculated R-value is, on average, 8.3% higher than the R-value calculated with the measured values as a basis. Further studies may also include the theoretical calculation of printed or switchable ETFE cushion when more detailed information on thermal and optical material data of the frit prints becomes available.

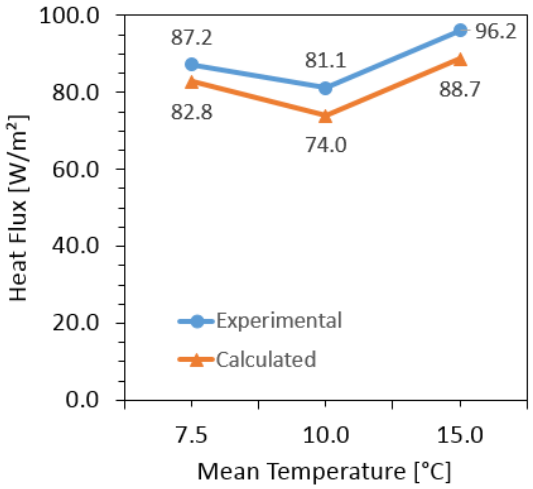


Figure 5. 51. Heat Flux through clear double layer ETFE cushion, sample No.1 (Temperature Difference 15°C)
(graph by the thesis author, unpublished)

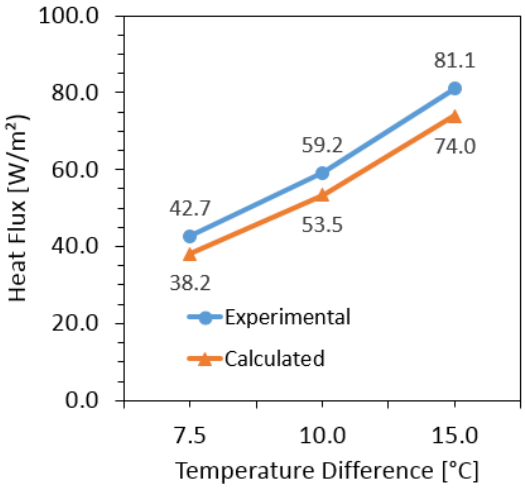


Figure 5. 52. Heat Flux through clear double layer ETFE cushion, sample No.1 (Mean Temperature 10°C)
(graph by the thesis author, unpublished)

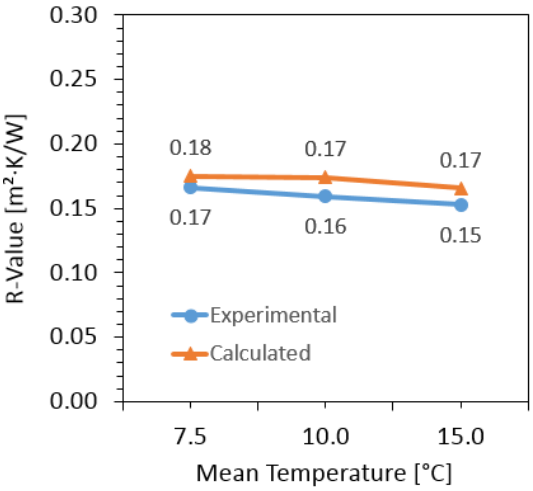


Figure 5. 53: R-Value for a clear double layer ETFE cushion, sample No.1 (Temperature Difference 15°C)
(graph by the thesis author, unpublished)

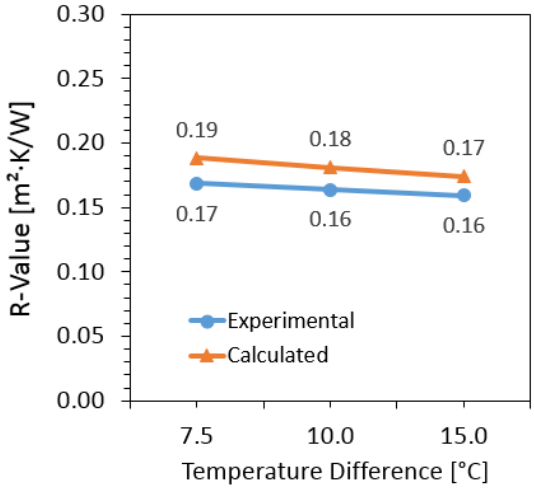


Figure 5. 54: R-Value for a clear double layer ETFE cushion, sample No.1 (Mean Temperature 10°C)
(graph by the thesis author, unpublished)

5.5. Chapter summary

The study presented in this chapter set out to investigate the thermal performance of switchable printed ETFE foil cushions under varying climate conditions. Experimental measurements were conducted in a large climate chamber on three ETFE cushion, comparing the performance of the switchable cushion with conventional clear and fritted. The obtained data was compared with numerical calculations which showed good agreement and provide confidence for further studies to use standard calculations as a tool for approximate preliminary estimations on the thermal performance of double and triple layer ETFE cushions without having to incur on time and resource expensive experiments or computer simulations. The most obvious, but also most important finding to emerge from this study is the high susceptibility of the thermal performance of pneumatic foil constructions to changing conditions of indoor and outdoor temperatures. This is of significance for the design of building envelopes using this type of construction and material in different climate zones.

While the comparison of the three distinctive designs showed only a minimal effect of air supply flow rates on the thermal performance of the cushion units, the analysis of the reflective frit print showed that the frit print reduces the heat flux of the whole cushion effectively. Switchable frit prints allow to modify the heat flux, which is hypothesized to come to effect due to the different emissivity of the printed and unprinted front and backside of the ETFE foil. The present study confirms previous findings and provides additional evidence of the importance of reflective frit prints for the overall thermal performance of ETFE foil cushions. Adaptive technologies like the switchable frit pattern might offer benefits beyond solar and daylighting control as they are capable of moderating the heat-flux effectively under different climate conditions. Further studies with a focus on heat transfer through solar radiation is therefore suggested, as well as whole building energy and daylighting simulations. These two topics will be explored and discussed in the following chapters six and seven incorporating material data of the investigated ETFE.

Chapter 6: Daylighting Performance

6.1. Introduction to chapter six

Natural lighting in buildings is essential for enhancing user comfort and reducing energy consumption. In chapter four, the optical performance of switchable ETFE cushion with different geometries types, frit patterns and ink types was investigated. This chapter builds up largely on the findings of the optical characterisation. It addresses the application in building envelopes with a focus on the natural daylighting qualities of spaces enclosed by multi-layer foil constructions and explores the potential for retrofits of outdated office buildings with ETFE double-skin façades (DSF). Building envelopes of ethylen-tetrafluorethylen (ETFE) allow daylight to enter the building almost unrestricted due to their high transparency [J. Knippers et al., 2011]. This can be beneficial when less light is available, for instance in high latitudes during winter, or may provoke problems of glare and excessive lighting during summer, in regions closer to the equator [Monticelli et al., 2013]. Novel switchable ETFE cushions have the capacity to control the incident daylight and moderate the internal lighting conditions of buildings by adapting actively according to weather and seasonal changes of solar radiation [Chiu & Lin, 2015]. Employing adaptive ETFE in double-skin façades may also improve the overall building energy performance while providing individual control autonomy to occupants over the environmental conditions of internal spaces. Validated daylighting simulation software Radiance was used to generate dynamic metrics data for a comprehensive understanding of the daylighting performance of ETFE double-skin façades. BSDF (Bidirectional-Scattering Distribution-Function) data of different cushion designs were derived from spectral analysis and used within the simulation process to accurately model the specular and diffuse light transmission and reflection of the different ETFE cushion designs. Aspects of cushion geometry, orientation and frit prints were considered in the modelling process. The combined use of various interconnected parametric software programs and plug-ins supported the five-phase simulation of different building and climate scenarios. The simulation results for useful daylight, glare probability and lighting uniformity provided

insights to the performance of switchable ETFE cushions for natural lighting in buildings by comparing them to conventional ETFE cushions and glazing systems. The results suggested that superior daylighting performance of the switchable ETFE cushion across different climates. However, the most significant advantages over conventional static DSF were achieved for façades with large window to wall ratios.

6.2. Retrofitting Office Façades: Improving daylighting performance with ETFE

The enhancement of natural daylighting in buildings is a physiological need, for human comfort and well-being, and a critical strand on the pathway to reducing the energy consumption of the building sector, which is necessary to achieve the goals of the agenda against climate change. Studies have shown that fenestration type and size in building envelopes have a significant impact on the overall energy consumption of buildings [Shen & Tzempelikos, 2012; Yu et al., 2015] and it is estimated that energy consumption for artificial lighting in buildings accounts for approximately 15-20% of the global electric energy consumption [Pellegrino et al., 2017]. While new buildings offer the opportunity to incorporate design considerations for sufficient natural daylighting, older buildings often lack this opportunity to save energy. Retrofitting of windows and shading devices of outdated buildings for improving the internal daylighting conditions is often limited by multiple factors. The building fabric of old buildings is either unsuitable for major changes due to structural limitations, or construction costs are too high for the modification of inflexible building systems [Bedon et al., 2018]. As a result of this situation demolition and new construction is preferred in most cases, which unfortunately might add to the problem of excessive energy and material consumption in the building industry. Added double-skin façades of ethylen-tetrafluorethylen ETFE might be a solution to the problem, offering a lightweight, flexible, and highly transparent building systems. Figure 6.55 A shows a picture of an office building built in 1959 on the campus of the University of Nottingham. Figure 6.55 B renders an artistic visualization of the proposed retrofit design of the building incorporating a secondary building envelope of switchable ETFE cushions.

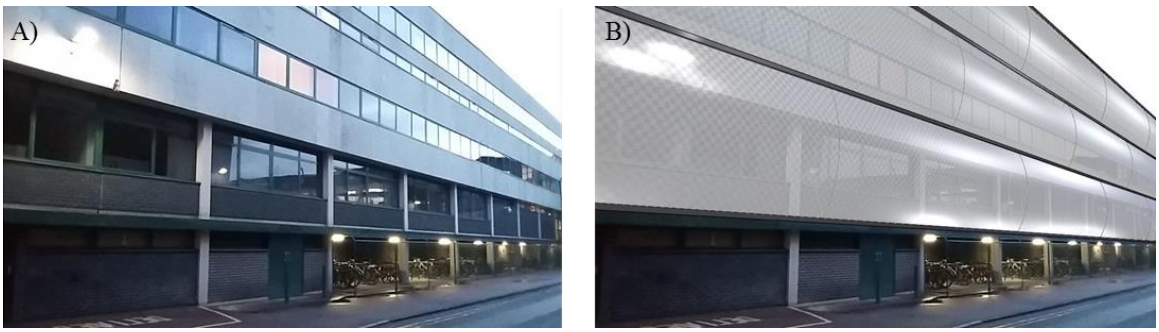


Figure 6. 55. A) Photography of a south-east facing façade of an office building, at the University of Nottingham, UK. Image B) shows an artistic rendering of a switchable ETFE double-skin façade added to the original building as a measure of retrofitting (photo and rendering by the thesis author, unpublished)

This retrofitting measure could improve the natural lighting condition having the cushions adapted with a switchable mechanism to different condition of solar radiation and potentially also lead to energy saving for heating and cooling [Gyeong et al. 2014]. Double-skin façades have been studied extensively and proven to enhance not only the daylighting and thermal performance but also to reduce the energy consumption the of the building [Shameri et al., 2011; Tang et al., 2018]. In architectural terms, the retrofit of the above-illustrated example might even contribute to creating a contemporary image of a high-tech University while conserving the original building. The same strategy may also apply for outdated office buildings in general as a good starting point for a financially sustainable process of upgrading old building stock in urban environments. Retrofitting of outdated office buildings with a double-skin façade of EFTE foil cushions would improve the energy performance of the global building stock much faster than replacing them with new buildings.

Additionally, this process could possibly lead to positive side effects on multiple levels, as it would make outdated buildings with better daylighting architecturally and therefore, financially more attractive [Turan et al., 2020]. The considerations about the value of daylighting go in hand with the changing global working culture, which is challenging traditional concepts on the design and use of office spaces. While open-plan

spaces populated with office cubicles were commonly introduced from the 1960s onward, nowadays a mix of single rooms, group rooms and rooms of flexible use is a more convenient space distribution scheme. Smaller room divisions with less room depth and access to operable light-controlling façade elements may lead to better natural daylighting conditions and a reduction of glare. Literature suggests that these measures could substantially improve the well-being and productivity of office occupants while reducing energy demand for artificial lighting [Al Horr et al., 2016]. However, it has been observed that while office spaces get subdivided and smaller, individuals tend to be less tolerant of comfort conditions and express their desire for a higher degree of control over their working environment. However, it is also known that people adjust environmental conditions of their working space only to a limited extent [Wienold, 2007], leaving windows open or sunscreens closed, for a longer time than needed, resulting in excessive energy use for air-conditioning, heating or artificial lighting. To avoid this dilemma between the individual demand for control autonomy of the environmental space conditions and the global goal of saving energy in the building sector, a second building envelope which acts as a buffer zone is proposed. An adaptive second building envelope, wrapping the building, could create independent of the individual user preference, favourable lighting and thermal condition, which would allow windows and shades of the primary building façade to operate without compromising the overall building performance. Low-rise office buildings with five to seven floors and a regular column–beam–slab concrete structure might exhibit the characteristics suitable for retrofit with a lightweight secondary skin of ETFE. A visualization of the building system and a detailed section of an office room with a double-skin façade integrating an ETFE foil cushion can be seen in Figure 6.56 A and B.

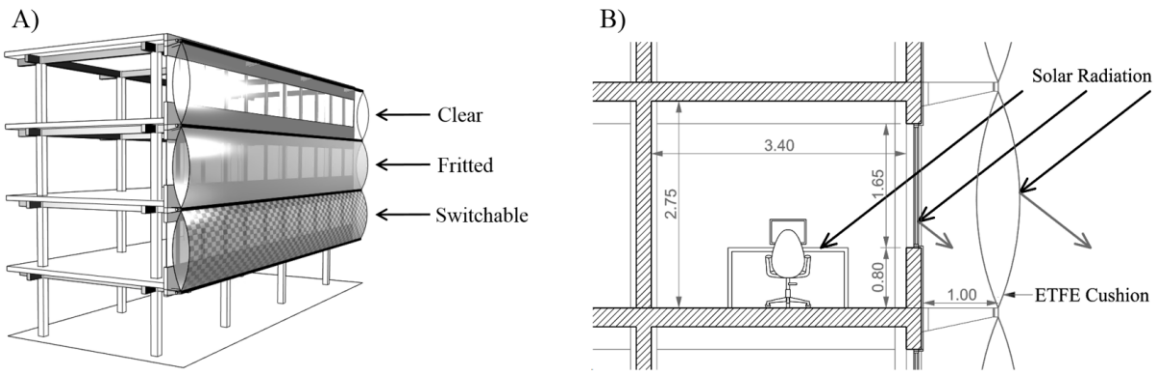


Figure 6. 56. A) Visualization of a structure of a typical low-rise office building with a double-kin façade with different ETFE foil types. B) Section of a typical single-unit office room with an ETFE double-skin façade showing the reflected and transmitted rays of solar radiation at the different layers of the building envelope
(images by the thesis author, unpublished)

Built examples for the use of ETFE in building envelopes are encountered frequently [Wieser, 2008; Risen, 2017] since the erection of the first permanent ETFE structure in 1983 in Arnheim, Netherlands. Most commonly ETFE foil has been employed as a structural or cladding material for coverings of large-scale sports or cultural constructions, where inflated multi-layer systems are usually preferred over single layer mechanically tensioned systems [Tanno, 1997; Moritz & Barthel, 2003]. In recent years the use of ETFE has been expanded to a greater variety of building typologies including educational, commercial or office buildings. However, a study which investigated sustainable trends of pneumatic skins in architecture found that only 15.6% of a sample of 412 projects where ETFE is employed were based on an existing building while most of the buildings with ETFE are new constructions [Gómez-González et al. 2011]. Within the group of newly built ETFE constructions, an emerging category using ETFE as a secondary layer of a double skin façade (DSF) has become more visible over the last decade [Grunwald, 2007]. Double-skin façades have the potential to improve the thermal and natural lighting performance of the building envelope and may lead to substantial energy savings of buildings [Ward et al., 2010; Cremers, 2011]. Current research suggests that

this might also be true for DSF with ETFE [Juaristi & Monge-Barrio, 2016]. Several built projects of this design approach are listed in Table 6.13 and examples can be seen in the pictures of Figure 6.57 A, B and C.

Table 6. 13

Double skin façade buildings with ETFE

(table by the thesis author, unpublished)

Project Name	Year of Completion	Location	ETFE façade type	Switchable
The Shed	2019	New York, US	multilayer	no
IIT Innovation Center	2018	Chicago, US	multilayer	yes
US Embassy	2017	London, UK	single layer	no
Canary Wharf Crossrail Station	2015	London, UK	multilayer	no
Tic-Media Building	2010	Barcelona, Spain	multilayer	yes
Unilever Headquarters	2009	Hamburg, Germany	single layer	no
Centre for Gerontology	2003	Bad Tölz, Germany	single layer	no

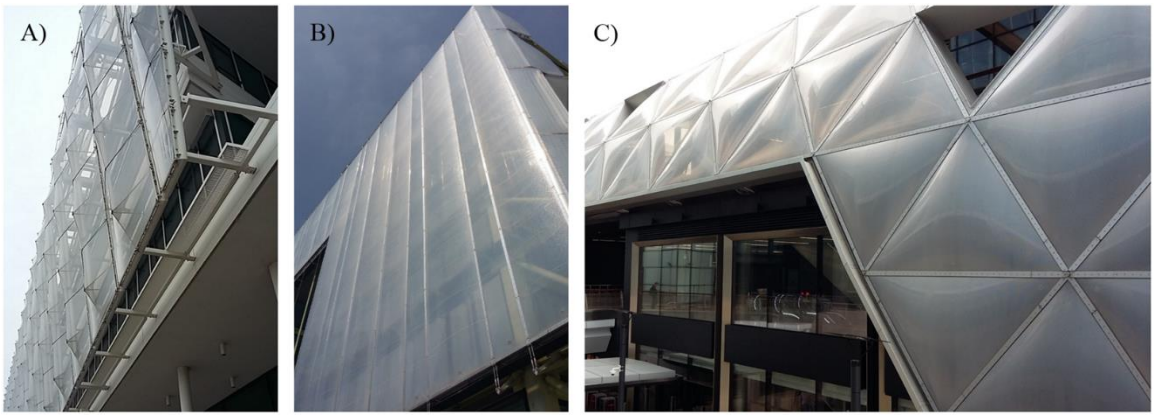


Figure 6. 57. Double-skin façades with ETFE A) Unilever Headquarter in Hamburg, with single-layer clear ETFE foil; B) Tic-Media Building in Barcelona with double layer ETFE foil cushion, switchable with nitrogen gas injection; C) Canary Wharf Crossrail Station in London with fritted double-layer ETFE foil cushion

(photos by the thesis author, taken during 2016 and 2017, unpublished)

While most of the ETFE buildings are located in the northern latitude between 50 and 60 degrees, the southern latitudes are less populated, with only rare examples to be found outside the temperate and humid conditions of the Köppen Cf climate zone [Gómez-González et al. 2011]. The applicability and benefits of DSF with ETFE in different climates is currently a question under investigation, and the hypothesis is that the employment of adaptive systems might be a part of the answer. A schematic section of an existing adaptive system for pneumatic ETFE foil cushion which has been employed in building envelopes and is investigated in this study, is shown in Figure 6.58 A and B. The air-inflated system consists of three layers of clear ETFE foil, with the outer and middle layer printed with a reflective shading mask. Each layer is shifted to cover the transparent areas of the other when overlapping. The middle layer can be changed in position from the outer to the inner layer by injecting air through valves into one or the other chamber. This process is reversible, allowing the cushion to switch from closed to open mode and back. When the two printed layers are separated from each other, the cushion is in 'open mode' (A), with one part of the incident light passing directly through the cushion while another part is reflected on the outer and middle layer with internal reflections. When the two printed layers are overlapping the cushion is in 'closed mode' (B), with only a minor part of the incident light passing through the cushion, diffused by the matching print masks. In the closed mode, the biggest part of the incident light is reflected by the reflective print mask on the overlapping outer and middle layer of the cushion. The interplay of specular and diffuse transmission and reflection between the clear and printed parts of the three ETFE layers is complex and further complicated by the three-dimensional double-curved geometry of the pneumatic structure. To accurately predict the daylighting qualities of spaces covered with switchable ETFE cushion a physics-based model describing the specular and diffuse light transmission and reflection, depicted in Figure 6.59 A and B is necessary. The methodological approach proposed in this chapter is to use the bidirectional scattering distribution function, to generate optical models of 3D ETFE foil cushions with mixed material combinations to investigate the impact of the adaptive shading mechanisms on DSF office spaces under different climate conditions.

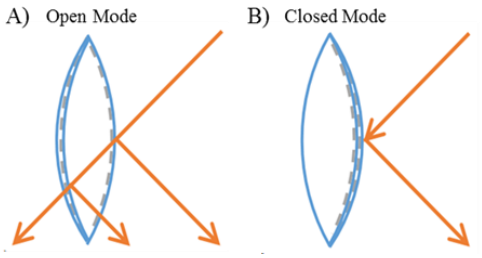


Figure 6. 58: Light transmission and reflection of a switchable ETFE cushion in the open (A) and closed mode (B)
(diagrams by the thesis author, unpublished)

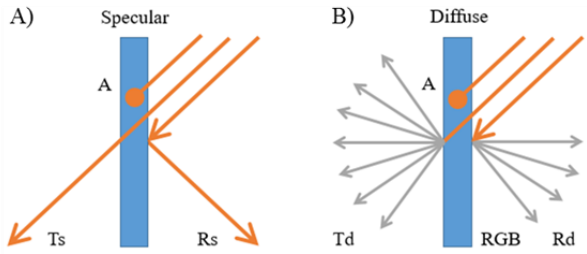


Figure 6. 59: Specular (A) and diffuse light transmission and reflection on a translucent material section
(diagrams by the thesis author, unpublished)

6.3. Methods

The workflow adopted for this daylighting study comprises a combination of experimental and digital methods supported by a network of simulation software [Roudsari et al., 2013; Roudsari, 2020]. Spectral analysis of ETFE material samples were conducted in a laboratory set-up provided the source data for applying the bi-directional scattering distribution function to generate detailed multi-angled optical models for the daylighting simulations. These were done with Radiance software (5.2.91 Release 2018-06-20, by Greg Ward at Lawrence Berkeley National Laboratory (LBNL) a part of the U.S. Department of Energy (DOE)), operated through HoneybeePlus (0.0.04 Release 2018-02-07, by Ladybug Tools LLC) as part of the Ladybug environmental analysis tools (0.0.65 Release 2017-28-07, by Ladybug Tools LLC) within the graphic programming plug-in Grasshopper (0.9 0076 Release 2014-08-27, by David Rutten at Robert McNeel & Associates) which operates on 3D modelling software Rhinoceros (5 SR7 64-bit 5.7.31213.18395 Educational Version Release 2013-12-13, by Robert McNeel & Associates),. Weather data and BSDF file are fed into Honeybee and compiled together with the model geometry, which is generated in Grasshopper/Rhinoceros, and sent to Radiance which acts as the calculation engine for the daylighting simulation. The results were transferred to the 3D environment

of Rhinoceros via the controls of Honeybee/Grasshopper for visualization and data post-processing [Subramaniam, 2018]. A simplified outline of the workflow and software tools used can be seen in Figure 6.60. A screenshot of the Grasshopper/Honeybee controls and the geometry with a result preview within the 3D environment of Rhinoceros is shown in Figure 6.61. The specific method for each of the above-resumed procedure is described in detail in the following sections.

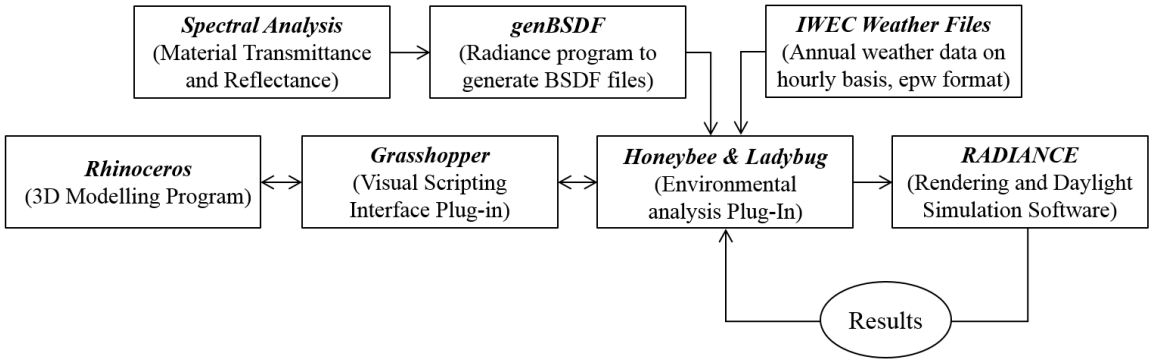


Figure 6. 60. Workflow diagram for daylight simulation, showing interconnectivity and data stream between software programs and plug-ins
(flow-diagram by the thesis author, unpublished)

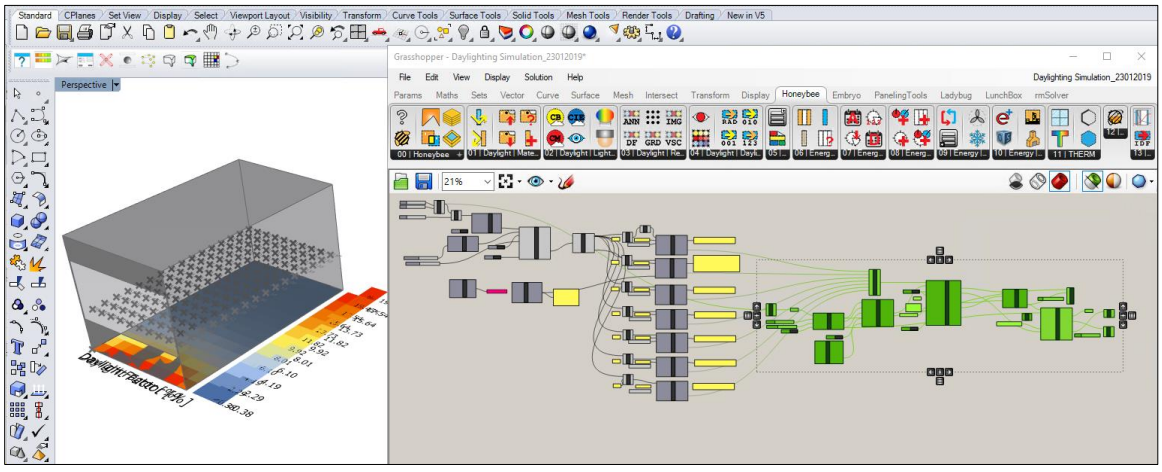


Figure 6. 61. Screenshot showing the office model generated in Rhinoceros with projected daylight simulation results and Grasshopper/Honeybee simulation definition
(screenshot by the thesis author, unpublished)

6.3.1. Measurement of optical properties of switchable ETFE foil

The approach adopted in this study for acquiring the optical properties of switchable ETFE foil was based on classical spectroscopy, where for each material section of printed foil the spectral characteristics of light transmission and reflection were determined individually. The post-processed data was then be applied in a second step to a virtual geometry which mirrors the inflated ETFE cushion which makes it then possible to generate the BSDF transmission matrix from the virtual model using the genBSDF program, which is part of Radiance software [Kohler, 2012]. The spectroscopy measurements necessary for this process were carried out for the visible light spectrum determining light transmittance and reflectance of the ETFE materials. Measurements were done on 210 mm x 297 mm material samples of clear 200 µm extruded ETFE foil printed with a silver ink pattern in two densities. The print pattern of the sample was composed in a square grid with unprinted, printed and densely printed areas containing all three types of material surface treatments used for the switchable ETFE cushion façade. All three surface areas were measured with a calibrated Ocean Optics spectrometer type USB+VIS-NIR-ES (H13465) and a Tungsten 4.75 W halogen light source with a wavelengths output from 360 to 2400 nm. The global and specular transmittance, as well as the global and diffuse reflectance, was measured at a wavelength ranging from 339 nm to 1024 nm. For the diffused light measurement, a collimating lens and an integrated sphere were utilized. The spectral data outputs were plotted with Ocean Optics, OceanView spectrometer operating software (1.6.7 Release 2018-08-03) and trimmed to a useful wavelength range from 380 nm to 780 nm, according to Dλ= relative spectral distribution of ISO 9050:2003(E) [ISO, 2003]. A picture of the material sample and spectroscopy set-up is shown in Figure 6.62 A and B. The global visual light transmittance T_{vis} and reflectance R_{vis} were calculated according to BS EN 410 [BS/EN, 2011]. The diffuse transmittance, specular reflectance and absorbance were calculated using the measured data according to the law of energy conservation [Jelle, 2013], where the sum of the transmittance *T*, absorbance *A* and reflectance *R* equals one over the range of measured wavelenght λ:

$$T(\lambda) + A(\lambda) + R(\lambda) = 1\ (100\ \%)$$

Equation 6. 4

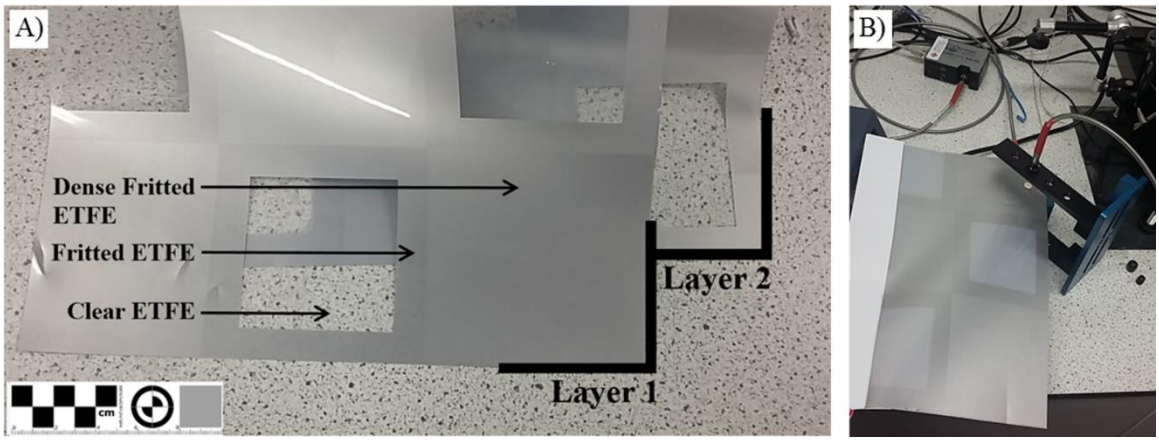


Figure 6. 62. Two layers of switchable ETFE foil samples *A)*, spectral analysis of ETFE standard light source and spectral sensor B)
(photos by the thesis author, unpublished)

In a second step, as part of the post-processing of the raw spectral distribution data and requirement for the generation of Radiance material definitions, measurement results were converted to RGB (red, green, blue) values, which can be represented on optical screens for rendering purposes. The data conversion process was guided by a theoretical description and calculation spreadsheets developed by Bruce Lindbloom [Lindbloom, 2019]. RGB values for the diffuse reflectance were calculated by using spectral measurements at a wavelength interval of 10 nm in the range of 380 to 780 nm, converting spectral data first to XYZ chromaticity coordinates for 2˚ and 10˚ of a standard observer and then transforming to RGB values, for different colour spaces of most used standards (CIE, Adobe, Apple). Outcomes for the RGB in different colour spaces for a D65 reference illuminance source generally present minor differences; therefore the CIE chromaticity coordinates were chosen as an appropriate standard since they are also used by Radiance to define the red green and blue channels [Ward & Shakespeare, 1998].

6.3.2. Modelling of ETFE Cushion and Material

The double-curved geometry of the inflated ETFE cushion was generated using RhinoMembrane V2.0 (64 Bit - 2.05 Release 2016-05-26, by ixRay ltd) [D'Anza, 2020], a plugin for Rhinoceros 3D software which uses the Update Reference Strategy (URS) [Bletzinger & Ramm, 1999] for modelling tensioned membrane structures. The URS is a generalized derivation of the force density method and applicable to tensioned membrane structures, such as an air-inflated ETFE foil cushion. Through a digital form-finding process, using Rhinoceros 5 (SR7 64-bit 5.7.31213.18395 Educational Version Release 2013-12-13, by Robert McNeel & Associates) in combination with the plug-in software Grasshopper (0.9 0076 Release 2014-08-27, by David Rutten at Robert McNeel & Associates) as a visual modelling space and control interface, respectively, a virtual ETFE cushion with analogue dimensions to a physical model was generated. The geometry represented an existing ETFE foil cushion of 1m x 1m with a maximum curvature displacement, or sag, of 10% on each side of the centerline, equating to a 0.2 m maximum distance between the layers at the centre of the cushion section. Although the chosen geometry is rather untypical compared to the type of geometry generally used for ETFE constructions (longitudinal, tube-like cushion modules are more common in the building industry), the symmetric layout makes it relatively easy to generate BSDF data which can be used independently of orientation. The form found geometry was meshed and re-edited to achieve a regularly laid out triangulated mesh which would facilitate a smoothed surface accelerated ray intersection during the daylight simulation [Ward & Shakespeare, 1998].

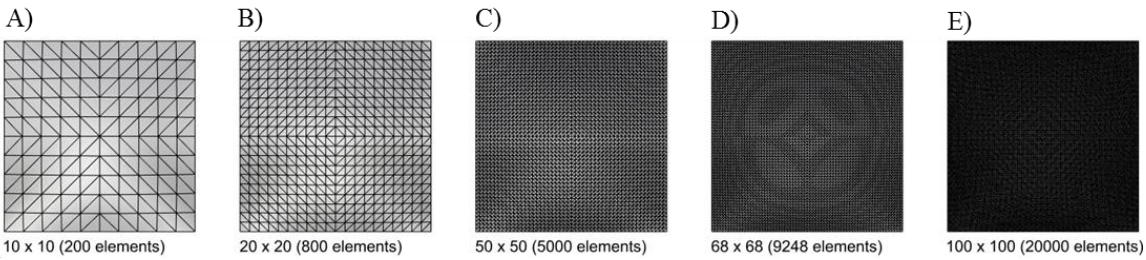


Figure 6. 63. Modelled cushion geometry with different mesh densities A), B), C), D), E) (images by the thesis author, unpublished)

To ensure accuracy of the shape, and a subsequent realistic optical behaviour, a mesh independence test with increasing mesh density was carried out. Five models, with a mesh density ranging from 200 to 20000 mesh face elements, were tested initially for curvature smoothness and mesh face planarity. Figure 6.63 shows the five cushion models in plan view with increasing mesh density from A) 10 x 10 to E) 100 x100. While the shape accuracy evidently increases with a higher number of mesh faces, so does the computational power to calculate and render the model. For the models D and E, the result deviation during the mesh independence test was found to be insignificant. Therefore, and for the sake of computational economy, it was opted for model D) as the final mesh geometry for the simulation campaign. With 9248 mesh faces Model D) has a high enough resolution for a smooth shape and a realistic simulation, but also can be handled computationally without the need for a high-performance computer (HPC). The mesh was further fine-tuned to accommodate the geometric pattern division of mesh faces necessary to fit the print pattern measures of the switchable ETFE material sample. The mesh was subdivided into three sub-meshes, and material definitions were assigned according to material sample to the mesh. The meshes of each material and layer were later recombined within Radiance to obtain a complete model of the triple-layer cushion. The ETFE material was modelled as a Radiance 'trans material' based on the results from the spectral analysis. A 'trans' material, selected as the closest fit to the characteristics of ETFE among the Radiance material options [Reinhart et al.; 2006], is described by Greg Ward the creator of Radiance as a:

"[…] translucent material, similar to plastic. The transmissivity is the fraction of penetrating light that travels all the way through the material. The transmitted specular component is the fraction of transmitted light that is not diffusely scattered. Transmitted and diffusely reflected light is modified by the material color. Translucent objects are infinitely thin." [Ward & Shakespeare, 1998].

Together with diffuse and specular transmittance and reflectance data, RGBs, surface roughness and the refractive index informed the input parameters for generating the material definition of clear, fritted and densely fritted ETFE foil. While for the semi-transparent fritted ETFE material the diffuse reflectance RGB values could be used directly, for the highly transparent ETFE material an average photopic value Rd of the RGB had to be calculated and adjusted to fit as an appropriate input for the diffuse reflectance channels (Rd = 0.052). The RGB transmission values were then converted to transmissivity to fit the requirements of the radiosity method of Radiance software.

To determine the surface roughness a comparable silver fritted 200 µm ETFE foil was measured with a Mitaka PF-60 point autofocus probe surface texture measuring instrument scanning the sample surface with (50µm/s) using a 100X (NA = 0.8, WD = 3.4mm) objective. The height parameters of measurements were evaluated according to ISO 25178 with values of Sz = 4.62µm and Sa = 0.270µm. From the section derived from the measurements, the surface roughness Ra for the clear ETFE and the fritted area was estimated to be very low similar to a polished surface. Even though the frit pattern of the measured sample was different from the switchable frit print, it was further assumed that the surface properties of the ETFE and frit surface would be comparable, and a dimensionless value of 0.001 was assumed for the simulation settings.

The refractive index of the material indicates how much the path of a light ray is bent by passing through the material relative to its initial incident angle on the surface. According to manufacturer's material data sheets (Norton® ETFE Fluoropolymere Film SAINT-GOBAIN Performance Plastics, Tefzel™ ETFE Fluoropolymer Film) ETFE has a refractive index of n = 1.40 following the ASTM testing method D-542. The summarized input parameters used for the material definition of the preliminary Radiance model is shown in Table 6.14. Figure 6.64 shows the 3D mesh model for the switchable triple-layer ETFE cushion in perspective, side and front view with all materials assigned. Figure 6.65 shows the initial custom-made 'trans' Radiance material definitions for the three different ETFE materials.

Table 6. 14

Grasshopper/Honeybee Input parameters for Radiance 'trans' material generator (table by the thesis author, unpublished)

Input Parameter		Clear ETFE foil	Fritted ETFE foil	Dense Fritted ETFE Foil
Diffuse Reflectance (Red Channel)	Cr	0.131	0.615	0.665
Diffuse Reflectance (Green Channel)	Cg	0.190	0.622	0.669
Diffuse Reflectance (Blue Channel)	Cb	0.271	0.652	0.696
Specular Reflectance	Rs	0.038	0.106	0.120
Diffuse Transmittance	Td	0.092	0.169	0.036
Specular Transmittance	Ts	0.818	0.061	0.004
Surface Roughness	Sr	0.001	0.001	0.001

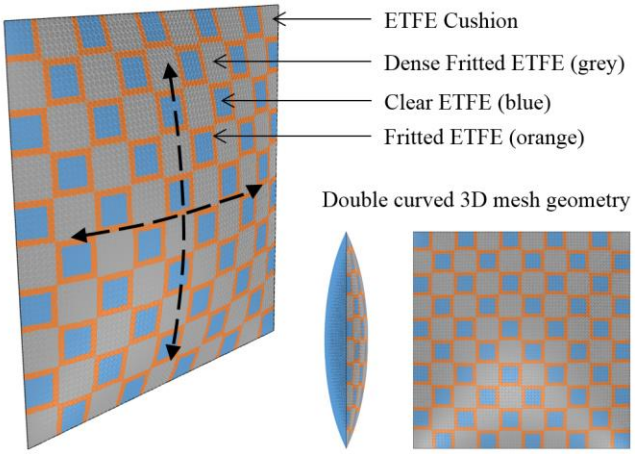


Figure 6. 64. Cushion geometry (perspective, section and plan view) with assigned materials (images by the thesis author, unpublished)

```
void trans DenseFrittedETFEspectrum
0
0
7 0.801 0.806 0.838 0.120 0.000 0.056 0.100

void trans ClearETFEspectrum
0
0
7 1.000 1.000 1.000 0.038 0.001 0.946 0.899

void trans FrittedETFEspectrum
0
0
7 0.942 0.953 0.999 0.106 0.001 0.270 0.265
```

Figure 6. 65. Radiance custom ETFE material definitions (codes by the thesis author, unpublished)

6.3.3. Bidirectional-scattering-distribution-function (BSDF)

Realistic physics-based simulations of the optical behaviour of complex fenestration systems, such as multi-layer ETFE foil cushions, require a high degree of computational power to calculate the multiple reflections between different layers of

material [Capperucci, 2019]. For materials with non-specular light transmittance properties, as in the case of printed ETFE foils, the scattered light is a considerable fraction of the overall transmitted light [Deroisy et al., 2013]. Understanding the angular distribution of specular and diffused light transmitted and reflected by the three-dimensional, multi-material and multi-layered shape of the ETFE cushion is crucial to quantify the overall lighting performance of covered spaces [McNeil, 2013]. The bidirectional-scattering-distribution-function takes a different approach to this problem. Instead of using a complete 3D model within the daylighting simulation, the model's transmittance, reflectance and absorbance are precalculated for a range of hemispherical incidence angles. Klems had proposed a system where a material geometry with assigned material properties is placed between two vertical hemispheres with a subdivision of 145 angular base patches. For each patch of the sphere an incident ray, perpendicular to the patch surface, is traced through the virtual material sample. On the backside of the material for each angular patch direction, the flux is accounted for. For the multi-layer cushion, also internal reflection and transmission are taken into account. The final model matrix holds the exact value of transmittance and reflectance on both sides of the model for each of the 145 angular patches of the vertical hemisphere [Klems, 1994]. A schematic diagram showing the principle of the BSDF generation with one incident ray on the Klems hemisphere angle basis is depicted in Figure 6.66 A. The distribution of the 145 angle basis patches on the coordinate system of the Klems hemisphere is shown in a plan view in Figure 6.66 B. The calculation for the above-described process is performed by the Radiance program genBSDF. BSDF data-based simulation models have been validated previously [McNeil, A., et al. 2013] and are the state-of-the-art practice for optical simulation studies of CFS [Ward, 2011; Molina et al., 2015; Grobe et al., 2015; Mainini et al., 2019]. However, due to the complexity of the model and compromised by the lack of validated simulation results of ETFE foil cushions in the literature, an indicative comparison test of the virtual and real size mock-up was performed, comparing the Radiance simulation results with the BSDF data for the switchable cushion in open mode, with the real switchable cushion. The testing conditions of a black non-reflecting testing

box were mirrored in the simulation as well as the diffuse sky conditions of a cloudy sky with approximately 10000 lux, measured on the day of the experiment. The measurement positions were ten aligned points in the depth direction of the test box on the lower (Z=0) horizontal centre line axis. The measurement device was a calibrated CEN multifunction environment meter, type DT-8820, attachable luxmeter with an accuracy of ±(5.0%+10d), manufactured by Shenzhen Everbest Machinery Industry CO., LTD. In Figure 6.67 pictures show the real mock-up of the switchable ETFE cushion (A), the lux-meter measuring probe for the experimental measurements inside the ETFE cushion mock-up (B) and an image of the mirrored virtual model with a horizontal test point grid (C).

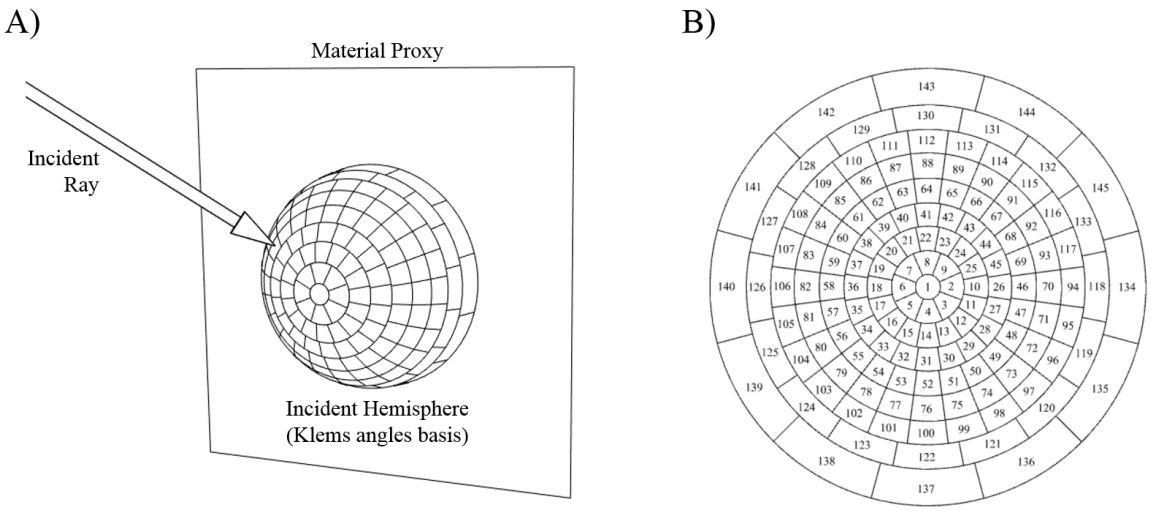


Figure 6. 66. A) Schematic diagram showing principle of BSDF generation. B) depicts a plan view of the Klems hemispheres with 145 subdivided patches of ray incidence angles (images by the thesis author, unpublished)

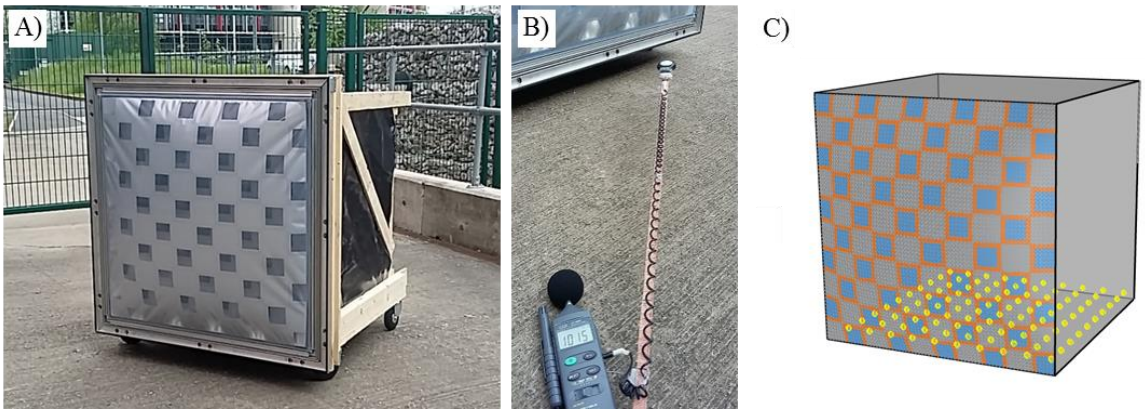


Figure 6. 67. A) Mock-up of switchable ETFE cushion with a solar shielded black box; B) Illuminance meter with extended luminance sensor that was introduced to the box; C) analogue digital model with assigned material data and black box with test points (photos and image by the thesis author, unpublished)

6.3.4. Simulation scenarios

The adaption of office spaces to the flexible working culture of emerging business models has implications on a building's space distribution and layout. Office space depths have been reduced over the last decades from 9.0 – 15.0 metres to 3.5 – 6.0 metres [Neufert 2012]. Assuming that outdated office buildings will be refurbished eventually to suit the contemporary working culture and organizational structures of the 21st century, this study will, therefore, focus on this range of office size. The office model adopted for simulation is based on the minimum standard size for a single unit office according to DIN EN 4543-1:1994-09 [DIN, 1994] measuring 3.4m (depth) x 2.9m (width) x 2.75m (height). Even though bigger offices spaces with multiple workstations or group meeting layouts are part of contemporary office buildings, in this study, the focus is on a single unit office, limiting the implied variable and enabling benchmarking and scaling for future studies. The simulation model was generated using parametric control functions of Honeybee/Grasshopper in the 3D environment of Rhinoceros [Qingsong et al., 2015]. The office room comprised four walls (A-D) a ceiling and floor represented by two-dimensional rectangular planes intersecting at the vertices. The south-oriented wall D represented the

outer façade while all other space dividing elements would have adjoining spaces. A parametric window with modifiable window to wall ratio was integrated into the façade. The ETFE cushion of the DSF would be located with a variable distance in front of the exterior wall D, covering the whole façade area. The inner space of the office room was laid out with a regular sensor grid for the readings of the simulated illuminance values of the daylight analysis. All elements used for the model were based on standard definitions for Radiance elements and compiled by Honeybee for the simulation files. A schematic diagram of the initial model is shown in Figure 6.68.

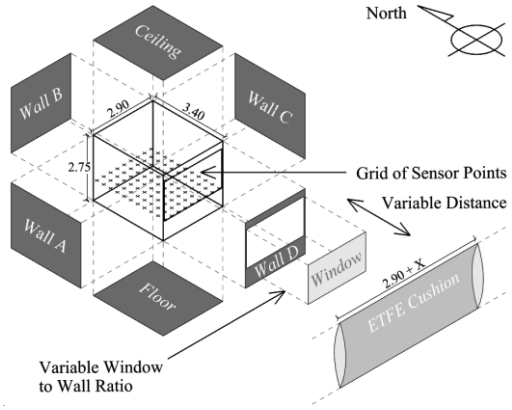


Figure 6. 68. Schematic diagram of the simulation model
(image by the thesis author, unpublished)

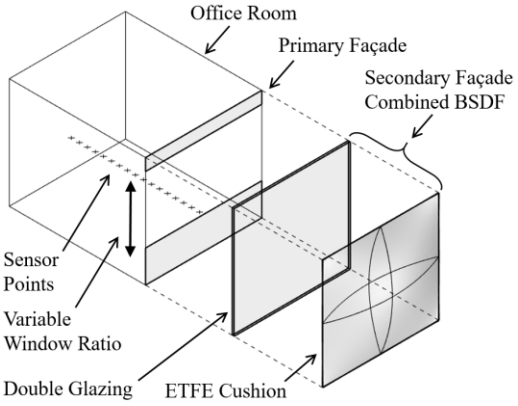


Figure 6. 69. Simplified DSF Model for Radiance including BSDF
(image by the thesis author, unpublished)

Due to the fact that the three and five-phase method includes only three flux phases and use of non-coplanar elements is limited [Wang et al., 2018], the two layers of the DSF window and ETFE had to be combined into one, covering the whole area of the façade, while the window to wall ratio was adjusted separately with two variable wall elements behind the window on the interior side of the façade. A scheme of this simplified model which was used for the simulation routines, is shown in Figure 6.69. Five window-to-wall-ratios were used for the different simulation scenarios, covering 30%, 45%, 60%, 75% and 90% of the façade area with glazing. The chosen range was intended to represent façade

designs common in office buildings and pursue the question of applicability and maximum benefit of the ETFE DSF, in terms of daylighting performance, for different cases of construction proportions. An overview of the window to wall ratio scenarios is shown in Figure 6.70 A to E representing a front view of the office room façade.

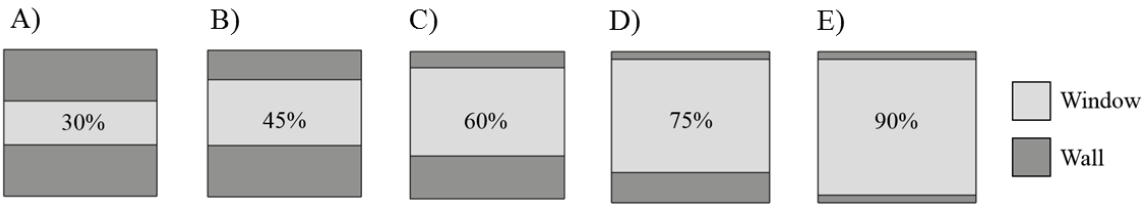


Figure 6. 70. Window to wall ratios of façade scenarios for daylighting simulation, A) 30% / 70%, B) 45% / 55%, C) 60% / 40%, D) 75% / 25%, E) 90% / 10%
(image by the thesis author, unpublished)

For the simulation scenarios, five material combinations were modelled and BSDF files generated. The first scenario is the reference scenario of clear double glazing. The four DSF scenario comprised a combination of the double glazing and an ETFE cushion as the second layer of DSF. For scenario number two, a clear double-layer ETFE cushion was added to the DG. Scenario three includes a double layer ETFE cushion with a silver fritted outer layer. Scenario four and five comprise triple-layer switchable ETFE cushion, were scenario four represents the existing measured material combination, and scenario number five represents an improved theoretic model with optimized reflectance and transmittance characteristics. An overview of the DSF material scenarios is listed in Table 6.15. All other walls, ceiling and floor elements were modelled using an opaque standard plastic material from the Radiance library, with a diffuse reflectance of 35% and a specularity of cero. The material roughness was also set to cero. A summary of the input data for the wall material is provided in Table 6.16. The simplification of the internal surfaces was intended to limit any further internal reflection within the office space and account in the daylight analysis primarily for the transmitted light from the DSF and allow an objective comparison between the different DSF.

Table 6. 15
Material combinations for double skin façade simulation
(table by the thesis author, unpublished)

Index	Material combinations for double skin facades
1	Clear Double Glazing
2	Clear Double Glazing + clear ETFE double layer foil cushion
3	Clear Double Glazing + fritted ETFE double layer foil cushion
4	Clear Double Glazing + printed ETFE triple layer foil cushion, switchable
5	Clear Double Glazing + printed ETFE triple layer foil cushion, switchable (modified)

Table 6. 16
Summary of the input data for the model wall material
(table by the thesis author, unpublished)

Building Element	Material Name *(Radiance)*	Colour RGB Channels *R*	*G*	*B*	Roughness	Specularity
Wall	Plastic	186	186	186	0	0

6.3.5. Geographic Location and weather data

Based on the findings of previous studies [Gómez-González et al. 2011] it is understood that most of the latest ETFE projects have been built in the northern hemisphere between a latitude of 50 to 60 degree. However, current trends suggest that ETFE is increasingly introduced in buildings located in the southern latitudes. This study is interested in understanding if DSF with ETFE can fulfil the expectations to improve daylighting performance of buildings as well in regions with intense solar radiation. And, if so, which are the best technical solutions between conventional and switchable ETFE foil cushions. The study, therefore, covers with three selected cities a wider range of 20 degrees of latitude. London, Barcelona and Shanghai, located at 51.5°, 41.4°, 31.2° N latitude respectively, were selected as the geographic locations for the parametric study. All three cities are large urban centres with a dynamically developing building stock likely to be incorporating lightweight building solutions for upgrading and retrofitting in the near

future. A world map indicating the geographic location of each city is presented in Figure 6.71.



Figure 6. 71. World map showing the geographic location of cities used for the climate-based Radiance simulation
(image by the thesis author, based on Google Maps world map, unpublished)

The climate of each city is distinct; however, all three locations are at sea level and exposed to a maritime climate influence. Annual weather file with hourly data in the Energy Plus weather format (EPW) with original source data from the American Society of Heating, Refrigerating and Air-Conditioning Engineers (ASHRAE 2001, *International Weather for Energy Calculations (IWEC Weather Files*)) was used as an input for the simulation. The annual weather data indicates that London is exposed to a total annual solar global horizontal irradiation (GHI) of 1023 kWh/m^2, Barcelona to 1621 kWh/m^2 and Shanghai to 1325 kWh/m^2. An extract of the hourly weather data file shows a more distinct image of the solar irradiation and the in consequence available amount of light in each city. London exhibits an average of 1460 hours of sunlight per year with an average of 3:59 of sunlight per day. It is sunny 33.3% of the daylight hours with overcast sky during the

remaining 66.7% of the hours. Barcelona has an average of 2437 daylight hours per year with an average of 6:40 of hours per day of which 55.6% are sunny. In Shanghai there is an average of 1874 hours of sunlight per year with an average of 5:07 of sunlight per day. It is sunny 42.8% of daylight hours and cloudy during the remaining daylight hours. The Figures in Annex A and B display annual graphs for the direct and diffuse solar radiation patterns of each city. The direct radiation is herein defined as the hourly direct normal radiation in Wh/m^2, which is the amount of solar radiation received directly from the solar disk on a surface perpendicular to the sun's rays. The diffuse radiation is herein defined as the hourly diffuse horizontal radiation in Wh/m^2, which is the amount of solar radiation received from the sky, excluding the solar disk, on a horizontal surface during the indicated time. From the graphs in Annex A it can be learned that London exhibits a seasonal pattern of solar radiation with lower values in the winter months and continuously increasing to the highest solar radiation values during the summer months with an approximately threefold difference between the extremes of the winter and summer season, with an, on average, slightly higher direct solar radiation. In Annex A it also can be seen that Barcelona has a similar seasonal pattern like London, with low values of solar radiation in winter and high values during the summer months. However, the direct solar radiation is on average, almost 50% higher than in London with a relative difference of approximately 30% to the much lower diffuse radiation. The annual solar radiation of Shanghai has a less pronounced seasonal pattern. Compared to London and Barcelona, the solar radiation is lower throughout the year on a monthly average basis, and the diffuse solar radiation is higher than the direct solar component in various months of the year. While this average monthly weather data provides a good overview on the solar radiation patterns in each of the chosen locations, it does not provide any information on the peak days and hours where shading might be required for the excess of light. The graphs in Annex B offer a more detailed view of the solar radiation patterns and potential critical peaks, showing the hourly global horizontal radiation in Wh/m^2 which is the total amount of the total sum of direct and diffuse solar radiation received by a horizontal surface during the indicated time. Observing the data, it becomes evident that independent of the geographical influences and seasonal

patterns all three cities receive peak values of solar radiation in the summer months between April and September in the hours between 10 am and 2 pm. While it is not a surprising fact, it further justifies investigating adaptive building envelopes which are able to mitigate the peaks of solar radiation.

6.3.6. Sky model and matrixes

To accurately predict the illuminance distribution of interior spaces, a realistic sky model is required. The sky model used for the simulation procedure of this study is a climate data based discretized hemisphere with a subdivision of 145 individual patches. The operation of projecting the irradiance data from the weather file to the subdivided hemisphere followed by the transformation into a sky matrix file is done with Radiance via the input through Honeybee. A sky matrix is the sum of a series of sky vectors for a period of time informed by the illuminance data provided by a weather file. Each sky vector contains an average sky luminance value of a discretized sky patch for the specific sky luminance pattern of a point-in-time [Reinhart et al.; 2000; Tregenza, 2016].

In a further step towards understanding the implications of the different modelling approaches of sky models, the total radiation of the annual weather file was projected on 145 subdivided patches based on a Tregenza discretized hemisphere and converted into a stereographic projection. This allowed the vectorized direction and intensity of averaged solar radiation for an entire year to be visualized. The diffuse and direct solar direction was plotted individually on separate stereographic projections. The generated images depicted in Figure 6.72 A, B and C are only for Barcelona, but the parametric tools of Ladybug/Grasshopper allow to generate images for any weather data at any point of time. The visualization of the sky models is expected to provide valuable input for the interpretation of the results of the annual daylight studies and produce additional confidence in the accuracy of the chosen sky model.

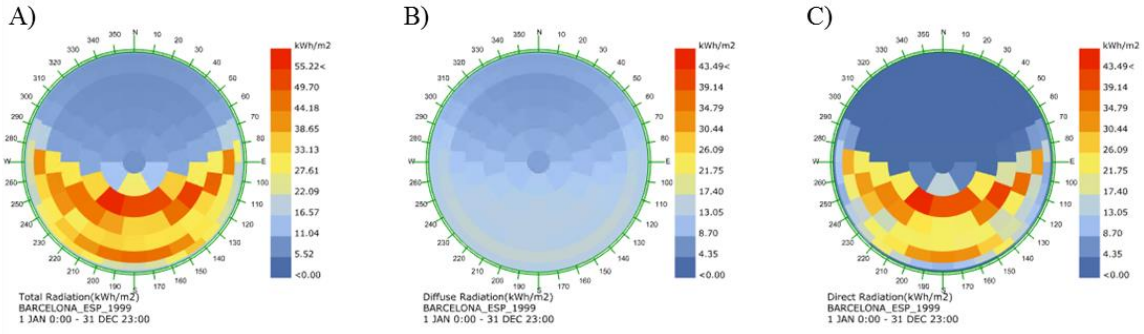


Figure 6. 72. Stereographic projection on discretized three-dimensional sky model for Barcelona showing the annual Total Radiation (A), Diffuse Radiation (B) and Direct Radiation (C)
(images by the thesis author, unpublished)

6.3.7. Simulation Parameters

The parameters for the daylight simulation are divided into input-, setting- and output-parameters. The daylight simulation is based on ray-tracing methods, and as such, requires precise adjustments of the simulation procedure. The Radiance parameters cover aspects such as accuracy, resolution and number of ambient bounces of the traced rays. The adjustment of parameters to the model size, available computing power and aspired results resolution was informed by several manuals and studies from the literature [Ward & Shakespeare, 1998; Reinhart, 2000; Sun et al. 2017]. For the ambient bounces (-ab), the most important parameter in terms of influence on result accuracy and computing cost, an independence test with incrementing ambient bounces was performed until reaching an acceptable level of accuracy for an affordable calculation time. An overview of the main Radiance input parameters chosen for the daylighting simulation procedure is shown in Table 6.17.

Table 6. 17

Simulation Parameters for Radiance daylighting simulation set-up

(table by the thesis author, unpublished)

Ambient Bounces (-ab)	Ambient Divisions (-ad)	Ambient Supersamples (-as)	Ambient Resolution (-ar)	Ambient Accuracy (-aa)
10	2048	2048	64	0.200

The setting input parameters comprised the climate files for different locations, window to wall ratio, BSDF matrix for different DSF material combinations and the schedule. The schedule chosen for the lighting analysis is based on a typical 9 am to 5 pm office hour schedule for five days of the week from Monday to Friday. No artificial lighting is scheduled in order to simulate only the effect of the natural daylight independent from other external factors. Another input parameter equally important for the outcome, and results is the setting of the sensor or analysis grid. Four illuminance-based simulations were performed. Each required a distinct sensor grid, for which the direction and distribution of the sensors define the quality of the result. Plan views of the room model depicted in Figure 6.73 A to D show the sensor grid distribution for the Radiance simulation for the useful daylight illuminance (UDI) (A) with a total of 221 vertical sensors in a regular grid of 0.2 x 0.2 m at 0.75 m height; illuminance (B) with a total of 17 vertical sensors across the longitudinal centre section of the room with a regular distance of 0.2 m between each sensor at 0.75 m height, according to; simplified daylight glare probability (DGPs) (C) with one single vertical sensor at a distance of 1.7 m from the window and 0.65 m meters from the west wall of the room at the height of 1.2 m for a typical view position of a person sitting on a centred desk; daylight illuminance uniformity ratio (UR) (D) with a regular 0.1 m x 0.1 m grid of 128 sensors distributed regularly over a task room centred area of 0.8 m x 1.6 m at the height of 0.75 m, representing an office desk surface. The sensor grid distribution for the illuminance simulation was defined in accordance with, specified in the British and European Standard 12464-1:2011, Light and lighting (Part 1), for lighting of indoor work places: Indoor work places [BS EN 12464-1, 2011].

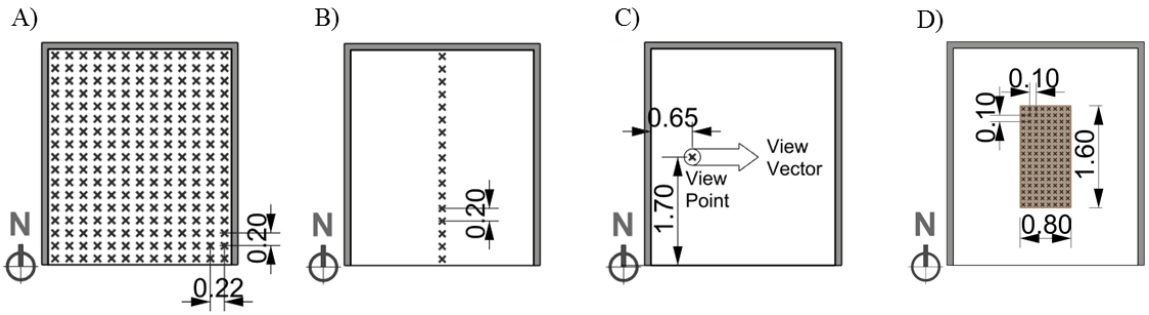


Figure 6. 73. Plan views of the room model showing the sensor grid distribution for the Radiance simulation of the Useful daylight illuminance (A), Illuminance (B), Simplified Daylight Glare Probability (C) and Daylight illuminance uniformity ratio (D) (images by the thesis author, unpublished)

6.3.8. Dynamic daylight performance metrics

The metrics used in this study to evaluate the daylighting performance of an office space are dynamic, meaning that rather than focussing on a specific point in time, dynamic metrics are intended to give a comprehensive annual overview. Weather data-based simulations generate a vast amount of hourly results, therefore the approach of this study was to summarize the data to percentages of time according to the established daylighting metrics of glare probability, illuminance uniformity and useful daylight illuminance, which will be outline in the following three sections.

6.3.8.1. Daylight glare probability metrics

Glare in office spaces can make it impossible to work productively. Bright, unfiltered sun light, direct or reflected, might create a visual discomfort which affects our capacity to focus on a specific task, manual or intellectually. The International Commission on Illumination (CIE) defines glare as: *"visual conditions in which there is excessive contrast or an inappropriate distribution of light sources that disturbs the observer or limits the ability to distinguish details and objects."* [CIE, 1995]. In office spaces, the contrast between the relatively dim internal lighting conditions and the bright direct

sunlight from a window view strain the human eye creating difficulty to focus and adapt to either one or the other lighting condition. Light reflections on computer screens are another known issue which can be challenging to adjust to at fixed workstations in an office room. Internal window curtains or adjustable lamella screens are the most common solution. Advanced versions of the sunscreen lamellas, either integrated into the glazing or externally attached to the façade, with or without automated control, are the common product solutions for controlling glare from solar radiation. Simulating their performance and the effects on the whole building, however, remain a challenging task [Konstantzos et al., 2015]. The Advanced lightweight building façades ad functionalities to the building faced. DSFs not only provide solar protection but also add with the second skin another layer of thermal insulation an enable controlled natural ventilation. Switchable ETFE cushions with reflective frit prints bring together these capabilities when employed as a second building skin. To quantify their capacity to reduce glare is the task developed in this section. Developed methods to estimate the glare probability in spaces have been presented and discussed extensively in the literature [Wienold & Christoffersen, 2006; Wienold, 2009; Wienold et al., 2017]. The method used in this study is the Simplified Daylight Glare Probability (DGPs) [Wienold, 2007]. DGPs is a simplified annual method to evaluate daylight glare based on vertical illuminance and is defined by the following equation 5.4 where E_v is the vertical illuminance in lux at eye level height, multiplied and summed with correction factors:

$$DGPs = 6.22 \times 10E\text{-}5 \times E_v + 0.184$$

Equation 6. 4

The daylight glare probability was assessed for a wall facing seating position in the near centre of the south-facing window of the office room. Illuminance values from an annual daylighting simulation were captured with a vertical sensor within the simulation scene. The simulation was performed with hourly weather data for a whole year using the weather file of London, Barcelona and Shanghai. The performance of different ETFE

double skin façades combined with different varying window to wall ratios (30%, 45%, 60%, 75%, 90%) façades was assessed. The obtained illuminance values were integrated into the above formula calculating the simplified glare probability. Four evaluation categories were assigned to limiting data bins, containing the filtered annual values for the glare probability, with less than 0.35 corresponding to imperceptible, 0.35 – 0.4 to perceptible, 0.4 – 0.45 to disturbing and 0.45 counting as intolerable.

6.3.8.2. Daylight illuminance uniformity metrics

In working environments such as offices, good lighting conditions are essential for the well-being and productivity of the workers. The lighting needs to provide enough illuminance intensity to perform the required tasks over a prolonged time without straining the eye vision while allowing the tasks to be carried out efficiently and in a timely manner. Besides the illuminance level, other aspects, such as the luminance distribution, light colour appearance, directionality of light and glare need to be considered according to BS EN 12464-1:2011 [BS EN, 2011]. Daylight uniformity is of importance for a task to be carried out on a specific area and may lead to higher productivity, a better quality of work and a high level of safety. However, achieving well-distributed lighting on a specific task area with natural lighting only is not an easy task. ETFE has been used previously for daylighting control in buildings [Monticelli, 2013]. But ETFE is not only a material suited for application in buildings but also has been used in agricultural structures such as greenhouses or winter gardens for its capabilities to scatter and evenly distribute light diffusely in a space [Tantau et al., 2012; Masih & Lau, 2015; Liu et al., 2016]. A requirement, which is as necessary for growing plants efficiently as it is essential for vision intensive tasks in working spaces such as offices. Daylight availability decreases drastically with the distance from the window, achieving a uniformly illuminated task area across the section of a room is, therefore, challenging when only daylight shall be used.

A metric to quantify the homogeneity of light availability over a certain area is the Daylight Illuminance Uniformity Ratio (UR) which is based on illuminance values and

provides a percentage of evaluated hours with the available daylight uniformity bins, of ≤ 0.4, 0.4 - 0.6, 0.6 – 0.7 and ≥ 0.7 for an evaluated task area. BS EN 12464-1:2011 requires office spaces to achieve a UR of 0.4 -0.6 in the task area and in the immediate surrounding area $\geq 0{,}40$ while the background area shall be $\geq 0{,}10$. For the simulation, a hypothetic task area with dimensions of a generic office desk was positioned in the centre of the virtual office room. The test points were spread out densely on a 0.2m x 0.2m grid for a high resolution of the UR results. Climate data from three cities, London, Barcelona and Shanghai, was used for the comparative simulation. The south-facing façade of the previously described office room was parametrically adjusted for five different windows to wall ratios, 30%, 45%, 60%, 75% and 90%, and successively equipped with five material and layer combinations of DSF design options, including DG, clear, fritted and switchable ETFE foil cushions. The daylighting simulations were weather data based annual matrix simulations using the 5-phase-method within Radiance software.

6.3.8.3. Useful daylight illuminance metrics

Daylight in offices has multiple benefits on comfort, health, productivity, and safety. Natural daylighting can also reduce the demand for energy use on artificial lighting in buildings when responding to occupancy patterns and making full use of controls. However, quantifying natural daylight in internal spaces and predicting whether it is sufficient for the task to be carried out and available during the time when needed is a challenging task. A variety of metrics have been used in the past to assess daylight using numerical scales which predict the daylight illuminance of a point in space for a specific time. The problem with this kind of approach is that if the study aims for a comprehensive understanding of the performance of a space with a variety of different design and material options the number of produced results might exceed the analysis capacity. To overcome this issue, a dynamic metric had been proposed, as a methodology to provide a comprehensive numerical value which can represent the time and space dimension at the same time [Nabil & Mardaljevic, 2006]. The concept of useful daylight illuminance (UDI)

looks on how often in the year daylight illuminances are achieved within a range which is useful for a certain space task or user profile. The UDI methodology considers hourly meteorological data for the period of a year to calculate the illuminance values for each point of a virtual sensor grid within the test space. Each of the points is evaluated for how many hours of the year it is exposed to useful daylight based on the preestablishes ranges of useful daylight illuminance. The UDI is expressed in percentage of time.

This study is about the useful daylighting of office spaces; therefore, a typical working schedule from Monday to Friday, from 9 am to 5 pm was adopted, and only the office hours were considered for the UDI evaluation. Useful daylight illuminance falls typically within the range of 100 to 2000 lux. However, the definition for the UDI was adjusted for this study to fit the purpose of evaluating precisely the daylighting conditions of office spaces. Several building standards and institutions recommend illuminance levels of minimum 500 lux for an office room, where tasks like writing, typing, reading and data processing are carried out [BS EN, 2011; CIBSE, 2015]. All values above 2000lux were considered as excessive oversupply, related to solar gains and glare, and all values falling below 500 lux as undersupply, which may not be enough light to carry out routine office tasks and additional artificial lighting would be required. This study evaluates the capabilities of different design options of double skin incorporating clear, fritted, and switchable ETFE cushions to moderate the UDI of an office space over the period of a year across different climates.

6.4. Results and Discussion

This section of the chapter presents and describes the results in a systematic and detailed way. As a mode of introduction, the first two subsections present and discuss measured data relevant to the optical characterisations of the simulated materials, followed by a partial validation of the generated simulation model. The following sub-sections display the results obtained from the annual daylighting simulation for one single unit office space. The individual sections discuss the daylighting condition for different performance criteria independently. The use of dynamic metrics offers a comprehensive

image of the annual performance and allow to compare the outcomes for different climate and design scenarios objectively. Results are displayed numerically in Tables and graphs.

6.4.1. Results of Spectroscopy and optical characterization

The optical characteristics and lighting qualities of ETFE foil have been well covered in the literature [Lau, B., et al., 2016; Good et al., 2016; Maywald, 2019]. However, the available data does not fit the purpose of this study as it is either not available in the required resolution and format or not available for the specular and diffuse optical compounds of the type of material necessary to model the switchable ETFE cushion. Pairing data from different sources for simulation set-up generates a high degree of uncertainty to the simulation results and reduces the possibilities of validating the results with physical measurements. Therefore, measurements of the visible light transmittance and reflectance were considered as necessary even though similar results had been published previously for different types of printed ETFE foils. Considerable variations in the optical characteristics have been observed for different foil types depending on a variety of parameters, for example, the manufacturer, foil thickness, foil tint saturation, foil tint colour, frit ink type, frit ink print density and percentage of frit pattern coverage. In consequence, the characterisation of the material provided by the manufacturer was essential in to compare and validate the results with experimental tests with a physical mock-up of the switchable cushion at a later stage of the project. The spectral measurements were taken from an A4-size (210 × 297 mm) sample sheet of a 200 µm switchable ETFE foil with clear, silver fritted and dense silver fritted areas, corresponding respectively to an approximate area of 26.8%, 23.2% and 50.0% of a one square metre sample. The light transmittance and reflectance of the three ETFE surface types were measured at different points of the sample in the visible range of the electromagnetic spectrum range. The absorbance was calculated according to the law of energy conservation. From the experimental data presented in Table 6.18, it can be seen that all three ETFE surface types have a distinct optical characteristics profile. As expected, the clear ETFE foil has the highest global transmittance value with 91.0%, which correlates

well with manufactures data and previous studies. Of the total transmitted light, 81.8% is direct or specular light transmittance, while 9.2% is diffused light, scattered by the material. The fritted foil has with 23.0% considerably lower light transmittance, with only 6.1% specular and 16.9% diffuse transmittance. The dense fritted ETFE foil has a total light transmittance of only 4%, which divides into 0.4% specular and 3.6% diffuse transmittance. The reflectance of a all three foil types is inversely distributed. The global reflectance of the clear ETFE is 6.2%, with a proportional 3.8% of specular and 2.4% diffuse reflectance. The fritted ETFE reflects 45.7% of the incident light, of which 10.6% is specular and 35.1% diffusely reflected. The densely fritted ETFE has a global reflectance of 53.2%, of which 12.0% is specular reflectance 41.3% diffuse reflectance. A graphical overview of the measurement results shown in the graphs of Figure 6.74 A, B and C. The underlying spectral data, which represents the directly measured results of the percentage of colour spectrum transmitted and reflected, provides a more detailed picture of the optical performance of each of the samples. An overview of the measured spectral transmittance, reflectance, and absorbance of all three samples is plotted in the graphs A, B and C in Figure 6.75. The absorbance, which is not measured directly, follows as a result of the function of the law of energy conservation. More detailed results are displayed in the graphs of Figure 6.76 A to D, where the spectral and diffused transmittance and reflectance is plotted separately for each of the samples.

Table 6. 18

Optical characteristics of visible light transmittance, reflectance and absorbance of three ETFE foil types (clear, fritted and dense fritted)

(table by the thesis author, unpublished)

Foil Type	***Global* T_{vis}** [%]	***Global* R_{vis}** [%]	***Specular* T_{vis}** [%]	***Specular* R_{vis}** [%]	***Diffuse* T_{vis}** [%]	***Diffuse* R_{vis}** [%]	A_{vis} [%]
Clear ETFE Foil	91.0	6.2	81.8	3.8	9.2	2.4	2.8
Fritted ETFE Foil	23.0	45.7	6.1	10.6	16.9	35.1	31.3
Dense Fritted ETFE Foil	4.0	53.2	0.4	12.0	3.6	41.3	42.8

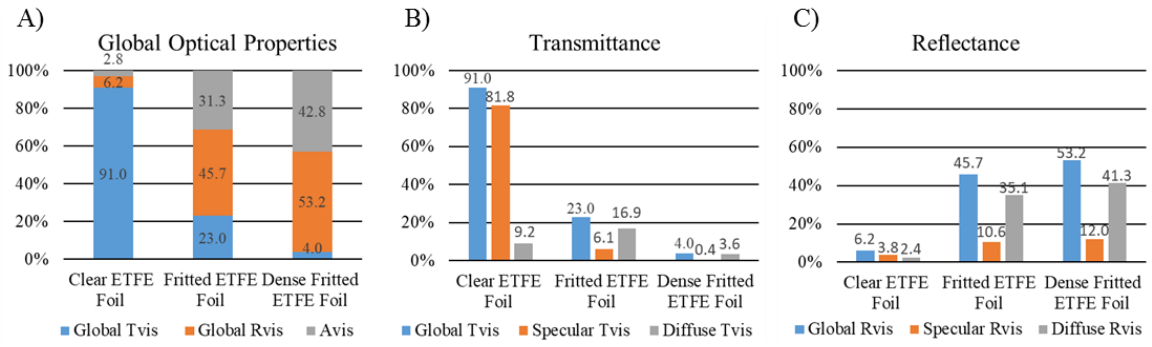


Figure 6. 74. General optical properties (A), global, specular and diffuse transmittance (B), global, specular and diffuse reflectance of three ETFE foil types (clear, fritted and dense fritted) taken from a switchable ETFE foil sample
(graphs by the thesis author, unpublished)

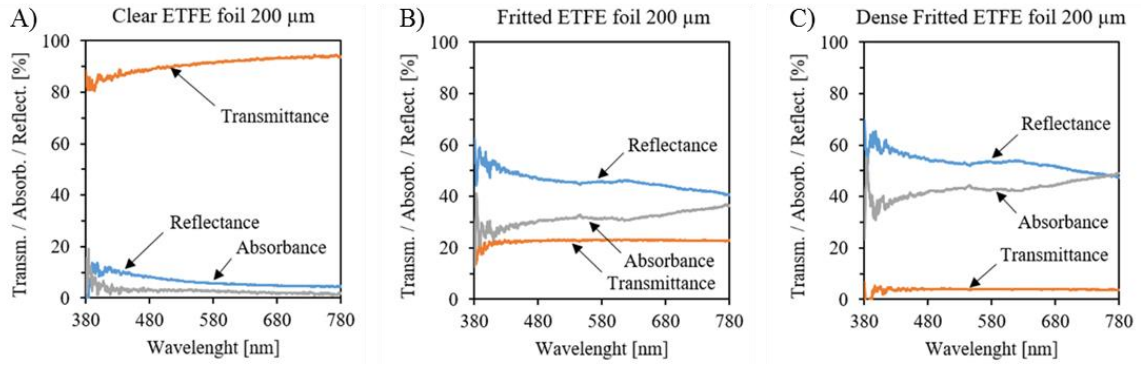


Figure 6. 75. Spectral distribution of visual light transmittance, reflectance and absorbance of three ETFE foil types taken from a switchable ETFE foil sample, A) clear, B) fritted and C) dense fritted
(graphs by the thesis author, unpublished)

Interestingly, there were also differing recognizable patterns between the tested samples in the ratios of spectral distribution in the specular and diffuse division, relating positively to similar observations from the global optical profiles of the samples. Overall, these results reaffirm observations from previous research studies about the relatively homogenous light distribution of ETFE across the visible spectrum. However, taken together with the results

from the specular and diffuse light analysis it becomes clear that ETFE light scattering properties might play an important role in the light transmittance and therefore the daylight distribution in internal spaces. The focus of this chapter section is turning now to the discussion of the generated BSDF models which bear the potential to replicate in daylighting simulations, the evidence obtained from the experimental measurements.

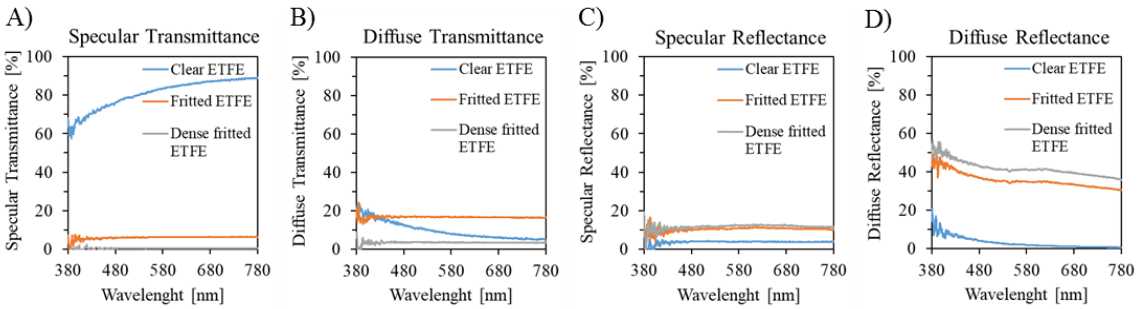


Figure 6. 76. Spectral distribution of specular transmittance (A), diffuse transmittance (B), specular reflectance (C) and diffuse reflectance (D) of three ETFE foil types (clear, fritted and dense fritted) taken from a switchable ETFE foil sample
(graphs by the thesis author, unpublished)

In order to generate material definitions for the input in Radiance daylighting software, the measured spectral data was converted into single values. The diffused reflectance was calculated individually for red, blue and green channels RGB according to the method by Lindbloom [Lindbloom, 2019]. An overview of the calculated diffuse RGB reflectance values for the different ETFE materials is shown in Table 6.19. The shown data represents the reflected colour of the material and defines hereby the colour of the material our eyes perceive. The RGBs were calculated according to the CIE colour model, using the CIE colour matching functions which were determined based on the spectral measurements for the visible light spectrum of the ETFE samples. In order to obtain RGB, values which can be displayed on computer screens with a mix of the three primary colours, CIE X, Y, and Z values, representative of the emitted light intensity weighted for each wavelength,

had to be calculated. The CIE standard model was adopted for this study because it is also used by Radiance simulation program.

Table 6. 19
Diffuse reflectance values of red, blue and green channels (RGB) according to different colour models for three ETFE foil types (clear, fritted and dense fritted)
(table by the thesis author, unpublished)

RGB Color Model	Clear ETFE			Fritted ETFE			Dense Fritted ETFE		
	R	*G*	*B*	*R*	*G*	*B*	*R*	*G*	*B*
CIE RGB	33	48	69	157	159	166	169	171	177

In the following modelling step, the material definitions, including the RGB values, were assigned to the individual mesh parts of the triple-layer cushion geometry. A preliminary test rendering of the switchable ETFE cushion in open and closed mode was performed in Radiance with photorealistic image output and false colour renderings showing luminance, highlighting the amount of light that passes through or is reflected for a specific lighting condition. Rendering time for one 2000 x 2000-pixel image was approximately three hours. After visual verification of the renderings and comparison with pictures from the real size mock-up (Figure 6.77), to reconfirm realistic representation of the materials and geometry, the model was exported to Radiance as material and geometry .rad files. Images of the test renderings are shown in Figure 6.78 A and B. The Radiance genBSDF program was used to recombine the material and geometry files of the individual layer parts of the ETFE cushion into on single unit file. The raytracing calculation to generate the BSDF file was then performed using genBSDF, which took, with the available calculation power, up to 72 hours for each of the 15 models listed in Table 6.20.



Figure 6. 77. Switchable ETFE cushion mock-up (photo by the thesis author, unpublished)

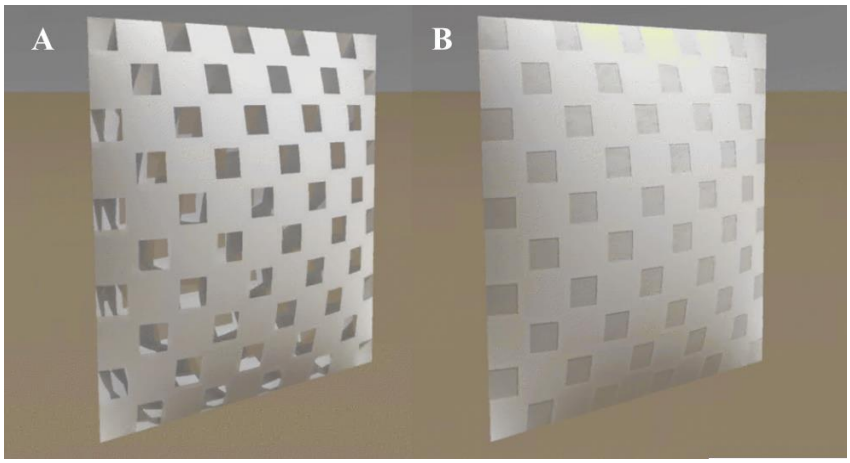


Figure 6. 78. Switchable ETFE cushion, in open (A) and closed mode (B), rendered in Radiance with material data from spectral analysis of material sample assigned (image by the thesis author, unpublished)

Table 6. 20

BSDF samples direct hemispherical visible transmittance and reflectance on front and backside for a perpendicular incidence angle

(table by the thesis author, unpublished)

BSDF Sample File (Data retrieved with: BSDFViewer_noTT Lawrence Berkeley National Laboratory)	**Direct hemispherical visible transmittance and reflectance**			
	T_{vis} (back) [%]	R_{vis} (back) [%]	T_{vis} (front) [%]	R_{vis} (front) [%]
Clear ETFE_flat Sample	91.0	9.0	91.0	9.0
fritted ETFE_flat sample	23.0	72.8	23.0	72.8
Dense Fritted ETFE_flat Sample	4.0	79.0	4.0	79.0
Dense Fritted ETFE modified_flat Sample	4.0	93.2	4.0	93.2
Glass Window Double Glazing (DG)	72.9	6.7	72.9	6.7
ETFE Clear Cushion	83.3	16.7	83.3	16.7
ETFE fritted cushion	23.6	72.2	23.6	72.2
ETFE switchable cushion OPEN	10.5	69.6	10.5	69.6
ETFE switchable cushion Closed	4.1	77.7	4.1	77.7
DG + ETFE Clear Cushion	61.5	16.5	61.5	16.5
DG + ETFE fritted Cushion	19.6	49.9	19.6	49.9
DG + ETFE switchable cushion OPEN	10.1	48.7	10.1	48.7
DG + ETFE switchable cushion CLOSED	5.4	53.2	5.4	53.2
DG + ETFE switchable cushion OPEN - *modified*	12.1	54.9	12.1	54.9
DG + ETFE switchable cushion CLOSED - *modified*	5.7	59.8	5.7	59.8

All listed transmittance and reflectance data corresponding to an incidence angle perpendicular to the sample, direct hemispherical visible transmittance, and reflection. Data varies considerably for each angle, especially for three-dimensional ETFE cushion samples and multi-layer component constructions. Therefore, the single incidence angle is only indicative and does not reflect the overall performance of the component as it has already been pointed out in previous ray-tracing studies on ETFE in chapter 3. For the generation of the BSDF of the ETFE cushion, the simplifying assumption was made to take the perpendicular optical characteristics of the perpendicular light incidence angle on the material samples obtained from the spectral analysis as the optical profile for modelling the ETFE foils as Radiance 'trans' materials. Therefore, the BSDF represents only the global optical performance of the ETFE cushion geometry with assigned materials but not the local BSDF of each of the material points on the cushion surface. In order to overcome this issue, a BSDF group within a BSDF unit is proposed. A mosaic of assembled multiple BSDF files would be necessary, where the angular spectral data is derived for each material from experimental goniophotomery. However, this idea is beyond the scope of this research and is instead recommended for future research. Another possible approach would be the development of a large scale goniophotometer to derive the BSDF of a full-size ETFE cushion directly; however, the difficulties associated with the up-scaling may appear to make this proposal unrealistic and justify the simplifications made for the time being. For the modelling of the DSF, the ETFE cushion models were combined with aligned windowpane geometry and assigned Radiance glass material. The switchable ETFE cushion had to be modelled in the open and closed mode as a requirement for the subsequent daylighting simulation which uses for the dynamic shading schedule, uses one model for each state to emulate the adaptive behaviour of the system. Following this requirement, a BSDF file was generated for each of the states. To verify generated BSDF for different angles and check for plausibility of overall transmittance and reflectance data, BSDF data files were loaded for visual crosscheck in the BSDFViewer program [McNeil, 2013]. Within the program transmission and reflection on all 145 angles of the Klems hemisphere for the front- and backside can be viewed for individual incidence angles. A

selection of the Klems BSDF diagrams with the datasets for the perpendicular incidence angle of the open (A) and closed (B) mode are shown in Figure 6.79 and 6.80, with distinct observable transmission and reflectance patterns for both optical states of the model. The direct hemispherical visible transmission at the front side is for this specific incidence angle 9.75% in open and 4.5% in closed mode. The reflectance at the front side in open mode is 70.0% and 77.7% in closed mode. However, the values vary drastically according to the incidence angle.

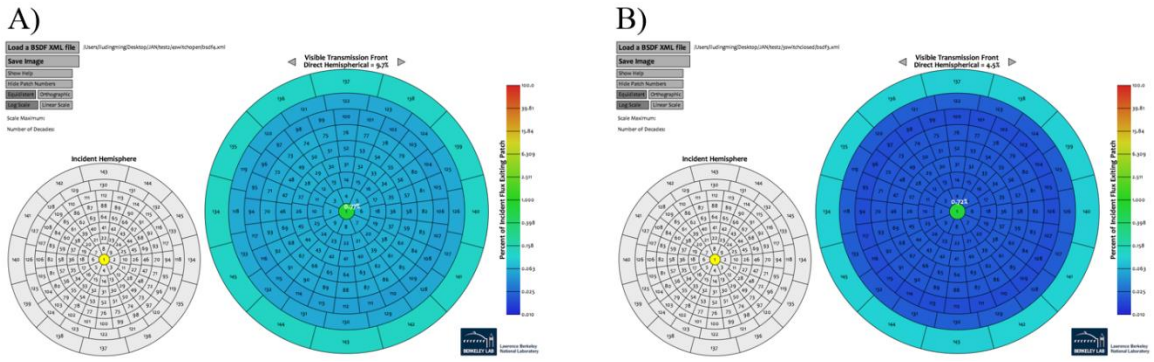


Figure 6. 79: Transmission on the frontside of the switchable ETFE cushion in (A) open mode (B) closed mode for a incidence angle perpendicular to the horizontal plane (images by the thesis author, unpublished)

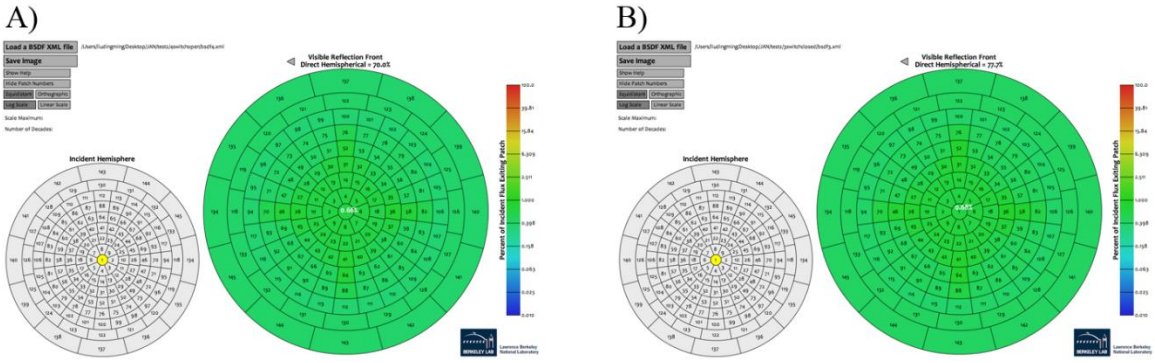


Figure 6. 80. Reflection on the frontside of the switchable ETFE cushion in (A) open mode (B) closed mode for an incidence angle perpendicular to the horizontal plane (images by the thesis author, unpublished)

6.4.2. Model calibration and partial validation

The BSDF of complex fenestration systems is an abstract matrix of numerical values which describes the light transmission and reflection of multiple incidence angles. Generated BSDF data was visualized using the LBNL BSDFViewer [McNeil, 2013] program for a plausibility check. However, evaluating the accuracy of the BSDFs virtual representation of the physical daylighting performance of a real size ETFE cushion is a challenge. While Radiance programs and daylighting simulations incorporating BSDFs have been validated previously in several studies [Reinhart, 2006; McNeil, 2013; Geisler-Moroder, 2018], switchable ETFE cushions with multiple assigned materials have never been assessed before, lacking reference data for comparison. Therefore, two comparative tests were carried out to verify the performance of the BSDFs. Firstly, a generic cubic test box measuring 1m x 1m x 1m with black non-reflective internal surfaces was generated. The south-oriented face of the box was replaced with a two-dimensional proxy geometry for the ETFE cushions. Four BSDF files for three different cushions (clear, fritted, switchable open, switchable closed) were assigned consecutively to the proxy geometry. The illuminance across the horizontal centre section from north to south was calculated with the 5-phase method for 10 test points with 0.1m distance from each other. A weather-based CIE sky (‘Sunny with Sun’) with the weather file of London was used to generate the lighting conditions for the 21st of June at 10 am. For all models, a clearly distinctive illuminance profile across the box section was observed confirming the expectations from the measurement of the spectral analysis.

For the second test, a physical black-box with non-reflective surfaces built around the switchable cushion mock-up. The illuminance was measured with an illuminance meter (type DT-8820, accuracy ±(5.0%+10d), manufactured by Shenzhen Everbest Machinery Industry CO., LTD) at different points aligned along the centre line section of the box depth with the switchable ETFE cushion in open mode. The conditions were then replicated with a CIE uniform cloudy sky with measured sky luminance of 10 k lux. Repeated simulations for comparison with the corresponding BSDF file were performed in Radiance. The results

of both tests are plotted in the graphs of Figure 6.81 and 6.82. The measured illuminance was higher near the back of the box, in comparison to the values from obtained from the simulated model. This difference could have many reasons, as for example, the solar exposure could have been not exactly the same in the experiment and the simulation, the position of the illuminance sensor might not have been completely horizontally aligned, or the black plastic did still generate some secondary reflections which were not taken into account in the simulation model. However, the results of the comparative test generated enough confidence in the BSDF models to proceed with the daylighting simulations.

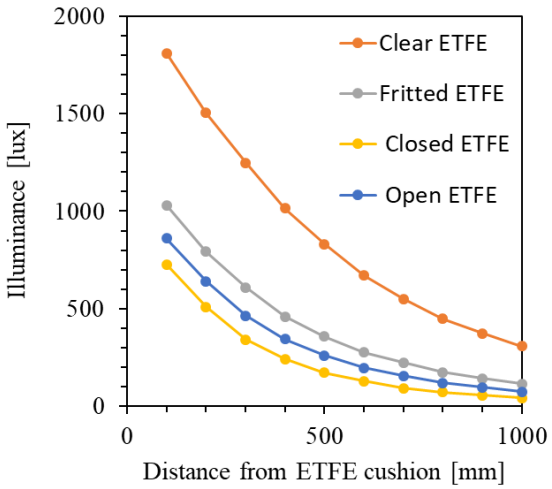


Figure 6. 81. Illuminance across the section in black test box for different ETFE BSDF models
(graph by the thesis author, unpublished)

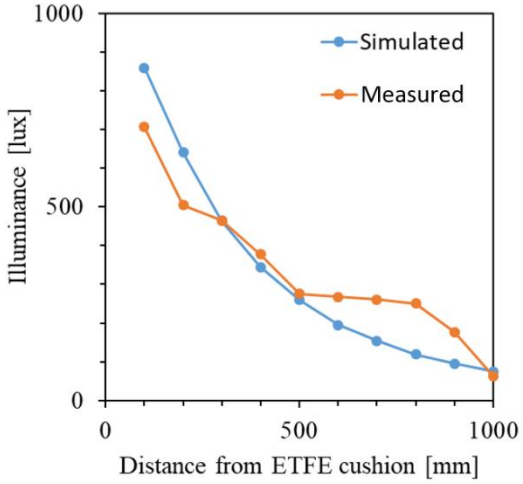


Figure 6. 82. Comparison of measured and simulated illuminance across the section in mock-up and virtual black box with ETFE switchable ETFE cushion in open mode
(graph by the thesis author, unpublished)

Another important aspect regarding the realistic representation of switchable ETFE cushions is the calibration of the switching mechanism control. The adjustment of the luminance threshold for the control sensors determines at which luminance level the

switchable cushion will change from one state to the other. Setting the luminance threshold is crucial to achieving the best daylight conditions within the space. If the threshold is too low the shading mechanism might switch to closed mode, only when glare is already unbearable, and switch back to open mode when daylight is still beyond comfort conditions. On the other hand, when the threshold is set too high, the adaptive mechanism might stay in closed mode during most of the working hours when natural daylight would be needed. In this case, also the visibility through the ETFE cushion is compromised for most of the time leading eventually to dissatisfaction with the view qualities of the glazing and loss of visible connection to the outdoors. In order to achieve an adaptive façade model which performs better than a conventional static system, it is a crucial task to calibrate the sensor threshold of the switching mechanism to a point where the equilibrium between the maximum hours of quality daylighting and minimal disturbance due to glare and inconvenient daylight distributions is achieved. The position and orientation of the virtual luminance sensor is also an elemental parameter for the performance of the adaptive shading mechanism; however, for this study, the switching sensor was located for all simulated scenarios at 0.75 m height within the principal task area in the centre of the room. Figures 6.83 to 6.85 show the annual switching schedule, for switching threshold from 0 lux to 500 lux and 1000 lux for the Barcelona weather file.

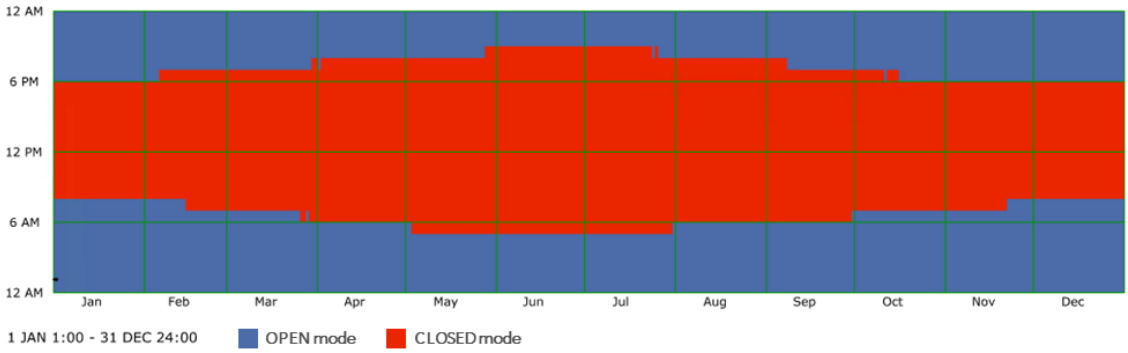


Figure 6. 83. Annual, hourly switching schedule for Barcelona climate with a luminance threshold of 0 lux set for the sensor
(chart by the thesis author, unpublished)



Figure 6. 84. Annual, hourly switching schedule for Barcelona climate with a luminance threshold of 500 lux set for the sensor
(chart by the thesis author, unpublished)

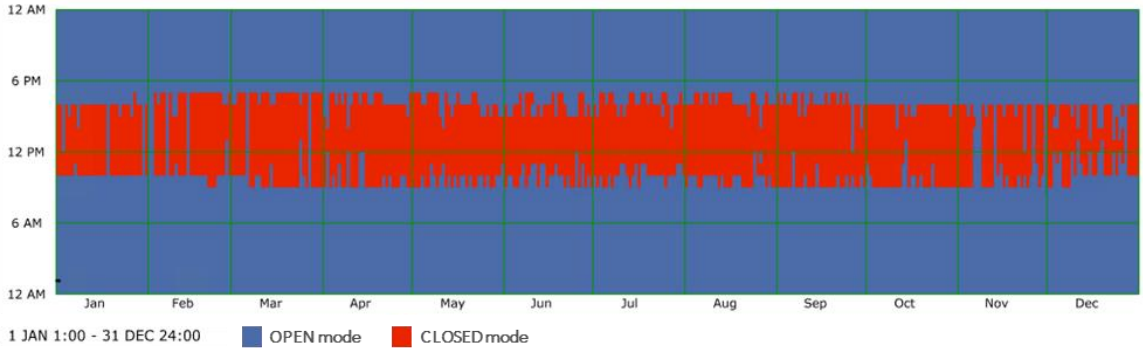


Figure 6. 85. Annual, hourly switching schedule for Barcelona climate with a luminance threshold of 1000 lux set for the sensor
(chart by the thesis author, unpublished)

After a preliminary analysis in all three chosen climates, the 1000 lux threshold was adopted, to limit the switching of the cushion to the peak hours of solar simulation and maximize the visibility of the glazing for the users. Figure 6.86 shows two graphs with the illuminance at a test point at the centre of the black-box simulated over 24 hours with a Barcelona climate file with switchable the ETFE cushion in the south face. Figure 6.86 A shows the illuminance plotted for both switching modes on the 21st of June, the summer solstice. Figure 6.86 B shows the on illuminance at the 21st of December, the winter solstice, for the open and closed mode. The graphs show clearly how the illuminance within

the box is affected by the application of one or the other switching mode. The illuminance can be reduced and kept within 2000 lux when switched in peak hours to the closed mode and increase the illuminance during morning and evening hours when switched to open mode. The increasing effect is more noticeable in summer, due to extended hours of solar daylight exposure, and the reducing effect in winter, due to lower solar angles with direct incidence on the ETFE cushion. A fine-tuning of the switching threshold for seasonal adaptation or weather dependent live calibration was out of the scope for this thesis but might be a topic for consideration in future studies.

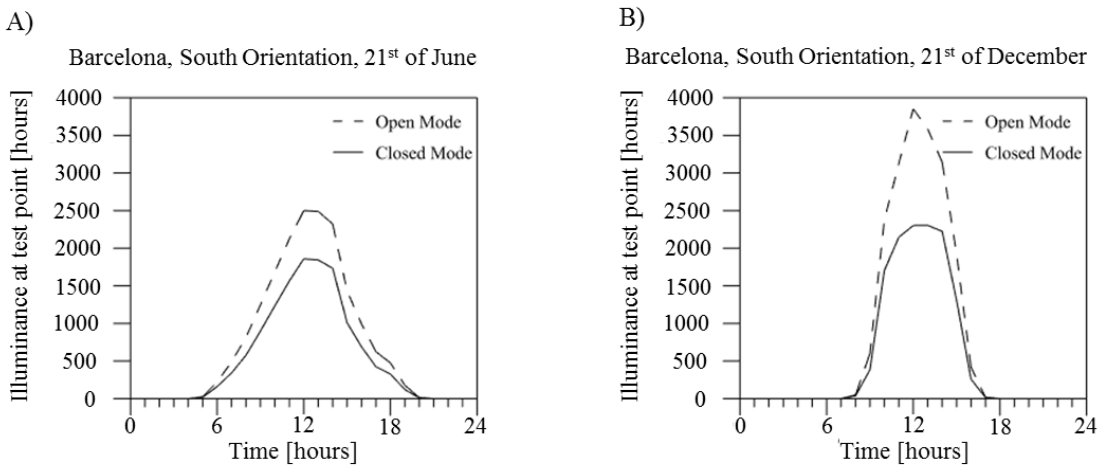


Figure 6. 86. Illuminance simulated over 24 hours with a Barcelona climate file at a centred sensor point in the generic test-box with switchable the ETFE cushion in the south face. A) shows the illuminance at the solstice of summer for the open and closed mode. B) shows the illuminance at the solstice of winter for the open and closed mode (graphs by the thesis author, unpublished)

6.4.3. Spatial light distribution and luminance of surfaces

The luminance distribution of the spatial surfaces of the office room (floor, ceiling, walls) was investigated through visual renderings of the room using the five-phase-method in Radiance. The renderings were generated for various material combinations and window-to-wall ratios for different days and hours, using the Barcelona weather data file.

The results in Figure 6.87 and 6.88 show a selection of dual renderings with the realistic view as the room would appear in front of the human eye (image 1, left side) and a corresponding false colour rendering showing the luminance of each surface rendered in a scaled colour scheme (image 2, right side). The image daylighting simulation, with the realistic rendering of the apparent brightness of the room, allows the human eye to visualise the brightness distribution and makes the identification of too bright or too dark areas, with the added false colour images, easier to be identified. With the parametric change of the window to wall ratio of the façade and the assignment of different material layer combinations of the DSF, it is possible to get a visual impression of the lighting effects resulting from the changes made to the façade. A comparison of the rendered images reveals that for the smaller window-to-wall ratios (30% to 60%) a higher contrast between the bright and darker areas can be noticed. This effect is reduced, smoothing the transition from bright to darker areas, with the addition of fritted or switchable ETFE cushions to the façade. The light scattering behaviour of the fritted cushions is the most likely reason for this effect. For the wider window to wall ratios, the brightness is more evenly distributed throughout the room over the wall, ceiling and floor surfaces. As expected, the room is overall much brighter as can be confirmed with the numerical scale of the false colour images. However, it must be taken into account for the evaluation of the luminance of the room surfaces that relatively dark surface colours with low reflectance were chosen for the simulation; therefore, internal reflections are limited, and the overall brightness of the room might appear low in comparison to rooms with white plastering finishes of internal surfaces. The switching effect of the adaptive ETFE cushion, depicted in Figure 6.87 C and D is noticeable but underestimated for the chosen luminance scale. A possible explanation for this might be that the wider window to wall ratio and the solar radiation angle and intensity at the chosen time and day for the point-in-time rendering might have a bigger effect on the luminance of the room surfaces than the different brightness condition caused by the open and closed mode of the switchable ETFE cushion. To investigate further the effects of the switchable ETFE cushion on the lighting conditions of the room, analysis of the annual behaviour is necessary to understand the advantages and disadvantages of the

DSF daylighting capabilities beyond individual point in time conditions, a topic outline in the following section of this chapter.

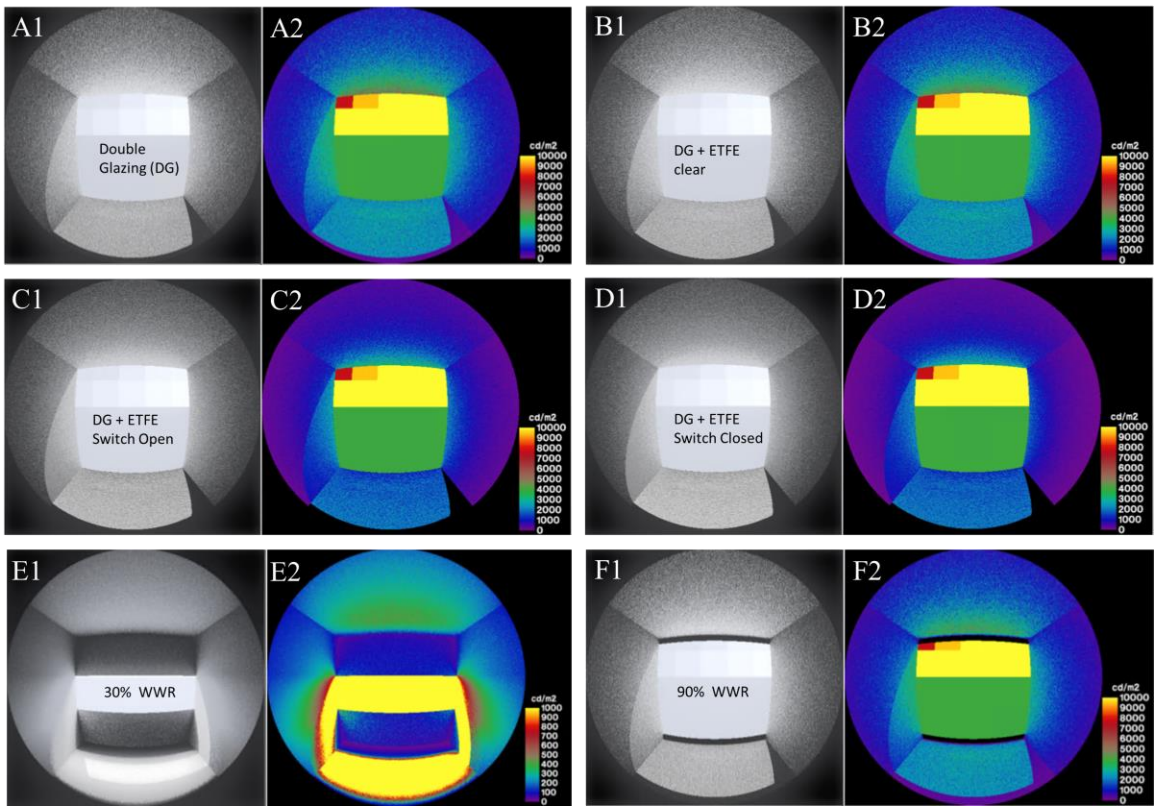


Figure 6. 87. Fish eye view realistic renderings and false colour illuminance renderings of south facing room for 12:00 am summer solstice in Barcelona, showing in A 1,2) double glazing with 100% WWR, B 1,2) double glazing + clear ETFE cushion with 100% WWR, C 1,2) double glazing + switchable ETFE cushion in open mode with 100% WWR, D1,2) double glazing + switchable ETFE cushion in closed mode with 100% WWR, E 1,2) double glazing + clear ETFE cushion with 30% WWR, F 1,2) double glazing + clear ETFE cushion with 90% WWR
(images by the thesis author, unpublished)

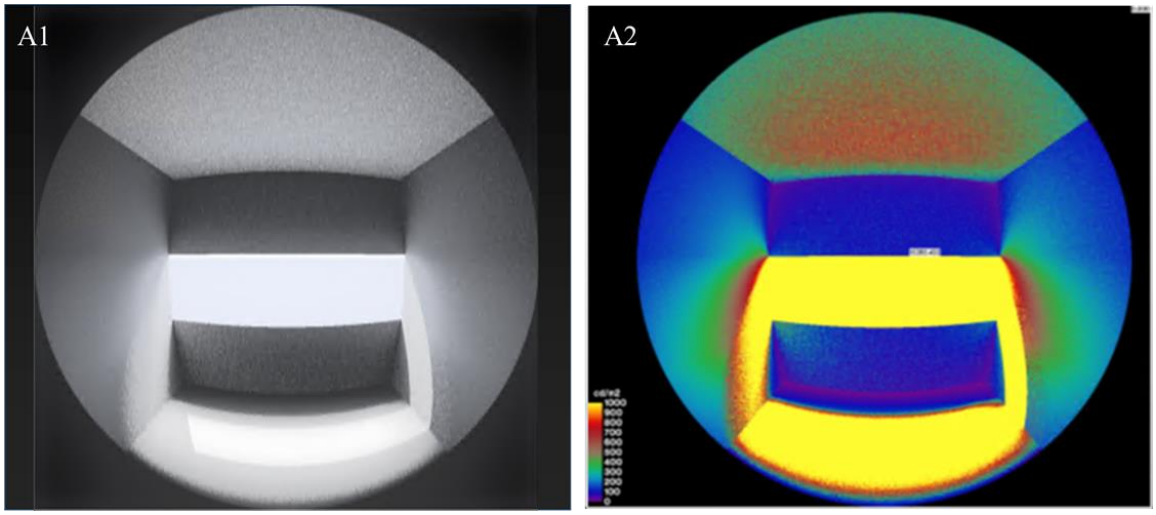


Figure 6. 88. Fisheye view realistic renderings and false colour illuminance renderings of south-facing room for 12 am summer solstice in Barcelona, showing in A 1 and A2 double glazing with 30% WWR
(images by the thesis author, unpublished)

6.4.4. Daylight Glare Probability results

The results for the daylight glare probability obtained for the different scenarios and DSF material combinations are summarized in the graphs of Figure 6.89, 6.90 and 6.91, indicating the percentage of the office schedule hours when glare is either intolerable, disturbing, perceptible, or imperceptible. The results obtained for London, depicted in Figure 6.89 show that the glare probability within the office room increases with larger window to wall ratios for façades with simple double glazing and DG with added clear ETFE cushion. With a 30% WWR, the glare is imperceptible for 92% to 93% of the office hours, for DG and DG + clear ETFE respectively. But for a WWR of 90%, the glare is perceptible up to 10% of the office hours, around 12% of the time disturbing and intolerable for up to 32% of the working hours. The immediate conclusion from the results might be that DG and clear ETFE double-skin façades are not suitable to control glare in south-facing office façades in London, especially when the WWR is large. Whereas the results from the other DSF material combinations, with fritted and switchable ETFE cushions,

clearly show a reduced glare probability for all WWR scenarios. Independent of large or small window openings in the façade, the glare inside the room is imperceptible during 92% to 97% of the office working hours when using fritted or switchable ETFE cushions as a second skin façade. In climates with intense solar radiation and more daylight availability throughout the year, the described trend is similar. In Barcelona (Figure 6.90), for most of the working hours throughout glare is imperceptible when using printed or switchable ETFE cushions. For the largest WWR of 90%, the glare is intolerable for only 10% of the working hours and shrinks considerably to 0.6% towards the smallest WWR with 30% window area. For the DG and the clear ETFE façade, the percentage of working hours with intolerable glare is considerably higher, with up to 47% for the largest WWR. In Shanghai (Figure 6.91) a similar behaviour can be observed for all simulated scenarios suggesting a consistent optical behaviour of the simulated façade design across different scenarios. The findings indicate that fritted or switchable could reduce the probability of glare for a range of climate locations when employed as a second layer in a DSF. The reflective properties of the frit prints in combination light scattering behaviour of the material and shape of the ETFE cushion might be suggested as the reason for the effective control of glare.

Additionally, the switching capabilities of the adaptive façade might reduce the glare even better during the peak hour of direct incident solar radiation; however, the results show that this was only true for the largest WWR of 90% façades. The density and smaller scale of the print pattern may have been a related factor, by scattering light more effectively over a large surface than a larger pattern with clear ETFE sections, as is the case for the switchable ETFE cushion, thus leading to reduced glare. This finding is of importance for the consideration in the development of new printing patterns for ETFE cushions to be applied specifically in building façades. The numerical values of the glare study are summarized at the end of this section in Table 6.21, 6.22 and 6.23.

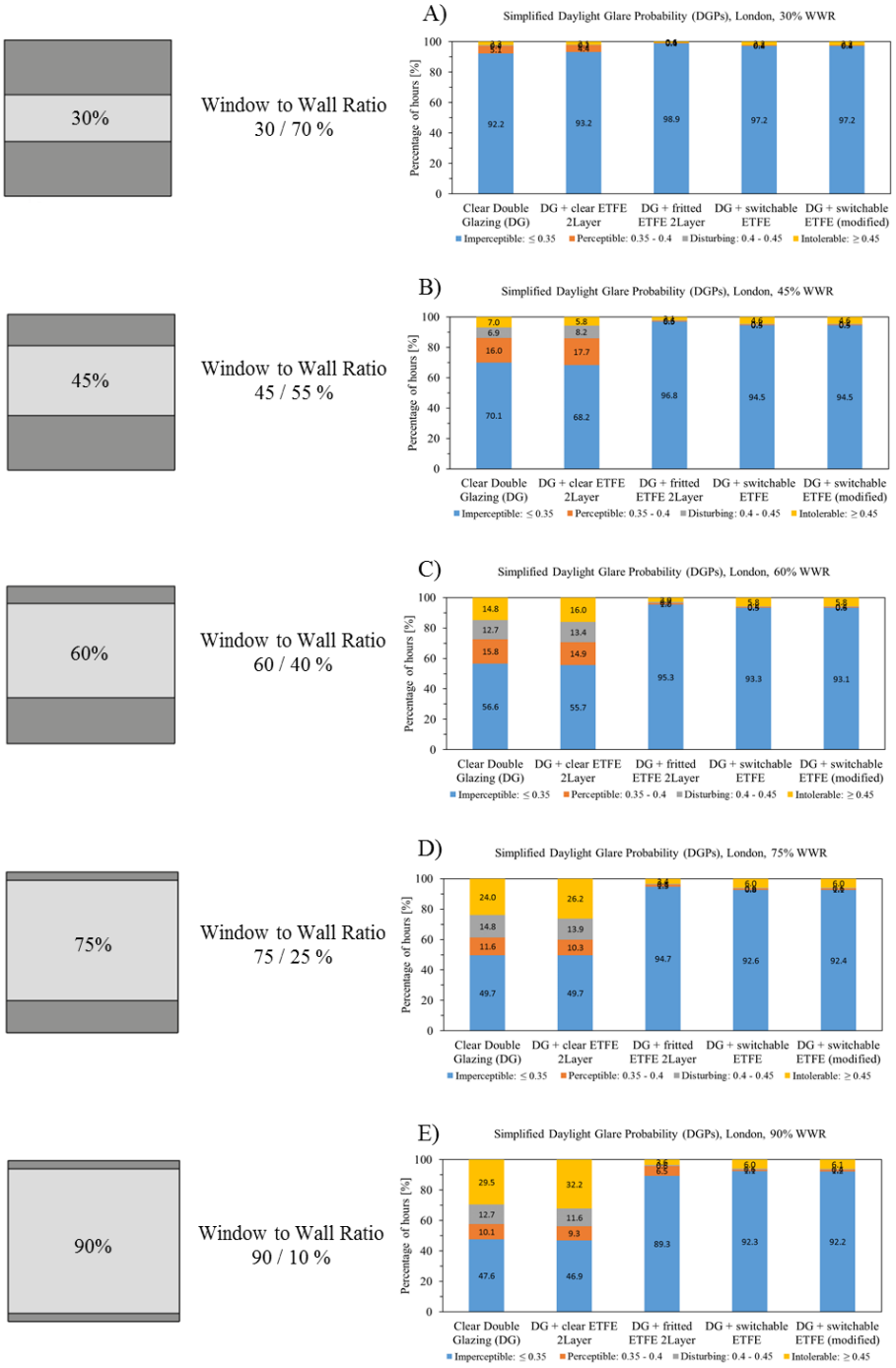


Figure 6. 89. Simplified Daylight Glare Probability (DGPs) at the viewpoint for south-facing office in London with different ETFE double-skin façades and varying window to wall ratio, A) 30%, B) 45%, C) 60%, D) 75%, E) 90%,
(graphs by the thesis author, unpublished)

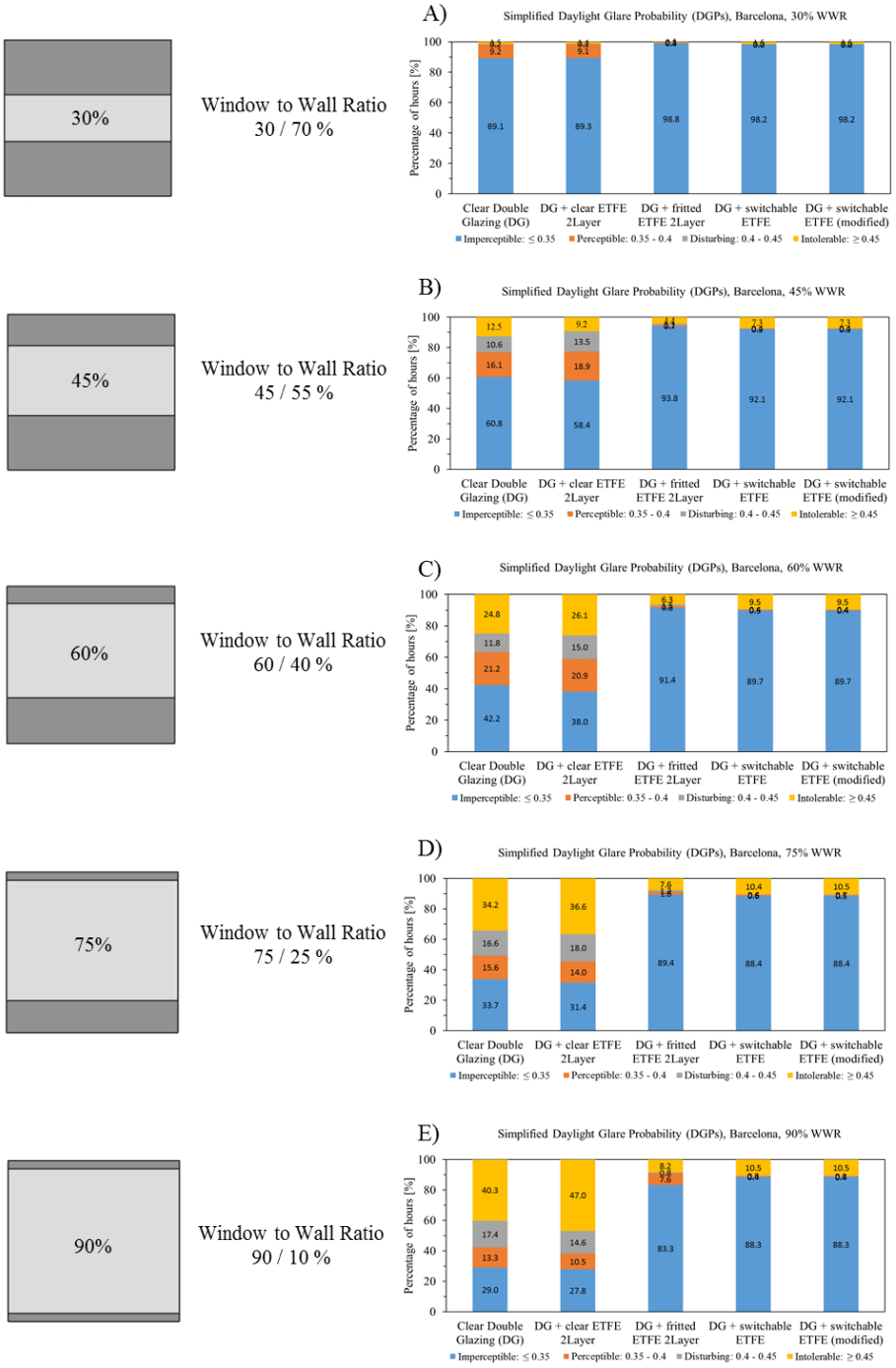


Figure 6. 90. Simplified Daylight Glare Probability (DGPs) at viewpoint for south facing office in Barcelona with different ETFE double-skin façades and varying window to wall ratio, A) 30%, B) 45%, C) 60%, D) 75%, E) 90%,

(graphs by the thesis author, unpublished)

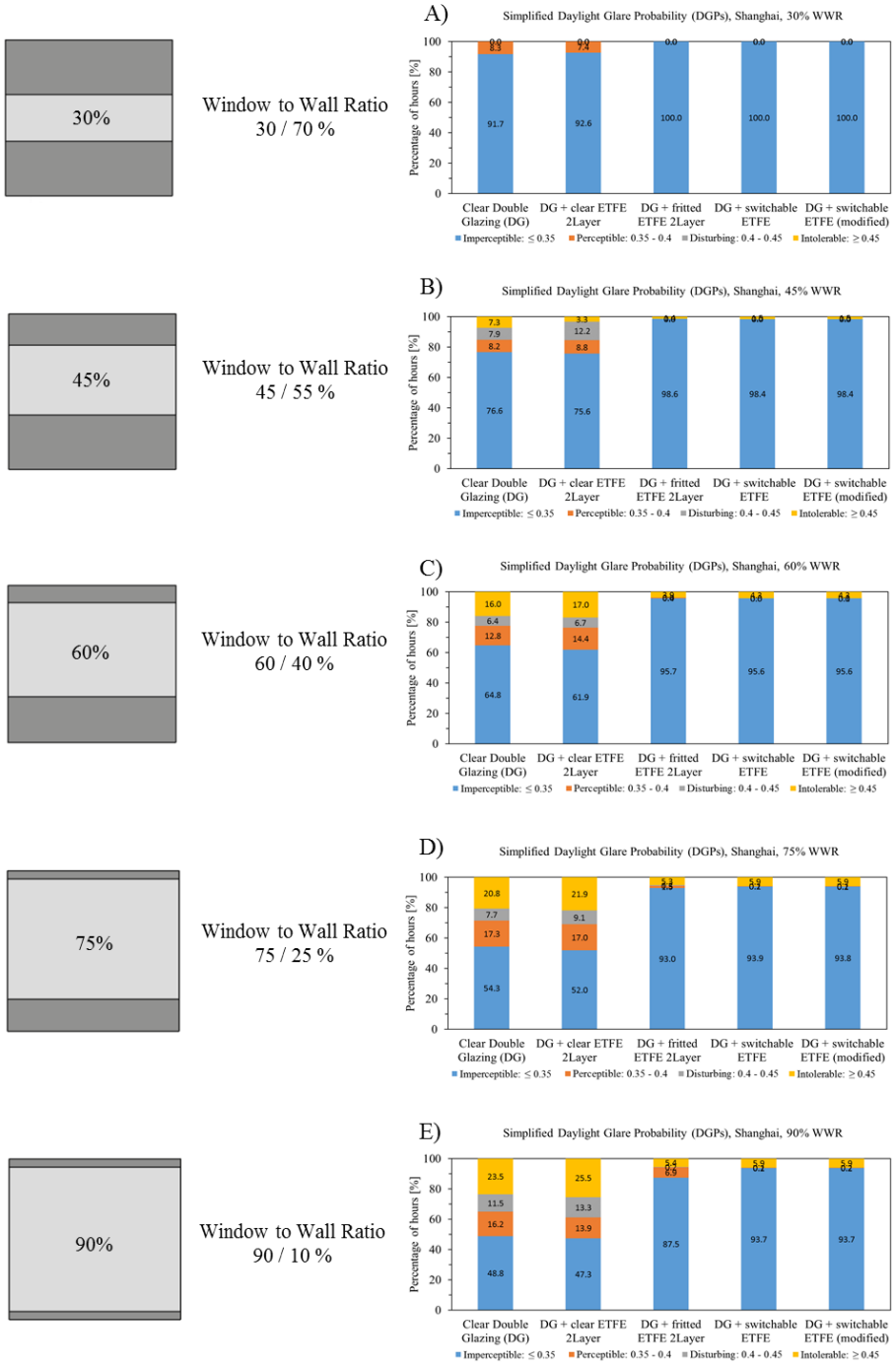


Figure 6. 91. Simplified Daylight Glare Probability (DGPs) at the viewpoint for south-facing office in Shanghai with different ETFE double-skin façades and varying window to wall ratio, A) 30%, B) 45%, C) 60%, D) 75%, E) 90%,
(graphs by the thesis author, unpublished)

Table 6. 21
Simplified Daylight Glare Probability (DGPs): numerical data summary for London
(table by the thesis author, unpublished)

WWR	Glare Perception	Bin	Clear Double Glazing (DG)	DG + clear ETFE 2 Layer	DG + fritted ETFE 2 Layer	DG + switch. ETFE 3 Layer	DG + switch. ETFE modif.
30%	Imperceptible:	≤ 0.35	92.16%	93.21%	98.87%	97.17%	97.17%
	Perceptible:	0.35 - 0.4	5.13%	4.44%	0.44%	0.44%	0.44%
	Disturbing:	0.4 - 0.45	0.36%	0.24%	0.12%	0.16%	0.16%
	Intolerable:	≥ 0.45	2.34%	2.10%	0.57%	2.22%	2.22%
45%	Imperceptible:	≤ 0.35	70.06%	68.20%	96.77%	94.51%	94.46%
	Perceptible:	0.35 - 0.4	16.04%	17.74%	0.53%	0.48%	0.48%
	Disturbing:	0.4 - 0.45	6.91%	8.24%	0.61%	0.40%	0.44%
	Intolerable:	≥ 0.45	6.99%	5.82%	2.10%	4.61%	4.61%
60%	Imperceptible:	≤ 0.35	56.61%	55.68%	95.31%	93.25%	93.13%
	Perceptible:	0.35 - 0.4	15.84%	14.87%	1.01%	0.53%	0.65%
	Disturbing:	0.4 - 0.45	12.73%	13.41%	0.69%	0.44%	0.40%
	Intolerable:	≥ 0.45	14.83%	16.04%	2.99%	5.78%	5.82%
75%	Imperceptible:	≤ 0.35	49.66%	49.66%	94.67%	92.61%	92.40%
	Perceptible:	0.35 - 0.4	11.56%	10.30%	1.33%	0.85%	1.05%
	Disturbing:	0.4 - 0.45	14.79%	13.86%	0.57%	0.57%	0.57%
	Intolerable:	≥ 0.45	24.00%	26.18%	3.43%	5.98%	5.98%
90%	Imperceptible:	≤ 0.35	47.60%	46.91%	89.29%	92.32%	92.24%
	Perceptible:	0.35 - 0.4	10.14%	9.25%	6.51%	1.13%	1.21%
	Disturbing:	0.4 - 0.45	12.73%	11.64%	0.65%	0.57%	0.44%
	Intolerable:	≥ 0.45	29.54%	32.20%	3.56%	5.98%	6.10%

Table 6. 22
Simplified Daylight Glare Probability (DGPs): numerical data summary for Barcelona
(table by the thesis author, unpublished)

WWR	Glare Perception	Bin	Clear Double Glazing (DG)	DG + clear ETFE 2 Layer	DG + fritted ETFE 2 Layer	DG + switch. ETFE 3 Layer	DG + switch. ETFE modif.
30%	Imperceptible:	≤ 0.35	89.05%	89.33%	98.83%	98.22%	98.22%
	Perceptible:	0.35 - 0.4	9.21%	9.09%	0.36%	0.04%	0.04%
	Disturbing:	0.4 - 0.45	0.20%	0.20%	0.28%	0.20%	0.20%
	Intolerable:	≥ 0.45	1.54%	1.37%	0.53%	1.54%	1.54%
45%	Imperceptible:	≤ 0.35	60.77%	58.38%	93.82%	92.12%	92.12%
	Perceptible:	0.35 - 0.4	16.08%	18.91%	0.73%	0.24%	0.24%
	Disturbing:	0.4 - 0.45	10.63%	13.49%	1.09%	0.36%	0.36%
	Intolerable:	≥ 0.45	12.53%	9.21%	4.36%	7.27%	7.27%
60%	Imperceptible:	≤ 0.35	42.22%	37.98%	91.35%	89.66%	89.66%
	Perceptible:	0.35 - 0.4	21.17%	20.89%	0.85%	0.48%	0.44%
	Disturbing:	0.4 - 0.45	11.80%	14.99%	1.45%	0.36%	0.36%
	Intolerable:	≥ 0.45	24.81%	26.14%	6.34%	9.49%	9.54%
75%	Imperceptible:	≤ 0.35	33.70%	31.43%	89.37%	88.36%	88.36%
	Perceptible:	0.35 - 0.4	15.56%	13.98%	1.82%	0.61%	0.48%
	Disturbing:	0.4 - 0.45	16.57%	17.98%	1.17%	0.61%	0.69%
	Intolerable:	≥ 0.45	34.18%	36.61%	7.64%	10.42%	10.46%
90%	Imperceptible:	≤ 0.35	29.01%	27.84%	83.31%	88.32%	88.28%
	Perceptible:	0.35 - 0.4	13.25%	10.55%	7.64%	0.40%	0.40%
	Disturbing:	0.4 - 0.45	17.41%	14.59%	0.81%	0.77%	0.77%
	Intolerable:	≥ 0.45	40.32%	47.03%	8.24%	10.51%	10.55%

Table 6. 23
Simplified Daylight Glare Probability (DGPs): numerical data summary for Shanghai
(table by the thesis author, unpublished)

WWR	Glare Perception	Bin	Clear Double Glazing (DG)	DG + clear ETFE 2 Layer	DG + fritted ETFE 2 Layer	DG + switch. ETFE 3 Layer	DG + switch. ETFE modif.
30%	Imperceptible:	≤ 0.35	91.68%	92.65%	100.00%	100.00%	100.00%
	Perceptible:	0.35 - 0.4	8.32%	7.35%	0.00%	0.00%	0.00%
	Disturbing:	0.4 - 0.45	0.00%	0.00%	0.00%	0.00%	0.00%
	Intolerable:	≥ 0.45	0.00%	0.00%	0.00%	0.00%	0.00%
45%	Imperceptible:	≤ 0.35	76.65%	75.64%	98.59%	98.42%	98.42%
	Perceptible:	0.35 - 0.4	8.20%	8.85%	0.00%	0.00%	0.00%
	Disturbing:	0.4 - 0.45	7.88%	12.24%	0.04%	0.04%	0.04%
	Intolerable:	≥ 0.45	7.27%	3.27%	1.37%	1.54%	1.54%
60%	Imperceptible:	≤ 0.35	64.77%	61.94%	95.72%	95.60%	95.60%
	Perceptible:	0.35 - 0.4	12.85%	14.38%	0.36%	0.04%	0.00%
	Disturbing:	0.4 - 0.45	6.42%	6.67%	0.04%	0.04%	0.08%
	Intolerable:	≥ 0.45	15.96%	17.01%	3.88%	4.32%	4.32%
75%	Imperceptible:	≤ 0.35	54.26%	51.96%	92.97%	93.86%	93.82%
	Perceptible:	0.35 - 0.4	17.25%	17.01%	1.45%	0.16%	0.16%
	Disturbing:	0.4 - 0.45	7.72%	9.09%	0.28%	0.08%	0.12%
	Intolerable:	≥ 0.45	20.77%	21.94%	5.29%	5.90%	5.90%
90%	Imperceptible:	≤ 0.35	48.81%	47.27%	87.47%	93.74%	93.70%
	Perceptible:	0.35 - 0.4	16.20%	13.86%	6.91%	0.24%	0.24%
	Disturbing:	0.4 - 0.45	11.47%	13.33%	0.24%	0.12%	0.16%
	Intolerable:	≥ 0.45	23.52%	25.54%	5.37%	5.90%	5.90%

6.4.5. Daylight illuminance uniformity

This section of the chapter discusses the simulation results for daylight uniformity. The results of the simulations are plotted in three groups of graphs in Figure 6.92, 6.93 and 6.94, with a summary of numerical data in Table 6.24, 6.25 and 6.26. The interpretation of the results suggests that the fritted double-layer ETFE cushion provides the highest percentage of working hours with a well-distributed daylight uniformity across all simulated scenarios. The double glazing and the DG with the added clear ETFE cushion tend to perform better with the smaller window to wall ratios of 30% to 45% while the switchable ETFE cushions deliver a better performance in terms of uniform daylight in the scenarios with larger window-to-wall ratios, from 60% to 90%. For climates like Shanghai, which already receive a higher proportion of diffuse daylight during the year, comfortable internal daylight uniformity ratios are available for comparatively more working office hours than in climates with a higher proportion of direct solar radiation. However, climates

like London with a pronounced variability of sunlight availability across the seasons do not not show reduction of UR in the 0.4 - 0.6 range; an effect which would have initially been expected due to shorter days during winter. The daylight uniformity ratio in the desired range between 0.4 and 0.6 was achieved on average for approximately 60% of the office hours across all scenarios in the London climate, with little variability among the samples. The only exception was the double glazing which had a smaller percentage of hours in the desired uniformity ratio in the scenarios with large window to wall ratios. For Barcelona, the daylight uniformity ratio was on average 50% of the hours within the targeted range, across the majority of WWR scenarios. Only with larger WWR of 65% and 90%, the percentage of hours dropped notably around 10% to 15%, due to intense direct solar radiation and the associated higher contrast of shade and light projected into the room, typical for a Mediterranean climate like Barcelona. For Shanghai, the uniformity ratio was throughout all scenarios high, ranging between 65% and 70 % on average, however, the double glazing showed a significant performance drop for the 90% WWR. Overall, the results suggest that satisfying illuminance uniformity can be achieved in small office spaces with natural daylight. Moreover, it seems possible to achieve illuminance uniformity across different climates and latitudes. Double-skin façades with inflated ETFE cushions as a second façade layer contribute to improve the illuminance uniformity and extend the number of working hours, with uniform daylight available up to 70% of the total scheduled working hours. Only an additional 30% of the hours would have to be supplied by artificial lighting. However, a high daylight uniformity value might also be interpreted as a sign for high light intensity, resultant from solar radiation, leading to sharp contrasts in the office space beyond the working area. A situation which may require more solar shading instead of additional artificial lighting. Fritted ETFE cushions with improved reflective print patterns performed best. The capacity to scatter and distribute diffused light evenly throughout the space is more effective than with glass or clear ETFE cushions, especially for façades with large window-to-wall ratios. However, only experimental settings or post-occupancy studies in real buildings might be able to provide a definite answer to this hypothesis and confirm the findings of this simulation campaign.

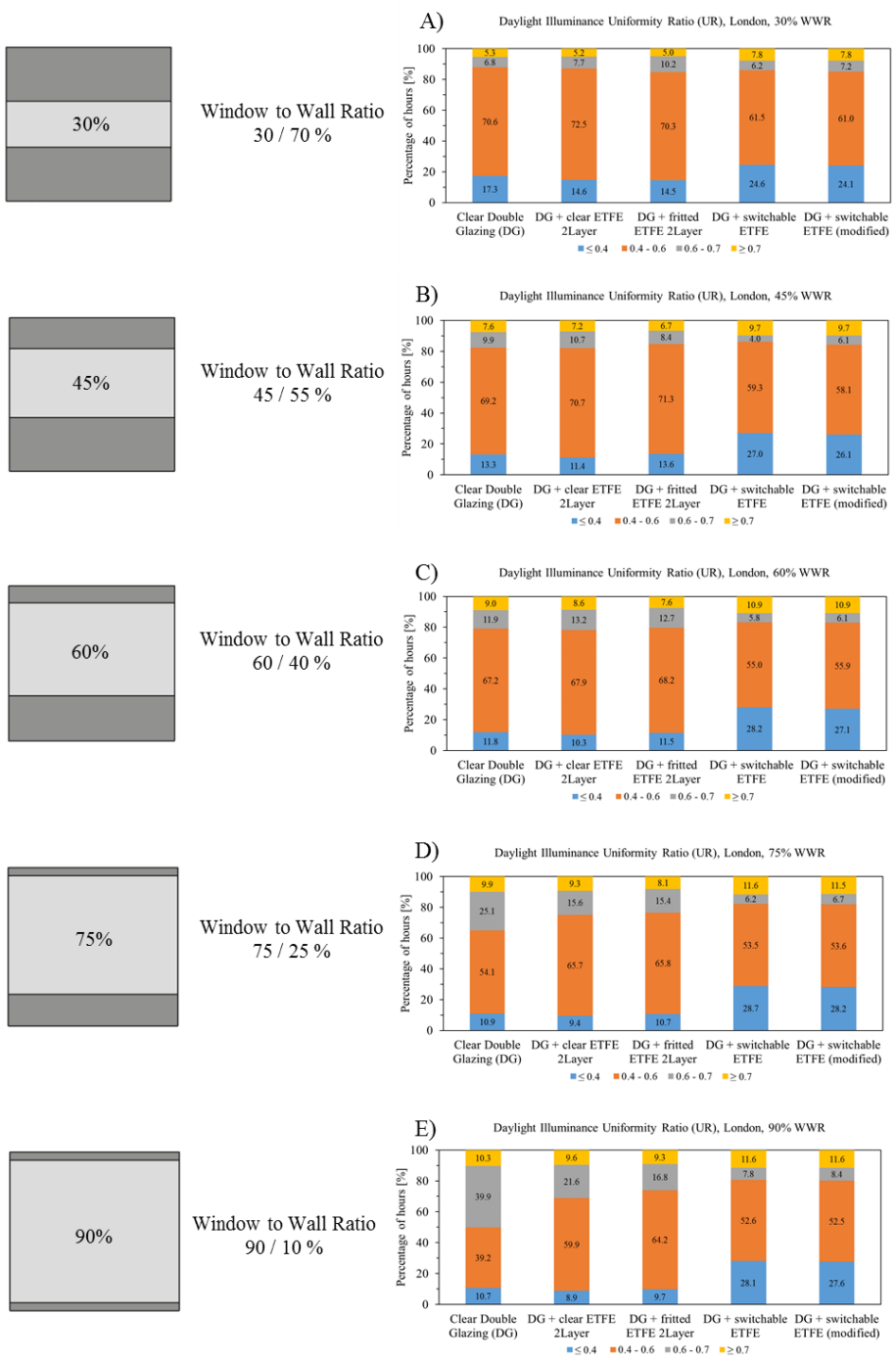


Figure 6. 92. Daylight illuminance uniformity ratio (UR) at task area for south-facing office in London with different ETFE double-skin façades and varying window to wall ratio, A) 30%, B) 45%, C) 60%, D) 75%, E) 90%

(graphs by the thesis author, unpublished)

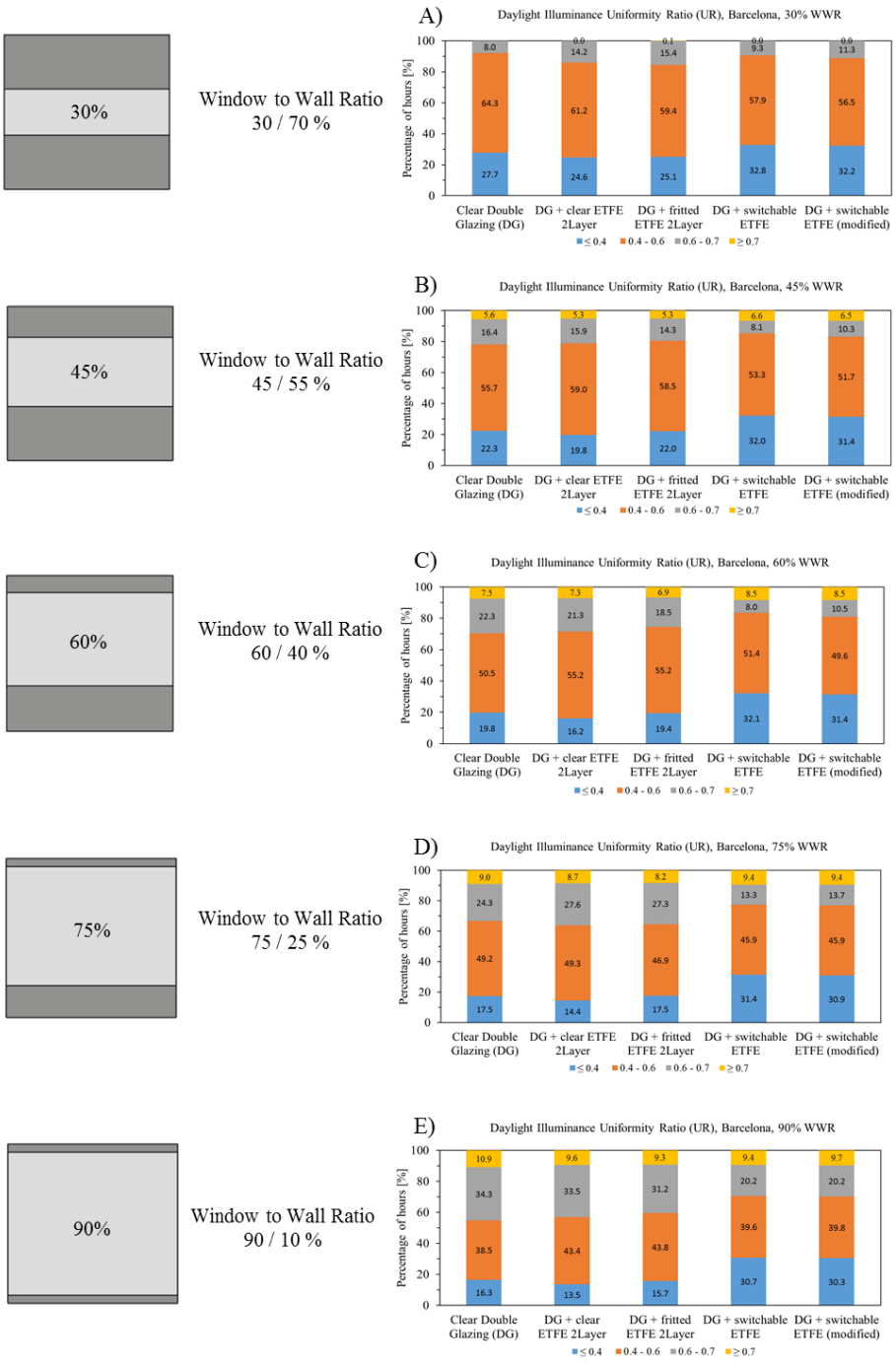


Figure 6. 93. Daylight illuminance uniformity ratio (UR) at task area for south-facing office in Barcelona with different ETFE double-skin façades and varying window to wall ratio, A) 30%, B) 45%, C) 60%, D) 75%, E) 90%

(graphs by the thesis author, unpublished)

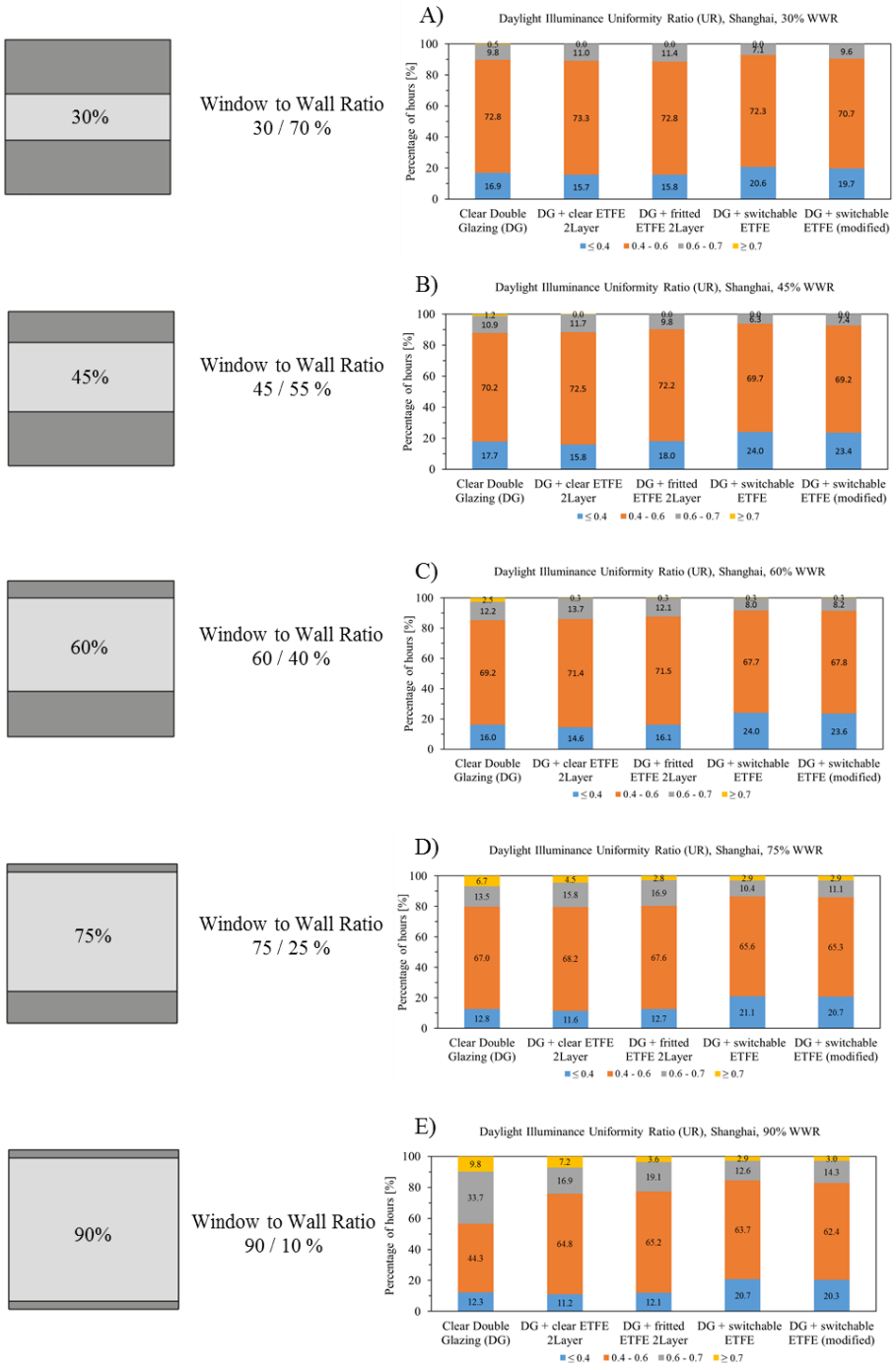


Figure 6. 94. Daylight illuminance uniformity ratio (UR) at task area for south-facing office in Barcelona with different ETFE double-skin façades and varying window to wall ratio, A) 30%, B) 45%, C) 60%, D) 75%, E) 90%

(graphs by the thesis author, unpublished)

Table 6. 24
Daylight illuminance uniformity ratio (UR): numerical data summary for London
(table by the thesis author, unpublished)

Window to Wall Ratio	Uniformity Ratio Bin	Clear Double Glazing (DG)	DG + clear ETFE 2 Layer	DG + fritted ETFE 2 Layer	DG + switch. ETFE 3 Layer	DG + switch. ETFE modif.
30%	≤ 0.4	17.29%	14.59%	14.51%	24.57%	24.08%
	0.4 - 0.6	70.59%	72.53%	70.26%	61.45%	60.97%
	0.6 - 0.7	6.79%	7.68%	10.22%	6.22%	7.19%
	≥ 0.7	5.33%	5.21%	5.01%	7.76%	7.76%
45%	≤ 0.4	13.25%	11.35%	13.58%	26.99%	26.10%
	0.4 - 0.6	69.17%	70.71%	71.27%	59.27%	58.14%
	0.6 - 0.7	9.94%	10.75%	8.44%	4.04%	6.06%
	≥ 0.7	7.64%	7.19%	6.71%	9.70%	9.70%
60%	≤ 0.4	11.84%	10.30%	11.52%	28.20%	27.07%
	0.4 - 0.6	67.23%	67.92%	68.16%	55.03%	55.88%
	0.6 - 0.7	11.92%	13.17%	12.73%	5.82%	6.10%
	≥ 0.7	9.01%	8.61%	7.60%	10.95%	10.95%
75%	≤ 0.4	10.95%	9.41%	10.71%	28.73%	28.20%
	0.4 - 0.6	54.14%	65.70%	65.82%	53.49%	53.62%
	0.6 - 0.7	25.05%	15.64%	15.39%	6.22%	6.71%
	≥ 0.7	9.86%	9.25%	8.08%	11.56%	11.47%
90%	≤ 0.4	10.67%	8.89%	9.74%	28.08%	27.56%
	0.4 - 0.6	39.15%	59.92%	64.16%	52.57%	52.48%
	0.6 - 0.7	39.88%	21.58%	16.85%	7.80%	8.40%
	≥ 0.7	10.30%	9.58%	9.25%	11.56%	11.56%

Table 6. 25
Daylight illuminance uniformity ratio (UR): numerical data summary for Barcelona
(table by the thesis author, unpublished)

Window to Wall Ratio	Uniformity Ratio Bin	Clear Double Glazing (DG)	DG + clear ETFE 2 Layer	DG + fritted ETFE 2 Layer	DG + switch. ETFE 3 Layer	DG + switch. ETFE modif.
30%	≤ 0.4	27.72%	24.61%	25.05%	32.77%	32.20%
	0.4 - 0.6	64.32%	61.17%	59.43%	57.94%	56.48%
	0.6 - 0.7	7.96%	14.22%	15.43%	9.29%	11.31%
	≥ 0.7	0.00%	0.00%	0.08%	0.00%	0.00%
45%	≤ 0.4	22.26%	19.80%	22.02%	32.00%	31.43%
	0.4 - 0.6	55.72%	58.99%	58.46%	53.33%	51.68%
	0.6 - 0.7	16.40%	15.92%	14.26%	8.08%	10.34%
	≥ 0.7	5.62%	5.29%	5.25%	6.59%	6.55%
60%	≤ 0.4	19.80%	16.16%	19.39%	32.12%	31.43%
	0.4 - 0.6	50.46%	55.23%	55.19%	51.39%	49.58%
	0.6 - 0.7	22.26%	21.33%	18.55%	8.00%	10.51%
	≥ 0.7	7.47%	7.27%	6.87%	8.48%	8.48%
75%	≤ 0.4	17.45%	14.42%	17.49%	31.43%	30.91%
	0.4 - 0.6	49.21%	49.25%	46.95%	45.86%	45.94%
	0.6 - 0.7	24.32%	27.64%	27.31%	13.29%	13.74%
	≥ 0.7	9.01%	8.69%	8.24%	9.41%	9.41%
90%	≤ 0.4	16.28%	13.45%	15.68%	30.71%	30.34%
	0.4 - 0.6	38.51%	43.43%	43.80%	39.64%	39.76%
	0.6 - 0.7	34.30%	33.54%	31.23%	20.24%	20.16%
	≥ 0.7	10.91%	9.58%	9.29%	9.41%	9.74%

Table 6. 26
Daylight illuminance uniformity ratio (UR): numerical data summary for Shanghai
(table by the thesis author, unpublished)

Window to Wall Ratio	Uniformity Ratio Bin	Clear Double Glazing (DG)	DG + clear ETFE 2 Layer	DG + fritted ETFE 2 Layer	DG + switch. ETFE 3 Layer	DG + switch. ETFE modif.
30%	≤ 0.4	16.89%	15.68%	15.76%	20.61%	19.72%
	0.4 - 0.6	72.81%	73.33%	72.85%	72.32%	70.71%
	0.6 - 0.7	9.82%	10.99%	11.39%	7.07%	9.58%
	≥ 0.7	0.48%	0.00%	0.00%	0.00%	0.00%
45%	≤ 0.4	17.70%	15.80%	17.98%	23.96%	23.43%
	0.4 - 0.6	70.22%	72.48%	72.24%	69.74%	69.21%
	0.6 - 0.7	10.87%	11.68%	9.78%	6.30%	7.35%
	≥ 0.7	1.21%	0.04%	0.00%	0.00%	0.00%
60%	≤ 0.4	16.04%	14.59%	16.12%	24.04%	23.60%
	0.4 - 0.6	69.17%	71.43%	71.52%	67.68%	67.84%
	0.6 - 0.7	12.24%	13.66%	12.08%	7.96%	8.24%
	≥ 0.7	2.55%	0.32%	0.28%	0.32%	0.32%
75%	≤ 0.4	12.77%	11.56%	12.69%	21.05%	20.69%
	0.4 - 0.6	67.03%	68.16%	67.60%	65.58%	65.29%
	0.6 - 0.7	13.49%	15.80%	16.93%	10.42%	11.07%
	≥ 0.7	6.71%	4.48%	2.79%	2.95%	2.95%
90%	≤ 0.4	12.28%	11.15%	12.08%	20.73%	20.28%
	0.4 - 0.6	44.28%	64.81%	65.17%	63.72%	62.42%
	0.6 - 0.7	33.66%	16.89%	19.11%	12.61%	14.30%
	≥ 0.7	9.78%	7.15%	3.64%	2.95%	2.99%

6.4.6. Useful daylight illuminance results

The results of the simulation provide a comprehensive analysis of the daylighting illuminance of the office space. The simulation was carried out for a number of scenarios investigating the influence of climate, window to wall ratios and material combinations of the proposed double-skin façades. The general trend observed in all analysed scenarios is that the UDI in the office with the double glazed and clear ETFE DSF increases gradually across the section of the room from small percentages of UDI at the window to higher values towards the back of the room. This can be explained with the total plotted illuminance levels which are far beyond the established UDI close to the window and then drop sharply after one-meter distance and levels down towards the back of the room where the UDI levels are achieved. For the cases with fritted and switchable ETFE double-skin façade, the incident solar radiation is considerably reflected by the outer layer of the ETFE cushions, and as a result, the internal illuminance levels reduced and are not contrasting as

severely across the section as in the case of the double glazing and clear ETFE. The UDI percentage of time with fritted and switchable ETFE is therefore also higher than with double glazing and clear ETFE, ranging between 50% and 70%, at the test points with the maximum UDI. The highest UDI is concentrated in the centre of the room, meaning that the useful daylight illuminance is for most of the time of the year concentrated in the centre area of the office room. In contrast, the highest UDI values for the double glazing and clear ETFE were shifted towards the back of the room. This is an observation which strengthens the idea that double-skin façades with fritted or switchable might deliver a better daylighting performance than a single façade with double-glazing, and that a double-skin façade with clear might not contribute to significant improvements. The above observations are supported by the graphs in Figure 6.95, 6.96 and 6.97 which compare the annual UDI with the point in time illuminance across the centre section of the room, starting from the south-facing window towards the north-facing internal wall. The UDI bins for the centre of the room are depicted in Annex C, D and E. Annex C shows the results for the London, Annex D for Barcelona and Annex E for Shanghai.

The horizontal UDI plots in Figure 6.98, 6.99 and 6.100 reinforce this interpretation, but deliver a bigger picture of the overall performance. The UDI plots in plan view show the annual UDI for every single point of the test grid and provide an overview of the useful daylight illuminance of the whole room at desk height. What becomes evident is that the switchable ETFE cushion provides a daylight exposure focussed in the centre area of the room while for the scenario with the fritted ETFE cushion the best-illuminated area is shifted from the centre towards the end of the room. In a room with a sizeable window-to-wall ratio, a widespread illuminated area in the centre of the room is more likely to be achieved with a switchable ETFE cushion, while for a small window-to-wall ratio this effect is more effectively achieved with a fritted ETFE cushion. The only scenario where the double-glazing without any additional façade skin was observed to be more beneficial in terms of useful daylight illuminance was the room with the smallest window-to-wall ratio. At 30% window-to-wall ratio double glazing provided more useful daylighting hours on a wider room area than any other investigated façade

designs, a pattern that was observed in all three climate scenarios. In Figure 6.101, the UDI performance trends were plotted for a selected test point at the centre of the room across all analysed window to wall ratio scenarios. While this type of analysis does not represent the performance of the whole room, it does give an idea about the effect that the parameters of climate, window to wall ratio and façade material have on the percentage of annual coverage with useful daylight illuminance. The general trend which can be observed from the graphs is that independently of the climate scenario, the annual hourly percentage of useful daylight illuminance in the office space decreases with augmenting window to wall ratios when double glazing single skin or clear ETFE double-skin façades are employed. The opposite performance trend is observed for the fritted and switchable ETFE cushion, which generates as a second-skin façade more annual hourly percentage of useful daylight illuminance with increasing window to wall ratio. In an attempt to generalize the result, it could be summarized, that for large window façades it would be better use fritted or switchable ETFE cushions as a measure for retrofitting and for façades with small window sizes, clear ETFE or double glazing would be more suitable.

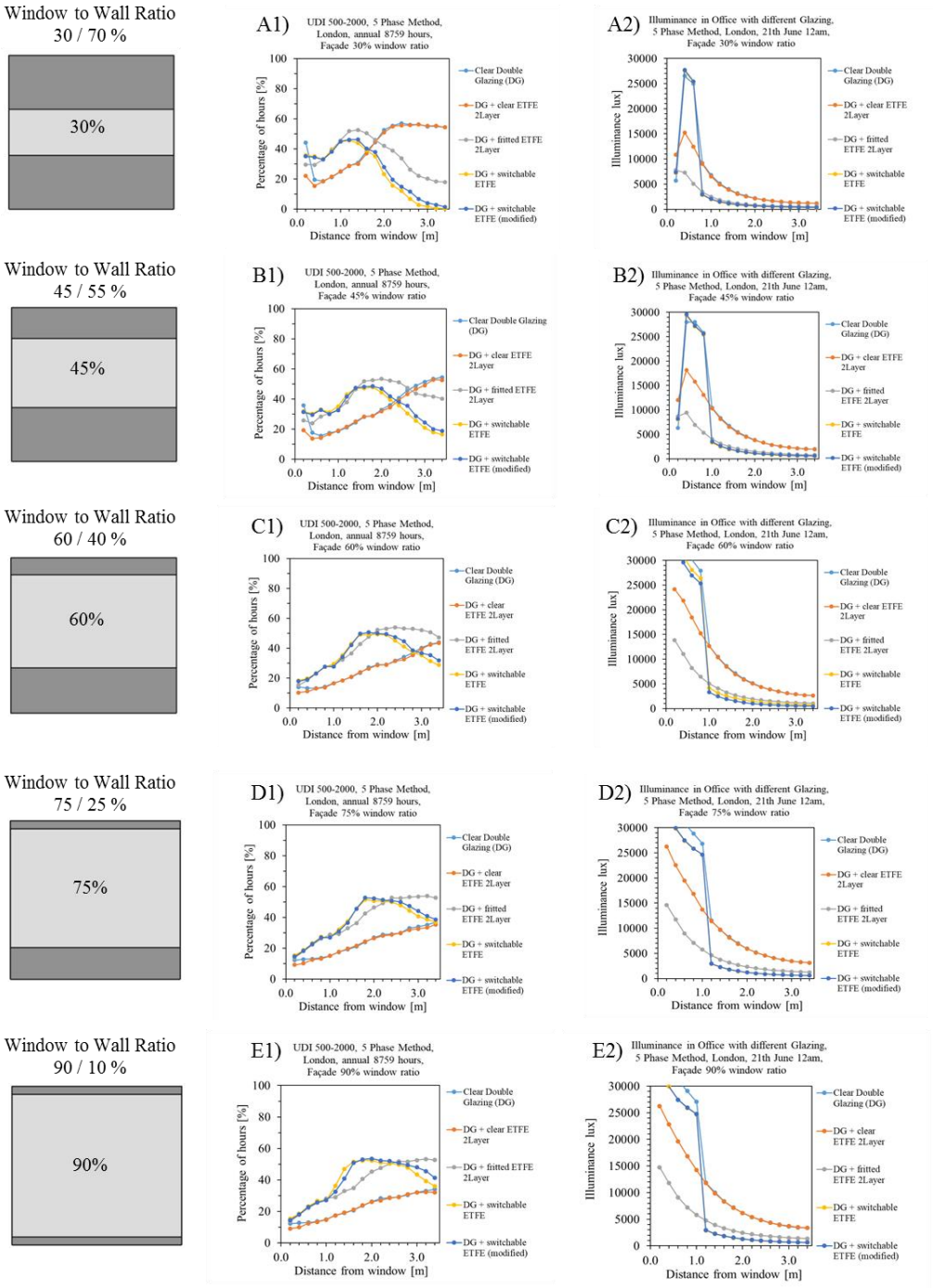


Figure 6. 95. UDI (1) and Illuminance (2) across the section of a south-facing office in London with different ETFE double-skin façades and varying window to wall ratio, A) 30%, B) 45%, C) 60%, D) 75%, E) 90%

(graphs by the thesis author, unpublished)

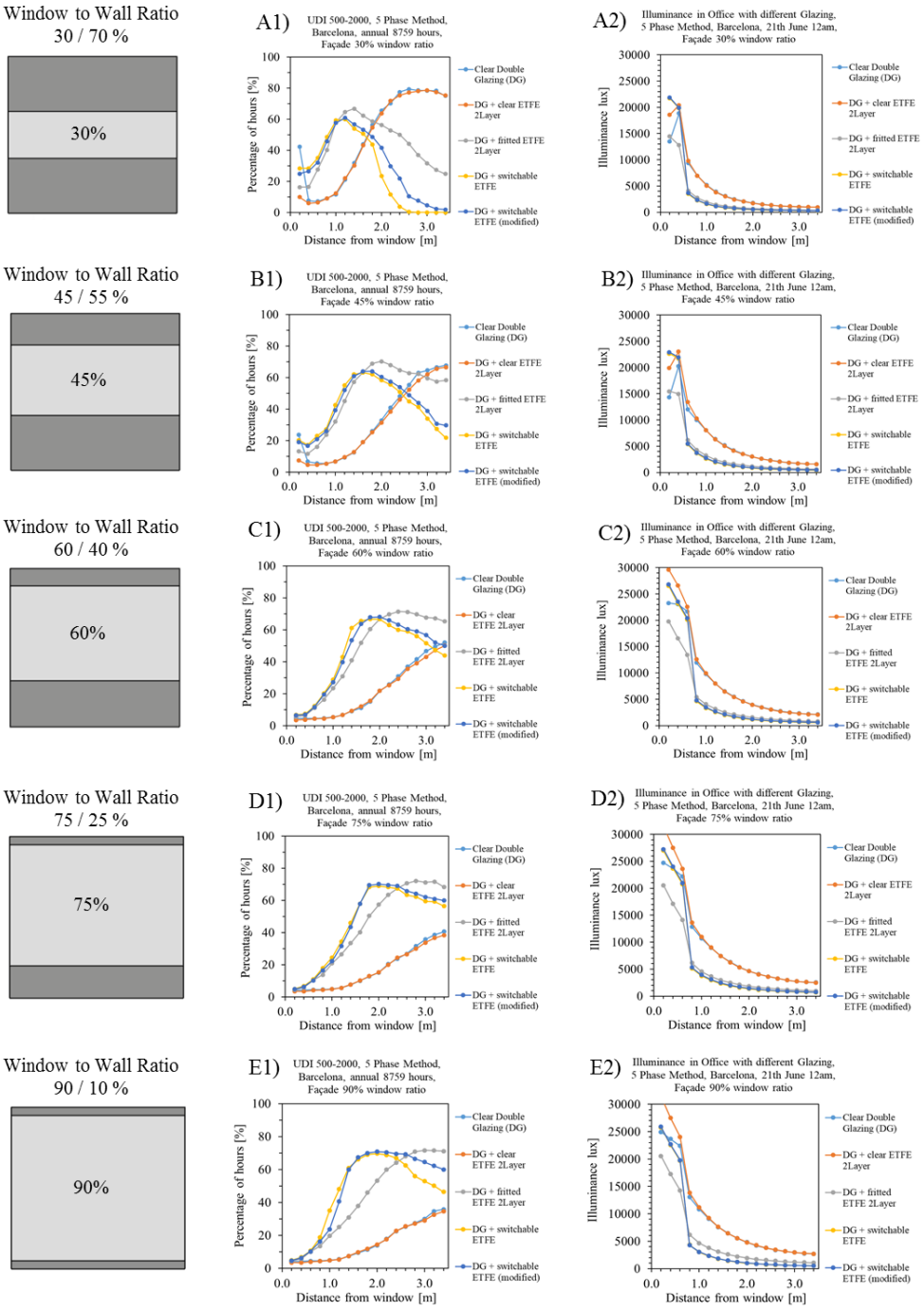


Figure 6. 96. UDI (1) and Illuminance (2) across the section of a south-facing office in Barcelona with different ETFE double-skin façades and varying window to wall ratio, A) 30%, B) 45%, C) 60%, D) 75%, E) 90%

(graphs by the thesis author, unpublished)

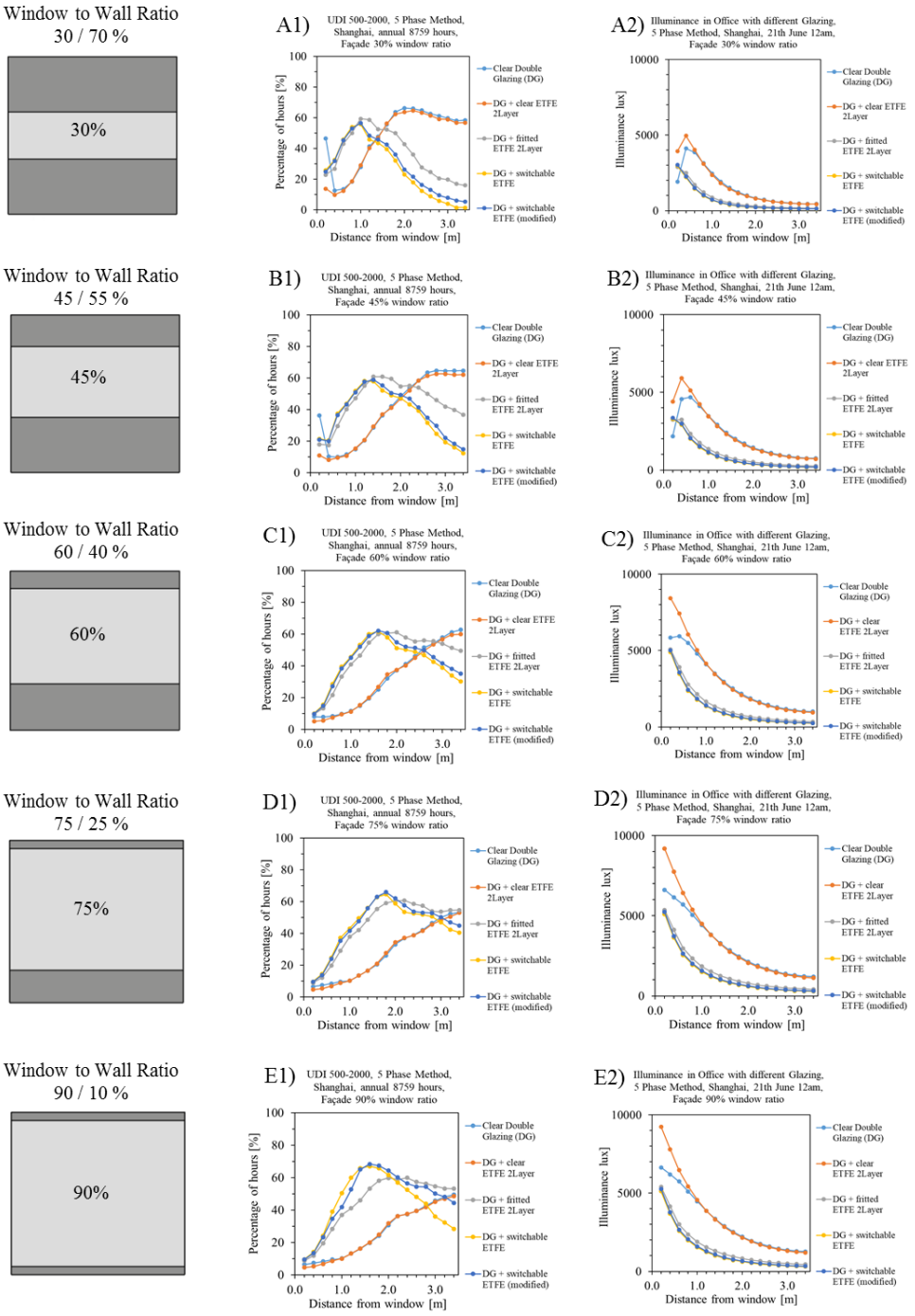


Figure 6. 97. UDI (1) and Illuminance (2) across the section of a south-facing office in Shanghai with different ETFE double-skin façades and varying window to wall ratio, A) 30%, B) 45%, C) 60%, D) 75%, E) 90%

(graphs by the thesis author, unpublished)

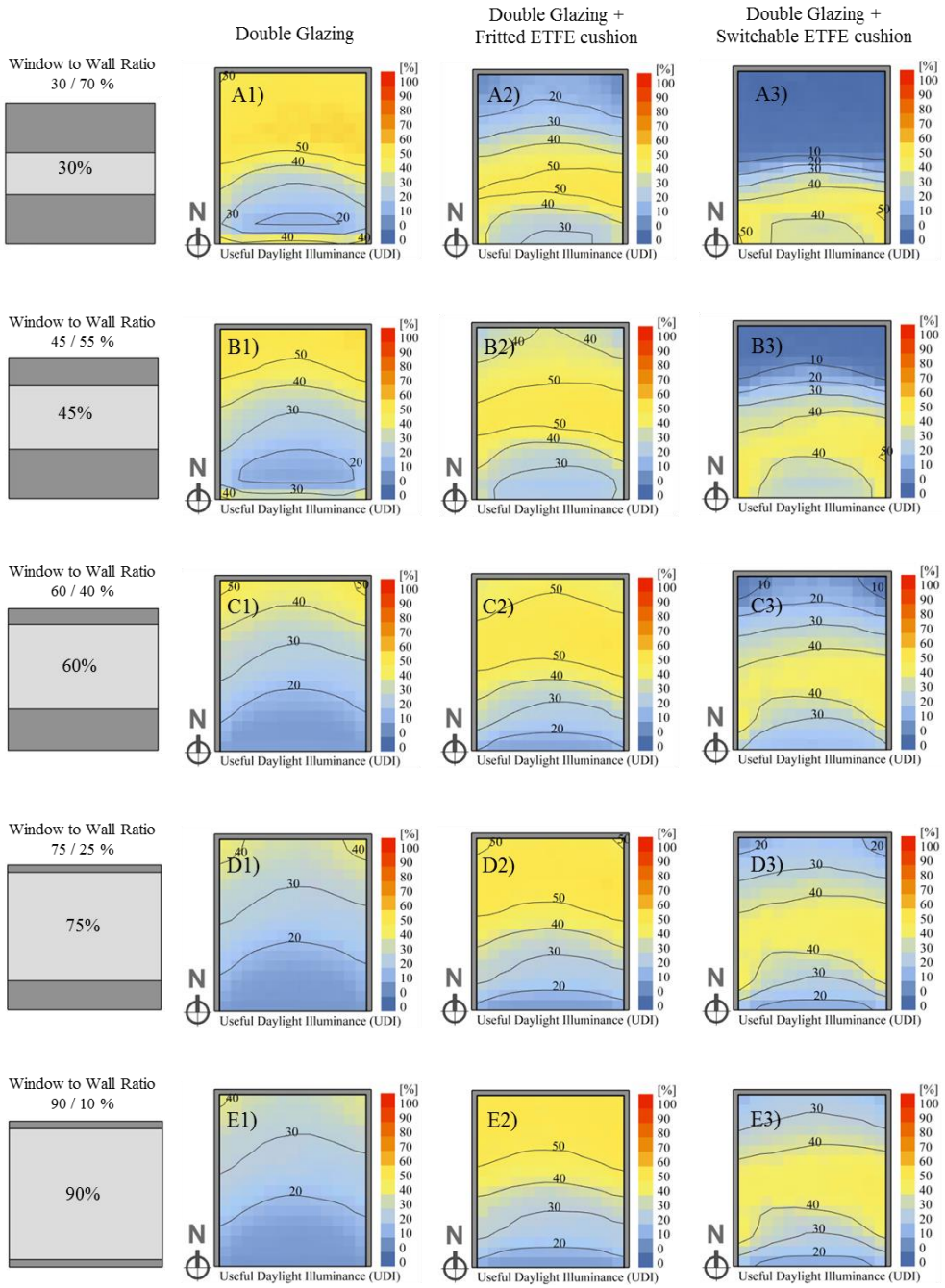


Figure 6. 98. UDI 500-2000lux bin at 0.75 m height horizontal plan for a 5-day working hours schedule of a south-facing office in London with double-skin façades comprising DG (1), DG+fritted ETFE cushion (2) and DG + switchable ETFE cushion (3) for different WWR ratios A) 30%, B) 45%, C) 60%, D) 75%, E) 90%
(graphs by the thesis author, unpublished)

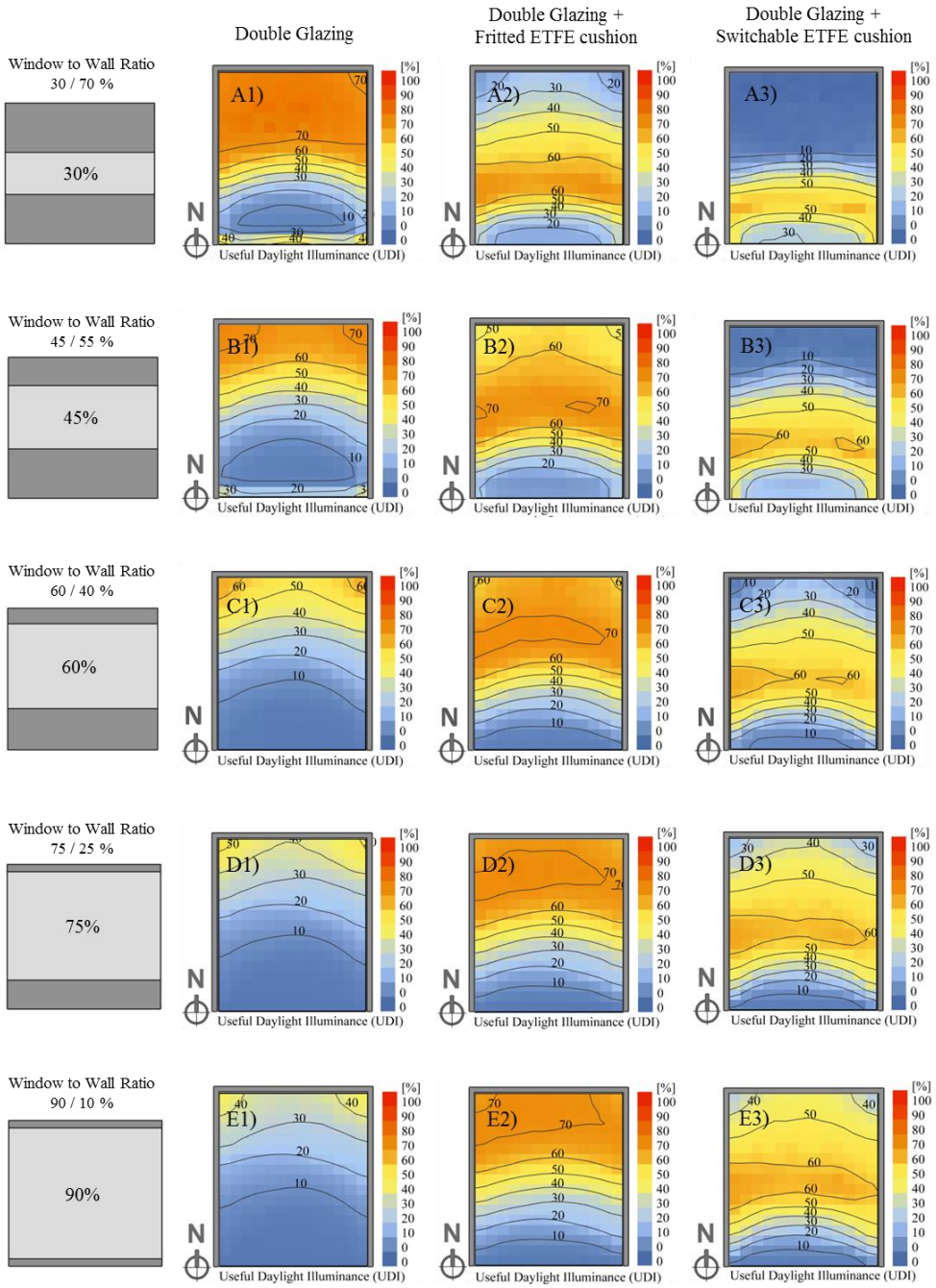


Figure 6. 99. UDI 500-2000lux bin at 0.75 m height horizontal plan for a 5-day working hours schedule of a south-facing office in Barcelona with double-skin façades comprising DG (1), DG+fritted ETFE cushion (2) and DG + switchable ETFE cushion (3) for different WWR ratios A) 30%, B) 45%, C) 60%, D) 75%, E) 90%,
(graphs by the thesis author, unpublished)

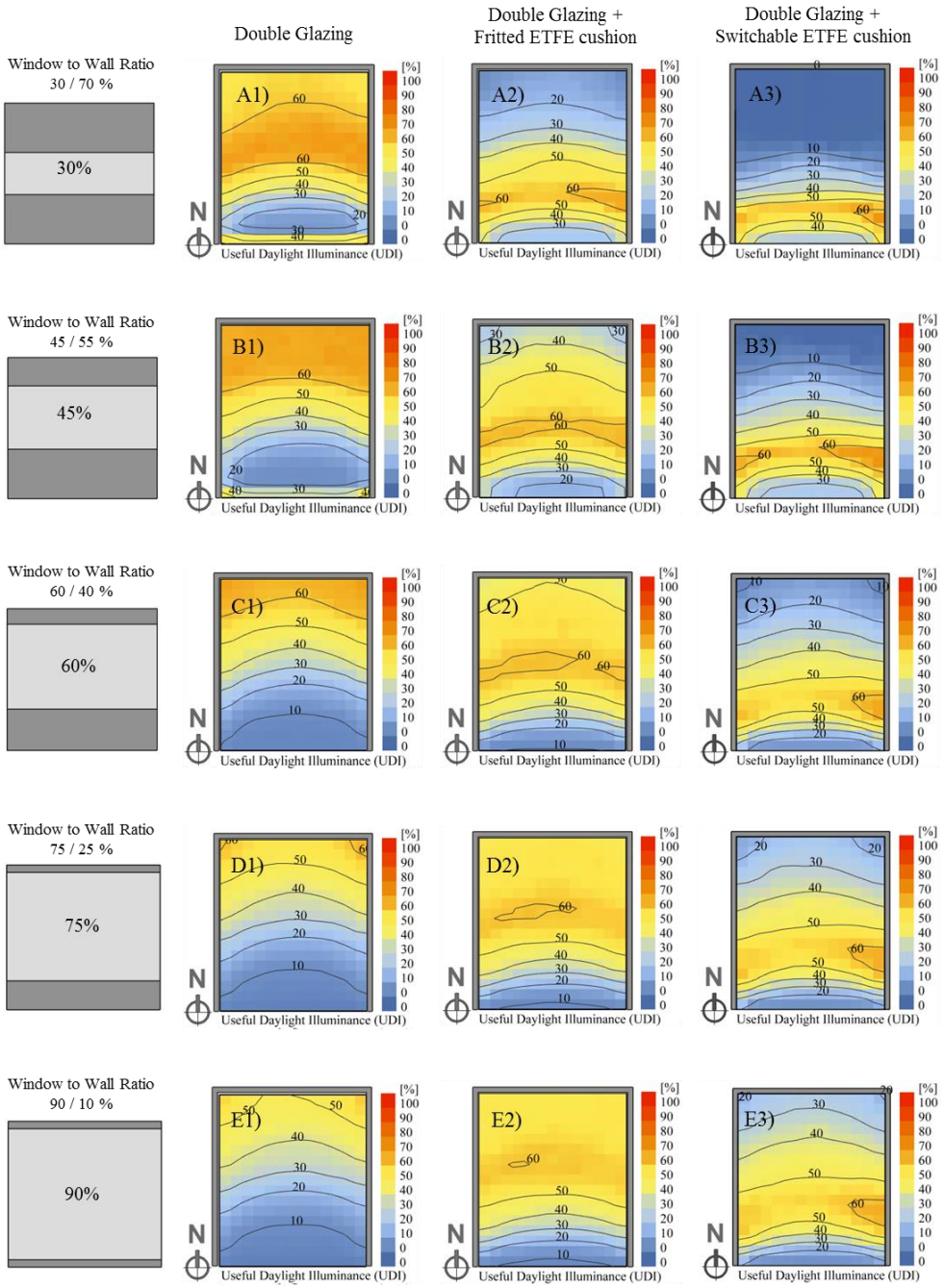


Figure 6. 100. UDI 500-2000lux bin at 0.75 m height horizontal plan for a 5-day working hours schedule of a south-facing office in Shanghai with double-skin façades comprising DG (1), DG+fritted ETFE cushion (2) and DG + switchable ETFE cushion (3) for different WWR ratios A) 30%, B) 45%, C) 60%, D) 75%, E) 90%
(graphs by the thesis author, unpublished)

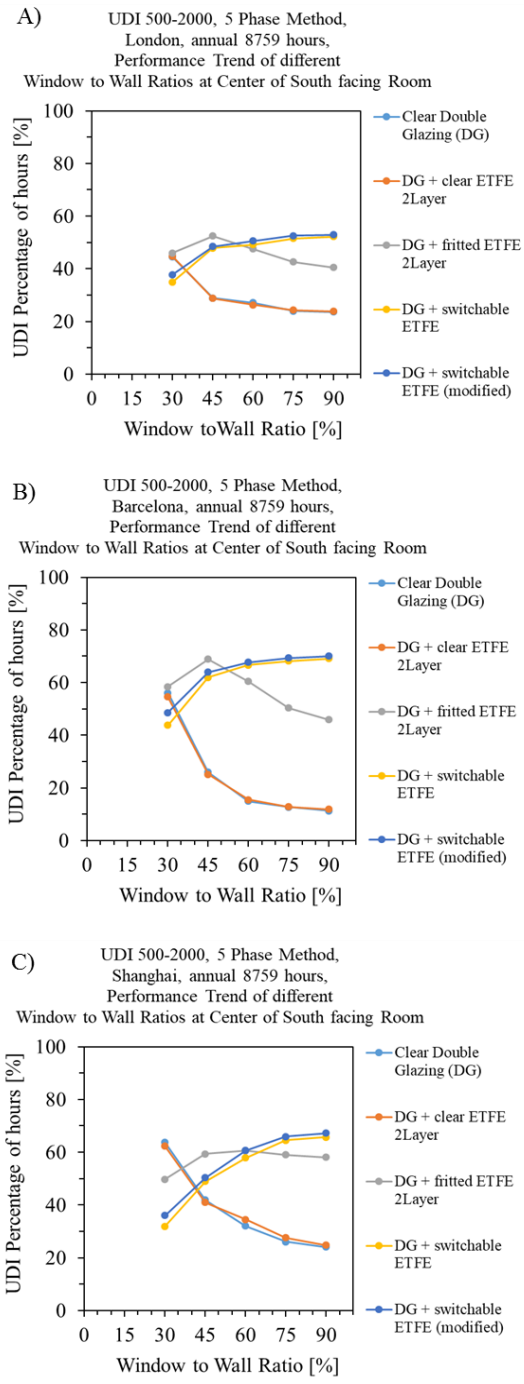


Figure 6. 101. UDI Performance trends at the centre of the room for different double-skin façades with varying window to wall ratio across different climates, A) London, B)Barcelona, C) Shanghai

(graphs by the thesis author, unpublished)

6.5.Chapter summary

This chapter investigated the daylighting performance of an office space retrofitted with different façade materials and designs. The study focussed on double-skin façades with clear, fritted and switchable ETFE cushions and evaluated the daylighting performance with criteria of illuminance uniformity, usefulness for a given purpose and disturbance through glare. The study was carried using ray-tracing methods and bidirectional scattering distribution function performing the calculations for the simulations with the validated Radiance software. The simulation was based on annual weather data and spectral analysis data of ETFE materials. An array of simulation scenarios was simulated testing the proposed double-skin façade materials under different climate conditions and a range of window to wall ratios.

The approach opted for in this study was to evaluate the daylight performance using annual hourly climate data, analysing and expressing daylight glare probability, daylight illuminance uniformity and useful daylight illuminance as a percentage of the analysed time frame at a point in a spatial grid. This approach allowed to make general judgements about the overall performance of the different DSF materials in each of the scenarios. It is however not to be forgotten that even if the performance of a specific system is exceptional over the course of the year that there will be still periods of time were glare, and illuminance over-or undersupply are affecting the daylighting qualities of the office space. In short, an adaptive double-skin façade with switchable ETFE cushions is not necessary a guarantee for a perfectly daylit space at all times.

The results had shown that glare could be effectively reduced, and a better daylight uniformity can be achieved when employing fritted or switchable ETFE cushions in double skin façades. The percentage of time when useful daylight illuminance was achieved augmented likewise when using fritted and switchable ETFE cushions as a second façade. However, it was observed that useful daylight was distributed more equally in the centre of the space when switchable ETFE cushions were employed in façade with large window to wall ratios, and fritted ETFE cushion tended to improve the daylighting distribution with

higher percentages in rooms with smaller windows. Single-skin façade with double-glazing and double skin façades with clear ETFE underperformed in all tested scenarios. The only exception was the climate scenario with less solar radiation, and the smallest of the analysed window-to-wall ratios; in this case, the double glazing outperformed all ETFE design options. The overall increase rate of the daylighting performance with switchable ETFE DSF in comparison to the original double-glazed façade was in the climate scenarios with the highest annual exposure to solar radiation.

While switchable ETFE cushions appear to perform well as daylighting control systems in double-skin façades, the question for future research remains if the adaptive shading mechanisms also enhance the energy performance of buildings. Further studies might need to be carried out to investigate whether the improved daylight performance and increased UDI has a direct effect on the electricity consumption, for lighting and cooling, or if this effect is neglectable from an energy point of view. Another question is if the fritted ETFE cushions provide enough visibility for a satisfying view experience. These questions will be addressed in the following two chapters, seven and eight.

Chapter 7: Energy Performance

7.1. Introduction to chapter seven

This chapter reports on the energy performance of spaces enclosed with ETFE. The objective of the study is to generate a general understanding of the energy performance and potential savings of office spaces when the building façade is retrofitted with a second building skin of inflated ETFE foil cushions. Based on the results from the previous chapters, a parametric, weather-data based whole building energy simulation, using EnergyPlus and Grasshopper/Honeybee, was conducted. Optical properties and U-values for the clear, fritted and switchable ETFE cushions, determined with computational and experimental methods in chapter four, five and six, were used for the simulation input and calibration of the energy simulation. Energy gains and losses with applied ETFE double-skin façades were analysed under different climate conditions, and the correlation between energy and daylighting performance was discussed. The parametrized office space used of the previous daylighting study served as a base unit for the whole building energy simulation of the present chapter. The study considered changing window to wall ratios to account for different façade configurations and the respective solar gains. In order to determine the suitability and effectiveness of ETFE DSF for different building situations and climate conditions, four façade constructions with different ETFE material layers and switchable mechanism were simulated. The testing scenarios covered three climate zones for which all DSF were tested for, with the goal to inquire which adaptive measure would be most suitable and beneficial for which climate in terms of annual energy savings.

The chapter structure includes one section covering background information on the state-of-the-art of double-skin ETFE façades and outlines a general body of knowledge regarding the energy performance of office spaces and DSF based on a review of previous studies from the literature. The following methods section covers the used software, simulation models and procedures, and the input parameters and assumptions used for the material and model generation. The results and discussion section include detailed data on

the annual electric energy use for heating, cooling and lighting for the different scenarios. The study further analyses the influence of the climate adaptive effect of the switchable multi-layer foil constructions on the energy performance of buildings under different climate conditions. The chapter concludes with a summary of the study's main findings and suggestion for future studies, including recommendations for the realistic simulation of ETFE cushions. The study outcomes are further set into the context of the built environment with a series of speculative scenarios for the future implementation of adaptive ETFE DSF in retrofitting office building façades.

7.2. Energy performance of building enclosed with ETFE

This section of the chapter outlines the background and motivation for the whole building energy simulation of office spaces enclosed with ETFE double-skin façades (DSF).

Buildings energy consumption contributes with 20-40% to the total globally consumed energy [International Energy Agency, 2013]. This is problematic when considering that the energy consumption in buildings is directly translatable to CO_2 emissions which accelerates climate change [Mardiana & Riffat, 2015]. Office buildings are notoriously known to use considerable amounts of energy for air conditioning and lighting to fulfil optimum working conditions and create productive environments on an extended schedule. Studies show that the annual average electric energy consumption in office buildings in the European Union is as high as 91.44 kWh/m2 of which 21.57% is used for lighting and 34.55% for heating and cooling for the analyzed building group and in the United States of America 293 kWh/m^2 of which 22% is used for lighting and 48% for heating and cooling [Pérez-Lombard et al., 2008; Bertoldi et al., 2012]. While the global climate change demands a reduction in CO_2 emissions from all sectors, measures for reducing energy consumption have been implemented only to a limited extent in the building sector, and emissions are effectively increasing [Wang, 2018]. The reason for this situation is partly the dynamics of the ever-growing global building stock, but also the fact that buildings are designed for a relatively long life-cycle, and therefore technologically

outdated buildings are replaced with energy efficient structures on a much slower rate than for example vehicles in the transport sector. While demolition and replacement are not sustainable solutions to this problem, a viable shortcut might be the implementation of energy retrofitting measures, such as replacement of heating cooling and lighting equipment with more efficient technologies [Caccavelli & Gugerli, 2002]. Because the technical limitations of these measures to holistically improve the overall energy performance of the building [Boyano et al., 2013], the energy study in this thesis focusses on the improvement of the building envelope. This building element directly affects the building's main thermal gains and losses. Great potential for energy savings in office buildings was forecasted in several studies. Annual energy savings of 56 kWh/m^2 were predicted for office buildings in hot Mediterranean climates [Spyropoulos & Balaras, 2011] and relative reduction of energy consumption of up to 60%, and even higher for offices built before 1980, were calculated in a case study in European countries investigating the implementation of different energy retrofitting measures in buildings [D'Agostino & Bertoldi, 2017].

Historically the thermal performance of building envelopes, windows and walls has improved gradually, a development which can be traced by tracking the benchmark U-values of building codes and standards over time. However, the actual current building stock is largely outdated with regards to the official requirements of energy performance [International Energy Agency, 2013]. Equipping buildings with a climate-adaptive second building skin appears therefore as a viable measure for energy retrofitting, a strategy which has been proposed and explored on a range of building types and scales with the literature reporting extensively on the different adaptive technologies and the impact on buildings energy performance [Haase et al., 2011; Karlsen et al., 2016; Tabadkani et al., 2020, Kunwar & Bhandari, 2020].

Double-skin façades can be described as a building envelope with two separate layers carrying out different functions linked to the aesthetics and formal appearance of the building, environmental shielding, energy generation, natural lighting and control of visibility [Shameri, 2011]. A variety of designs, material applications and operational

concepts can be found in the built environment and literature, demonstrating multiple examples also for offices buildings [Poirazis, 2004]. However, generally, double-skin façades are defined by a dual building skin where the innermost layer defines the boundary of the internal space and seals the building against the environment. The second, outer layer, which is usually separated from the inner layer by an air gap, defines the visible façade of the building and performs as a moderating element for environmental influences, such as noise, solar radiation, wind loads and other adverse weather conditions. The space in between the two layers, which can vary from a narrow gap to a walkable space, acts as a thermal buffer zone between the inside and the outside environment. Forced or natural ventilation of the air gap between the inner and outer façade may lead to enhanced environmental, and energy performance of the building and several concepts and design studies have investigated exploiting the occurring thermodynamic effects for heat and energy generation [Tang et al., 2018]. Ventilation and direct energy generation are, however, not part of this study, and instead, the focus has been put on the application of novel materials and switchable systems, investigating the impact on the energy performance under different climate conditions.

While novel building systems such as ETFE cushions have been used extensively for new build structures of multiple scale and typology, ETFE has become only recently a choice of material for façade retrofit designs [Hu et al., 2017]. While some examples of new build ETFE double-skin façades have achieved international attention during the last decade, as for example the TicMedia building shown in Figure 7.102 an anticipated widespread implementation on a bigger scale for retrofits of outdated buildings has not yet materialized. One of the main reasons may reside in the unavailability of system performance data and the lack of suitable methods and tools to predict reliably the energy savings which would justify the implementation of an ETFE double-skin façade [Kim & Park, 2011; Foucquier et al., 2013].

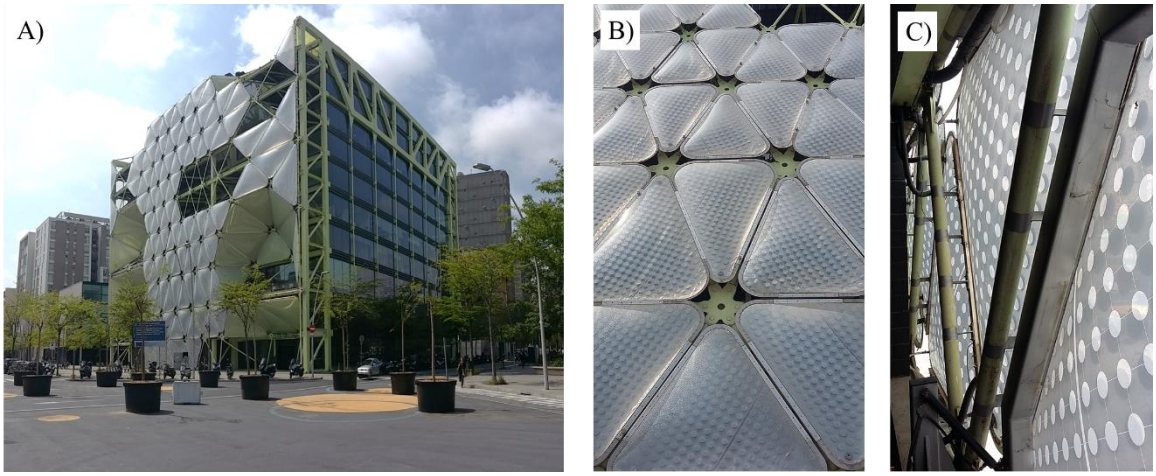


Figure 7. 102. TicMedia building in Barcelona, Spain, A) street view of the building with switchable ETFE double-skin façade, B) close-up view of the switchable ETFE cushion façade, C) backside view of the switchable ETFE cushion seen from the space between primary and secondary façade
(photos by the thesis author, taken in April 2017, unpublished)

The adaptive mechanism of the switchable ETFE cushion described in this chapter is based on a system which has been extensively analysed in the previous chapters and was specified according to findings from the optical and thermal characterisation in chapter four and five. The triple-layer inflated ETFE cushion has an alternated reflective frit print on the middle and outer layer. With a sensor-controlled air-supply, the position of the middle layer can be reversibly changed from open to close mode and hence modify the transmission of solar radiation when the internal illuminance levels rise beyond a preset threshold. A more detailed description of the optical aspects and daylighting performance of the switchable ETFE cushion is provided in chapter four and six, whereas in this chapter, the focus is on the energy performance. Investigating the adaptive capacities of switchable ETFE cushions in double-skin façade systems is directly linked to the initial questions of this thesis, whether active shading systems have the capacity to adapt to the variability of different climates scenarios and enhance the energy performance of buildings. Modelling and simulating the system and its behaviour in a realistic setting is part of the task endeavoured in this study in order to quantify the effect on the annual energy consumption of the office space. As a mode of introduction to the simulation approach of this study a

simplified approximation to the underlying energy model of the DSF is outlined below, intended to support the visualization and interpretation of the building simulation. Figure 7.103 exemplifies with a simplified diagram of a schematic building section the heat transfer mechanisms thru an ETFE double-skin building façade.

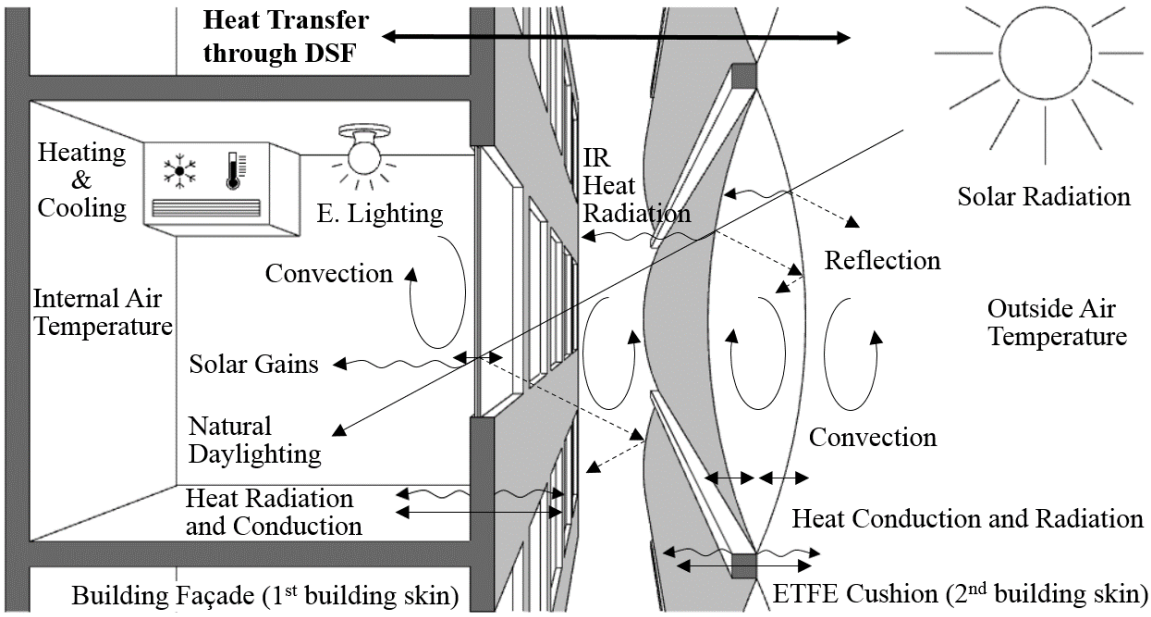


Figure 7. 103. Heat transfer mechanisms through double-skin façades with ETFE cushion (image by the thesis author, unpublished)

The diagram shows the multiple interactions of radiation, conduction and convection within the ETFE foil cushion and in between the two layers of the DSF building envelope. The heat transfer mechanisms and interactions of transmitted and reflected solar radiation thru and in between the two façade skins define, apart from electrical equipment or human presence, are the primary heat gains and losses of the internal office space. Depending on how much heat is transferred thru the building envelope into or out of the office, mechanical systems must be employed using electric energy to heat, cool or illuminate the space to establish comfort conditions for a productive environment. Testing and quantifying the potential energy savings of switchable ETFE cushions in comparison to conventional double-glazing façades and static ETFE double-skin façades is the

objective of this chapter. The methods employed to achieve this objective are outlined in the following section.

7.3.Methods

This section of the chapter describes the methods used for the whole building energy simulation, assessing the capabilities of switchable ETFE cushions to improve the energy performance of buildings across different climate zones. Consulted literature and international standards provided the technical framework and normative benchmarks for the simulation set-up. A description of the used simulation tools and outline of the workflow is provided together with a detailed account of the parameters used for the material generation and the assumptions made for the model set-up.

7.3.1. Workflow and Software tools

The software program chosen for the whole building energy simulation study reported in this chapter is OpenStudio (1.14.0 Release 2016-12-16, by the National Renewable Energy Laboratory, a part of the U.S. Department of Energy (DOE)) which uses EnergyPlus (8.6.0 Release 2016-09-27, by the U.S. Department of Energy (DOE)) in combination with Radiance 5.0.a.8 Release 2016-10-02, by Greg Ward at Lawrence Berkeley National Laboratory (LBNL) a part of the U.S. Department of Energy (DOE)) as calculation engines for the simulation processs; EnergyPlus is a widely acknowledged software for this type of study and has been validated in previous studies [US Department of Energy, 2018]. EnergyPlus is used in this study in combination with Honeybee (0.0.62 Release 2017-28-07, by Ladybug Tools LLC), an add-on program for the Grasshopper plug-in (0.9 0076 Release 2014-08-27, by David Rutten at Robert McNeel & Associates) of Rhinoceros 3D modelling program (5 SR7 64-bit 5.7.31213.18395 Educational Version Release 2013-12-13, by Robert McNeel & Associates), a software coupling which provides capabilities for parametric modelling and automatization of simulation routines [Sargent et al., 2011]. With Grasshopper's generative modelling tools, a generic office building is

modelled within the Rhinoceros 3D environment. The input data for the model and simulation parameters is assigned through the Honeybee/Grasshopper interface. Honeybee is able to read, write and execute EnergyPlus data and simulation procedures. The numerical results generated with the EnergyPlus simulation engine are automatically imported to Honeybee for read-out and visualization in the 3D graphic environment of Rhinoceros, achieving a circular and reiterative data flow [Roudsari, 2020]. An overview of the workflow between the different programs can be seen in the diagram of Figure 7.104.

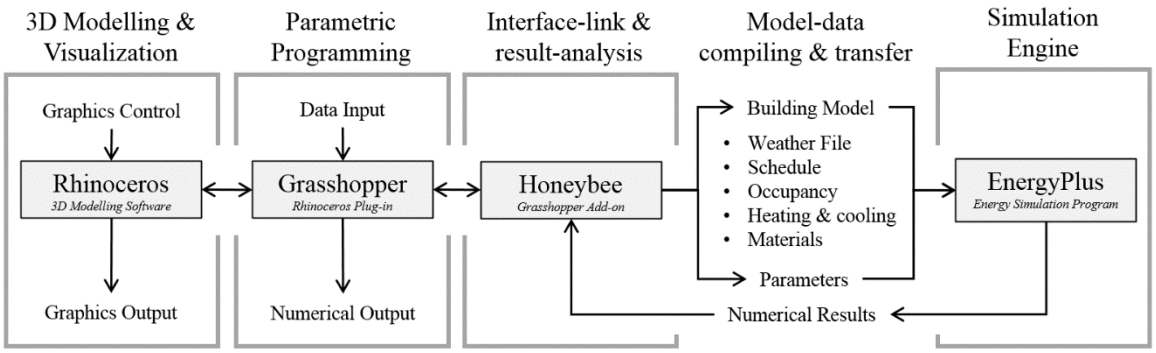


Figure 7. 104. Workflow diagram of energy simulation showing data stream between programs and plug-ins
(flow-diagram by the thesis author, unpublished)

7.3.2. Location and climate data

The whole building energy simulation described in this chapter was carried out for three different climate zones between the 30th and 50th degrees of northern latitude. The purpose of this approach was to get an understanding of the impact of ETFE façades on the energy performance of buildings under different climate conditions, a common approach in advance building simulation studies [Sun et al., 2018]. The analyzed climates in this study were Oceanic, Mediterranean and Subtropical, according to the Köppen-Geiger climate classification system [Köppen, 1900; Kottek et al., 2006], and were represented by the cities of London, Barcelona and Shanghai, respectively. The city climates were also classified according to the climate categories of the ASHRAE standard 90.1-2019 [ANSI/ASHRAE, 2019]. While the ASHRAE climate classification system is not as

precise and descriptive as the Köppen-Geiger climate classification, it provides an ample normative catalogue of recommendations for material, comfort and building services benchmarking for energy simulations. An overview of the climate classification and characteristic climate attributes for each of the chosen locations is shown in Table 7.27.

Table 6. 27
Climate classification of simulated locations
(table by the thesis author, unpublished)

Representative City	Geographic Coordinates	Climate Zone (ASHRAE)	Climate Zone (Köppen)	General Climate Characteristics
London	51.5° North 0.1° West	4 A (Mixed - Humid)	Cfb (Oceanic)	temperate oceanic climate, with mild summers and cool winters
Barcelona	41.4° North 2.1° East	3 C (Warm - Marine)	Csa (Mediterranean)	warm-temperate subtropical climate, with hot summers and mild winters
Shanghai	31.2° North 121.5° East	3 A (Warm - Humid)	Cfa (Humid Subtropical)	humid subtropical climate with hot and humid summers, and chilly and damp winters

For the energy simulation, IWEC weather files in epw format with hourly meteorological data of the three locations were used for the annual whole building energy simulation. An overview and data summary of the most relevant climate parameters considered for this study is shown in Table 7.28.

Table 6. 28
Meteorological data for London, Barcelona and Shanghai
(table by the thesis author, unpublished)

Meteorological data	Unit	London		Barcelona		Shanghai	
(average monthly)	[ ]	Min	Max	Min	Max	Min	Max
Dry-bulb temperature	[°C]	3.9	17.3	8.2	24.1	4.3	28.2
Dew point temperature	[°C]	1.5	12.4	3.2	18.5	-0.1	24.0
Relative humidity	[%]	70.8	88.5	66.2	82.5	70.6	83.5
Wind speed	[m/s]	2.3	4.4	2.4	4.4	2.6	4.0
Direct normal radiation	[Wh/m^2]	22.0	143.4	81.6	235.7	58.2	136.7
Diffuse horizontal radiation	[Wh/m^2]	17.6	123.1	35.7	117.2	47.5	107.7
Global horizontal radiation	[Wh/m^2]	22.9	209.2	69.5	279.0	88.8	210.9
Horizontal infrared radiation	[Wh/m^2]	288.1	350.9	289.9	382.0	284.1	415.8
Global horizontal illuminance	[lux]	2496.0	23149.2	7447.2	30820.3	9671.8	23770.0
Total sky cover	[tenth]	5.7	8.0	3.3	5.4	4.8	7.7
Barometric pressure	[Pa]	100146.8	101349.2	101263.9	101913.8	100300.0	102853.4

7.3.3. Building model and zone configuration

The building model for the energy simulation is based on a standard single unit office room, used for the daylighting simulation in the previous chapter five. The office dimensions are in accordance with the minimal office dimension of the normative DIN EN 4543-1:1994-09 [DIN, 1994], measuring 3.4 m (depth) by 2.9 m (width) by 2.8 m (height), with a floor area of 9.86 m^2 and a total space volume of 27.1 m^3. Recent, up-to-date international building standards do not provide a clear indication of office space dimensions; therefore, it was opted to follow this reference which had also been used previously for the office model of the daylighting simulations in chapter five. The office building itself is composed of three zones, namely office, corridor and staircase, containing 60 equal office units. The office building is three stories high 35.4 m long, 9.0 m high and 8.3 m wide. The total floor area of the building is 955.8 m^2 with a volume of 2628.5 m^3. The testing office, which was analyzed in detail throughout the study in this chapter, is located on the second floor on the south-facing façade. The office building's shape and spatial layout were based on a generic configuration designed to represent a standard office building as it could be existing in many places and therefore could serve as a comparative model for other building simulations. A visualization of the building and investigated office space is shown in Figure 7.105 and 7.106 A and B.

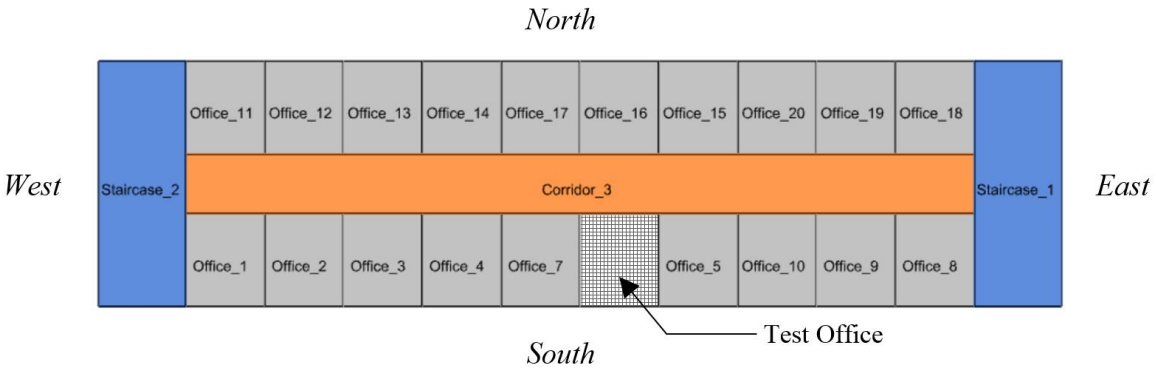


Figure 7. 105. Plan view of building model with indicated test office
(image by the thesis author, unpublished)

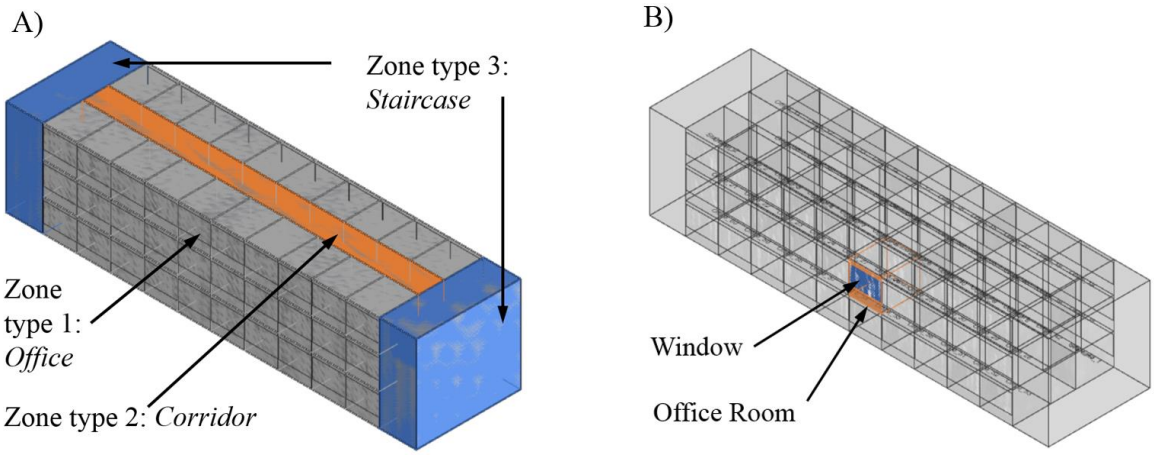


Figure 7. 106. Isometric view of building model and zones (A) and test office room (B) (images by the thesis author, unpublished)

The building façade was modelled with an adjustable parameter for the window-to-wall ratio, with the purpose to compare the impact of the ETFE double-skin façade on different configurations of the façade. The window-to-wall ratio had been identified previously in several studies as one of the main parameters that affect buildings' energy performance [Marino et al., 2017; Sun et al., 2020]. The window-to-wall ratio of the office test room façade in this study represented five different scenarios shown in Figure 7.107, which ranged in a proportional window size from 30% to 90% in steps of 15%. The WWR scenarios were analogue and, therefore, comparative to the daylighting simulation in chapter five, where results had shown that this range of WWRs provided sufficient daylight in all climate scenarios. The glazing parameters and DSF configurations are also based on the previous daylighting studies in chapter five. The materials which were assigned to the glazing surfaces with DG, DG + clear ETFE cushion, DG + fritted ETFE cushion and DG + switchable ETFE cushion were alternated throughout the different scenarios of the study. This allowed the same office building model, with different WWR and glazing materials, hence façade configurations, to be compared. Due to constraints in the modelling options of EnergyPlus, it was not possible to model the double-skin façade for the whole model outer façade, as the modelling conventions of EnergyPlus only allow materials to be assigned to coplanar planes of the space limiting geometry. An alternative approach would

have been to model the DSF as a separate zone, which, however, would have led to other secondary modelling problems. The chosen modelling approach is considered the most appropriate to represent the ETFE DSF, but has implications not only on the daylighting performance but also on the heat transfer through the façade and will be discussed in detail in the following sections.

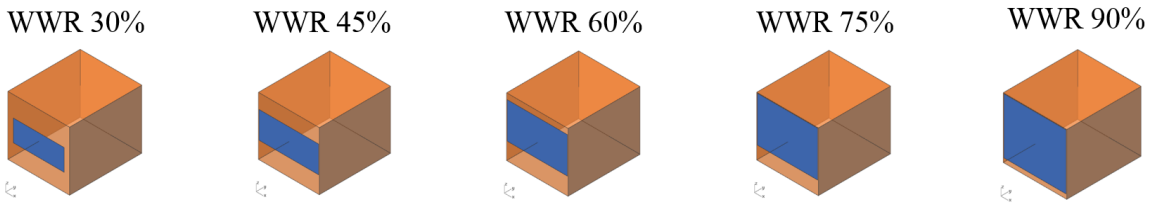


Figure 7. 107. Office test room with incremental window to wall ratios ranging from 30% to 90% in steps of 15%
(image by the thesis author, unpublished)

7.3.4. Model and zone parameters

This section gives an overview of the simulation parameters and illustrates the rationale behind the chosen parameter values and assumptions made for modelling the office building. International standards were consulted to provide criteria for setting the inputs of the simulation parameters. Decisions about material choices, zone schedule and occupancy, lighting, cooling and heating as well as equipment loads were informed by the recommendations of the international standards. The model is meant to represent an outdated office building with buildings materials and performance parameters typically underachieving the requirements of current standards. While the standard requirements may arguably vary for different time periods and locations, the building model projected for this study considers the minimal requirements of previous building practices to simulate an aged building.

The ASHRAE standard 55-2013 [ANSI/ASHRAE, 2013] defines the thermal environmental conditions for human occupancy and establishes an adaptive comfort model which was used for calculating the lower and upper comfort temperatures based on annual, hourly climate data for the three analysed locations. However, it was reasoned to use the

same comfort conditions for all three climates scenarios in favour of a reduced number of variables and better comparability of the results. The upper and lower limits of the calculated comfort temperature band defined the parameters of heating and cooling set-points for the annual energy simulation of the building.

The ASHRAE energy standard for buildings 90.1 [ANSI/ASHRAE, 2010], provides a material and construction component database with recommendations for assigning materials and components to building models according to climate zones. The chosen materials and construction components follow the recommendations for climate zone 3 and 4. While the U-value used for the building construction components of walls, roofs, and windows is considerably higher than current versions of building standards recommend, they reflect the outdated building stock proposed to be retrofitted within this study. The alternative façade constructions, which constitute the simulation scenarios for double-skin façades equipped with ETFE cushions are based on the experimental measurements in chapter four and the optical properties derived in chapter three and five. The optical material characteristics for the different layers are based on measurements for the visible part of the spectrum presented in chapter five and data from the literature for the solar transmittance and reflectance [Knippers et al., 2011, Flor et al., 2018]. The transmittance and reflectance values for the open and closed mode of the switchable cushion is based on the published raytracing study presented in chapter three. A summary of the input data for the material definition of the glazing and ETFE is shown in Table 7.29.

Table 7. 29
Input data for the material definition of the glazing and ETFE (source: Knippers et al. 2011; Flor et al., 2018, experimental data chapter 5 and 6)
(table by the thesis author, unpublished)

Double Skin Facade Layers	Transmittance [%]		Reflectance [%]		Emissivity		Conductivity	Thickness
(DSF material types)	T_{sol}	T_{vis}	R_{sol}	R_{vis}	ε_{front}	ε_{back}	ƙ [W/m·K]	[m]
Glazing	83.7	89.8	7.5	8.1	0.84	0.84	0.90	0.0030
Clear ETFE	91.1	91.0	8.0	6.2	0.82	0.82	0.23	0.0002
Fritted ETFE	54.0	33.0	23.0	45.7	0.82	0.57	0.23	0.0002
Switchable ETFE (open mode)	20.6	20.6	42.3	42.3	0.82	0.57	0.23	0.0002
Switchable ETFE (closed mode)	2.5	2.5	57.5	57.5	0.82	0.57	0.23	0.0002

Within the Honeybee/EnergyPlus construction material editor, ETFE multi-layer cushions were modelled using the optical and thermal properties from the previous chapters as input data. While the optical data from chapter three and five was used directly for the EnergyPlus input, the experimental U-values meassured in the climate chamber, reported in chapter five, section 4.1 were used for a validating comparison with the U-values of the three ETFE cushion types calculated within EnergyPlus. The comparative table 7.30 shows the similarity between the calculated and measured values with a mean deviation of 8.8%, which compares to the deviation from the standard calculation in chapter five, section 3.8 and provided sufficient confidence to proceed with the calculated values.

Table 6. 30.
Comparison between measured and calculated U-values of ETFE cushions (table by the thesis author, unpublished)

ETFE Cushion Samples	Meassured (Climate Chamber) U-Value [W/(m^2·K)]	Calculated (EnergyPlus) U-Value [W/(m^2·K)]
Clear ETFE cushion (double-layer)	2.2	2.4
Fritted ETFE cushion (double-layer)	2.1	2.4
Switchable ETFE cushion (triple-layer)	1.8	1.7

Therefore, it was decided to use the generated U-values of the ETFE cushions for the future building simulation. Combined double-skin façades were modelled with the respective layer build-up, using the previously modelled ETFE cushions and standard wall components from the EnergyPlus catalogue following the recommendation of ASHRAE [ANSI/ASHRAE, 2010] A schematic diagram showing the layer build-up of the DSF options is shown in Figure 7.108. The U- and R-value for the combined DSF models were also calculated within EnergyPlus. A summary of the main building components, material layers and thermal characteristics is laid out in Table 7.31.

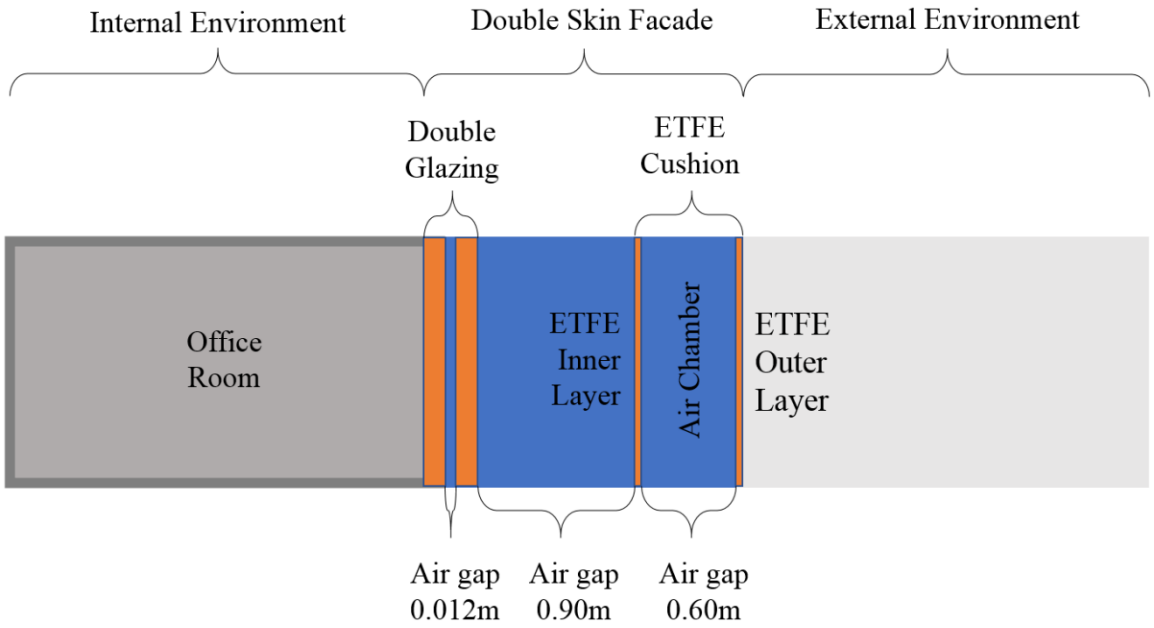


Figure 7. 108. Schematic diagram showing the layer composition of the double-skin façade with ETFE
(image by the thesis author, unpublished)

Table 7. 31
Construction components and materials' thermal resistance
(table by the thesis author, unpublished)

Construction Component	Component Material Layers	U-Value [W/m^2·K]	R-Value [K·m^2/W]
Roof	roof membrane, roof insulation, metal decking	0.3	3.5
Wall	metal siding, metal building wall insulation, gypsum board	0.5	1.9
Floor	carpet pad, acoustic tile, ceiling air space resistance, lightweight concrete	1.3	0.8
Window	clear glazing, air-gap, clear glazing (Double Glazing = DG)	2.4	0.4
DSF Clear	DG, air-gap, double layer clear ETFE cushion (IL, OL clear)	0.8	1.3
DSF Fritted	DG, air-gap, double layer fritted ETFE cushion (IL clear, OL frited)	0.8	1.3
DSF Switchable	DG, air-gap, triple layer switchable ETFE cushion (Il clear, ML fritted, OL fritted)	0.6	1.7

The lighting parameters of the simulation model were assigned by zone and informed by international standards. Chapter 9 of the ASHRAE 90.1-2019 edition defines the maximum, whole building interior lighting power for quantitative analysis of building models. For small commercial offices, a lighting power density (LPD) per area of 1 W/ft^2 is recommended, which equals 10.8 W/m^2. This value matches well with the lighting

requirements for interior areas stated in the international standard BS EN 12464-1:2011 when converting luminous levels to lighting load, assuming luminous efficacy of standard LED light sources. The suggested illuminance levels range between 300 lux 750 lux for offices [BS EN, 2011.]. However, for specific office tasks like writing, typing, reading and data processing an illuminance level of 500 lux is suggested. Lighting levels for the transit zones of corridors and stairs were set to a considerably lower LDP. The switching threshold for dimming electrical lights when sufficient natural daylight is available was set to 500 lux in all zones. The switching threshold of the switchable ETFE cushion in the DSF construction for switching from open to closed mode was equally set to 500 lux. A detailed zone parameters overview of the building model is listed in Table 7.32.

Table 7. 32
Zone parameters
(table by the thesis author, unpublished)

Zone Parameters *EnergyPlus Input*	Zone 1 *Office*	Zone 2 *Corridor*	Zone 3 *Stairs*
Total Volume [m^3]	1627	526	475
Total Area [m^2]	592	191	173
Occupancy density [m^2 per person]	10	20	20
Equipment load per area [W/m^2]	5	1	1
Lighting Power density [W/m^2]	11.3	2.3	2.3
Standard maintained illuminance [lx]	500	100	100
Lighting dimm set-point [lx]	500	500	500
Cooling set-point [°C]	25	25	25
Heating set-point [°C]	20	20	20
Infiltration rate [ACH]	0.25	0.25	0.25

7.3.5. Simulated parameters and scenarios

This section gives an overview of the parameters for the different simulation scenarios. The analysed parameters of this simulation study comprise annual values for cooling, heating and lighting load of the test office, normalized with the area of the test

office room, and expressed kilo Watt-hour per meter square. The annual loads for heating, cooling and lighting are calculated based on a standard office working schedule with high-level occupancy from 7 am to 11 am, and 12 am to 4 pm, five days a week from Monday to Friday, and Saturdays with half-day occupancy on a medium level. The result outputs are given for three different DSF façade options in comparison with double glazing. The simulation scenarios cover five different window-to-wall ratios. All scenario cases are simulated for the three locations, hence different climate scenarios, with annual hourly data weather files. The results of total energy consumption are further transformed to a percentage value of energy savings relative to the energy consumption of the office with double glazing, which is the benchmark case in this study, to provide an indicative evaluation for the effectiveness of the proposed DSF application as a measure of energy retrofitting.

7.4. Results and discussion

This section reports on the results from the energy simulation and discusses the outcomes of the different scenarios. The purpose of this simulation campaign was to get a general understanding of the energy performance of office spaces when retrofitted with a double-skin façade of inflated ETFE cushions. A particular interest of the study was focused on the adaptive performance of switchable ETFE cushions in comparison to static ETFE cushions. Furthermore, the study followed-up with the hypothesis of the previous daylighting chapter, that ETFE double-skin façades might improve the building performance relatively more effective in buildings which exhibit glass façades with a large window-to-wall ratio and are located in climate zones with a high degree of solar radiation throughout the seasons. Therefore, for better comparability of the results, and confirmation of the hypothesis, the window-to-wall ratios were equally established as scenarios for the energy simulation and analyzed for the same annual weather data stations as in the previous chapter. The performance indicator for the energy performance of the office space in this study is the total annual electric energy per area used for heating, cooling and lighting, expressed in kilo Watt-hour per square meter. Although these three categories provide only

a partial picture of the overall energy consumption of a building, they do give an informative indication for the most energy-intensive services of a building, and allow, due to their sensitivity to changes in the building envelope, an indirect comparative evaluation of the performance of the ETFE double-skin façade.

The graphs in Figure 7.109, 7.110 and 7.111 show an overview of the results obtained from the energy simulation. Each of the graphs represents the result for the three chosen locations (London, Barcelona, Shanghai) in the respective climate zones (Oceanic, Mediterranean and Subtropical). The heating, cooling, and lighting results are depicted as a bar chart, for the reference case (double glazing) and the different DSF designs (clear ETFE DSF, fritted ETFE DSF, switchable ETFE DSF) in different window-to-wall ratio scenarios. The total annual electric energy consumption can be derived directly from the charts below by addition of the individual sums for heating, cooling and lighting. While the amount of energy consumed for electric daylighting is mainly dependent on the window size and daylight transmission through the double-skin façade layer, the energy required for heating and cooling depends on the heat gains and losses through the different surfaces of the building envelope.

7.4.1. Results for the London climate scenario

The results for London, depicted in Figure 7.109, show an overall increasing trend of energy consumption relative to the window wall ratio, being lowest for a mall glazing area, and highest for an almost totally glazed façade. The lowest annual energy consumption of an annual total of 98 kWh/m^2 for heating, cooling and lighting is achieved with double-skin façade with a clear double layer ETFE cushion in an office building with a window to wall ratio of 30%. In contrast, the scenario with the highest annual energy consumption sums up to a total of 171 kWh/m^2 for a building façade with a window to wall ratio of 90%, with double glazing windows without the DSF. The switchable ETFE DSF performs well across all window-to-wall ratios without much deviation between the different scenarios, showing a range of total annual energy consumption between 120 and 128 kWh/m^2. However, the DSF with the fritted ETFE cushion delivers on average the best

performance, outperforming all material choices of this study, especially for the scenarios with a higher window to wall ratio, from 60 to 90%. For the smaller window-to-wall ratios of 30 and 45%, the DSF with the clear ETFE cushion delivers the best performance. The results for London are coherent with the meteorological data and daylight study of the previous chapter, which shows a reduced daylight availability for the office space with smaller window-to-wall ratios. Whereas the proportion for lighting on the overall energy consumption is consistently low, the energy consumption for heating is for all London scenarios significantly high. Therefore, transparent DSF designs, which provide more substantial solar gains, might be suggested for climates with a seasonal need for heating and lighting. The switchable ETFE cushion does not provide sufficient material transparency for the required solar transmittance in a London like climate.

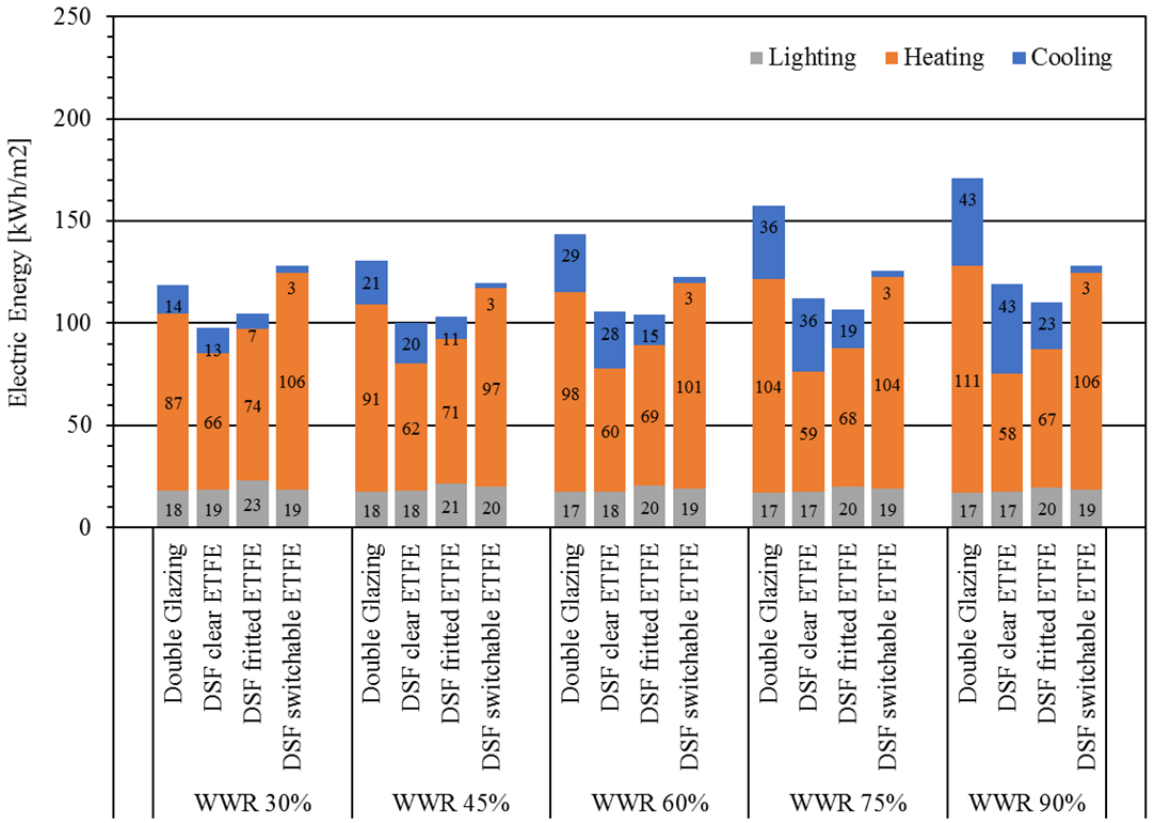


Figure 6. 109. Annual lighting, heating and cooling electric energy consumption of an office room in London, with different façades and window to wall ratio
(chart by the thesis author, unpublished)

7.4.2. Results for the Barcelona climate scenario

The results for Barcelona, shown in Figure 7.110, contrast drastically from the London results, even though the general trend of increasing energy consumption relative to enlarging proportions continues, as has been highlighted in the previous section. However, the proportional increase of energy consumption across the different window-to-wall ratio scenarios is much more pronounced, and the energy consumption required for cooling is disproportionally high compared to the energy required for heating and lighting. This picture, however, is entirely coherent with the climate data of Barcelona. The high energy demands for cooling can be explained with Mediterranean climate characteristics, which require cooling during hot summers and less energy for heating during winter due to the intense solar radiation throughout the annual seasons.

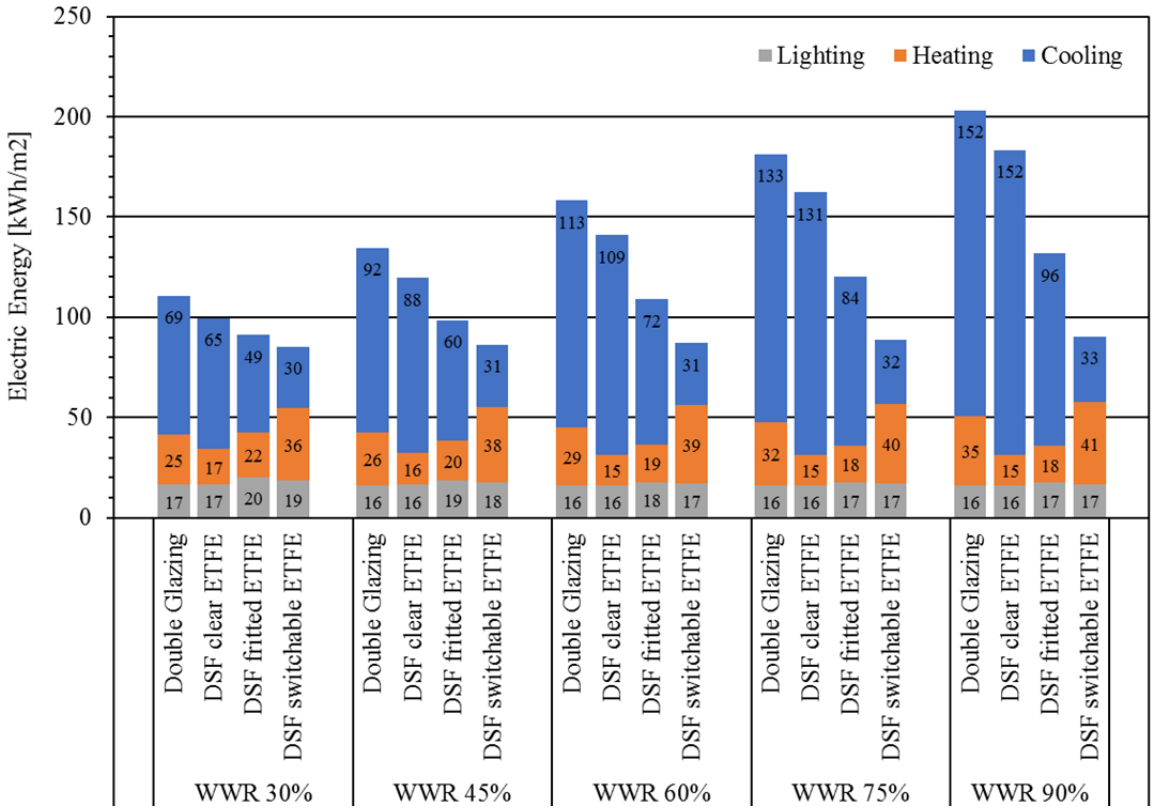


Figure 7. 110. Annual lighting, heating and cooling electric energy consumption of an office room in Barcelona, with different façades and window-to-wall ratio (chart by the thesis author, unpublished)

The scenario with the lowest annual energy consumption in Barcelona has a window-to-wall ratio of 30% with and achieves with a double-skin façade with the switchable ETFE cushion a total of 85 kWh/m^2 for heating, cooling and lighting. On the other end of the performance spectrum, the scenario with the highest annual energy consumption sums up to a total of 203 kWh/m^2 for a building façade with a window to wall ratio of 90%, with double glazing windows, without the DSF. Similarly, as in the previous London climate scenario, the switchable ETFE DSF performs well across all window to wall ratios without much deviation between the different scenarios, showing a range of total annual energy consumption between 85 and 91 kWh/m^2. The second best-performing DSF across all window-to-wall ratio scenarios is the fritted ETFE cushion, which reflects a considerable fraction of the incoming sunlight with the reflective frit print on the outer layer, thus, reducing solar gains, and saving energy to cool the office with mechanical air-conditioning. The proportion of energy required for lighting is consistently low, compared to the overall energy consumption, and is only negligibly affected by the different window-to-wall ratios, as highlighted previously in the discussion of the result of the London climate scenario. What is interesting to note is that the benefit of significantly reducing the energy required for cooling with the implementation of a switchable DSF is traded off with a gain in energy demand for heating. However, the overall energy consumption is not affected and outweighs in the overall performance the gains for heating, which might result from the very effective solar shading mechanism of the switchable ETFE cushion which is triggered by an illuminance sensor. Therefore, switchable ETFE cushions might be recommendable for Mediterranean climates with the characteristics similar to the local climate of Barcelona. The switchable ETFE cushion has the adaptive capacity to effectively control with the active shading mechanism the solar gains of the office space while providing at the same time additional thermal insulation to the building envelope. Shading the buildings' primary façade significantly reduces the energy consumption for cooling, which in comparison with standard double-glazing façades would represent otherwise a large proportion of the overall energy use in office buildings within the Mediterranean climatic zone.

The comparison of the results for the climate scenarios of London and Barcelona reveals a very distinctive energy performance of the office space even though all building and material parameters are equally applied in both scenarios. If we now turn to the Shanghai climate scenario, the same strong dependence between climate and energy performance can be observed. The range of moderation on the energy consumption achieved with the application of the different double-skin façades in the subtropical climate of Shanghai is discussed in the following section.

7.4.3. Results for the Shanghai climate scenario

The overall picture of the annual energy consumption in the Shanghai climate scenario is illustrated in Figure 7.111, and clearly demonstrates that offices under these climate conditions have the highest demand for cooling, heating and lighting among the three studied cases. Cooling requires, on average over half of the total consumed energy, followed by energy for heating, and considerably less energy for lighting. This trend is consistent across all window to wall ratio scenarios; however, augments proportionally with the glazing area. The scenario with the highest annual energy consumption sums up to a total of 230 kWh/m^2 for a building façade with a window to wall ratio of 90%, with double glazing windows, without the DSF. This value is 12% and 37% higher than the maximum energy consumption in the Barcelona and London scenarios, respectively. As noted in the previously discussed climate scenarios also for Shanghai, the window-to-wall ratio scenario with the lowest annual energy consumption is the office façade with the smallest glazing proportion of 30%. Within this scenario, the best energy performance was achieved with the applied switchable ETFE DSF. The annual energy consumption for cooling, heating and lighting totals 136 kWh/m^2, which is approximately 35% higher than the minimum value for the London and Barcelona scenario and highlights again the dependency of the energy consumption on the climate conditions.

Similarly, as in the London and Barcelona climate scenario, the switchable ETFE DSF performs well across all window to wall ratios without much deviation between the different scenarios, showing a range of total annual energy consumption between 136 and

143 kWh/m^2. This is of importance for the application in building retrofits, as the outer ETFE façade, due to the adaptive capacity, can almost be considered as a general measure of improvement for the energy performance of a building without much dependencies on the window-to-wall ratio of the formerly existing building design. The second best performing DSF across all window to wall ratios in the Shanghai climate scenario is the fritted ETFE cushion, followed by the clear ETFE cushion DSF. As observed in the previous scenarios, the double-glazing façade without a second skin is the case with the highest annual energy consumption in all studied cases under Shanghai climate condition.

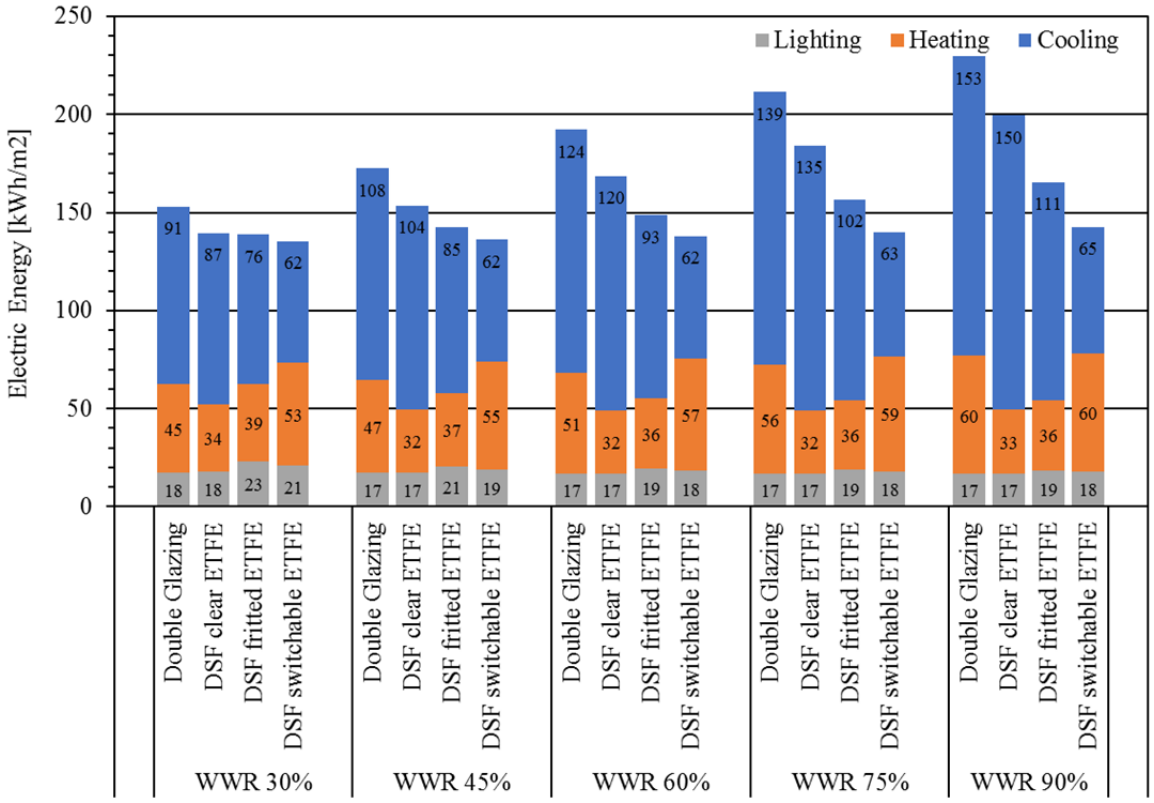


Figure 7. 111. Annual lighting, heating and cooling electric energy consumption of an office room in Shanghai, with different façades and window-to-wall ratio
(chart by the thesis author, unpublished)

7.4.4. Energy gains and losses

The heat gains and losses are defined by the intrinsic capacity of the building envelope components and materials to resist the thermal conductive flow from the outside to the inside and vice versa. The extrinsic component to the heat gains and losses are the solar gains from solar radiation and the seasonal change of climate conditions. Depending on the differential between external climate conditions and the internal loads of the building, energy is transferred with varying amount and direction through the building envelope. The heat transfer mechanisms through the building envelope are radiation, conduction, and convection. While the latter is neglected in this study, the solar gains through radiation and the heat gains and losses through conduction were analyzed in detail for the different double-skin façades in comparison to the original double-glazed office façade. In Figure 7.112 to 7.115, an annual energy balance for the office room with a 90% window-to-wall ratio is plotted with the total monthly loads for the totality of considered parameters for this study. The two graphs highlight the office space's different energy performance with and without the adaptive second building skin. The graph in Figure 7.115 shows that the switchable ETFE cushion façade effectively reduces the solar gains during the summer month in the hot Barcelona climate, and with this diminishes the energy required for cooling. This annual behaviour has also been observed for the Shanghai climate but is inverted in the case of London (Figure 7.113); heat losses during the winter season are reduced which effectively lead to savings for heating, due to the improved insulative capacity of the double-skin façade, while solar radiation still enters the room.

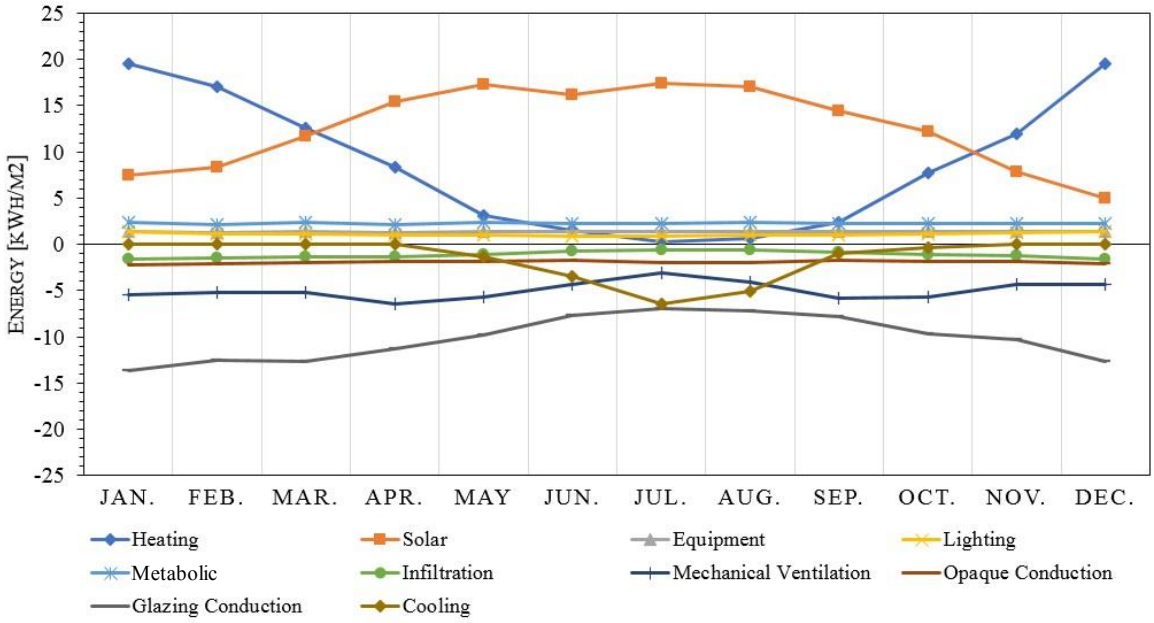


Figure 7. 112. Annual energy balance on a monthly basis - London climate, double Glazing, 90% WWR
(chart by the thesis author, unpublished)

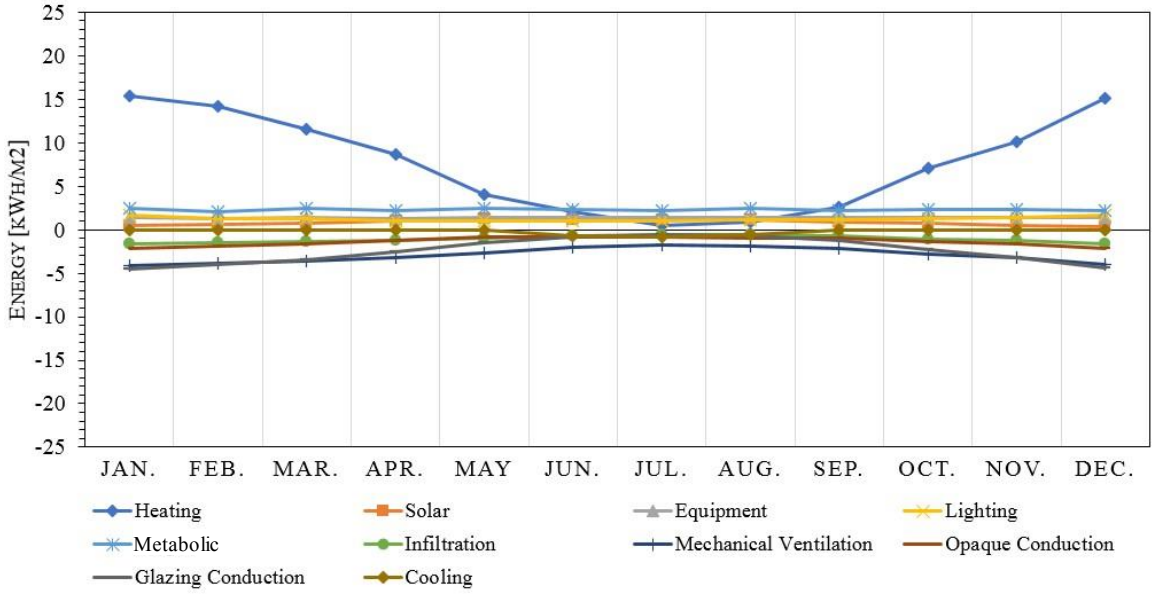


Figure 7. 113. Annual energy balance on a monthly basis - London climate, switchable ETFE double-skin façade, 90% WWR
(chart by the thesis author, unpublished)

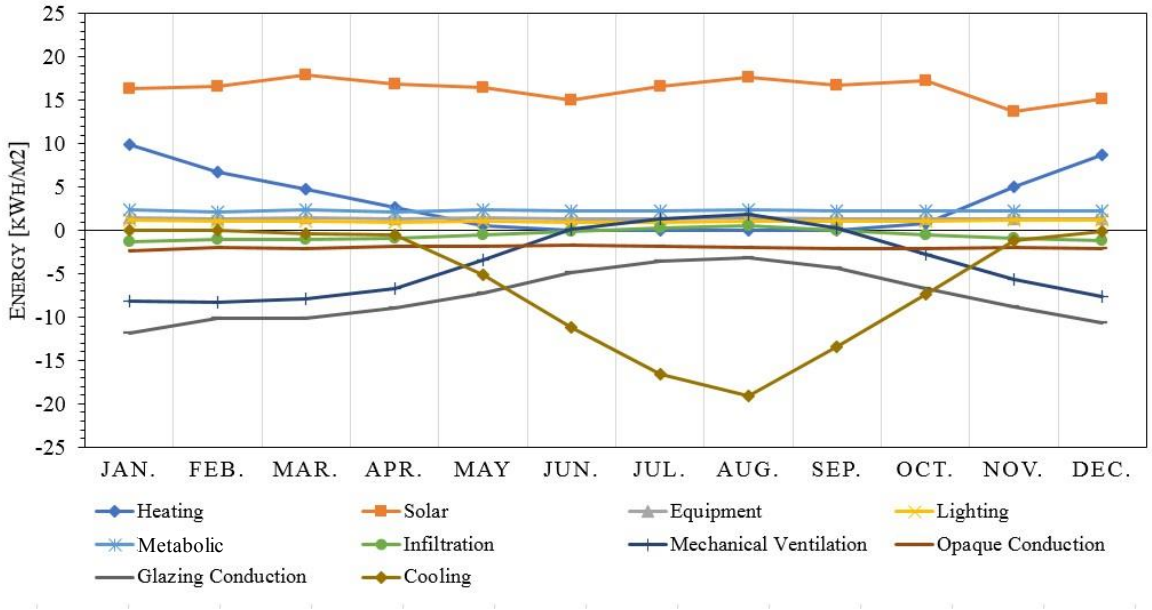


Figure 7. 114. Annual energy balance on a monthly basis - Barcelona climate, double Glazing, 90% WWR
(chart by the thesis author, unpublished)

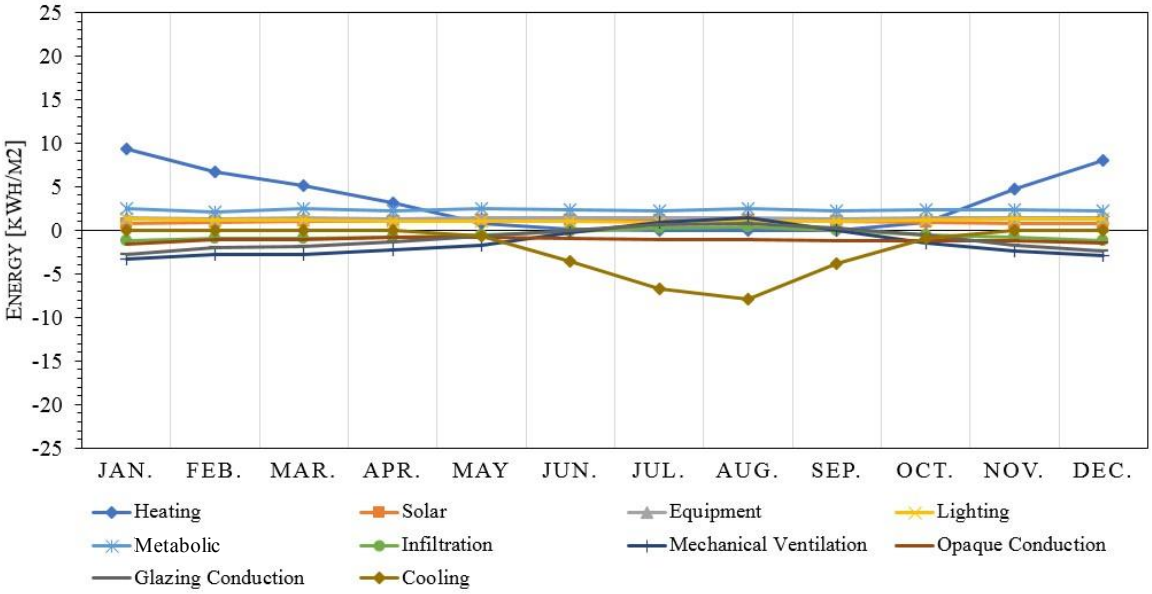


Figure 7. 115. Annual energy balance on a monthly basis - Barcelona climate, switchable ETFE double-skin façade, 90% WWR
(chart by the thesis author, unpublished)

What the data also shows is that one of the major limiting factors to improve further the energy performance of the office room with the switchable cushion façade is the limitation of the switching mechanism to one single control parameter, which is, in this case, the daylighting illuminance in the center of the room. What can be seen is that the adaptive system effectively reduces the energy consumption for one parameter, but as a consequence, another parameter rises. This is only of little significance for the overall energy consumption, which is reduced in the overall energy balance. However, the implementation of a multi-objective control system for the switching mechanism's decision-making would lead to even more energy savings and a higher level of comfort and control for the user of the space. Integrating not only one but two, or multiple parameters, such as internal air temperature or façade surface temperatures into self-evaluating close loop control systems with additional override options would convert switchable ETFE into truly smart building façades.

In order to understand where the main heat gain and losses are generated, an additional detailed analysis of the main building skin components was carried out. The charts depicted in figure 7.116 and 7.117 show that proportionally the most important heat gain is transferred through the window, in the case of the single skin-façade with double glazing, while for the double-skin façade the largest part of the heat gain is generated internally. Proportional changes in the heat loss are attributed to the different window-to-ratio according to the changing proportional area and the corresponding U-value for the façade. Air infiltration and internal loads played no major role in the heat loss of the double-skin façade showing constantly low proportional values. This is only true for the window-to-wall-ratios under Barcelona's Mediterranean climate conditions, and a wider range of testing scenarios would be recommended for future investigations. The comparison of the conventional building façade with double glazing and double-skin façade also reconfirmed the findings of the previous section that a switchable ETFE cushion added as an additional layer to the building envelope decreases the thermal transfer through the building envelope reducing the total energy gains of the office space.

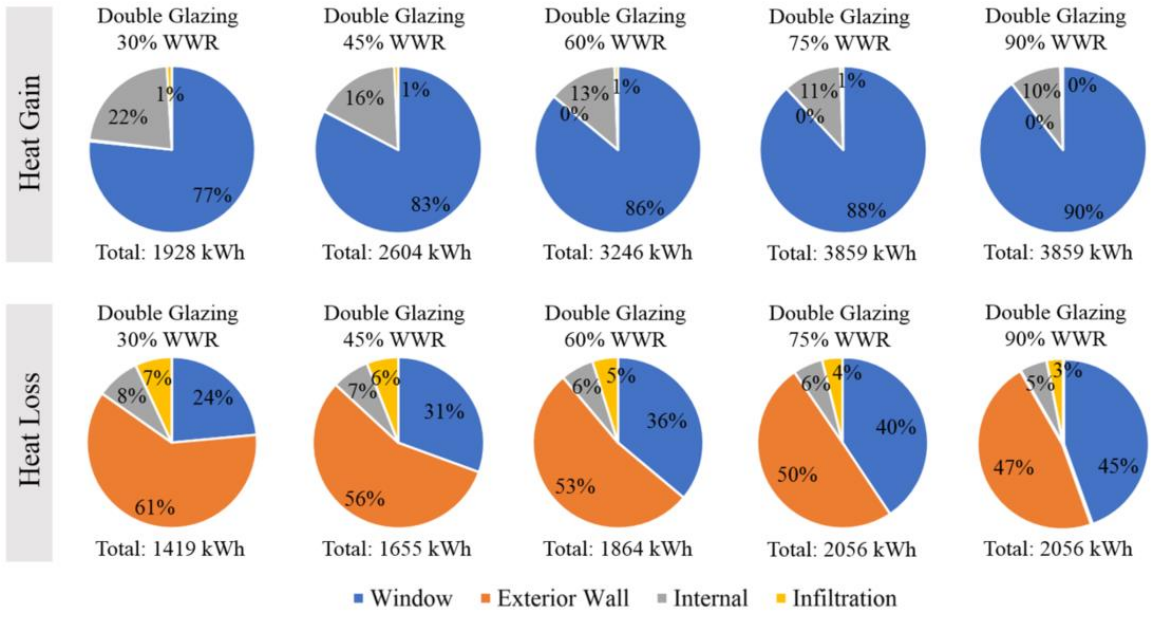


Figure 7. 116. Proportional annual heat gains and losses through the main building components of an office room with double glazing under Barcelona climate conditions
(chart by the thesis author, unpublished)

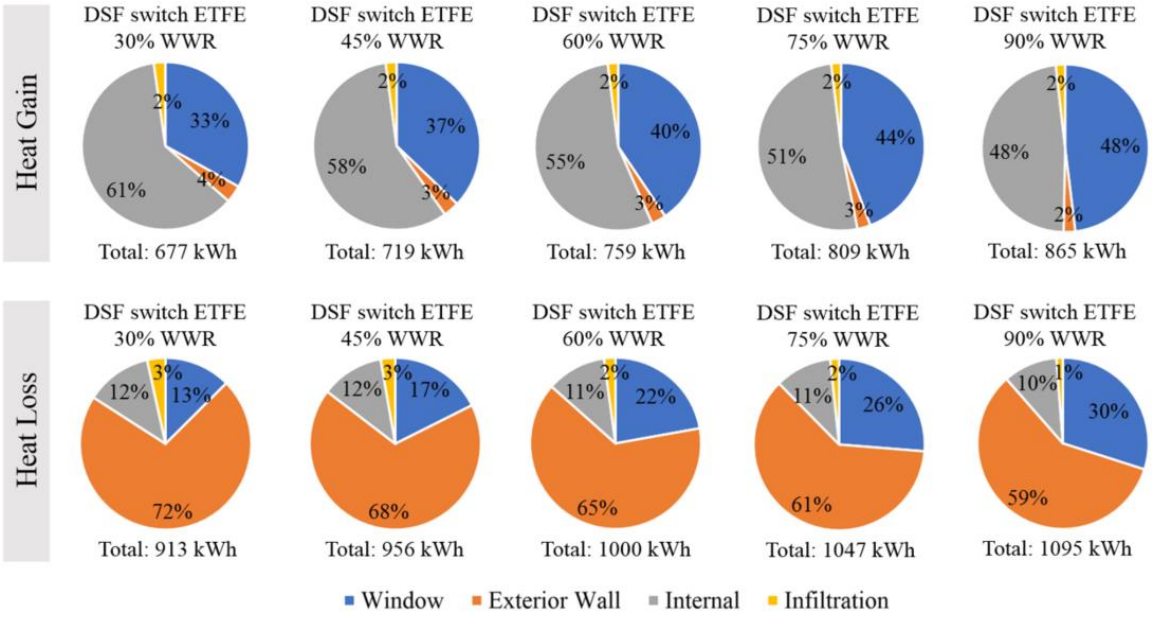


Figure 7. 117. Proportional annual heat gains and losses through the main building components of an office room with a double-skin façade with switchable ETFE cushions, under Barcelona climate conditions
(chart by the thesis author, unpublished)

On continuation, it is discussed how much of thermal transfer can be attributed to DSF's thermal resistance, and how much to the responsive shading mechanism itself. Figure 7.118 and Figure 7.119 show the proportional energy gains and losses through an office façade with a 90% window-to-wall ratio for the different DSF design options and climate scenarios for summer and winter season. The focus of the analysis is here on the solar radiation and heat conduction component of the energy transfer mechanisms during Summer and Winter season. The graphs show a significant reduction of energy being transferred through the façade when comparing a single-skin to a double-skin façade with ETFE. As pointed out already in the previous analysis, the switchable ETFE cushion increases with its additional material layers and air gaps the thermal resistance of the façade reducing conductive heat losses through the façade during summertime (equinox of spring to equinox of autumn) by up to 80% on average. The energy gains through solar radiation are reduced on average by up 95% when comparing the switchable ETFE double-skin façade with a double-glazed façade. During wintertime (equinox of autumn to equinox of spring), the DSF transmits more solar radiation, maintaining an equally low thermal conduction loss. In regions with mild or warm climates, this seasonal behaviour can be considered beneficial for thermal comfort and energy consumption.

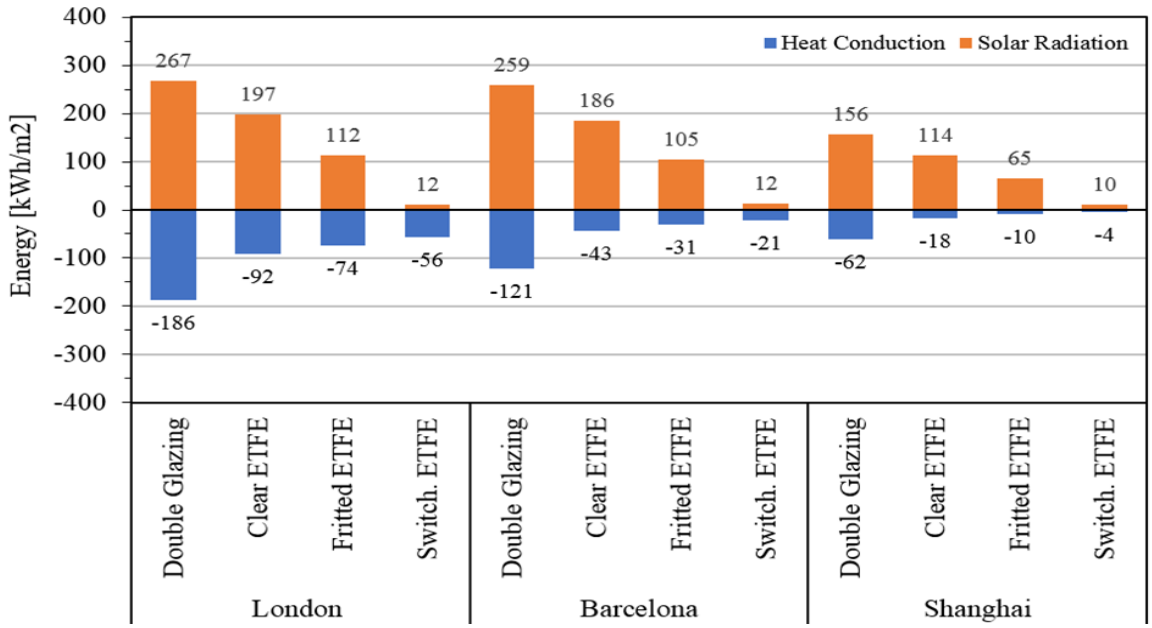


Figure 7. 118. Energy gains and losses by heat conduction and solar radiation for a DSF with a WWR of 90% in different climates, from 22nd of Mar. to 21st of Sept.
(chart by the thesis author, unpublished)

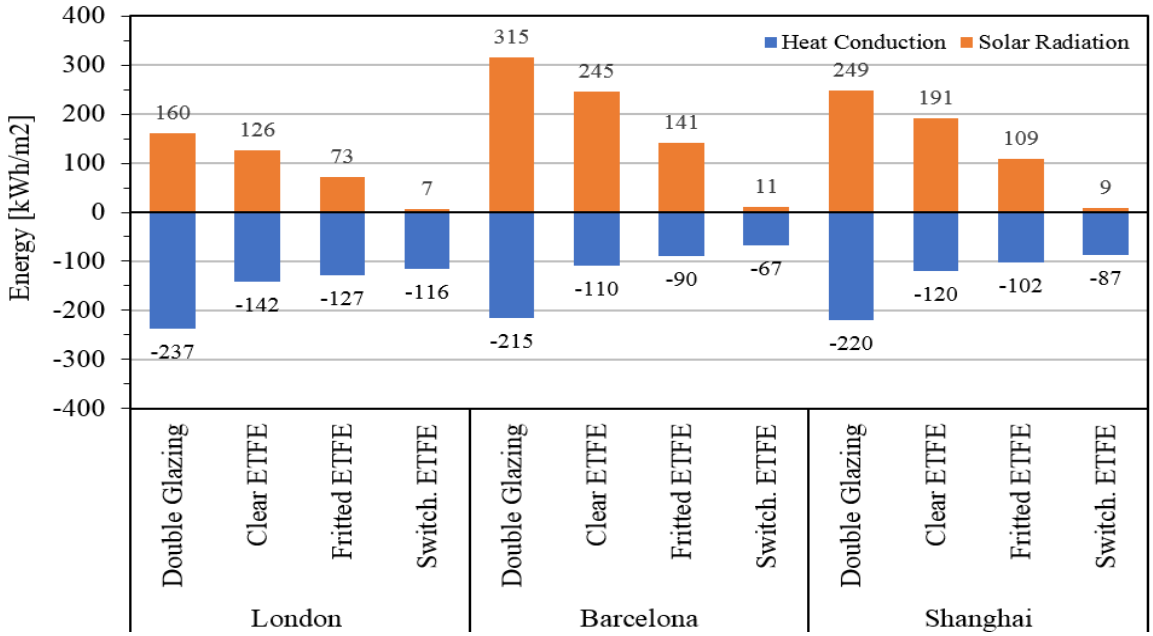


Figure 7. 119. Energy gains and losses by heat conduction and solar radiation for a DSF with a WWR ratio of 90% in different climates, from the 22nd of Sep. to 21st of Mar.
(chart by the thesis author, unpublished)

7.4.5. Energy savings

When discussing measures to reduce energy consumption to limit carbon dioxide emissions and mitigate climate change, the scalability for a global effect is an important criterion to promote or argue against one or the other technology. To decide whether it is worth investing in a novel building technology a critical factor to take into account for the evaluation of the energy performance is the benchmark case against which the forecasted energy savings are compared to. It is out of the scope of this study to provide feasibility or cost-benefit evaluations for the proposed ETFE double-skin façades. Neither are the three studied scenarios covering enough climate zones nor is the performance of office buildings representative for other typologies of the existing building stock. However, in this study, it is suggested to express the potential energy-saving as a percentage relative to the benchmark of a standard office building with a simple double-glazed façade. The graphs of Figure 7.120, 7.121 and 7.122 depict the relative potential energy saving for the three proposed double-skin façades relative to the double-glazing single-skin façade. The trends for the three façade designs are plotted along with the changing window-to-wall ratios for each of the studied climate scenarios.

Figure 7.120 shows the potential energy savings for the London climate scenario. The data shows that the potential energy savings grow with increasing window to wall ratios. The forecasted energy savings with the DSFs are calculated relative to the energy consumption with a standard double-glazing façade which increases with larger window to wall ratio. Therefore, also the expected energy savings of the DSFs grows as a function of the incrementing performance difference e between the double glazing and the ETFE double-skin façades.

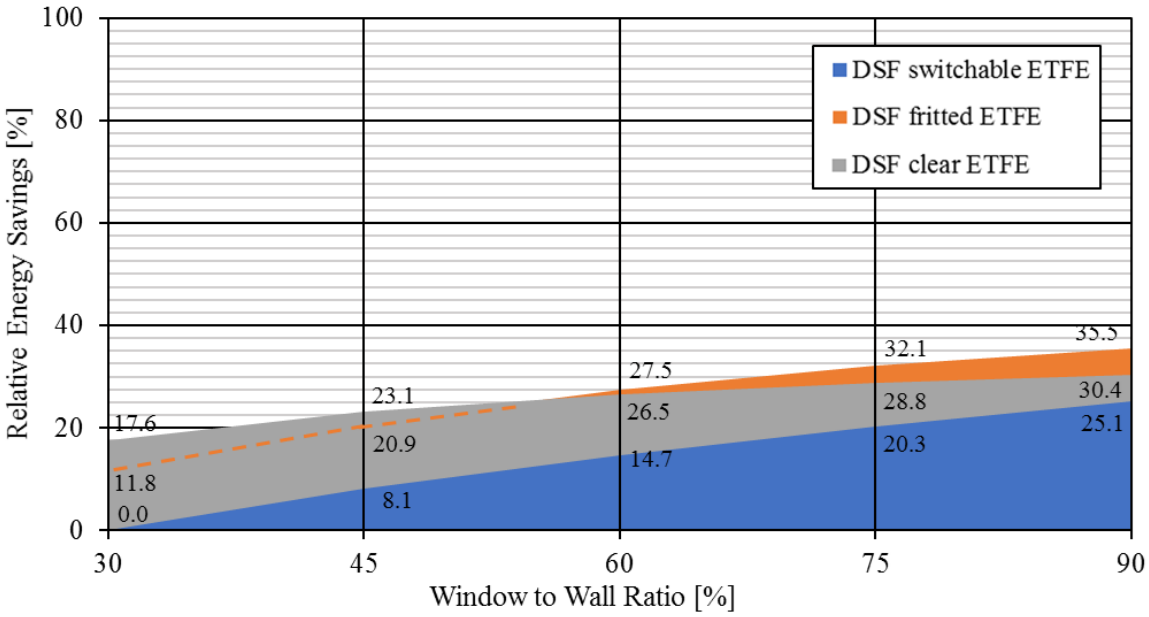


Figure 7. 120. Percentage of annual energy savings with DSF relative to the reference case with Double Glazing – London
(chart by the thesis author, unpublished)

Under the London climate conditions, the most significant energy savings are predicted to be achieved with the fritted ETFE DSF, with potential savings of up to 35.5% for large window-to-wall ratios, followed by the clear and the switchable ETFE façade, with 30.4% and 25.1% respectively. For small window-to-wall ratios of 30% and 45%, the clear ETFE DSF is predicted to achieve with 17.6% greater energy savings than the clear and the switchable double-skin façade.

Figure 6.121 shows the potential energy savings for the Barcelona climate scenario. Again, the ETFE double-skin façades are compared to the double-glazed façade without the DSF, which acts as a benchmark for a comparative prediction of potential energy savings for the different window-to-wall ratios. Under the Barcelona climate conditions, the switchable DSF is predicted to achieve the greatest energy saving across all tested window to wall ratio scenarios, with a minimum of 23% for the façades with the smallest ratio and 55.5% for the façades with 90% glazing area. The second-best performing façade is the DSF with the fritted ETFE cushion, achieving for the simulated window to wall

scenarios annual energy savings ranging from 17.8% to 35.1%. The lowest energy savings are predicted for the DSF with clear ETFE cushions, with 10.0% to 9.7%.

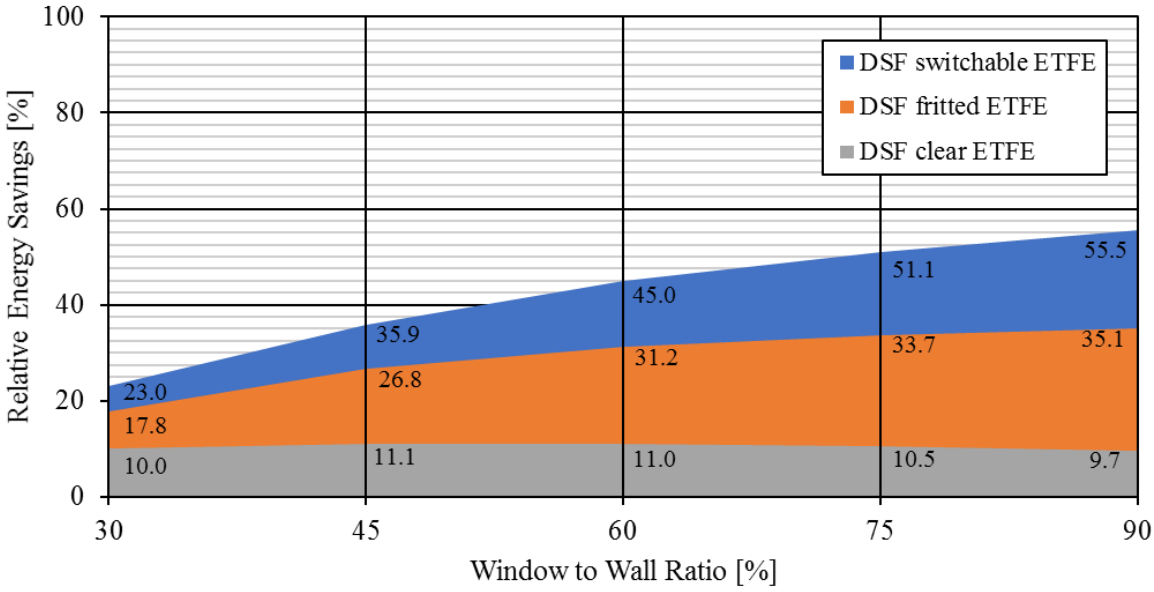


Figure 7. 121. Percentage of annual energy savings with DSF relative to the reference case with Double Glazing – Barcelona
(chart by the thesis author, unpublished)

Figure 7.122 shows the potential energy savings for the Shanghai climate scenario. The calculated relative percentage of energy-saving follows a similar trend as in the previous Barcelona scenario, with increasing energy-savings relative to a growing ratio of window-to-wall area. However, in general, the predicted energy savings for Shanghai are approximately 10% to 20% lower than for Barcelona. In Shanghai, double-skin façades with switchable ETFE cushions show the best performance among the tested façade options, achieving a potential annual energy saving in the range of 11.7% to 37.9%. Double-skin façades with fritted ETFE cushion show the second-best performance with annual energy savings ranging from 9.4% to 27.9%. Double-skin façades with clear ETFE cushion achieve only 8.9% to 13.1%, but with a relatively consistent performance across all calculated window to wall ratio scenarios. The overall outlook for saving energy under Shanghai climate conditions by retrofitting or upgrading offices buildings with ETFE

double-skin façades is evaluated positively, especially for façades with large areas of glazing.

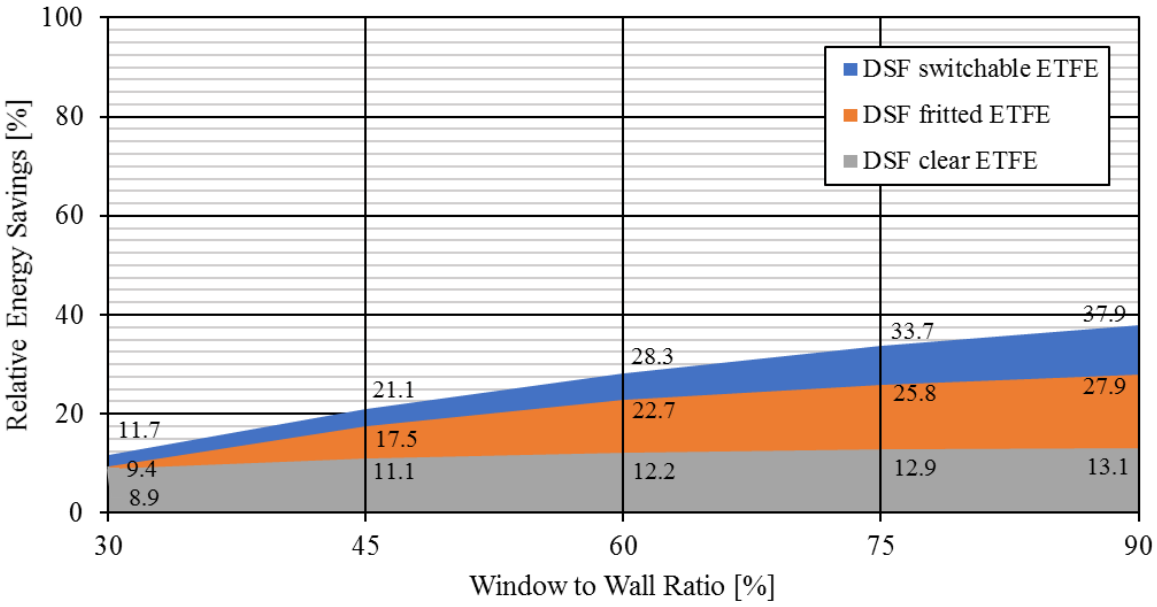


Figure 6. 122. Percentage of annual energy savings with DSF relative to the reference case with Double Glazing – Shanghai
(chart by the thesis author, unpublished)

In order to create an approximate guide of applicability for the analysed façade systems, a summarized data set of the predicted energy savings for the different scenarios was considered based on the numerical results presented in this chapter. Table 7.33 on the following page outlines the suitability for each individual case.

Table 7. 33
Applicability of ETFE double-skin façade design options for different climate scenarios and window-to-wall ratios
(Table by the thesis author, unpublished)

Window to Wall Ratio	London	Barcelona	Shanghai
30% WWR	• Double Glazing • DSF fritted ETFE • DSF clear ETFE	• DSF clear ETFE • DSF fritted ETFE • DSF switch.ETFE	• DSF clear ETFE • DSF fritted ETFE • DSF switch.ETFE
45% WWR	• DSF clear ETFE • DSF fritted ETFE • DSF switch.ETFE	• DSF clear ETFE • DSF fritted ETFE • DSF switch.ETFE	• DSF clear ETFE • DSF fritted ETFE • DSF switch.ETFE
60% WWR	• DSF clear ETFE • DSF fritted ETFE • DSF switch.ETFE	• DSF fritted ETFE • DSF switch.ETFE	• DSF clear ETFE • DSF fritted ETFE • DSF switch.ETFE
75% WWR	• DSF clear ETFE • DSF fritted ETFE • DSF switch.ETFE	• DSF fritted ETFE • DSF switch.ETFE	• DSF fritted ETFE • DSF switch.ETFE
90% WWR	• DSF clear ETFE • DSF fritted ETFE • DSF switch.ETFE	• DSF fritted ETFE • DSF switch.ETFE	• DSF fritted ETFE • DSF switch.ETFE

7.5. Energy and daylighting performance

This section summarizes and discusses the correlation between energy and daylighting performance, with the purpose to detect synergies or functional contradictions under different climate and building scenarios. It is of great interest for the implementation of double-skin façades with switchable ETFE foil cushions to verify that energy-saving

measures are not compromising the natural daylighting conditions, and vice versa, that the operation of the active shading mechanism does not produce undesired effects on the energy performance of the building. Since the switchable shading mechanism is controlled in this study by a single illuminance sensor, contradictions between the goals for daylighting and energy-saving can not be guaranteed at all times and under all conditions. Therefore, the following discussion focusses on the annual energy consumption for heating, cooling and electric lighting, discussed in section 7.4.1 – 7.4.3 of this chapter, and the annual useful daylight illuminance at the center of the test room, presented in section 4.6 of the previous chapter six. These values are the sum of the hourly simulation results for a whole year under the climate conditions of London, Barcelona and Shangai. The focus on the annual values ensures to obtain an overview of the general macro-performance of the proposed system. Future investigations might find an interest in carrying out seasonal daily or even hourly analysis for critical periods in order to estimate the potential benefits of smart multi-objective control logics to enhance the building performance further.

The graphs in Figure 7.123 to 7.125 show the overlap of the annual energy and daylighting performance, comparing a conventional double-glazing with a double-skin façade with switchable ETFE cushion. What can be seen from the three different climate scenarios is that the energy consumption for the office room with double glazing rises with increasing window-to-wall ratio while the percentage of the useful daylight performance drops. With larger window size the solar gains rise, which leads to a significant increase of the heating load in colder climates like for example in London, due to the energy loss through the window, and a higher energy demand for cooling in warmer climates like Barcelona or Shanghai, due to the solar gains. At the same time the illuminance levels in the center of the room rise, proportionally to the augmenting window-to-wall ratios, beyond the limits of useful daylight for an increasing percentage of the hours of the year.

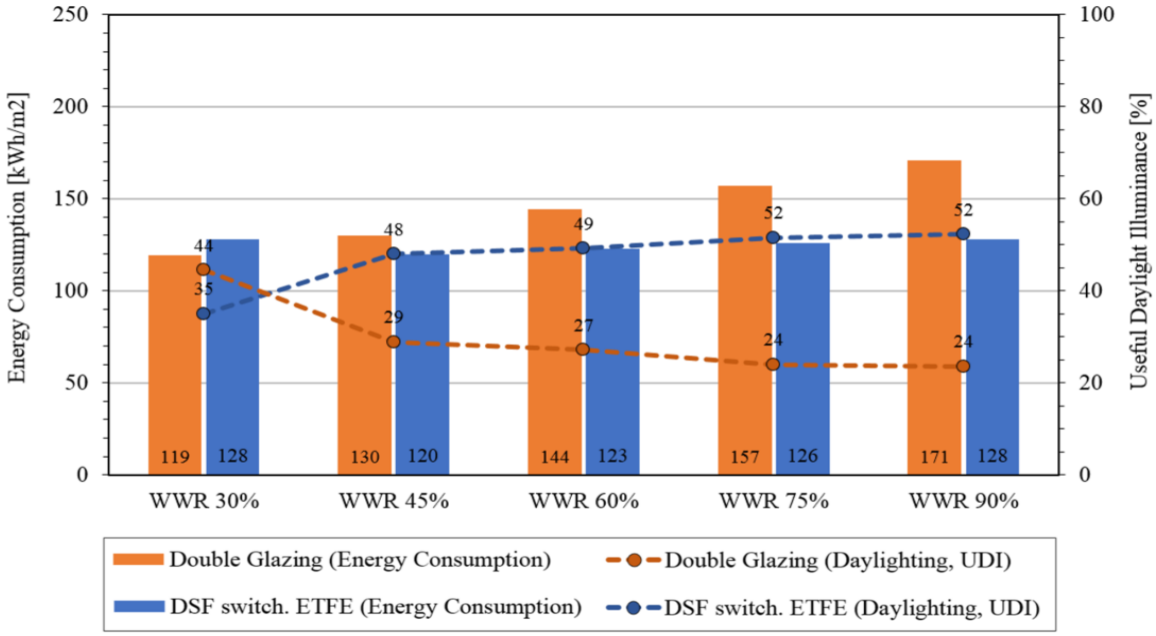


Figure 7. 123. Correlation of the annual energy and daylighting performance for a façade with double-glazing compared to a double-skin façade with switchable ETFE cushions, with different window-to-wall-ratios under London climate conditions
(chart by the thesis author, unpublished)

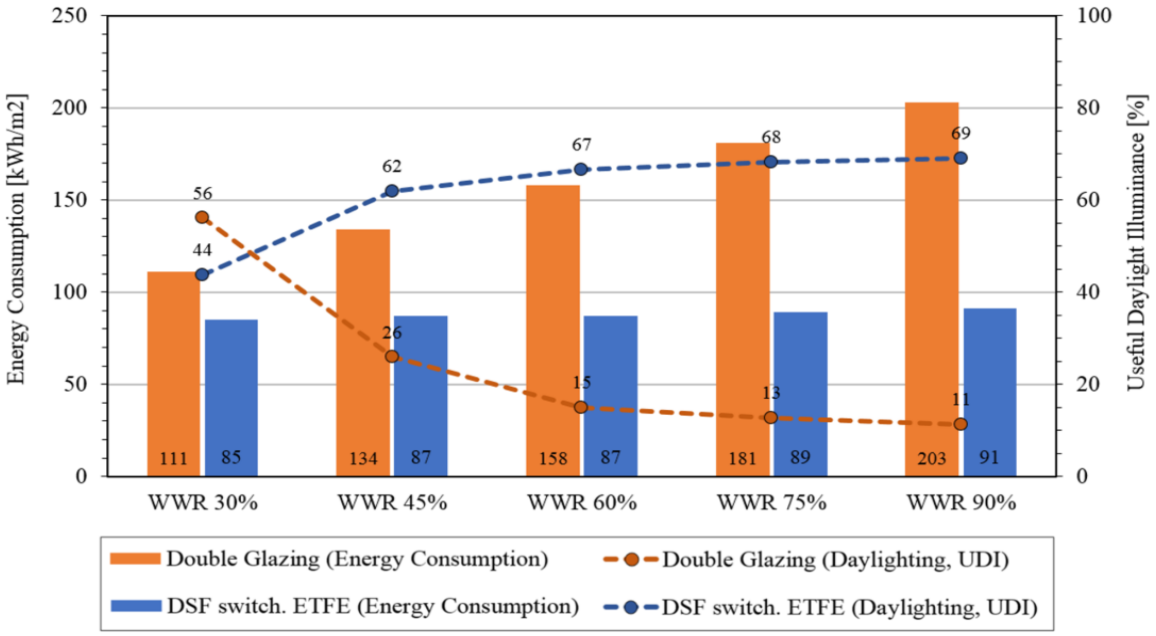


Figure 7. 124. Correlation of the annual energy and daylighting performance for a façade with double-glazing compared to a double-skin façade with switchable ETFE cushions, with different window-to-wall-ratios under Barcelona climate conditions
(chart by the thesis author, unpublished)

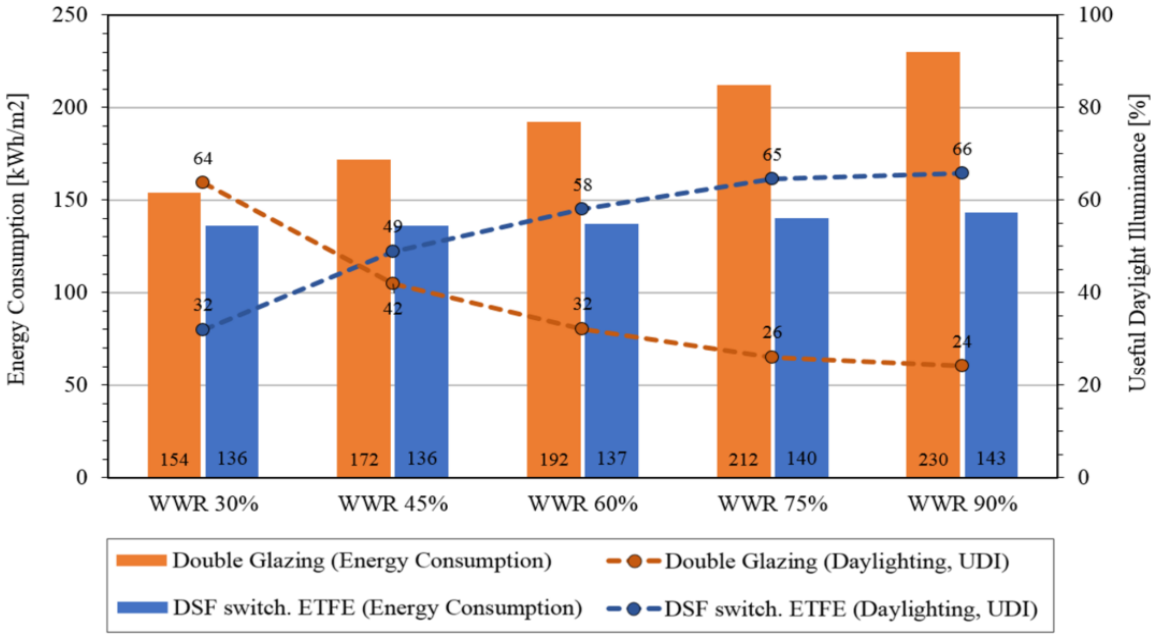


Figure 7. 125. Correlation of the annual energy and daylighting performance for a façade with double-glazing compared to a double-skin façade with switchable ETFE cushions, with different window-to-wall-ratios under Shanghai climate conditions
(chart by the thesis author, unpublished)

Juxtaposed, to the performance data of the double-glazing, the double-skin façade with the switchable ETFE cushion shows a very different trend of the annual energy consumption and daylighting illuminance. Independent of the different window sizes the energy consumption is kept at a consistently low level, relative to the façade with double glazing only. This can be attributed to the higher thermal resistance of the façade, caused by the additional layers of the building envelope, reducing thermal gains and losses. Nevertheless, the superior thermal performance might be additionally attributed to the adaptive shading mechanism of the ETFE cushion which reflects the incident solar radiation and shades the primary building façade during the most critical periods, reducing the overall solar gains and energy demand for cooling. Diagramed schematic building sections in Figure 7.126. A and B exemplify the above-described principle. The useful daylight illuminance increases with augmenting window-to-wall ratios, which can again be attributed to the switchable shading mechanisms, which actively moderates the incident solar radiation and keeps the light levels within the range of the useful daylight illuminance.

These findings are evaluated overall positively considering that the single factor control logic of the switchable mechanism can enhance, both, daylighting and energy performance of the office space, for a range of window to wall ratios under different climate conditions. This poses a significant advantage of adaptive, switchable ETFE double-skin façades, over conventional double glazing and static ETFE façades. Therefore, double-skin façades with switchable features were considered according to the findings of this study as a suitable building system for energy retrofitting measures of outdated office buildings.

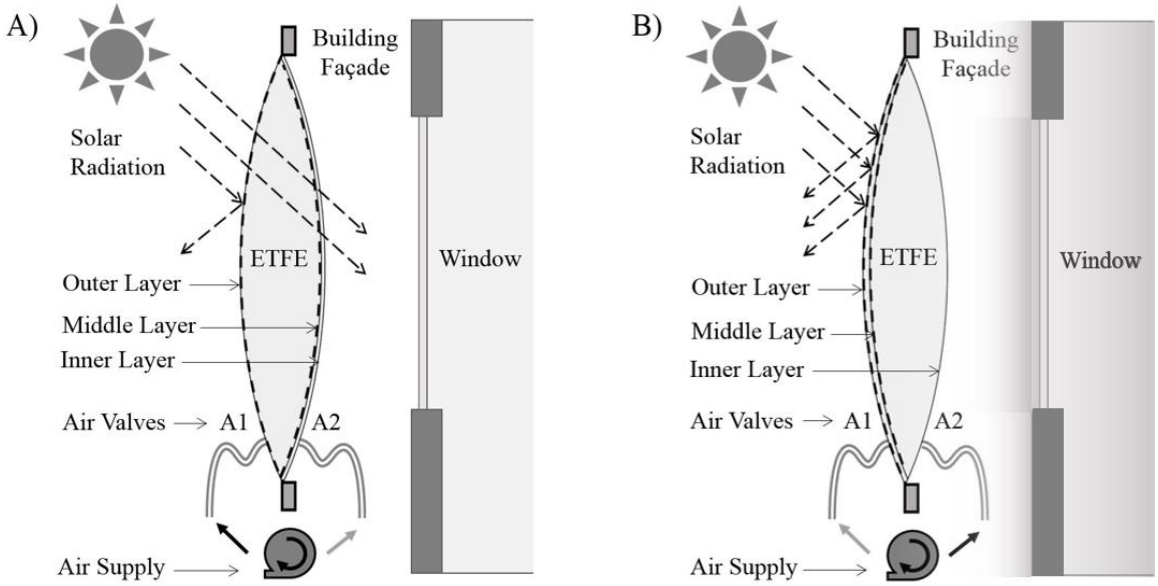


Figure 7. 126. Schematic section showing double-skin façade with switchable ETFE cushion in open mode (A) and closed mode (B) shading the primary building façade (images by the thesis author, published in: Flor et al., 2021)

7.6.Chapter summary

This section summarizes the conclusions drawn from the energy simulation study and highlight some of the limitations and suggestions for future studies. A whole building energy simulation based on climate data was conducted using EnergyPlus, with the aim to quantify the potential energy saving of proposed retrofits of the building envelope with ETFE double-skin façades and adaptive switchable features. A generic building was modelled to represent a typical low-rise office building, based on ASHRAE international

standards. The model was generated with Rhinoceros 3D modelling software and Grasshopper/Honeybee plugin tools. These tools allowed to create a parametric model where parameters can easily be adjusted and modified for a streamlined simulation procedure, that allows processing a large number of simulation scenarios in a short time. Three DSF façades were modelled based on material data from the literature and measurements from previous experiments. The main parameters tested in this simulation campaign were the façade materials, window-to-wall ratios and climate. The criteria for evaluating the performance of the proposed double-skin façades was the annual energy consumption, for heating, cooling and lighting services of a south-facing single unit office space, within the modelled building. The study comprised three climate scenarios based on the annual hourly climate data of London, Barcelona and Shanghai, representing an Oceanic, Mediterranean and Subtropical climate, respectively. The results showed an improved energy performance for the office space for all three climate scenarios when an ETFE double-skin façade was added to the original double-glazed building façade. Under the London climate conditions, the most significant energy savings were achieved by a reduction of heating demand. Whereas for the climate conditions of Barcelona and Shanghai, the primary annual energy savings were generated by a significant reduction in the cooling demand. The demand for electric lighting contributed only to a limited extent to the overall energy consumption and was consistently low across all scenarios. The energy demand for lighting increased even marginally for the DSF scenarios with fritted and switchable ETFE cushions due to the reflective properties of the outer layers, but again, this had no significant effect on the overall energy performance of the office space.

The maximum values for the overall predicted energy savings ranged from 35.5% in London to 37.9% in Shanghai and up to 55.5% in Barcelona. For the climate condition of Barcelona and Shanghai, the most effective material choice for the DSF was the switchable ETFE cushion which generated the highest energy savings. For the London climate, the fritted ETFE was predicted to be the best material choice to achieve the highest energy saving compared to the original building double glazed building façade. These results, however, can only be considered relative to the U-values of the building envelope

components of the pre-existing building. A new building with a well-insulated building envelope might not yield the same energy savings when a switchable ETFE double-skin façade is applied.

Nevertheless, the significance of the results of this study for the design and construction industry is evident. When it comes to the choice of materials for different building designs and requirements, the climate should be considered one of the foremost important criteria. However, only south-facing façades have been investigated in this study, as a scenario where highest annular solar gains can be expected in any of the studied climates. Future studied might also consider the effect on energy consumption of other cardinal building orientations, or situations with mixed façade orientation relative to the overall building envelope proportions. Optional frit patterns and print densities, as well as the façade orientation, might be a consideration to take into account as well for the for future studies of energy performance analysis.

Another potential vector for the reduction of energy consumption is the fine-tuning of the control system for the kinetic mechanism of the switchable ETFE. A multi-objective control system with a combination of weighted mean radiant temperature, air temperature and illuminance sensor readings for the control of the switching mechanisms might be an up-grade for more sophisticated future systems which could further enhance the energy savings and adapt to changes in the environment more effectively by using combined climate criteria for the shading control. Seasonal calibration of the system, as well as the incorporation of override options for individual user choices, might also be an option to consider for enhanced user experience and satisfaction. The simulation of such a control system, however, remains a challenge with the currently available simulation programs and might be a topic for future research.

The following and last chapter of the main body of the thesis will focus on the user experience in office spaces covered with ETFE double-skin façades, investigating the view clarity and emotional response through different types of clear and printed ETFE cushions in virtual environments.

Chapter 8: View Perception

8.1. Introduction to chapter eight

The study reported in this chapter evaluates the user experience and satisfaction with the window view of an office space equipped with a double-skin façade with different pneumatic ETFE cushions, including a switchable unit which is compared to a standard façade with double-glazed windows. Double-skin façades (DSF) with automated switchable glazing elements are promising developments for improving the lighting and energy performance of office buildings, as it has been demonstrated in the previous chapter six and seven. However, the acceptance and experience of occupants working in spaces equipped with novel switchable DSF has not yet comprehensively been addressed in the literature. While the reduction of glare and a general improvement of natural lighting conditions are perceived as positive, a limited view to the outside and loss of control autonomy is generally pointed out as a negative factor for automated climate-responsive shading systems, such as switchable ETFE cushions. However, the lack of experimental data and user feedback makes it currently difficult to evaluate the suitability of these systems for application in building envelopes on a bigger scale. Virtual Reality is explored in this chapter as a new tool for virtual prototyping and evaluating the user response of novel complex fenestration systems. In addition to the evaluation of different ETFE double-skin façade materials, this study showcases how physics-based virtual reality can be used to evaluate architectural spaces and to gain user feedback with predictive methods, assessing novel building applications prior to their implementation.

The experimental and theoretical work described in this chapter was carried out at the University of Nottingham during the summer period 2019 in a collaborative effort by the applicant, and fellow PhD colleagues, Marina Aburas, Fedaa Abd-AlHamid supervised by Dr Yupeng Wu. The development of the research idea, planning and execution was conducted by the applicant with the individual contributions of co-authors listed in

Appendix S. The study has recently been published and the first page of the article is shown in Appendix T. The citation details are listed below:

> *Flor, J.-F., Aburas, M., Abd-AlHamid, F., & Wu, Y., Virtual reality as a tool for evaluating user acceptance of view clarity through ETFE double-skin façades. Energy and Buildings, 2021, 231: 110554.*

8.2. View qualities and user acceptance of ETFE double-skin façades

To close the gap between climate goal projections and realities of the built environment development of novel technologies and materials are necessary. In order to address the twofold challenge of reducing CO_2 emission and respond to extreme weather situations of a changing climate, buildings must be equipped with adaptive and energy-saving building envelopes. Building concepts and standards such as the Passive House, nearly Zero Energy Building (nZEB) and Plus Energy Building (PEB) [D'Agostino et al., 2019; Marino, 2019] target the building envelope as a crucial element to improve indoor comfort conditions and save or even generate energy at the same time [Cao et al., 2016]. Switchable building components have the capacity to adapt to climate and moderate daylighting and heat flux of the building [Loonen et al., 2013], and are an innovative technical solution to achieve this objective as shown in the previous chapters of this thesis. Equipped with reflective printing frits truly adaptive building envelopes can be achieved [Zanelli et al., 2011; Morenoet et al., 2019], suitable for application in double-skin façades and retrofitting of outdated buildings to enhance energy performance with an additional functional layer in the building envelope [Poirazis et al., 2004]. An artistic rendering showing a visualization of how an ETFE double-skin façade could be implemented in an existing office building is shown in Figure 8.127 A and B.

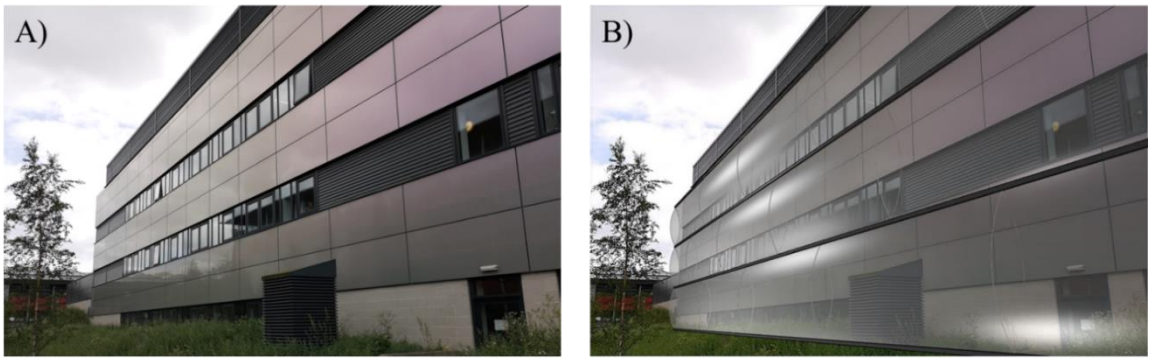


Figure 8. 127. Energy Technology Building at The University of Nottingham Jubilee Campus. Image A) original building office building. Image B) artistic rendering showing the same building with an ETFE double-skin façade
(photo and rendering by the thesis author, published in: Flor et al., 2021)

While the energy and lighting performance of such advanced building envelopes is currently extensively investigated [Hu et al., 2017], the user acceptance relating to the viewer experience and emotional response has not received the same attention so far. However, the human component is of crucial importance for the success of the implementation of such systems on a larger scale. ETFE is a highly transparent material; however, in building practice, potential issues regarding view clarity and haze have been highlighted by designers and manufacturers. A post-occupancy study conducted in an office building in Barcelona, where adaptive ETFE foil cushions had been implemented in the façade, investigated the user satisfaction in relation to thermal comfort and natural lighting under summer and winter conditions. The results suggested that even though user satisfaction for the thermal and lightings conditions varied widely without a clear trend, a general issue with perceived glare and lack of natural lighting was persistent. Glare was reported by 25% of the participants during winter and 45% during summer, while 20% noted a lack of natural lighting during summer and 15% during winter. The cause of this contrary perception of lighting condition was identified to be related to the different location of each participant within the building but also to the slow response of the switching mechanisms of the ETFE façade to the changing solar radiation. The authors of

the study further suggested that a dialogue between users and designers should be established before the implementation of novel adaptable systems and to recalibrate the system control after a certain time of operation with feedback data from user surveys [Juaristi & Monge-Barrio, 2016]. The limitations of the study result from the uncontrolled survey conditions and a relatively small number of participants, of which all where located at, and reporting consequently on, different comfort and lighting conditions. View perception through the ETFE façade was not investigated at all; however, this study is of some value since it represents the only reported survey on the user satisfaction of switchable ETFE cushions, so far. In general, there has been little discussion in the literature regarding the view qualities of ETFE, mainly due to the fact that this technology has been implemented in only in a small number of building façades (Projects: Beijing National Aquatics Center, PTW Architects CSCEC, CCDI and Arup, Beijing 2007; Unilever-Haus, Behnisch Architekten, Hamburg, 2009; Media-TIC building, Architect Enric Ruiz Geli and Cloud 9 Barcelona). In consequence, exposure of the general public to such technologies is limited and factual user experience has been publicized to date only in a single case. Considering the potential for energy savings and the benefits on health and productivity in office spaces [Hartig et al., 1997; Gyeong et al. 2014; Chilton & Lau, 2015; Konstantzos & Tzempelikos, 2017; ElGhazi, 2018; Masoudinejad & Hartig, 2018] this lack of knowledge demands and justifies an empirical investigation to be carried out, to outline the limitations and challenges of such technologies before implementation on a larger scale is initiated. Therefore, the present study investigates the user acceptance and view experience of a variety of ETFE foil façade constructions in order to deepen the understanding of design parameters for future applications. The objective of the study is to provide insights into how people's view from indoor office spaces is affected by different ETFE foil types. For the first-time immersive virtual reality tools are used as a novel methodical approach to evaluating the different ETFE foil constructions. It is expected that outcomes of this study inform future developments of printed and switchable ETFE foil constructions and trigger further improvements of the view characteristics for the implementation in building envelopes. The contents of this chapter are organized in four

parts. The first part deals with the method and explains in detail the procedure of generating the virtual reality views of the different ETFE façade systems. The second part outlines the experimental design and provides details on the sample population and testing conditions. Part three analyses the results of interviews and part four summaries the findings and concludes with a series of recommendations for future research and design developments of ETFE double-skin façades.

8.3.Experimental methods

The use of virtual reality as a tool for assessing the view qualities of windows in architectural spaces is a relatively new methodological approach [Chamilothori et al., 2014]. Commonly, physical material samples and mock-up rooms are being used to investigate the human response to novel glazing developments [Liang et al., 2019]. The method described in this study, using a virtual environment instead, is based on a previously developed method which was validated with an experimental study using visual performance tasks [Abd-Alhamid et al., 2019]. The actual experiment is an audio questionnaire which was applied to a group of individuals during immersion into virtual reality, evaluating different aspects of view perception through a window in an office space with an array of different ETFE foil assemblies. The developed questionnaire was based on previous research studies relating to the view clarity index and emotional responses on view [Bülow-Hübe, 1995; Cetegen et al., 2008; Cauwerts, 2013; Konstantzos et al., 2015]. The experiment design, facilities, equipment and imaging technique used for this study will be described in the following subsections.

8.3.1. Test facility

The room used in this study to assess the view qualities of the different ETFE foils is an office room within a three-story building located at the Jubilee Campus of The University of Nottingham, in Nottingham, UK at a latitude of 52° on the northern hemisphere. The office, with three workstations, has a floor area of approximately 15 m^2,

with two northward facing windows of standard double glazing. The north-facing façade, which was chosen due to the general office orientation in the investigate building, has a metal cladding façade which is earth walled and greened up to the windowsill of the ground floor. The dimensions and spatial configuration of the room is shown in Figure 8.128 A, B and C.

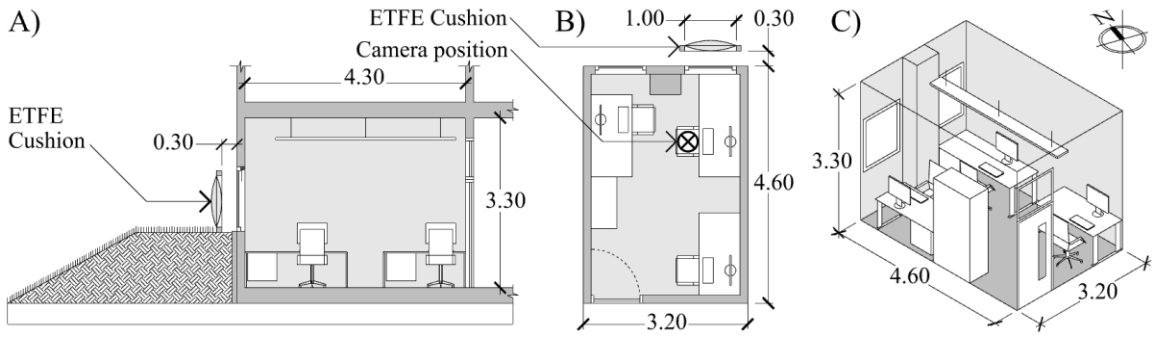


Figure 7. 128: Dimension and spatial configuration of the test room, showing in A) a transversal section, in B) a plan view, and in C) an isometric view
(drawings by the thesis author, published in: Flor et al., 2021)

8.3.2. Experimental equipment

For the generation of the virtual environment and the experimental phase, specialized technical equipment was used. The essential instruments used in this study are described in the following section:

To generate the images for the creation of the virtual environment, a Hagner S3 photometer was used to measure the luminance, and a DSLR camera equipped with a fish-eye lens and mounted on a rotating tripod. For the generation of the virtual environment, a HPC Vive Headset virtual reality headset was used. The headset has a refresh rate of 90 Hz and a 110-degree field of vision. Two OLED panels project the images through Fresnel lenses, one per eye, with a combined resolution of 2160 × 1200 pixels. The headset includes a gyroscope and proximity sensor to determine the location in space and update the projected images accordingly. During the experimental phase, a digital handheld voice

recorder was used to record and double-check the answers given by the participant during the questionnaire. Additionally, a digital timer was used to control the view time in the virtual environment and the time reserved for applying the questionnaire.

8.3.3. Generation of the virtual environment

To recreate the view experience of a double-skin building façade in a virtual environment, firstly a physical scene had to be designed, and photo scanned using previously developed physics-based photography method [Abd-Alhamid et al., 2019]. In order to create the physical test scene, a mock-up of an ETFE façade unit measuring 1.2 m by 1.2 m was installed with 0.3 m distance from the building façade as can be seen in Figure 8.129 A. The mock-up frame developed during a previous stage by the authors [Flor et al., 2019], allowed inflatable ETFE foil cushions with different print designs and layer configurations, as specified in the following section, to be installed and exchanged. Inside in the test room, the camera position for obtaining the stereographic 3D images was chosen as a natural viewing point with the intent to limit the view of the participants from the inside to the outside through the false double-skin building façade, as can be seen in Figure 8.129 B. The camera tripod was placed in front of a desk with approximately 1m to the window. It was necessary to block the upper part of the window with a solar lamella shading screen in order to maintain the illusion of the view through the double-skin façade. Additionally, the second window in the room was entirely covered with a lamella screen to avoid any possibility of accidental reference views to the outside without the ETFE cushion.



Figure 7. 129. A) External view of the building façade showing the installed ETFE cushion mock-up. B) Inside view showing the camera in the view position for the 360-degree stereographic imaging
(photos by the thesis author, published in: Flor et al., 2021)

The camera used for the 3D imaging, a Canon type EOS 5D equipped with a fish-eyelens (Sigma 4.5 mm f/3.5 EX DG), was mounted on a rotating tripod at the height of 1.65 m height corresponding to the approximate eye position of the participants in standing position. A Hagner S3 photometer was used to measure the luminance. The camera was rotated around a 360-degree angle, and six overlapping image sets with different light exposures were taken for each of the three ETFE samples and the reference sample. The procedure was repeated to take one set for the left and one for the right eye with a 65 mm separation to account for the human binocular vision that allows a three-dimensional effect to be perceived in the virtual environment. The images were taken on a summer day in June over a period of 1 hour and 40 minutes from 11:50 am to 1:30 pm under sunny and clear sky conditions. Inside and outside illuminance was monitored for post-processing of the photos to achieve HDRI quality with realistic illuminance levels for the final combined image, according to the method described in [Abd-Alhamid et al., 2019].

The photos were then combined using a specialized ‘stitching’ software (PTGui Pro - 11.13 - Release 2019-04-11, by New House Internet Services BV) obtaining a continuous 360 -degree image of the room in two dimensions. In the following step, the image was converted into a file type readable by the communication software of the virtual reality headset and projected onto a three-dimensional sphere with the viewpoint of the user in the centre of the sphere. In the final step, the three-dimensional stereographic images were projected onto the Fresnel lenses equipped imaging screens of the virtual reality headset. The steps of the above-described procedure can be seen in a diagrammatic flowchart in Figure 8.130, step one to four. An impression of one of the researchers wearing the virtual reality headset can be seen in Figure 8.131 A, a view of the user’s perspective on the inner side of the virtual reality headset is shown in Figure 8.131 B. An example of the stereographic images projected through the lenses of the headset, is depicted in Figure 8.132.

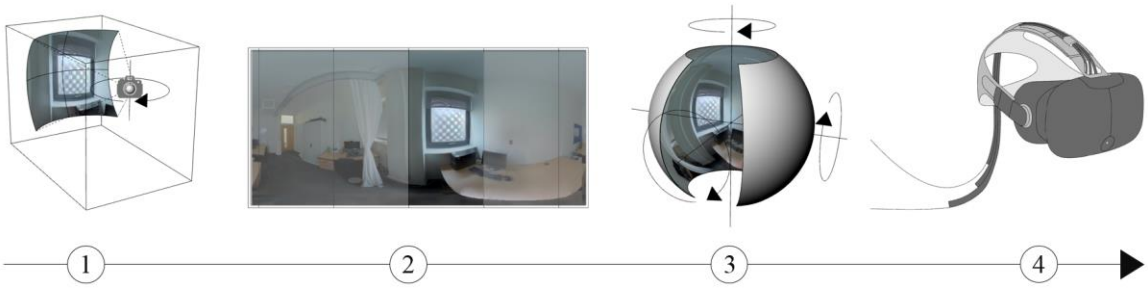


Figure 8. 130. Process of VR image generation, 1. stereographic HDRI photography of test room, 2. stitching of images, 3. Post-processing and 3D projection of images to spherical geometry, 4. projection of imagery to VR headset
(images by the thesis author, published in: Flor et al., 2021)

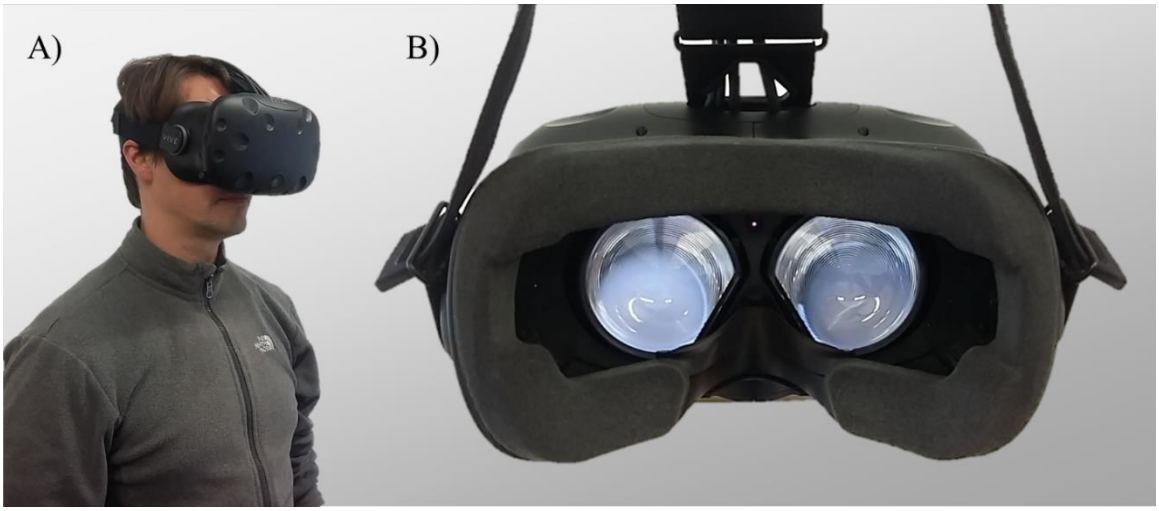


Figure 8. 131. A) Participant equipped with the virtual reality headset as used during the experimental sessions. B) Close-up view of the virtual reality mask from the participant's perspective, showing the two Fresnel lenses through which, the stereoscopic images of the room are projected
(photos by Marina Aburas (A) and the thesis author (B), published in: Flor et al., 2021)



Figure 8. 132. An example of the stereographic images projected through the lenses of the virtual reality headset
(stitched photos by Fedaa Abd-AlHamid, published in: Flor et al., 2021)

8.3.4. Material definitions and view scenarios

During the experiment, four scenarios with three ETFE cushions with different material combinations plus one neutral reference without any additional ETFE layer were viewed and assessed by the participants. The reference scenario coded REF was the view

through the unmodified as-built clear double pane glass window. Sample No. 1, named DSF 1, was the view sample of the combined double-skin façade of the double-glazing window with the externally added inflated ETFE cushion with two layers of clear ETFE foil. Sample No. 2, named DSF 2, was the view sample of the combined double-skin façade of the double glazing window with the externally added inflated ETFE cushion with two layers of clear ETFE foil, of which the external layer was printed with a hexagon pattern of approximately 71% surface cover in standard silver ink with a print density of 28%. Sample No. 3, named DSF 3, was the view sample of the combined double-skin façade of the double-glazing window with the externally added switchable ETFE cushion in open mode. The switchable ETFE cushion is composed of three layers, one clear and two, with a square pattern of approximately 74% surface cover in standard silver ink with a print density of 28%. The printed layers are shifted in a way that the printed areas of one layer overlap with the clear areas of the other. This makes it possible to modify the light transmittance of the cushion, switching from open to closed mode. The sample was only viewed in the open, transparent mode. All ETFE samples measured 1000 mm by 1000 mm with a rise of 100 mm of the main section curvature on each side of the centre plane. All samples were composed of extruded ETFE foil with a thickness of 200 μm. The cushion edges were clamped into an extruded aluminium profile and mounted on a structural wooden frame to support the cushion and withstand tension forces. The whole unit measured 1200 x 1200 mm. The cushions were fully inflated with a nominal pressure of 300 Pa during the time the images were taken. The detailed sample specifications are listed in Table 8.34 and a close-up view through each of the samples is shown in Figure 8.133 A to D.

Table 8. 34
Material description and layer composition of ETFE double-skin façades used in the experiment
(table by the thesis author, published in: Flor et al., 2021)

ID	Description	Configuration
REF	Double Glazing (DG)	14mm Double Glazing Window
DSF 1	DG + Clear ETFE Cushion	14mm Double Glazing Window / 300mm Air Gap / 250µm clear ETFE foil / 200mm Air Gap / 250µm clear ETFE foil
DSF 2	DG + Fritted ETFE Cushion	14mm Double Glazing Window / 300mm Air Gap / 250µm clear ETFE foil / 200mm Air Gap / 250µm silver fritted (71%) ETFE foil
DSF 3	DG + Switchable ETFE Cushion	14mm Double Glazing Window / 300mm Air Gap / 250µm clear ETFE foil / 200mm Air Gap / 250µm silver fritted (74%) ETFE foil / 250µm silver fritted (74%) ETFE foil

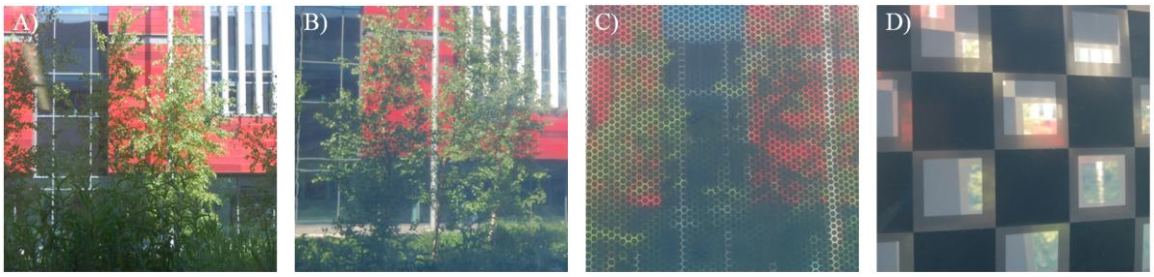


Figure 8. 133. Views through DSF material samples, A) REF double glazing, B) DSF 1, double glazing + clear ETFE, C) DSF 2, double glazing + fritted ETFE, D) DSF 3, double glazing + switchable ETFE
(photos by Marina Aburas and the thesis author, published in: Flor et al., 2021)

8.3.5. Design of the experiment

The purpose of this study is to evaluate the user acceptance of novel glazing systems in double-skin façades, using virtual reality as a predictive tool, which could be implemented in the future by architect practices. This study was specifically designed to look at how different combinations of glazing with ETFE cladding materials in a second skin façades affect the view and have an impact on the perception of colour, scenery and

weather in a virtual environment. Also, the emotional response to the lighting conditions created by the different glazing combinations is being investigated. The different glazing combinations within the virtual environment is only one independent variable within the experiment. The experiment is based on a repeated-measures design, with each participant taking part in tests for all the environments within the study. The Virtual Environment was aimed to be as similar as possible to the real-world space. The participants viewed the different glazing combinations in a random order to avoid bias. The dependent variables in the experiment were the response of participants to the luminance, colour and view perception, regarding subjective questionnaires and task performance.

8.3.6. Experimental procedure

Prior to undertaking the investigation, ethical clearance was obtained from The University of Nottingham Faculty Research Ethics Committee. Participants were recruited by personal invite through an e-mail request. After confirming their interest, potential participants received an information sheet with an overview of the process. A one-hour time slot was then scheduled for the test, with the agreement of the participant. The experiment took place at the University of Nottingham facilities at the Energy Technology Building, on Jubilee campus. Following a brief introduction and check on their well-being, participants were asked for their written consent to take part in the study. This included providing basic personal information and checking on VR related simulator sickness symptoms before the test. The immersed virtual environment test took place in a neutral test room, containing all the virtual reality equipment, headset, computer and a desk for the researcher conducting the experiment. The participants were familiarized with the head-mounted VR equipment and given instructions for the VR viewing and questionnaire. Participants were asked to stay during the test within a colour-marked floor 1 m x 1 m. This zone was covered by the VR spatial location sensors communicating with the VR headset. Within this zone, participants could freely move but would be guided back by the experimenter in case of stepping accidentally out of the zone. After the introduction, four different test scenarios (double glazing + clear ETFE cushion, double glazing + fritted

ETFE cushion, double glazing + switchable ETFE cushion) were shown to the participants. The scenarios were assigned in a random order to counterbalance the presentation order effect. Each immersive environment session was timed to not exceed 5 minutes with a 5 minute recovery break between each session. At the beginning of each session, participants were allowed 2 minutes to familiarize and visually adjust to the environment. Then participants were asked questions by the researcher on their view within the immersive environment. The questions were read out loud by the researcher from a 10-item questionnaire form in a randomized order. Answers were to be given by the participants in a multiple-choice scheme on a scale from one to seven, where one is the lowest and seven the highest rating. The participants' answers were noted down on individual questionnaire forms and audio recorded with the consent of the participants for later verification. After completing the virtual reality test followed by a recovery period, participants were assessed again on any motion sickness symptoms through a questionnaire. All collected information was processed and stored according to the standards established by the ethics committee of the University of Nottingham. A summary flowchart of the experimental procedure can be seen in Figure 8.134.

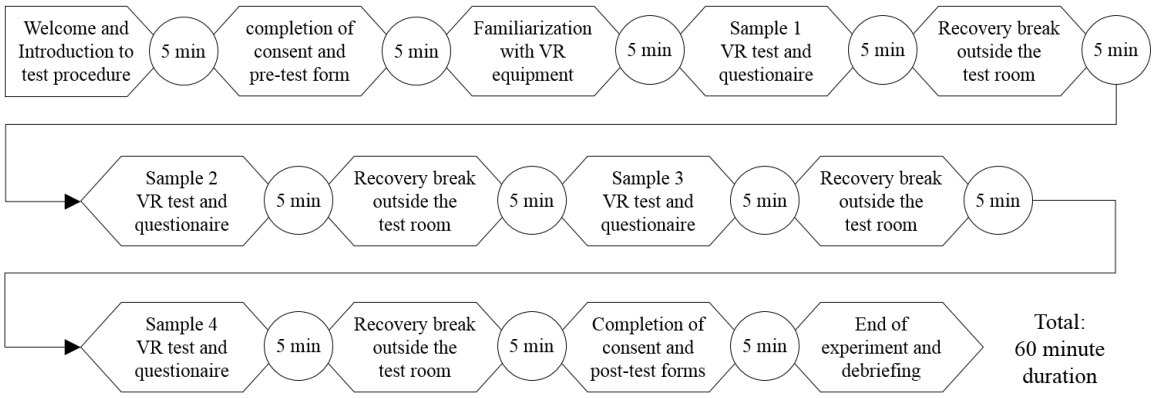


Figure 7. 134. Flowchart of the experimental procedure
(flow-chart by the thesis author, published in: Flor et al., 2021)

8.3.7. Studied parameters

The questionnaire is composed of rating scales developed around view clarity through window shades, based mainly on the work of Konstantzos et al. [2015] with variations reported in many studies since [Konstantzos et al. 2015; Konstantzos et al. 2017]. The questions included responding to visual tasks such as recognizing and counting elements outside the room, as well as making judgements about the view and corresponding emotional state with the goal to identify the preference and user acceptance of participants towards the different ETFE samples. The parameters to rate the preference were linked to the concepts of view clarity, amount of view, view appearance and emotional states of pleasure, arousal and dominance. Each parameter was assessed with a set of questions derived from previous research studies [Bülow-Hübe, 1995; Cetegen et al., 2008; Chamilothori et al., 2018.; Bakker et al., 2014; Hartig et al., 1997; Konstantzos & Tzempelikos, 2017; Masoudinejad & Hartig, 2018]. The questions address the perception of the view, scenery, colours, weather and the emotional response to it, as for example: “How would you grade the vividness of the outside colours”, “How satisfied are you with the amount of view?”, “How pleasant do you feel about the space?”. Ultimately the questionnaire aims to evaluate the user acceptance of ETFE façade systems measuring the view perception and emotional response within each of the four proposed scenarios assessing the view through the DSF ETFE foils with different print patterns and resulting view clarities. The full catalogue of questions and parameters addressed with the questionnaire is listed in Table 8.35 with a sample of the randomized questionnaire shown in Appendix F.

Table 8. 35

Evaluated Parameters in the questionnaire

(table by the thesis author, published in: Flor et al., 2021)

Parameter		Question	Bipolar description	Reference
View clarity		Which outside objects can you distinguish from the following?	Columns/Trees/W.Shades	[Konstanzos 2017]
		How clear is your outside view through the glazing?	Not Clear - Very Clear	[Konstanzos 2017]
		How satisfied are you with the view from the window?	Dissatisfied - Satisfied	[Masoudinej.2009]
Amount of view		How satisfied are you with the amount of view?	Dissatisfied - Satisfied	[Cetegen 2008]
View appearance		How clear is the weather outside?	Hazy - Clear	[Bülow-H. 1995]
		How sunny is the weather outdoor?	Grey - Sunny	[Bülow-H. 1995]
		How would you grade the vividness of the outside colours?	Faded - Strong	[Konstanzos 2017]
Emotional state:	Pleasure	How pleasant do you feel about the space	Unpleasant - Pleasant	[Bakker 2014]
	Arousal	How energized or soporific you feel due to the space	Soporific - Energized	[Bakker 2014]
	Dominance	How controlling versus controlled you feel due to the space	Submissive - Dominant	[Bakker 2014]

8.3.8. Sample population of participants

The questionnaire Twenty-two participants of diverse ethnicity were recruited for this virtual reality experiment. Of these, eight were female, and fourteen were male. The mean age was 29 years, with a standard deviation of 4 years. Thirteen participants self-reported short-sightedness, however only eleven of them wore glasses during the experiment. No other eye problems were reported by any other participant. All test participants volunteered for the experiment without receiving any benefits. All of them spoke fluent English, the language used for the test instructions. The University of Nottingham Faculty Research Ethics Committee, managed by the Chair of the Ethics Committee and the Faculty Research Ethics Officer, reviewed and approved the research protocol and questionnaires (26 April 2019) and all participants signed an informed consent form before and after taking part in this study. A copy of the ethics documentation and approval, as well as a sample of the participant consent form, is included in Appendix G and H.

8.4. Results and discussion

The first set of analyses examined the ratings on the different view samples given by the participants during the questionnaire. The response of the participants to the questionnaire was given during the virtual environment experience they were immersed in, reflecting their immediate response to the perceived visual stimulus. The answers to the 9 questions were given on a bipolar scale from 1 to 7, where 1 is the lowest and 7 the highest score. The average scores of the 22 participants were compared in order to determine difference and preferences in the view perception of the three ETFE samples and the reference sample of the double glazing.

8.4.1. Sample Rankings

This section describes and discusses the preference rankings for the tested façade samples obtained from the experimental data. Each data set of the tested parameters and corresponding asked questions in the applied questionnaire was discussed in the following:

At the beginning of each virtual reality session, the first question was always “Which outside object can you distinguish from the following?”, asking the participants to recognize and count three types of objects (columns, trees, window shades) visible on the outside view. The answers to this question were not included in the analysis of the results since the question was only intended to make the participants engage with the virtual environment and focus their attention on the window view before initiating the questions, which would rate the participants' viewing experience. Additionally, the experimenter was able to observe at the same time on a computer screen a projection of the view the participant was looking at through the virtual reality headset.

The results from the preliminary results outlined in Figure 8.135 show across all investigated parameters that the highest ratings were given to the reference sample REF with the clear glazing, followed by the DSF 1 sample with the added on clear ETFE cushion and the DSF 2 sample with the fritted ETFE cushion. The DSF 3 sample with the

switchable ETFE cushion was the lowest ranking in all nine questions. The highest rating for the reference sample REF was for question number 5 “How sunny is the weather outdoor?” with an average score of 6.8 translating to ‘very sunny’ on the bipolar scale. The other three samples achieved their highest rating within the questionnaire for the same question, with 6.5 for DSF 1, 5.9 for DSF 2 and 5.6 for DSF 3, meaning that regardless of the visibility participants were still able to perceive the external weather condition and judge if it is sunny or not.

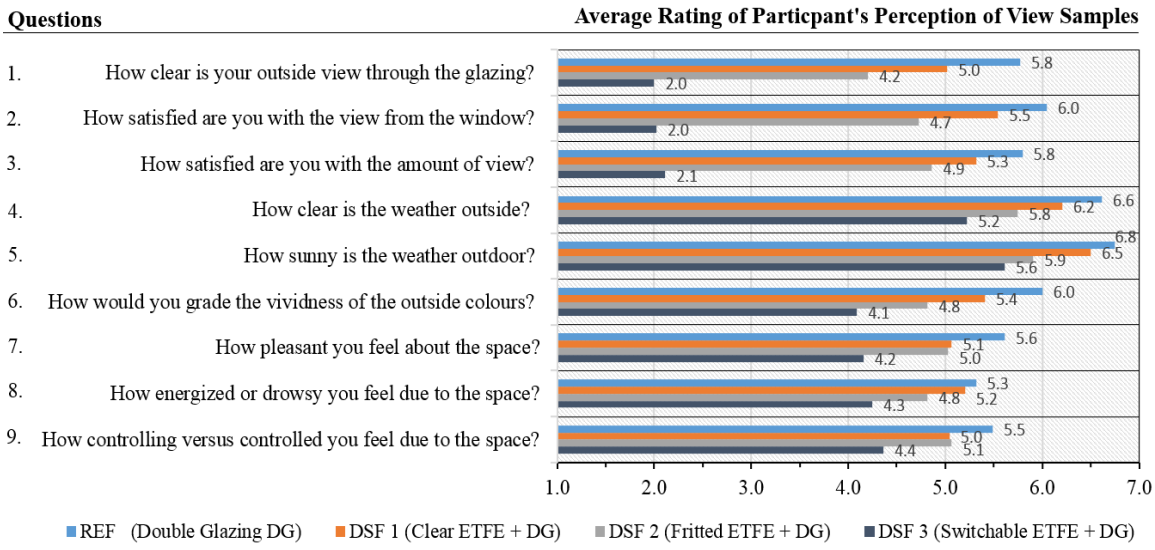


Figure 7. 135: Results of the questionnaire showing average ratings of samples (chart by the thesis author, unpublished)

A similar trend was observed for questions number 4 and 6, asking about the clearness of the weather and the vividness of the outside colours. Again, the visibility of the different view samples had only a limited influence on the participants' perception of external environmental conditions but showing again a clear preference for the reference sample REF, followed by DSF 1, DSF 2 and the least preferred DSF 3. The overall lowest rating for the questionnaire was scored by sample DSF 3 with 2.0, 2.0 and 2.1 for question number 1, 2 and 3 respectively. Participants stated the view through the switchable ETFE cushion not to be clear and were particularly dissatisfied with the view from the window

and the amount of view. The participants rating is not surprising as the view through the overlapping squared printing pattern of the foil layers of the switchable cushion limits the view through the window considerably as can be observed in Figure 8. 133 D. Interestingly, for the same questions participants reported much higher scores for the sample DSF 1, DSF 2 and the reference sample REF, stating a general satisfaction with the view. This reinforces the intuitive impression from an early stage of the study that the view satisfaction and related user acceptance of ETFE foils in building façades is directly linked to the proportional amount and grade of clear view through the window, which is in the case of switchable ETFE cushion directly influenced by the pattern of the frit. The squares of the switchable frit print are very dominant but distributed dots, like in the outer layer of cushion sample DSF 2, are less intrusive and probably need further investigation. In the final part of the questionnaire, participants were asked about their emotional state during the view experience within the virtual environment using the dimensions of pleasure, dominance and arousal, developed by Mehrabian and Russel [Bakker et al., 2014]. A majority of participants perceived their emotional state as positive towards the virtual space they were immersed in. Most participants reported experiencing a pleasant feeling, were energized and feeling dominant within the space. This emotional response was reported for all four viewing samples; however, the switchable DSF 3 sample received with an average of 4.3 the lowest ratings, and the reference sample REF with 5.5 the highest, while the clear and printed ETFE sample, DSF 1 and DSF 2, scored on average 5.1 and 5.0 respectively for all three dimensions. Detailed ranking charts with standard error indication for each of the parameters evaluated with corresponding questions asked to the participants on viewing the samples is shown in Figure 8.136, for those relevant to the emotional response, and in Figure 8.137 for view clarity. Descriptive statistical data will be discussed in the following section adding in support for the validity of the presented ranking data.

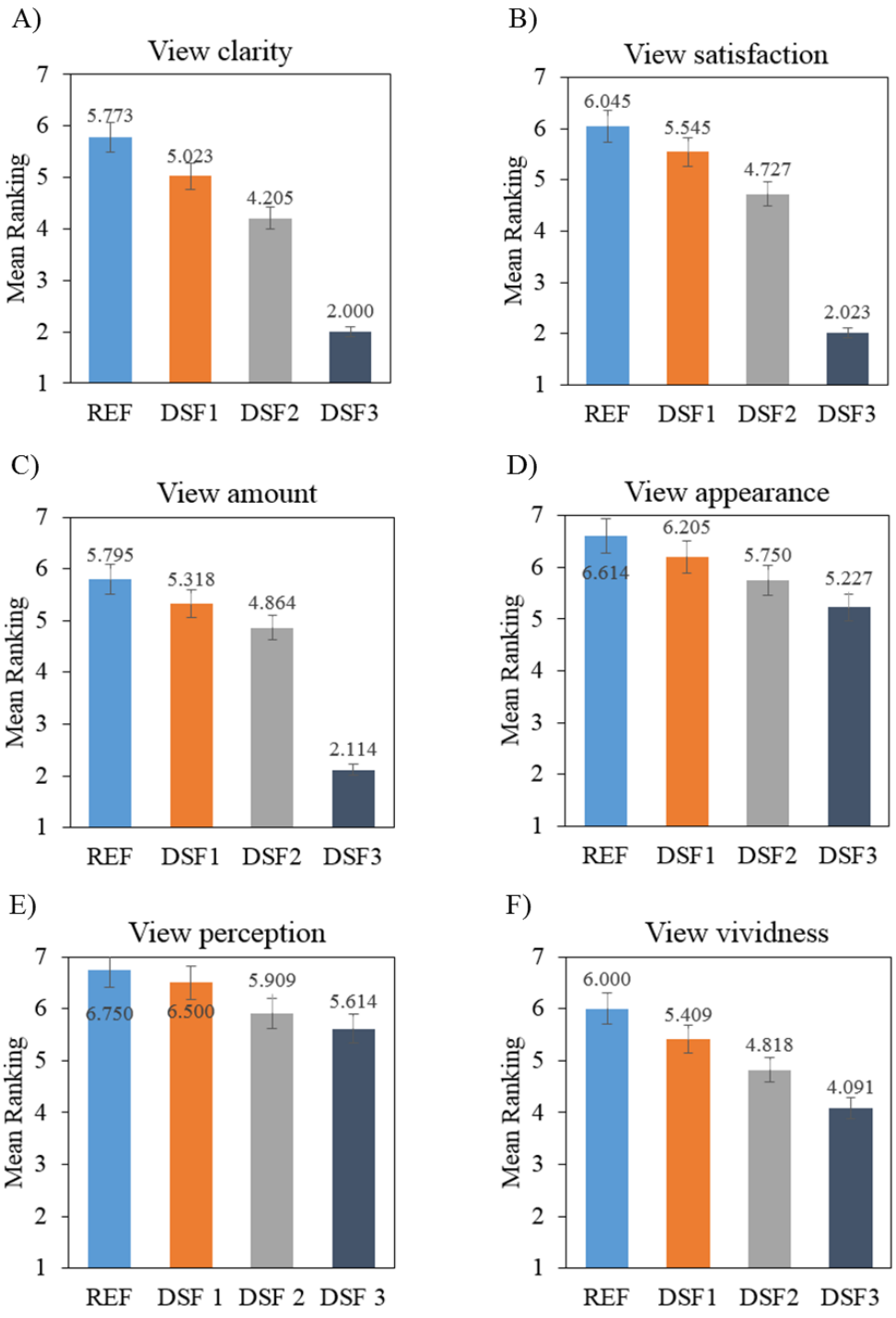


Figure 8. 136: Ranking charts of mean values corresponding to the view clarity parameters of the different view samples, A) View clarity (Question No. 1), B) View satisfaction (Question No. 2), C) View amount (Question No. 3), D) View appearance (Question No. 4), E) View perception (Question No. 5) , F) View vividness (Question No. 6)
(charts by the thesis author, unpublished)

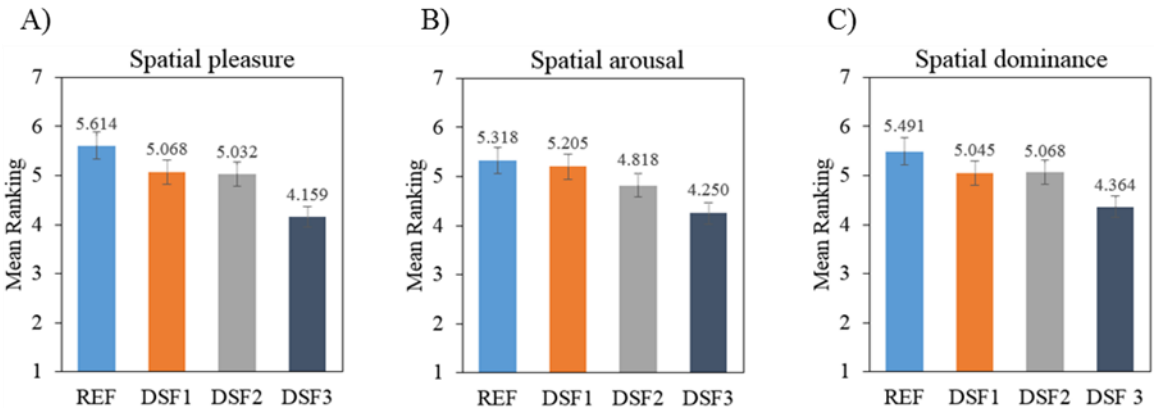


Figure 8. 137: Ranking charts of mean values for those parameters corresponding to the emotional response on the different view samples, A) Spatial pleasure (Question No. 7), B) Spatial arousal (Question No. 8), C) Spatial dominance (Question No. 7)
(charts by the thesis author, unpublished)

8.4.2. Statistical data

This section summarizes descriptive statistical data on the collected data-sets that was used to support the analysis and interpretation of the sample rankings. An overview of the descriptive statistical data outlining the experimental sample rating results is shown in Table 8.36 at the end of this section.

The view qualities of three samples of ETFE double-skin facades and a reference glazing sample had been investigated, inquiring with a questionnaire of nine questions on view perception and emotional response. Questions one to six addressed parameters of perception while questions seven to nine looked at the emotional response. For all questions, a continuous scale from one to seven was used, with 22 participants rating their subjective perceptions with bipolar concepts such as: “How clear is the outside view?”, where the provided possible answers were between one and seven with “not clear”, being the lowest possible rating (1) and “clear” the highest (7).

For question number one, which addressed the view clarity of the samples, the mean value ratings positioned the reference sample at 5.7 with a minimum of 3 and a maximum of 7. Sample DSF 3 was placed on the lowest mean ranking for this parameter, with a more considerable sample variance of 1.8 compared to 1.3 of the REF sample. The Calculated

standard error ranged between 0.2 and 0.3. The standard deviation of the sample data sets for question one ranged between 0.9 and 1.8 with the fritted sample DSF2 accounting for the lowest value. This indicated that participants view satisfaction levels differed distinctly between REF and DSF 2/DSF 3 and DSF 3 and DSF1/DSF 2. Overall participants were more satisfied with the view through the clear ETFE, followed by the fritted ETFE. The view through the switchable ETFE was ranked less satisfying than clear and fritted ETFE.

Question number two addressed view satisfaction, asking how satisfied participants were with the view from the window, rating from "dissatisfied" (1) to "satisfied" (7). Reference sample REF received the highest-ranking position with a mean ranking of 6.0, ranging between a minimum of 4 and a maximum of 7. The error for this data-set was 0.2, with a standard deviation of 0.8 and a sample variance of 0.6. The switchable sample DSF3 received the lowest mean ranking with 2.0 and range between min.= 1 and max= 4. The standard error for this data set was 0.2, standard deviation 1 and sample variance also 1. This indicated that participants view satisfaction levels differed distinctly between REF and DSF 3. Overall participants were more satisfied with the view through the clear ETFE, followed by the fritted ETFE. The view through the switchable ETFE was evaluated as less satisfying than clear and fritted ETFE.

In question three, participants were asked how satisfied they were with the amount of view from "dissatisfied" (1) to "satisfied" (7). Mean rankings ranged between 5.8 and 2.1 with REF in the highest rank and DSF3 in the lowes. The standard error was consistently low across all four data-sets for this parameter, ranging between 0.2 and 0.3. The standard deviation ranged between 0.9 and 1.2, with a sample variance between 0.7 and 1.3. Participants reported much higher scores for REF, DSF 1 and DSF 2 stating a general satisfaction with the view through those conditions, and less satisfaction with the view amount of switchable ETFE cushions.

Question four investigated the view appearance asking about the clearness of the weather. Answers were reported continuously from 1 for "hazy" to 7"clear". The standard error for this data-set ranged between 0.1 and 0.3. The standard deviation oscillated between 0.5 and 1.5, with a sample variance between 0.3 and 2.3. Not surprisingly,

participants rated the view through the ETFE cushion without any frit prints as the clearest among the ETFE samples. Unlike the response to questions on "view clarity", "satisfaction" and "amount", no significant difference was noted for DSF 2 compared to DSF 3. The maximum mean difference between all samples was only 1.4.

Question number five addressed the view perception asking participants to rate how sunny the weather was outdoors from "grey" (1) to "sunny" (7). Participants perceived the weather to be sunnier when viewed through the clear ETFE, sample DSF1 (mean= 6.5), followed by the fritted sample DSF2 (mean= 5.9), and last, the switchable ETFE sample DSF3 (mean= 5.6). It is noted that the highest rating for all ETFE types was found for this question, meaning that regardless of the visibility, participants were still able to perceive the outside weather conditions. The standard error for this data-set ranged again between 0.1 and 0.3. The standard deviation oscillated between 0.5 and 1.5, with a sample variance between 0.5 and 2.0.

Question number 6 asked participants to grade the vividness of the outside colours from "faded" (1) to "strong" (7) enquiring on the view vividness of the DSF samples. The lowest rating was scored by sample DSF 3 with a mean value of 4.1 compared to 6 of the double glazed reference sample REF. The standard error for this data-set ranged between 0.2 and 0.4. The standard deviation was between 0.7 and 1.6, with a marginally higher sample variance between 0.6 and 2.7.

Despite low deviation among individual responses and high consistency of the rating across the view samples, participants frequently asked for further explanation of the questions seven, eight and nine, addressing the emotional aspects of the view perception, and reported being unsure how to respond. Further, during the debriefing sessions after the test, some participants disclosed that they were unfamiliar with the concepts of emotional state and how to evaluate an architectural space in these dimensions. However, the results from the questionnaires show a very consistent rating compared with the rest of the sample, with a standard deviation between 0.5 to 1.6 and a standard error between 0.1 and 0.3, independent of the order of the viewed samples. This further adds confidence to the results of the experiment.

Table 7. 36

Overview of descriptive statistical data of the experimental sample rating results (table by the thesis author, unpublished)

Parameter	Sample	Mean	Median	Min.	Max.	Standard Error	Standard Deviation	Sample Variance	Count
View clarity	REF	5.773	6.000	3.000	7.000	0.246	1.152	1.327	22
(Question 1)	DSF1	5.023	5.000	2.000	7.000	0.262	1.229	1.511	22
	DSF2	4.205	4.000	3.000	6.000	0.199	0.934	0.873	22
	DSF3	2.000	1.750	1.000	5.500	0.285	1.336	1.786	22
View satisfaction	REF	6.045	6.000	4.000	7.000	0.161	0.754	0.569	22
(Question 2)	DSF1	5.545	6.000	4.000	7.000	0.218	1.022	1.045	22
	DSF2	4.727	5.000	3.000	6.000	0.160	0.752	0.565	22
	DSF3	2.023	2.000	1.000	4.000	0.217	1.017	1.035	22
View amount	REF	5.795	6.000	3.000	7.000	0.222	1.043	1.087	22
(Question 3)	DSF1	5.318	5.750	3.000	6.500	0.193	0.907	0.823	22
	DSF2	4.864	5.000	3.000	6.000	0.178	0.834	0.695	22
	DSF3	2.114	2.000	1.000	5.000	0.246	1.154	1.332	22
View appearance	REF	6.614	7.000	5.500	7.000	0.109	0.510	0.260	22
(Question 4)	DSF1	6.205	6.000	4.000	7.000	0.182	0.854	0.730	22
	DSF2	5.750	6.000	4.000	7.000	0.232	1.088	1.185	22
	DSF3	5.227	5.750	2.000	7.000	0.327	1.533	2.351	22
View perception	REF	6.750	7.000	5.500	7.000	0.097	0.456	0.208	22
(Question 5)	DSF 1	6.500	6.750	4.000	7.000	0.154	0.724	0.524	22
	DSF 2	5.909	6.250	1.000	7.000	0.306	1.436	2.063	22
	DSF 3	5.614	5.750	4.000	7.000	0.205	0.963	0.927	22
View vividness	REF	6.000	6.000	4.000	7.000	0.158	0.740	0.548	22
(Question 6)	DSF1	5.409	5.500	3.000	7.000	0.222	1.042	1.087	22
	DSF2	4.818	5.000	3.000	7.000	0.278	1.305	1.703	22
	DSF3	4.091	4.000	1.000	7.000	0.349	1.638	2.682	22
Spatial pleasure	REF	5.614	6.000	3.000	7.000	0.230	1.079	1.165	22
(Question 7)	DSF1	5.068	5.000	2.000	7.000	0.247	1.158	1.340	22
	DSF2	5.032	5.000	3.000	7.000	0.212	0.992	0.984	22
	DSF3	4.159	4.000	2.000	6.000	0.254	1.189	1.414	22
Spatial arousal	REF	5.318	5.250	3.000	7.000	0.243	1.140	1.299	22
(Question 8)	DSF1	5.205	5.000	3.000	7.000	0.239	1.120	1.254	22
	DSF2	4.818	5.000	3.000	6.500	0.241	1.129	1.275	22
	DSF3	4.250	4.000	2.000	6.000	0.237	1.110	1.232	22
Spatial dominance	REF	5.491	5.250	4.000	7.000	0.205	0.962	0.926	22
(Question 9)	DSF1	5.045	5.000	2.000	7.000	0.265	1.243	1.545	22
	DSF2	5.068	5.000	2.500	7.000	0.206	0.967	0.936	22
	DSF 3	4.364	4.250	2.000	6.000	0.266	1.246	1.552	22

Taken together, these results suggest that there is an association between user satisfaction and view clarity, where those DSF with higher clarity and less obstruction through reflective frit prints are preferred and provoke a more positive emotional response in users towards the spaces they are in. For the future applications of these foil constructions, which have been extensively used for canopy and roof constructions, these results might appear as a negative indicator for the use in façade systems, where visibility and view clarity is much more important to the user. This is especially true for the switchable ETFE cushion, which promises so much benefit in terms of energy performance. However, the results are not per se a negative outcome for the question of future applicability of printed and switchable ETFE foils in double skin façades (DSF), but rather suggest that the frit prints must be carefully designed to fulfil the users need to interact with the exterior visually. Virtually reality and immersive environments have been demonstrated within this study to be a practical and reliant tool to experience in advance the view and feeling of being in a room with an innovative and novel façade system without incurring the costs of a large size mock-up or running the risk of exposing users to work for decades in an unsatisfying environment. Overall the results provide important insights into view perception and emotional response of DSF with ETFE foils.

8.4.3. Limitations

The biggest limitation of this virtual reality study might be that the sceneries viewed during the experiment are instead of a virtually created environment only a three-dimensional image of a physically existing scenery represented by a virtual reality viewing tool. Although for this particular experiment a preexisting physical mock-up was used to create the illusion of a view through a double skin façade, for future studies the exclusive use of calibrated physics-based virtual models is envisioned to further increase time- cost-effectiveness, design flexibility and alterability of climate and location. Which leads to the second big limitation of the test, which is the restriction of the view conditions to the point in time when the images of the room were taken. For future tests, it would be desirable to view the test samples under different weather conditions, hence cloudy or rainy sky. Also,

different view sceneries, urban vs rural would be of interest to explore. Different window orientation north vs south and different daytime with alternative sun angle and solar radiation intensity would be recommended to investigate as well as testing the effect of direct vs indirect solar incidence on the window and include different artificial indoor lighting scenarios. A method which would allow the change of the virtual scenery and to modify the window materials and façade design digitally would, therefore, be of much interest. The development and validation of such method which would facilitate the physically correct modelling and editing of virtual environments for mock-up testing of novel designs would be a task for future research. A further limitation of this study was the static nature of the VR scenarios. Participants could not interact with the scene, hence moving in virtual space for a different viewing angle or touching and moving objects was not possible. To enhance a deeper immersion during the viewing experience, giving the full illusion of being there might be beneficial for the comprehensive evaluation of novel façade and window systems in the future. It is also hoped that the development of virtual reality hardware itself will continue to advance and provide higher resolution screens for even more realistic representations of immersive environments which truly recreate the physical correct lighting conditions of windows in architectural spaces.

8.5. Chapter summary

The study in this chapter set out to investigate the viewing experience and emotional response to different ETFE materials in double-skin building façades using virtual reality equipment. The goal was to determine the user acceptance towards the different design options simulating the viewing experience in immersive environments with physically correct imagery. The method had been validated in a previous study, however, was used in this case for a practical application of investigating the view clarity of printed and switchable ETFE cushions in building façades. The current findings clearly support the relevance of using virtual reality for early design evaluation and user feedback. While the results obtained from the applied questionnaire was consistent and coherent, participants reported, in general, positive testing experience and confirmed the adequacy

of the method for the chosen purpose. One of the more significant findings to emerge from this study is that even though several options of commonly used printed ETFE foils were displayed during the viewing sessions, none of them would outperform in any of the tested parameters the clear double-glazing reference sample. Even though this outcome is, at first sight, discouraging, considering the fact that these printed foils were not purpose-designed for the application in building façades puts the result into perspective and instead should be interpreted as suggestive criteria for the development of better foil frit prints, inks and patterns with a higher view clarity for the application in novel façade systems. Although the current study is based on a small sample of participants, the findings suggest that this is especially true for the switchable ETFE cushion which on one side offers many opportunities for energy savings and enhanced daylight performance, but on the other side was not well accepted by the participants of this study due to its limited view clarity and amount of clear view to the outside environment. This outcome is of significance for the future application of switchable ETFE cushions in its current form. Even though this is the first time that virtual reality has been used to explore the view clarity and user acceptance of printed and switchable ETFE foils in double skin building façades the effectivity of this method has been demonstrated in this study. Further research regarding the role of the switching process itself of the adaptive ETFE cushion would be worthwhile, especially under different weather and lighting conditions, which could lead to even more complex questions of user acceptance when incorporating the users' autonomy to control the switching process in a dynamic interactive virtual environment testing set up of future studies.

Chapter 9: Conclusions

9.1. Conclusions

The research presented in this thesis aimed to examine the potential of the climate adaptive capabilities of switchable multi-layer ETFE foil cushions to enhance the environmental performance of façades and buildings, in comparison to conventional, static systems. The following secondary aim of this study was to investigate the effects of influencing parameters on the system and the performance, to understand under which conditions it would be reasonable to incorporate adaptive ETFE systems into building envelopes.

This study has shown that switchable ETFE cushions undeniably have a great potential to improve the environmental performance of buildings, especially when applied as a double-skin façade for retrofitting measures. Providing an answer to the initial research questions of this study it can be said that the application of adaptive ETFE structures as a second building skin and measure of retrofit to reduce the energy consumption and improve the daylighting performance of outdated multi-story buildings is completely viable from a building physics perspective. The study focused on two major aspects of the environmental performance and evaluated the energy consumption of buildings and the daylighting qualities of the internal spaces. Simulations results revealed several important findings, first: those office buildings covered with a switchable ETFE double-skin façade consume considerably less energy for heating cooling and lighting. Annual energy savings of up to 56% were predicted in comparison to buildings with a standard double-glazing façade. Second: the daylighting exposure and distribution in an office space can be significantly improved when the façade is retrofitted with switchable ETFE cushions. Useful daylight illuminance was made available for up to 69% time of the year when a switchable ETFE double-skin façade was applied, compared to 11% without. The results further showed that glare from direct sunlight could be minimized with the responsive shading mechanism to an unperceived level for most of the time. The switchable ETFE cushions could reduce

glare by up to 59%, compared to a double-glazing façade without the ETFE double-skin façade. Overall, the switchable ETFE cushion outperformed double glazing façades in all test scenarios. While conventional, static ETFE cushions with clear foil and reflective frit prints improved the environmental performance of the investigated spaces also considerably, yet, when applied as double-skin façades, they did not achieve the same energy savings and daylighting qualities reached with the application of switchable ETFE cushions.

The main parameters affecting the effectivity of the adaptive shading mechanism were identified to be the incidence angles of solar radiation and the optical characteristics of the reflective fritting patterns, imprinted on the ETFE foil. Ray-tracing simulations revealed that with increasing reflectance and decreasing transmittance of the frit print the climate-adaptive capabilities of the switching ETFE cushion were augmented, hence the difference of the overall light transmittance in the open and closed switching state was maximized. Simulation scenarios with different solar angles demonstrated the angle-dependent optical behaviour of the switchable system. In open mode, counterintuitively, the light transmittance is higher for steeper angles and lower for ray angles perpendicular to the horizontal axis of the cushion geometry. Angle dependent variations of up to 20% were found, depending on the selected frit print transmittance. This phenomenon was explained with the shifted frit patterns of the outer and middle layer, which in the open mode, allow for more transversal permeability at lower ray angles. In closed mode, this effect was not as pronounced due to the changed position of the fritted middle layer. Experiments in a large climate chamber confirmed that there is also a thermal aspect related to the switching mechanism, finding that the thermal resistance of the cushion is higher in open mode and lower in closed mode. The overall horizontal heat-flux through the switchable ETFE was observed to be 17% lower in open mode. It was hypothesized that this thermal behaviour might be related to the different emissivities of printed and unprinted foil surfaces which overlap during the switching process and result in the overall change of the thermal performance of the ETFE cushion. A second possible explanation relates to small air pockets between the middle and outer layer, resulting from residual air

trapped between the layer during the switching process, which might add to the overall thermal resistance of the ETFE cushion. However, further research is needed to provide a satisfactory explanation and evaluate the potential for multi-objective performance controls.

Supported by the simulation results, the most significant potential for achieving energy savings and enhanced daylighting performance with switchable ETFE cushions is predicted for climatic regions of the lower latitudes, where intense solar radiation is available all year long Whereas in colder climates in higher latitudes the application of switchable ETFE in double-skin façades is still beneficial, but might not yield the same percentage of energy savings and daylighting enhancement as in lower latitudes, and is therefore not likely to justify the investment for a façade retrofit unless new frit prints become available which provide a better material performance. Together with the arguments of the previous section, this offers an answer to the second initial research question of this thesis. However, a wider range of climatic regions is suggested to be investigated to obtain a more differentiated conclusion on this topic. Another defining factor for the feasibility and effectiveness of the climate adaptive capacity of switchable ETFE cushion is the window-to-wall ratio of the building where the ETFE double skin façade is to be applied to. The results of the study showed that buildings with large window façades might benefit the most from an additional ETFE second-skin façade, in terms of energy savings and daylighting enhancement, while for the smaller window-to-wall ratios also conventional static ETFE cushions with reflective fritting could achieve similar performance. Nevertheless, a factor which reduces the feasibility of implementing switchable ETFE cushion as a second skin façade is the visibility. Virtual reality was used in this research study to objectively evaluate the view clarity and user acceptance of double skin façades with different ETFE fol constructions. The obtained results generally showed a visual dissatisfaction of users with current switchable ETFE constructions in building façades. The results suggested that this might be strongly related to the visibility impaired by the frit patterns, and answers the third of the initial research questions of this thesis. Therefore, it is argued here for a reconsideration of the frit pattern designs and inks to suit

the specific requirements of fenestration and façade applications and consider the users' emotional needs beyond concerns about daylighting efficiency and energy consumption.

In summary, it has been shown in this study that the climate-adaptive capacity of switchable ETFE cushions can significantly improve the environmental performance of buildings. Taken these findings together, they suggest convincing arguments for promoting switchable ETFE cushions as a viable technology for climate-adaptive double-skin façades, and as an effective retrofitting measure to reduce energy consumption and enhance daylighting performance in office buildings. However, frit inks and patterns of switchable ETFE cushions must be adapted to suit the user expected visibility and view clarity of common fenestrations in façade applications. Overall, this study strengthens the idea that an outdated building stock, which currently contributes to a large extent to global energy consumption and CO_2 emissions, could possibly be energetically upgraded, rather than demolished and rebuilt.

This thesis is one of the first attempts to thoroughly examine the energy and daylighting performance of ETFE in building façade. The conducted studies have provided a more in-depth insight into the thermo-optical characteristics and behaviour of ETFE cushions in general and is the most extensive study so far, documenting the switching mechanism of climate adaptive, switchable ETFE cushions. Prior to this study, it was difficult to make predictions about how an ETFE double-skin façade would affect the energy and daylighting performance of a building. This new understanding could help to improve predictions of the impact of different types of ETFE double-skin façades on the environmental performance of office spaces and other typologies in commercial building projects. Additionally, the insights gained from this study may be of assistance for the development of new switchable materials and systems, as well as providing guidance for designers and manufacturers to assess the material choices for the energy and daylighting requirements of future building projects.

9.2. Limitations

The generalizability of the results presented in this thesis is, however, subject to certain limitations. For instance, the sample of climate scenarios which this study is based on covers only a small percentage of global climate regions and the results might need to be reconfirmed with further research, also on other building types and scales, in a broader climate range. Another major limitation of this study is the lack of experimental data for the solar component of the thermal performance of the ETFE cushion samples. Due to time limitations, it was not possible to assess the solar heat gain coefficient of switchable ETFE cushions; therefore, the degree of accuracy with which the simulated results reflect the solar gains of buildings with climate-adaptive ETFE double-skin façades realistically can only be estimated and rely mainly on the software validations of previous studies. Thirdly, the study did not evaluate any fundamentally new proposals that could have led to advance the engineering developments for the second generation of switchable ETFE cushions. However, the research has investigated with virtual reality studies, the view experience of switchable ETFE cushion in building façades, highlighting possible pathways and criteria for redesigning frit prints and patterns to adapt the existing switchable ETFE cushion to applications more suitable to the user expectations on building façades. Despite its limitations, the study certainly adds to our understanding of the thermo-optical behaviour of switchable ETFE cushions and contributes to the general knowledge of climate adaptive light-weight structures in building façades.

9.2. Future work

This research has brought up many questions in need of further investigation. Considerably more work will need to be done to determine the solar heat gain coefficient of ETFE cushions, as mentioned previously. A greater focus on the solar radiation could produce interesting findings that account more precisely for the solar gains in the thermal performance of ETFE foil construction in general and the switchable ETFE cushion

specifically. Research in this direction could possibly lead to new discoveries on the pathway to developing novel material applications and advance multi-objective control systems for climate-adaptive foil constructions. Related to this research direction, another fruitful area for future work would be the development of a new type of frit print ink with superior thermo-optical properties, but which would also take into account to improve the visual performance and user experience of ETFE for applications in building fenestrations. Further research should be undertaken to explore how virtual environments can support the experimental development of novel materials and systems on a small scale with performance evaluation of large-scale virtual mock-ups. Finally, post-occupancy studies would be highly recommended to verify the predicted energy savings and daylighting performance on an existing building and obtain feedback on the performance from a user perspective, regarding effectiveness, operability, potential issues and suggestions for improvement.

Climate change is a pressing issue for global economies and is starting to affect human communities and the natural world as a whole on an unprecedented scale. The building sector and commercial buildings particularly are one of the main contributors to global CO_2 emissions and climate change. Given the current situation, there is a definite need for upgrading the energy efficiency of a large, outdated building stock on a global scale. The challenge is to reduce the energy consumption of building in the short term, and the vision to transform the current building stock from energy-consuming to energy-producing structures in the future. Vast potential is seen in climate adaptive building envelopes as a measure to retrofit old buildings and to reduce their energy consumption and related emissions. It is hoped that the information contained in this thesis might find potential use for architects and engineers to promote targeted interventions aimed to implement switchable ETFE cushions for energy retrofits of office buildings and inspire researchers to develop even better materials and systems to support this task.

References .

Abd-Alhamid, F., Kent, M., Bennett, C., Calautit, J., & Wu, Y. (2019). Developing an Innovative Method for Visual Perception Evaluation in a Physical-Based Virtual Environment. *Building and Environment, 162*, 106278.

Afrin, S. (2016). *Thermal Performance Analysis of ETFE-foil Panels and Spaces Enclosed with ETFE-foil Cushion Envelope.* (Doctorate Doctoral Thesis). University of Nottingham, Nottingham, UK.

AGC - Asahi Glass Co., L. (2016). *Fluon ETFE film - Technical Datasheet (ETFE film structures).*

Al Horr, Y., Arif, M., Kaushik, A., Mazroei, A., Katafygiotou, M., & Elsarrag, E. (2016). Occupant productivity and office indoor environment quality: A review of the literature. *Building and Environment, 105*, 369-389.

Andersen, M., Rubin, M., Powles, R., & Scartezzini, J. L. (2005). Bi-directional transmission properties of Venetian blinds: experimental assessment compared to ray-tracing calculations. *Solar Energy*, 78(2), 187-198.

Andrew, M. (2013). BSDFViewer: A utility for interactive exploration of BSDF datasets.

ANSI/ASHRAE. Standard 90.1 – 2019, Energy Standard for Buildings Except Lo-Rise Residential Buildings. In.

ANSI/ASHRAE. (2010). Standard 90.1 – 2010, Energy Standard for Buildings Except Lo-Rise Residential Buildings. In.

ANSI/ASHRAE. (2013). Standard 55-2013, Thermal Environmental Condition for Human Occupancy. In.

Attia, S., Favoino, F., Loonen, R., Petrovski, A., Monge-Barrio. (2015). *Adaptive Façades System Assessment: An initial review*. Paper presented at the 10th Conference on Advanced Building Skins, Bern, Switzerland.

Bakker, I., van der Voordt, T., Vink, P., & de Boon, J. (2014). Pleasure, Arousal, Dominance: Mehrabian and Russell revisited. *Current Psychology, 33*(3), 405-

Barozzi, M., Lienhard, J., Zanelli, A., & Monticelli, C. (2016). The Sustainability of Adaptive Envelopes: Developments of Kinetic Architecture. *Procedia Engineering, 155*, 275-284.

Beccarelli, P. (2015). The Design, Analysis and Construction of Tensile Fabric Structures. In *Biaxial Testing for Fabrics and Foils - Optimizing Devices and Procedures* (pp. 138): Springer International Publishing.

Bedon, C., Honfi, D., Kozłowski, M., Machalická, K., Santos, F., Wüest, T., . . . Vokáč, M. (2018). Key structural aspects for adaptive façades - Activity progress from the EU-COST Action TU1403 'Structural' Task Group. 2, 135-154.

Berger, J., & Mendes, N. (2017). An innovative method for the design of high energy performance building envelopes. *Applied Energy, 190*, 266-277.

Bertoldi, P., Hirl, B., & Labanca, N. (2012). Energy efficiency status report 2012. In I. f. E. a. T. J. R. C.) (Ed.), *Electricity consumption and efficiency trends in the EU - 27 - Study*. Luxembourg: Publications Office of the European Union.

Biloria, N., & Sumini, V. (2009). Performative Building Skin Systems: A morphogenomic approach towards developing real-time adaptive building skin systems. *International journal of architectural computing, 07*(04), 643 - 675.

Bletzinger, K.-U., & Ramm, E. (1999). A General Finite Element approach to the form finding of tensile structures by the updated reference strategy. *International Journal of Space Structures, 14*(2), 131-145.

Boer, B. d., Jan Ruijg, G., Loonen, R., Trčka, M., Hensen, J., & Kornaat, W. (2011). *Climate adaptive building shells for the future - optimization with an inverse*. Paper presented at the ECEEE 2011 Summer study, Belambra Presqu'île de Giens, France.

Boyano, A., Hernandez, P., & Wolf, O. (2013). Energy demands and potential savings in European office buildings: Case studies based on EnergyPlus simulations. *Energy and Buildings, 65*, 19-28.

Brembilla, E., Chi, D. A., Hopfe, C. J., & Mardaljevic, J. (2019). Evaluation of climate-based daylighting techniques for complex fenestration and shading systems. *Energy and Buildings, 203*, 109454.

BS EN 12464-1:2011 - Light and lighting. Lighting of work places. Indoor work places. (2011).

Buchner, A. (2015). dyAna®-membran : Hygrothermische Simulation und Anlagentechnik Software Version 1.0. In A. E. GmbH (Ed.), *Brochure*. Fröndenberg, Germany.

Bueno, B., Wienold, J., Katsifaraki, A., & Kuhn, T. E. (2015). Fener: A Radiance-based modelling approach to assess the thermal and daylighting performance of complex fenestration systems in office spaces. *Energy and Buildings, 94*, 10-20.

Bülow-Hübe, H. (1995). Subjective reactions to daylight in rooms: Effect of using low-emittance coatings on windows. *International Journal of Lighting Research and Technology, 27*(1), 37-44.

Caccavelli, D., & Gugerli, H. (2002). TOBUS — a European diagnosis and decision-making tool for office building upgrading. *Energy and Buildings, 34*(2), 113-119.

Cao, X., Dai, X., & Liu, J. (2016). Building energy-consumption status worldwide and the state-of-the-art technologies for zero-energy buildings during the past decade. *Energy and Buildings, 128*, 198-213.

Capperucci, R., Loonen, R. C. G. M., Hensen, J. L. M., & Rosemann, A. L. P. (2019). Angle-dependent optical properties of advanced fenestration systems—Finding a right balance between model complexity and prediction error. *Building Simulation, 12*(1), 113-127. doi:10.1007/s12273-018-0466-4

Cardoso, D., Michaud, D., Sass, L. (2007). *Soft Façade: Steps into the Definition of a Responsive ETFE Façade for High-rise Buildings*. Paper presented at the 25th eCAADe Conference: Predicting the Future, Frankfurt am Main, Germany.

Cauwerts, C., & Bodart, M. (2013). *Validation of a questionnaire for assessing perceptions of lighting characteristics in daylit spaces* Paper presented at the

29th Conference, Sustainable Architecture for a Renewable Future, Munich, Germany.

Cellura, M., Guarino, F., Longo, S., & Tumminia, G. (2018). Climate change and the building sector: Modelling and energy implications to an office building in southern Europe. *Energy for Sustainable Development, 45*, 46-65.

CEN. (2011). BS EN 673:2011 Glass in building - Determination of thermal transmittance (U value) - Calculation method. In (Vol. BS EN 673).

Cetegen, D., Veitch, J., & Newsham, G. (2008). View size and office illuminance effects on employee satisfaction. *Proceedings of Balkan light, 2008*, 242-252.

Chamilothori, K., Wienold, J., & Andersen, M. (2018). Adequacy of immersive virtual reality for the perception of daylit spaces: Comparison of real and virtual environments. *LEUKOS*, 1-24.

Chan, Y.-C., & Tzempelikos, A. (2012). A hybrid ray-tracing and radiosity method for calculating radiation transport and illuminance distribution in spaces with venetian blinds. Solar Energy, 86(11), 3109-3124.

Chartered Institution of Building Services Engineers. (2015). Environmental design : CIBSE guide A. In (Vol. 8th edition). London, UK.

Chen, X., & Yang, H. (2017). A multi-stage optimization of passively designed high-rise residential buildings in multiple building operation scenarios. *Applied Energy, 206*, 541-557.

Chilton, J. (2013). Lightweight envelopes: ethylene tetra-fluoro-ethylene foil in architecture. *Proceedings of the Institution of Civil Engineers - Construction Materials, 166*(CM6), 343–357.

Chilton, J., & Lau, B. (2015). Lighting and the visual environment in architectural fabric structures. 203-219.

Chiu, S. K., & Lin, E. S. (2015). *Transformable Tensile Façade: Performance assessment on energy, solar and daylighting*. Paper presented at the Advanced Building Skins, Graz.

Chiu, S. K., & Lin, E. S.-H. (2015). *Tensile Membrane Façade: Performance Analysis of Energy, Daylighting and Material, Optical Properties*. Paper presented at the ENERGY FORUM.

CIE. (1995). 117-1995 Discomfort Glare in Interior Lighting. In C. T. C. T. 3-13 (Ed.), (pp. 39).

Connelly, K., Wu, Y., Chen, J., & Lei, Y. (2016). Design and development of a reflective membrane for a novel Building Integrated Concentrating Photovoltaic (BICPV) 'Smart Window' system. *Applied Energy, 182*, 331-339.

Connelly, K., Wu, Y., Ma, X., & Lei, Y. (2017). Transmittance and Reflectance Studies of Thermotropic Material for a Novel Building Integrated Concentrating Photovoltaic (BICPV) 'Smart Window' System. *Energies, 10*(11), 1889.

Cremers, J. (2011). *Energy saving design of membrane building envelopes*. Paper presented at the Structural Members: International Conference on Textile Composites and Inflatable Structures, Barcelona.

Cremers, J. (2011). *Innovative Membranarchitektur mit Folien und Geweben* (Vol. 2011).

Cremers, J., & Marx, H. (2016). Comparative Study of a New IR-absorbing Film to Improve Solar Shading and Thermal Comfort for ETFE Structures. *Procedia Engineering, 155*, 113-120.

Cremers, J., & Marx, H. (2017a). 3D-ETFE: Development and evaluation of a new printed and spatially transformed foil improving shading, light quality, thermal comfort and energy demand for membrane cushion structures. *Energy Procedia, 122*(Supplement C), 115-120.

Cremers, J., & Marx, H. (2017b). *Improved daylight comfort by a new 3D-foil that allows to trade off solar gains and light individually*. Paper presented at the Structural Membranes 2017, Munich, Germany.

Cremers, J., Mirbach, D., Marx, H., & Hajek, O. (2019). The ideal ETFE fenestration: The influence of material properties on the thermal performance.

Cremers, J., Palla, N., Buck, D., Beck, A., Biesinger, A., & Brodkorb, S. (2016). Analysis of a Translucent Insulated Triple-layer Membrane Roof for a Sport Centre in Germany. *Procedia Engineering, 155*, 38-46.

Cruz, N. C., Redondo, J. L., Berenguel, M., Álvarez, J. D., & Ortigosa, P. M. (2017). Review of software for optical analyzing and optimizing heliostat fields. Renewable and Sustainable Energy Reviews, 72, 1001-1018.

D'Agostino, D., Cuniberti, B., & Bertoldi, P. (2017). Energy consumption and efficiency technology measures in European non-residential buildings. *Energy and Buildings, 153*, 72-86.

D'Agostino, D., & Mazzarella, L. (2019). What is a Nearly zero energy building? Overview, implementation and comparison of definitions. *Journal of Building Engineering, 21*, 200-212.

D'Anza, G. http://www.ixray-ltd.com.

Davey, M., Bellew, P., Er, K., Kwek, A., & Lim, J. (2010). Gardens by the Bay: High performance through design optimization and integration. *Intelligent Buildings International, 2*(2), 140-157.

Deng, Q.-G., Cao, G.-Y., Liu, Z.-C., Wang, Z.-S., Yang, Y., He, X.-Y., & Yu, J.-J. (2016). Annual daylight glare evaluation: Impact of weather file selection. Lighting Res. Technol.(50), 446–455.

Deroisy, B., Deneyer, A., Lethé, G., & Flamant, G. (2013). *Bi-directional scattering distribution data of solar shading: characterization and performances*. Paper presented at the CIE Centenary Conference 2013, Paris, France.

Deroisy B., D. A., Lethé G., Flamant G. (2013). Performance analysis of common solar shading devices: experimental assessment and ray-tracing calculations using bi-directional scattering distribution data.

Devulder, T. (2004). *The thermal response of textile membrane constructions.* (PhD). University of Nottingham, Nottingham, United Kingdom.

Devulder, T., Chilton, J.C., Wilson, R. and Blum, R. (2007). *Advanced textile skins: predicting the thermal response of complex membrane constructions*. Paper presented at the Ephemeral Architecture: Time and Textiles, Milan.

Dimitriadou, E. A. (2013). *Computational modelling of the thermal behaviour of an ETFE cushion using IES*. Paper presented at the SB13 Portugal - Contribution of Sustainable Building to meet EU 20-20-20 Targets, Guimarães, Portugal.

Dimitriadou, E. A. (2015). *Experimental Assessment and Thermal Characterisation of Lightweight Co-Polymer Building Envelope Materials.* (PhD). University of Bath,

Dimitriadou, E. A., & Shea, A. (2015). Experimental Assessment and Thermal Characterization of Ethylene TetraFluoroEthylene ETFE Foil. *Athens Journal of Technology & Engineering, 2*(1), 25-38.

DIN. (1994). DIN EN 4543-1:1994-09 Office work place - Part 1: Space for the arrangement and use of office furniture; safety requirements, testing. In.

Do, C. T., & Chan, Y.-C. (2018). *Development of a New Framework for Daylighting Simulation with Dynamic Shading Devices*. Paper presented at the International High Performance Buildings Conference, Purdue University, Purdue, US.

Dunston, P. S., Arns, L. L., & McGlothlin, J. D. (2010). Virtual reality mock-ups for healthcare facility design and a model for technology hub collaboration. *Journal of Building Performance Simulation, 3*(3), 185-195.

Ebeling, S. (2016 / 1926). *Space as Membrane / Der Raum als Membran*. London / Dessau.

EIA. (2019). Annual Energy Outlook 2019 with projections to 2050. In. Washington: U.S. Energy Information Administration Office of Energy Analysis U.S. Department of Energy.

ElGhazi, Y., Hamza, N., & Dade-Robertson, M. (2018). *Modelling and Simulation of Integrated Responsive Solar-Shading with Double Skin Façades in Hot Arid Climates* Paper presented at the 4th Building Simulation and Optimization Conference, Cambridge, UK.

Eltaweel, A., & Su, Y. (2017). Controlling venetian blinds based on parametric design; viaimplementing Grasshopper's plugins: A case study of an officebuilding in Cairo. *Energy and Buildings, 139,* 31–43.

Energy, U. S. D. o. (2018). *EnergyPlus Engineering Reference - The Reference to EnergyPlus Calculations* (T. B. o. T. o. t. U. o. I. a. t. R. o. t. U. o. C. t. t. E. O. L. B. N. Laboratory Ed.): University of Illinois, Ernest Orlando Lawrence Berkeley National Laboratory, U.S. Department of Energy.

Fang, Y., & Cho, S. (2019). Design optimization of building geometry and fenestration for daylighting and energy performance. *Solar Energy*, 191, 7-18.

Favoino, F., Giovannini, L., & Loonen, R. C. G. M. (2017). *Smart glazing in intelligent buildings : what can we simulate?* Paper presented at the Glass Performance Days 2017, Tampere, Finland.

Favoino, F., Goia, F., Perino, M., & Serra, V. (2016). Experimental analysis of the energy performance of an active responsive and solar (ACTRESS) façade module. *Solar Energy, 133,* 226–248.

Fela, R., Utami, S., Mangkuto, R., & Suroso, D. (2019). The Effects of Orientation, Window Size, and Lighting Control to Climate-Based Daylight Performance and Lighting Energy Demand on Buildings in Tropical Area.

Flor, J.-F., Aburas, M., Abd-AlHamid, F., & Wu, Y., Virtual reality as a tool for evaluating user acceptance of view clarity through ETFE double-skin façades. Energy and Buildings, 2021, 231: 110554.

Flor, J.-F., Liu, D., Sun, Y., Beccarelli, P., Chilton, J., & Wu, Y. (2018). Optical aspects and energy performance of switchable ethylene-tetrafluoroethylene (ETFE) foil cushions. *Applied Energy*, *229*, 335-351.

Flor, J.-F., Sun, Y., Beccarelli, P., Wu, Y., & Chilton, J. (2019). *Switchable ETFE cushion: designing and building a model for experimental testing*. Paper presented at the IASS Annual Symposium 2019 – Structural Membranes 2019, Barcelona, Spain.

Flor, J.-F., Wu, Y., Beccarelli, P., & Chilton, J. (2017). *Dynamic environmental control mechanisms for pneumatic foil constructions*. Paper presented at the International Conference on Advances in Energy Systems and Environmental Engineering (ASEE17), Wroclaw, Poland.

Flor, J. F., Sun, Y., Beccarelli, P., Rowell, C., Chilton, J., & Wu, Y. (2019). Experimental study on the thermal performance of ethylene-tetrafluoroethylene (ETFE) foil cushions. *IOP Conference Series: Materials Science and Engineering, 556*, 012004.

Florian Antretter, W. H., Andreas Holm. (2008). *Thermal Transfer through Membrane Cushions Analyzed by Computational Fluid Dynamics*. Paper presented at the Nordic symposium on building physics, Copenhagen, Denmark.

Forster, B., & Mollaert, M. (2004). *European Design Guide for Tensile Surface Structures*: Tensinet.

Foucquier, A., Robert, S., Suard, F., Stéphan, L., & Jay, A. (2013). State of the art in building modelling and energy performances prediction: A review. *Renewable and Sustainable Energy Reviews, 23*, 272-288.

Gan, G. (2009). CFD modelling of transparent bubble cavity envelopes for energy efficient greenhouses. *Building and Environment*(44), 2486-2500.

Geisler-Moroder, D., Lee, S. E., & Ward, J. G. (2018). Validation of the Five-Phase Method for Simulating Complex Fenestration Systems with Radiance against Field Measurements. In *15th International Conference of the International Building Performance Simulation Association*.

Ghobad, L. (2018). *Daylighting and energy simulation workflow in performance based building simulation tools*. Paper presented at the 2018 Building Performance Analysis Conference and SimBuild co-organized by ASHRAE and IBPSA-USA, Chicago, IL.

Giovannini, L., Favoino, F., Lo Verso, V. R. M., Pellegrino, A., & Serra, V. (2018). A Simplified Approach for the Annual and Spatial Evaluation of the Comfort Classes of Daylight Glare Using Vertical Illuminances. *Buildings, 8*(12), 171.

Goia, F., Perino, M., Serra, V., & Zanghirella, F. (2010). Towards an Active, Responsive, and Solar Building Envelope. *Journal of Green Building, 5*(4), 121-136.

Gonzalez-Franco, M., & Lanier, J. (2017). Model of Illusions and Virtual Reality. *Frontiers in Psychology, 8*(1125).

Good, P., Cooper, T., Querci, M., Wiik, N., Ambrosetti, G., & Steinfeld, A. (2016). Spectral reflectance, transmittance, and angular scattering of materials for solar concentrators. *Solar Energy Materials & Solar Cells*(144), 509-522.

Grobe, L. O., Noback, A., Wittkopf, S., & Kazanasmaz, Z. T. ç. (2015). *Comparison of Measured and Computed BSDF of a Daylight Redirecting Component*. Paper presented at the CISBAT 2015, Lausanne, Switzerland.

Grunwald, G. (2007). *Mechanisch vorgespannte, doppellagige Membranmodule in ihrer Anwendung als zweite Gebäudehülle.* (PhD). Technische Universität Berlin, Berlin, Germany.

Gyeong Yun, K. C. Y., Kang Soo Kim. (2014). The influence of shading control strategies on the visual comfort and energy demand of office buildings. *Energy andBuildings, 84*, 70–85.

Gómez-González, A., Neila, J., & Monjo, J. (2011). Pneumatic Skins in Architecture. Sustainable Trends in Low Positive Pressure Inflatable Systems. *Procedia Engineering, 21*, 125-132. doi:10.1016/j.proeng.2011.11.1995

Haase, W., Klaus, T., Knubbe, E., Mielert, F., Neuhäuser, S., Schmid, F., & Sobek, W. (2011). *Adaptive Multi-layer Textile Building Envelopes*. Retrieved from Stuttgart:

Haase, W., Klaus, T., Knubben, E., Mielert, F., Neuhäuser, S., Schmid, F., & Sobek, W. (2011). *Adaptive mehrlagige textile Gebäuedehüllen*. Retrieved from Universität Stuttgart:

Haase, W., Klaus, T., Schmid, F., Sobek, W., Sedlbauer, K., Schmidt, T., & Synold, M. (2011). Adaptive textile und folienbasierte Gebäudehüllen. *Bautechnik, 88*(2), 69-75.

Hanke, T. (2013). Einsatzverhalten von ETFE-Membrankissenkonstruktionen.

Hanke, T., Michael, H., & Köhler, M. (2016). *ETFE-Solarthermie: schaltbare Verschattungen für Membrankissen aus Ethylen-Tetrafluorethylen-Hochleistungs-Copolymerfolie mit integrierter Solarthermienutzung*. Retrieved from Germany:

Harder, N., Schlegl, F., Albrecht, S., Park, S., & Leistner, P. (2018). Bauphysikalische und ökologische Potenziale von adaptiven Leichtbaukonstruktionen. *Bauphysik, 40*(5), 307-318.

Harder, N., Schlegl, F., Flemming, D., Di Bari, R., Albrecht, S., Leistner, P., & Park, S. (2019). Bauphysikalische und ökologische Bewertung adaptiver Fassadenkonstruktionen auf Raumebene. *Bauphysik, 41*(6), 302-313.

Hartig, T., Korpela, K., Evans, G. W., & Gärling, T. (1997). A measure of restorative quality in environments. *Scandinavian Housing and Planning Research, 14*(4), 175-194.

Harvie, G. (1996). *An Investigation into the thermal behaviour of spaces enclosed by fabric membranes.* (PhD). University of Wales, Cardiff, United Kingdom.

Harvie, G. N. (2015). 8 - Thermal behaviour in architectural fabric structures A2 - Llorens, Josep Ignasi de. In *Fabric Structures in Architecture* (pp. 221-240): Woodhead Publishing.

Hausladen, G. (2007). *Climate skin_concepts for building skins that can do more with less energy, Flight test facility HolzkirchenHausladen*. Basel: Birkhäuser.

Hensel, M. (2013). *Performance-Oriented Architecture*. West Sussex, UK: John Whiley & Sons Ltd.

Heydarian, A., Carneiro, J. P., Gerber, D., & Becerik-Gerber, B. (2015). Immersive virtual environments, understanding the impact of design features and occupant choice upon lighting for building performance. *Building and Environment, 89*, 217-228.

Heydarian, A., Carneiro, J. P., Gerber, D., Becerik-Gerber, B., Hayes, T., & Wood, W. (2014). *Immersive virtual environments: Experiments on impacting design and human building interaction*. Paper presented at the 9th International Conference

on Computer Aided Architectural Design Research in Asia CAADRIA Hong Kong.

Heydarian, A., Carneiro, J. P., Gerber, D., Becerik-Gerber, B., Hayes, T., & Wood, W. (2015). Immersive virtual environments versus physical built environments: A benchmarking study for building design and user-built environment explorations. *Automation in Construction, 54,* 116-126.

Hinz, K., Alvarenga, J., Kim, P., Park, D., Aizenberg, J., & Bechthold, M. (2018). Pneumatically adaptive light modulation system (PALMS) for buildings. *Materials & Design, 152*, 156-167.

Houtman, R. (2015). Materials used for architectural fabric structures. In J. I. de Llorens (Ed.), *Fabric Structures in Architecture* (pp. 101-121): Woodhead Publishing.

Höpfner, J. (2002). Integriertes Lichtlenkungs- und Verschattungssystem in 2-3 - lagigen Pneukonstruktionen in Dächern und geneigten Fassaden. Gebrauchsmusterschrift DE 201 19 761 U1, Deutsches Patent- und Markenamt, Bundesrepublik Deutschland, retrieved from: Google Patents (accessed 2018).

Hu, J., Chen, W., Qu, Y., & Yang, D. (2020). Safety and serviceability of membrane buildings: A critical review on architectural, material and structural performance. *Engineering Structures, 210*, 110292.

Hu, J., Chen, W., Zhao, B., & Yang, D. (2017). Buildings with ETFE foils: A review on material properties, architectural performance and structural behavior. *Construction and Building Materials, 131*, 411-422.

Hu, J. H., Chen, W. J., Qiu, Z. Y., Zhao, B., Zhou, J. Y., & Qu, Y. G. (2015). Thermal performances of ETFE cushion roof integrated amorphous silicon photovoltaic. *Energy Conversion and Management, 106*, 1201-1211.

Hu, J. H., Chen, W. J., Yang, D. Q., Zhao, B., Song, H., & Ge, B. B. (2016). Energy performance of ETFE cushion roof integrated photovoltaic/thermal system on hot and cold days. *Applied Energy, 173*, 40-51.

Huntington, C. G. (2013). *Tensile Fabric Structures - Design, Analysis, and Construction*. US: American Society of Civil Engineers.

IEA. (2019). *World Energy Outlook 2019*. Retrieved from Paris: https://www.iea.org/reports/world-energy-outlook-2019

International Energy Agency. (2013). *Transition to sustainable buildings - Strategies and oportunities to 2050 - Executive Summary*. Retrieved from

Ipcc, Masson-Delmotte, V., Zhai, P., Pörtner, H.-O., Roberts, D., Skea, J., . . . Waterfield, T. (2018). *Global warming of 1.5°C. An IPCC Special Report on the impacts of global warming of 1.5°C above pre-industrial levels and related global greenhouse gas emission pathways, in the context of strengthening the global response to the threat of climate change, sustainable development, and efforts to eradicate poverty*.

ISO. (2003). ISO 9050:2003 Glass in building — Determination of light transmittance, solar direct transmittance, total solar energy transmittance, ultraviolet transmittance and related glazing factors.

ISO. (2010). BS EN ISO 12567-1:2010 Thermal performance of windows and doors - Determination of thermal transmittance by the hot-box method. In *Part 1: Complete windows and doors*.

ISO. (2014). BS ISO 9869-1-2014-Thermal insulation - Building Elements - In-situ meassurements of thermal resistance and thermal transmittance - Part 1- Heat flow meter method. In.

Jelle, B. P. (2013). Solar radiation glazing factors for window panes, glass structures and electrochromic windows in buildings—Measurement and calculation. *Solar Energy Materials and Solar Cells, 116*, 291-323.

Jeska, S. (2008). *Transparent Plastics - Design and Technology*. Basel - Boston - Berlin Basel, Switzerland printed in Germany: Birkhäuser Verlag AG.

Jones, A. C. (2000). Civil and structural design of the Eden Project. In M. Barnes & M. Dickson (Eds.), *Widespan Roof Structures* (pp. 89-99). Bath, United Kingdom.

Juaristi, M., & Monge-Barrio, A. (2016). *Adaptive façades in temperate climates. An in-use assessment of an office building*. Paper presented at the 11th Conference on Advanced Building Skins, Bern, Switzerland.

Karwath, M. (2011). *Membrane structures with improved thermal properties*. Paper presented at the Structural Membranes - International Conference on textile composites and inflatable structures.

Kaufmann, A., Sedlbauer, K., & Sieder, M. (2013). Wärmetechnische Besonderheiten von Membrankissenkonstruktionen. *Bautechnik 90*(Heft 7), 7.

Kim, D.-W., & Park, C.-S. (2011). Difficulties and limitations in performance simulation of a double skin façade with EnergyPlus. *Energy and Buildings, 43*(12), 3635-3645.

Kim, D. Y. (2019). A Design Methodology Using Prototyping Based on the Digital-Physical Models in the Architectural Design Process. *Sustainability, 11*(16), 4416.

Klems, J. H. (1994). A new method for predicting the solar heat gain of complex fenestration systems. *ASHRAE Transactions, 100*, 16.

Knippers, J., Cremers, J., Lienhard, J., & Gabler, M. (2011). *Construction Manual for Polymers + Membranes*. Basel: Birkhauser Verlag AG.

Kohler, C. (2012). *Simulation of complex glazing products; from optical data measurements to model based predictive controls*. Paper presented at the BEST 3 Conference.

Konstantoglou, M., & Tsangrassoulis, A. (2016). Dynamic operation of daylighting and shading systems: A literature review. *Renewable and Sustainable Energy Reviews, 60*, 268-283.

Konstantzos, I., Chan, Y.-C., Seibold, J. C., Tzempelikos, A., Proctor, R. W., & Protzman, J. B. (2015). View clarity index: A new metric to evaluate clarity of view through window shades. *Building and Environment, 90*, 206-214.

Konstantzos, I., & Tzempelikos, A. (2017). A Holistic Approach for Improving Visual Environment in Private Offices. *Procedia Environmental Sciences, 38*, 372-380.

Konstantzos, I., Tzempelikos, A., & Chan, Y.-C. (2015). Experimental and simulation analysis of daylight glare probability in offices with dynamic window shades. *Building and Environment, 87*, 244-254.

Kottek, M., Grieser, J., Beck, C., Rudolf, B., & Rubel, F. (2006). World Map of the Köppen-Geiger climate classification updated. *Meteorologische Zeitschrift, 15*(3), 259-263.

Kuhn, T. E. (2017). State of the art of advanced solar control devices for buildings. *Solar Energy, In Press*.

Kunwar, N., & Bhandari, M. (2020). A Comprehensive Analysis of Energy and Daylighting Impact of Window Shading Systems and Control Strategies on Commercial Buildings in the United States. Energies, 13(9).

Kämpf, J. H., & Scartezzini, J.-L. (2011). *Ray-tracing simulation of complex fenestration systems based on digitally processed BTDF data*. Paper presented at the CISBAT Conference, Lausanne, Switzerland.

Köppen, W. (1900). Versuch einer Klassifikation der Klimate, vorzugsweise nach ihren Beziehungen zur Pflanzenwelt. *Geographische Zeitschrift, 6*(11), 593-611.

Köster, H. (2003). *Entwicklung von retroflektierenden Oberflächenkonturen fuer Licht lenkende Fassadenbauteile und Entwicklung zugeordneter Herstellungsverfahren_*. Retrieved from Frankfurt, Germany:

Lamnatou, C., Moreno, A., Chemisana, D., Reitsma, F., & Clariá, F. (2018). Ethylene tetrafluoroethylene (ETFE) material: Critical issues and applications with emphasis on buildings. *Renewable and Sustainable Energy Reviews, 82*, 2186-2201.

Lau, B., Masih, D. A. A., Ademakinwa, A. A., Low, S. W., & Chilton, J. (2016). Understanding Light in Lightweight Fabric (ETFE Foil) Structures through Field Studies. *Procedia Engineering, 155*, 479-485.

LeCuyer, A. (2008). *ETFE. Technology and Design*. Basel, Switzerland: Birkhauser Verlag AG.

Leicht, R. M., Kumar, S., Abdelkarim, M., & Messner, J. I. (2010). *Gaining end user involvement through virtual reality mock-ups: a medical facility case study*. Paper presented at the CIB W78 2010: 27th International Conference, Cairo, Egypt.

Li, P., & Yang, Q. (2013). Form Finding and Loading Analysis of ETFE Cushions Using Interaction Numerical Model. *Applied Mechanics and Materials*(438-439), 1812-1815.

Liang, R., Kent, M., Wilson, R., & Wu, Y. (2019). Development of experimental methods for quantifying the human response to chromatic glazing. *Building and Environment, 147*, 199-210.

Lin, Y.-H., Tsai, K.-T., Lin, M.-D., & Yang, M.-D. (2016). Design optimization of office building envelope configurations for energy conservation. *Applied Energy, 171*, 336-346.

Lindbloom, B. J. http://www.brucelindbloom.com.

Lippke, R. (2009). *Folien als transparente Elemente in der Fassade - mechanische und bauphysikalische Eigenschaften.* (PhD). Technische Universität Berlin, Berlin, Germany.

Liu, H. B., Li, B., Chen, Z. H., Zhou, T., & Zhang, Q. (2016). Solar radiation properties of common membrane roofs used in building structures. *Materials & Design, 105*, 268-277.

Liu, X., Gao, H., Sun, Y., Wu, Y., Martin, B., Chilton, J., . . . Lau, B. (2016). Thermal and Optical Analysis of a Passive Heat Recovery and Storage System for Greenhouse Skin. *Procedia Engineering, 155*, 472-478.

Llorens, J. (2015). *Fabric Structures in Architecture*: Woodhead Publishing.

Lombardi, S., & Canobbio, R. (2016). Textile Structures for Climate Control. *Procedia Engineering, 155*, 163-172.

Loonen, R. C. G. M., Trčka, M., Cóstola, D., & Hensen, J. L. M. (2013). Climate adaptive building shells: State-of-the-art and future challenges. *Renewable and Sustainable Energy Reviews, 25*(Supplement C), 483-493.

Mainini, A. G., Poli, T., Paolini, R., Zinzi, M., & Vercesi, L. (2014). Transparent Multi-layer ETFE Panels for Building Envelope: Thermal Transmittance Evaluation and Assessment of Optical and Solar Performance Decay due to Soiling. *Energy Procedia, 48*, 1302-1310.

Mainini, A. G., Speroni, A., Zani, A., & Poli, T. (2016). The Effect of Water Spray Systems on Thermal and Solar Performance of an ETFE Panel for Building Envelope. *Procedia Engineering, 155*, 352-360.

Mainini, A. G., Zani, A., De Michele, G., Speroni, A., Poli, T., Zinzi, M., & Gasparella, A. (2019). Daylighting performance of three-dimensional textiles. *Energy and Buildings*.

Majumdar, T., Fischer, M., A., Schwegler, B., & R. (2006). *Conceptual design review with a virtual reality mock-up model*. Paper presented at the Joint International Conference on Computing and Decision Making in Civil and Building Engineering, Montréal, Canada.

Mardiana, A., & Riffat, S. B. (2015). Building Energy Consumption and Carbon dioxide Emissions: Threat to Climate Change. *Journal of Earth Science & Climatic Change, s3*.

Marino, C., Nucara, A., Panzera, M. F., & Pietrafesa, M. (2019). Towards the nearly zero and the plus energy building: Primary energy balances and economic evaluations. *Thermal Science and Engineering Progress, 13*, 100400.

Marino, C., Nucara, A., & Pietrafesa, M. (2017). Does window-to-wall ratio have a significant effect on the energy consumption of buildings? A parametric analysis in Italian climate conditions. *Journal of Building Engineering, 13*, 169-183.

Martin, B. A. J., Lau, B., Beccarelli, P., Chilton, J., & Wu, Y. (2015). *Modular Transparent ETFE Panels for Building Envelopes Thermal Transmittance Assessment and Evaluation*. Paper presented at the Proceedings of the International Association for Shell and Spatial Structures (IASS) Symposium 2015, Amsterdam, Future Visions, Amsterdam, Netherlands.

Masoudinejad, S., & Hartig, T. (2018). Window View to the Sky as a Restorative Resource for Residents in Densely Populated Cities. *Environment and Behavior*, 0013916518807274.

Masih, D., & Lau, B. (2015). *The Investigation of the Luminous Environment in ETFE Structures.* 14th International Conference on Sustainable Energy Technologies – SET 2015 25th - 27th of August 2015, Nottingham, UK

Maxa, J. F. J., Reisingera, G., Hofmann, T., Hinkend, J., Tantaud, H.-J., Ulbrich, A., . . . Schurr, U. (2012). Glass–film-combination: Opto-physical properties and energy saving potential of a novel greenhouse glazing system. *Energy and Buildings, 50*, 298–307.

Maywald, C., & Riesser, F. (2016). Sustainability – The Art of Modern Architecture. *Procedia Engineering, 155*, 238-248.

Maywald, C. (2019). Coating of ETFE solar shading for architectural applications. Paper presented at the 6th International TensiNet Symposium " Softening the Habitats : Sustainable Innovations in Minimal Mass Structures and Lightweight Architectures", Politecnico di Milano, Milan, Italy.

McNeil, A. (2013a). *BSDFViewer: A utility for interactive exploration of BSDF datasets.*

McNeil, A. (2013b). *The Five-Phase Method for Simulating Complex Fenestration with Radiance*. Retrieved from https://facades.lbl.gov/publications/

McNeil, A. (2013c). *The three-phase method for simulating complex fenestration with Radiance*. Retrieved from https://facades.lbl.gov/publications/

McNeil, A., Jonsson, C. J., Appelfeld, D., Ward, G., & Lee, E. S. (2013). A validation of a ray-tracing tool used to generate bi-directional scattering distribution functions for complex fenestration systems. *Solar Energy, 98*, 404-414.

McNeil, A., & Lee, E. S. (2013). A validation of the Radiance three-phase simulation method for modelling annual daylight performance of optically complex fenestration systems. *Journal of Building Performance Simulation, 6*(1), 24-37.

Menéndez, A., Martínez Díez, A. L., Santos, A., Ruiz, B., Moritz, K., Klein, I., . . . Gomez, D. (2017). *A multifunctional ETFE module for sustainable façade lighting: Design, manufacturing and monitoring* (Vol. 161).

Mikkonen, R., Lahokallio, S., Frisk, L., & Mäntysalo, M. (2018). Processing of printed silver patterns on an ETFE substrate. In (pp. 1-7): IEEE.

Molina, G., Bustamante, W., Rao, J., Fazio, P., & Vera, S. (2015). Evaluation of radiance's genBSDF capability to assess solar bidirectional properties of complex fenestration systems. *Journal of Building Performance Simulation, 8*(4), 216-225.

Monticelli, C. (2015). Membrane claddings in architecture. In J. I. d. Llorens (Ed.), *Fabric structures in Architecture* (pp. 449 - 480): Woodhead Publishing.

Monticelli C., L. S., Würfl C. , Mohamed Ibrahim H. (2013). Ellipsoidal shape and daylighting control for the ETFE pneumatic envelope of a winter garden.

Moreno, Á., Chemisana, D., Vaillon, R., Riverola, A., & Solans, A. (2019). Energy and Luminous Performance Investigation of an OPV/ETFE Glazing Element for Building Integration. *Energies, 12*(10), 1870.

Moritz, K. (2007). *ETFE-Folie als Tragelement.* (PhD). Technische Universität München, Munich, Germany.

Moritz, K., & Barthel, R. (2003). Bauen mit ETFE-Folien. In *DETAIL Praxis - Transluzente Materialien* (pp. 70– 78). Institut für Internationale Architekturdokumentation, München.

Moritz, K., Brengelmann, T., & Schiemann, L. (2005). Tankstellendächer aus Stahl und Folie / Steel service station roofs with plastic membranes. *DETAIL Zeitschrift für Architektur + Baudetail, 7/8*, 798-804.

Morris, B. (2000). *Foil Climatic Envelope*. Paper presented at the International Symposium on Widespan Enclosures, University of Bath, UK.

Nabil, A., & Mardaljevic, J. (2006). Useful daylight illuminances: A replacement for daylight factors. *Energy and Buildings, 38*(7), 905-913.

Naz, A., Kopper, R., McMahan, R. P., & Nadin, M. (2017, 18-22 March 2017). *Emotional qualities of VR space.* Paper presented at the 2017 IEEE Virtual Reality (VR).

Neufert, E. (2012). *Architects' data / Ernst and Peter Neufert* (4th ed. / updated by Johannes Kister ... [et al.] ; translated by David Sturge. ed.). Chichester: Chichester : Wiley-Blackwell.

Otto, F. (1954). *Das hängende Dach.* (PhD). TU Berlin, Berlin, Germany.

Otto, F., Trostel, R., & Schleyer, F.-K. (1973). *Tensile Structures - Design, Structure, and Calculation of Buildings of Cables, Nets, and Membranes* (D. Ben-Yaakov & T. Pelz, Trans. F. Otto Ed. MIT Press paperback edition, combining Volumes 1 and 2 ed. Vol. 1 and 2). Cambride, Massachustts, and London, England: The MIT Press.

Pacheco, R., Ordó˜nez, J., & Martínez, G. (2012). Energy efficient design of building: A review. *Renewable and Sustainable Energy Reviews*(16), 3559– 3573.

Paech, C. (2016). Structural Membranes Used in Modern Building Façades. *Procedia Engineering, 155*, 61-70.

Pellegrino, A., Cammarano, S., Lo Verso, V. R. M., & Corrado, V. (2017). Impact of daylighting on total energy use in offices of varying architectural features in Italy: Results from a parametric study. Building and Environment, 113, 151-162.

Peng, J., Curcija, D. C., Lu, L., Selkowitz, S. E., Yang, H., & Zhang, W. (2016). Numerical investigation of the energy saving potential of a semi-transparent photovoltaic double-skin façade in a cool-summer Mediterranean climate. *Applied Energy, 165*, 345-356.

Peng, J., Lu, L., & Yang, H. (2013). An experimental study of the thermal performance of a novel photovoltaic double-skin façade in Hong Kong. *Solar Energy, 97*, 293-304.

Peng, J., Lu, L., Yang, H., & Han, J. (2013). Investigation on the annual thermal performance of a photovoltaic wall mounted on a multi-layer façade. *Applied Energy, 112*, 646-656.

Perino, M., & Serra, V. (2015). Switching from static to adaptable and dynamic building envelopes: A paradigm shift for the energy efficiency in buildings. *Journal of Façade Design and Engineering, 3*, 143–163.

Pohl, G. (2010). *Textiles, Polymers and Composites for Buildings*: Woodhead Publishing.

Poirazis, H. (2004). *Double Skin Façades for Office Buildings - Literature Review Report*. Retrieved from

Poirazis, H. (2009). Energy modelling of ETFE membranes in building applications.

Poletto, M., & Pasquero, C. (2019). ecoLogicStudio.

Portman, M. E., Natapov, A., & Fisher-Gewirtzman, D. (2015). To go where no man has gone before: Virtual reality in architecture, landscape architecture and environmental planning. *Computers, Environment and Urban Systems, 54*, 376-384.

Pérez-Lombard, L., Ortiz, J., & Pout, C. (2008). A review on buildings energy consumption information. *Energy and Buildings*(40), 394–398.

Qingsong, M., & Fukuda, H. (2015). *Parametric office building for daylight and energy analysis in the early design stages*. Paper presented at the Urban Planning and Architecture Design for Sustainable Development, UPADSD 2015, Lecce, Italy.

Rayner, H. (2020). http://www.solarbubblebuild.com.

Reinhart, C. F., & Andersen, M. (2006). Development and validation of a Radiance model for a translucent panel. *Energy and Buildings, 38*(7), 890-904.

Reinhart, C. F., & Herkel, S. (2000). The simulation of annual daylight illuminance distributions — a state-of-the-art comparison of six RADIANCE-based methods. *Energy and Buildings, 32*(2), 167-187.

Risen, C. (2017). Award: Dynamic ETFE Façade. *ARCHITECT The Journal of The American Institute of Architects*.

Robbin, T. (1996). *Engineering a new architecture*. Printed in United States of America Quebecor-Eusey Press, Leominster, Massachusetts: Yale University Press New Haven and London.

Robinson-Gayle. (2003). *Environmental impact and performance of transparent building envelope materials and systems.* (PhD). Brunel University,

Robinson-Gayle, S., Kolokotroni, M., Cripps, A., & Tanno, S. (2001). ETFE foil cushions in roofs and atria.

Roudsari Sadeghipour, M. (2020 (accessed)). Honeybee Primer. In (web ed., pp. 511). https://www.scribd.com/document/303440360/Honeybee-Primer: GitBook.

Roudsari Sadeghipour, M., Pak, M., Smith, A., & Architecture, G. G. (2013). *Ladybug: a parametric environmental plugin for grasshopper to help designers create an*

environmentally-conscious design. Paper presented at the 13th Conference of International Building Performance Simulation Association, Chambery, France.

Roudsari Sadeghipour, M., & Waelkens, A. (2015). A New Approach to Modeling Frit Patterns for Daylight.

Salz, C., & Schepers, H. (2006). *Arup's ETFE Material note*. Retrieved from

Santos, L., Leitão, A., & Caldas, L. (2018). A comparison of two light-redirecting fenestration systems using a modified modeling technique for Radiance 3-phase method simulations. *Solar Energy, 161*, 47-63.

Sargent, J. A., Niemasz, J., & Reinhart, C. F. (2011). *Shaderade: combining rhinoceros and energyplus for the Design of static exterior shading devices*. Paper presented at the Conference of International Building Performance Simulation Association, Sydney.

Schiemann, L. (2009). *Tragverhalten von ETFE-Folien unter biaxialer Beanspruchung_*. (PhD). TECHNISCHE UNIVERSITÄT MÜNCHEN, Munich.

Schmid, G. (2009). Neues Bauen mit ETFE-Folien. *AB Archiv des Badewesens(04)*.

Scorpio, M., Ciampi, G., Spanodimitriou, Y., Laffi, R., Rosato, A., & Sibilio, S. (2020). *Double-Skin Façades with Semi-Transparent Modules for Building Retrofit Actions: Energy and Visual Performances*.

Shahin, H. S. M. (2019). Adaptive building envelopes of multistory buildings as an example of high performance building skins. *Alexandria Engineering Journal, 58*(1), 345-352.

Shameri, M. A., Alghoul, M. A., Sopian, K., Zain, M. F. M., & Elayeb, O. (2011). Perspectives of double skin façade systems in buildings and energy saving. *Renewable and Sustainable Energy Reviews, 15*(3), 1468-1475.

Shen, H., & Tzempelikos, A. (2012). Daylighting and energy analysis of private offices with automated interior roller shades. Solar Energy, 86(2), 681-704.

Singh, R., Lazarus, I. J., & Kishore, V. V. N. (2016). Uncertainty and sensitivity analyses of energy and visual performances of office building with external venetian blind shading in hot-dry climate. *Applied Energy, 184*, 155-170.

Sinnesbichler, H. (2015). Membrankissen mit integriertem Sonnenschutz. Fraunhofer Institut für Bauphysik IBP, Valley, Germany.

Spencer, G. H., & Murty, M. V. R. K. (1962). General Ray-Tracing Procedure. *Journal Of The Optical Society Of America, 52*(6), 672-678.

Spyropoulos, G. N., & Balaras, C. A. (2011). Energy consumption and the potential of energy savings in Hellenic office buildings used as bank branches—A case study. *Energy and Buildings, 43*(4), 770-778.

Srisuwan, T. (2017). Article Review: Fabric Façade: An Intelligent Skin *BUILT, 9*.

Standardization, E. C. f. (2011). BS EN 410 Glass in building - Determination of luminous and solar characteristics of glazing. In. Brussels, Belgium: CEN-CENELEC Management Centre BSI Standards Publication.

Stegmaier, T., Sarsour, J., Gresser, G. T., Wagner, R., Kröplin, B., Kungl, P., . . . Bögner-Balz, H. (2018). Energy-Efficient Textile Building with Transparent Thermal Insulation for the Solar Thermal Use According to the Model of the Polar Bear's Fur. *Innovative Energy & Research, 7*(3), 1-4.

Ströbel, D., Singer, P., & Holl, J. (2013). *Holistic Calculation of (Multi)-Chambered ETFE-Cushions'*. Paper presented at the Tensinet Symposium [RE]THINKING lightweight structures, Istanbul, Turkey.

Subramaniam, S. (2018). *Parametric modeling strategies for efficient annual analysis of daylight in buildings.* (Doctor of Philosophy). The Pennsylvania State University, US.

Subramaniam, S. et al., (2020). A Tool for Assessing Visual Comfort Through an Immersive Environment. PLEA 2020, A Coruña Planning Post Carbon Cities.

Sun, Y., Liu, D., Flor, J.-F., Shank, K., Baig, H., Wilson, R., . . . Wu, Y. (2020). Analysis of the daylight performance of window integrated photovoltaics systems. *Renewable Energy*, 145, 153-163.

Sun, Y., et al., (2018). A Review of Thermal and Optical Characterisation of Complex Window Systems and Their Building Performance Prediction. *Applied Energy, 222C*, 729-747.

Sun, Y., Liang, R., Wu, Y., Wilson, R., & Rutherford, P. (2017). Development of a comprehensive method to analyse glazing systems with Parallel Slat Transparent Insulation material (PS-TIM). *Applied Energy, 205*, 951-963.

Sun, Y., Liu, D., Flor, J.-F., Shank, K., Baig, H., Wilson, R., Wu, Y. (2020). Analysis of the daylight performance of window integrated photovoltaics systems. *Renewable Energy, 145*, 153-163.

Sun, Y., Wu, Y., & Wilson, R. (2017). Analysis of the daylight performance of a glazing system with ParallelSlat Transparent Insulation Material (PS-TIM). *Energy and Buildings*(139), 616–633.

Sun, Y. Y., Wu, Y. P., Wilson, R., & Lu, S. X. (2016). Experimental measurement and numerical simulation of the thermal performance of a double glazing system with an interstitial Venetian blind. *Building and Environment, 103*, 111-122. doi:10.1016/j.buildenv.2016.03.028

Sun, Y. Y., Wu, Y. P., Wilson, R., & Sun, S. Y. (2016). Thermal evaluation of a double glazing façade system with integrated Parallel Slat Transparent Insulation Material (PS-TIM). *Building and Environment, 105*, 69-81.

Suo, H., Angelotti, A., & Zanelli, A. (2015). Thermal-physical behavior and energy performance of air-supported membranes for sports halls: A comparison among traditional and advanced building envelopes. *Energy and Buildings, 109*, 35-46.

Tang, H., Zhang, T., Liu, X., Liu, X., Xiang, X., & Jiang, Y. (2018). On-site measured performance of a mechanically ventilated double ETFE cushion structure in an aquatics center. *Solar Energy, 162*, 289-299.

Tanno, S. (1997). *ETFE foil cushions as an alternative to glass for atriums and rooflights*. Paper presented at the International conference on Building, Envelope Systems and Technology, Bath, United Kingdom.

Tantau, H.-J., Hinken, J., von Elsner, B., Max, J., Ulbrich, A., Schurr, U., . . . Reisinger, G. (2012). Solar transmittance of greenhouse covering materials. *Acta Horticulturae, 956*, 441-448.

Toutou, A., Fikry, M., & Mohamed, W. (2018). The parametric based optimization framework daylighting and energy performance in residential buildings in hot arid zone. *Alexandria Engineering Journal, 57*(4), 3595-3608.

Tregenza, P. R. (2016). Uncertainty in daylight calculations. *Lighting Research & Technology, 49*(7), 829-844.

Turan, I., Chegut, A., Fink, D., & Reinhart, C. (2020). The value of daylight in office spaces. *Building and Environment, 168*, 106503.

U.S. Energy Information Administration. (2017). *International Energy Outlook - Executive Summary*. Retrieved from

UN Environment and International Energy Agency. (2017). *Towards a zero-emission, efficient, and resilient buildings and construction sector - Global Status Report*. Retrieved from

UnitedNations. (2016). Paris Agreement. In. Paris, France.

US-Department-of-Energy. (2018). *EnergyPlus Engineering Reference - The Reference to EnergyPlus Calculations* (T. B. o. T. o. t. U. o. I. a. t. R. o. t. U. o. C. t. t. E. O. L. B. N. Laboratory Ed.): University of Illinois, Ernest Orlando Lawrence Berkeley National Laboratory, U.S. Department of Energy.

Vlasceanu, E., Lienhard, J., & Knippers, J. (2013). *Responsive Textiles*. Paper presented at the VI International Conference on Textile Composites and Inflatable Structures STRUCTURAL MEMBRANES 2013, Barcelona, Spain.

Wang, H., Chen, W., & Shi, J. (2018). Low carbon transition of global building sector under 2- and 1.5-degree targets. *Applied Energy, 222*, 148-157.

Wang, H., Flor, J.-F., Sun, Y., & Wu, Y. (2019). Numerical investigations on the thermal performance of adaptive ETFE foil cushions. *Energy Procedia, 158*, 3191-3195.

Wang, J., Beltran, L., & Kim, J. (2012). *From Static to Kinetic: A Review of Acclimated Kinetic Building Envelopes*. Paper presented at the Solar Conference, World renewable energy forum, Boulder, Colorado, USA.

Wang, M., Peng, J., Li, N., Lu, L., Ma, T., & Yang, H. (2016). Assessment of energy performance of semi-transparent PV insulating glass units using a validated simulation model. *Energy, 112*, 538-548.

Wang, M., Peng, J., Li, N., Yang, H., Wang, C., Li, X., & Lu, T. (2017). Comparison of energy performance between PV double skin façades and PV insulating glass units. *Applied Energy, 194*, 148-160.

Wang, T., Ward, G., & Lee, E. S. (2018). Efficient modeling of optically-complex, non-coplanar exterior shading: Validation of matrix algebraic methods. *Energy and Buildings, 174*, 464-483.

Ward, G. (2011). Computing and applying variable-resolution data for bidirectional scattering distribution functions. DOE/LBNL, Berkeley, USA.

Ward, G., Mistrick, R., Lee, E. S., McNeil, A., & Jonsson, J. (2011). Simulating the Daylight Performance of Complex Fenestration Systems Using Bidirectional Scattering Distribution Functions within Radiance. *LEUKOS, 7*(4), 241-261.

Ward, G. L., & Shakespeare, R. (1998). *Rendering with radiance: the art and science of lighting visualization*: Morgan Kaufmann Publishers Inc.

Ward, J., Chilton, J., Heslop, A., & Rowell, L. (2010). ETFE foil in building envelopes.

Ward, J., Chilton, J. C., Heslop, A., & Rowell, l. (2010). *Internal environment in ETFE foil covered building enclosures*. Paper presented at the TensiNet Symposium 2010 - Tensile Architecture: Connecting Past and Future, University of Architecture, Civil Engineering and Geodesy (UACEG), Sofia, Bulgaria.

Whalley, A., & Nicholas Grimshaw & Partners. (2000). The Eden Project glass houses world environments. In M. Barnes & M. Dickson (Eds.), *Widespan Roof Structures* (pp. 75 - 84). London, UK: Thomas Telford books.

Wienold, J. (2007). *Dynamic simulation of blind control strategies for visual comfort and energy balance analysis*. Paper presented at the Building Simulation.

Wienold, J. (2009). *Dynamic daylight glare evaluation*. Paper presented at the Building Simulation 2009, the 11th International IBOSA Conference, Glasgow, UK.

Wienold, J., & Christoffersen, J. (2006). Evaluation methods and development of a new glare prediction model for daylight environments with the use of CCD cameras. *Energy and Buildings, 38*(7), 743-757.

Wienold, J., Kuhn, T., Christoffersen, J., & Andersen, M. (2017). *Annual glare evaluation for fabrics*.

Wieser, C. (2008). Luftkissenarchitektur : Geschäftshaus "La Miroiterie" in Lausanne von Brauen + Wälchli. *Werk, Bauen + Wohnen*, *95*(4), 30-35.

Wu, Y., Connelly, K., Liu, Y., Gu, X., Gao, Y., & Chen, G. Z. (2016). Smart solar concentrators for building integrated photovoltaic façades. *Solar Energy, 133*, 111-118.

Wyckmans, A. (2005). *Intelligent building envelopes-architectural concept and applications for daylighting quality.* (PhD). Norwegian University of Science and Technology, Trondheim.

Wypych, G. (2016). *Handbook of Polymers* (Second Edition ed.): ChemTecPublishing.

Xie, F. (2011). *A novel clear foil cushion construction incorporating an additional water layer.* (PhD). University of Nottingham, Nottingham, UK.

Yu, J., Liu, Y., Xiong, C., & Huang, J. c. (2015). Study on Daylighting and Energy Conservation Design of Transparent Envelope for Office Building in Hot Summer and Cold Winter Zone. Procedia Engineering, 121, 1642-1649.

Yu, X., & Su, Y. (2015). Daylight availability assessment and its potential energy saving estimation –A literature review. *Renewable and Sustainable Energy Reviews, 52*, 494-503.

Zaker, R., & Coloma, E. (2018). Virtual reality-integrated workflow in BIM-enabled projects collaboration and design review: a case study. *Visualization in Engineering, 6*(1), 4.

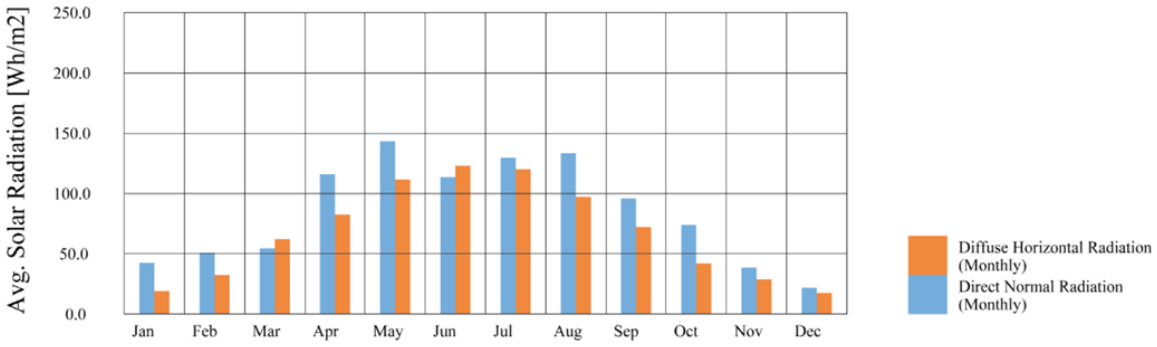
Zanelli, A., Monticelli, C., Beccarelli, P., & Ibrahim, H. (2011). *Experimental Manufacture Of A Pneumatic Cushion Made Of Etfe Foils And Opv Cells*.

Zhang, T., Tan, Y., Yang, H., & Zhang, X. (2016). The application of air layers in building envelopes: A review. *Applied Energy, 165*, 707-734.

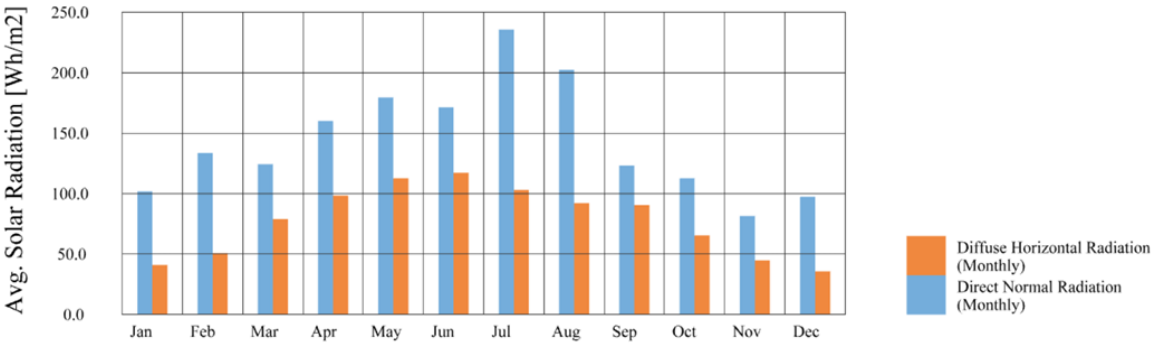
Zhao, Z., Liu, H., & Chen, Z. (2017). Thermal behavior of large-span reticulated domes covered by ETFE membrane roofs under solar radiation. *Thin-Walled Structures, 115*, 1-11.

Appendix A: Annual solar radiation graph showing average diffuse horizontal and direct normal radiation for London, Barcelona and Shanghai

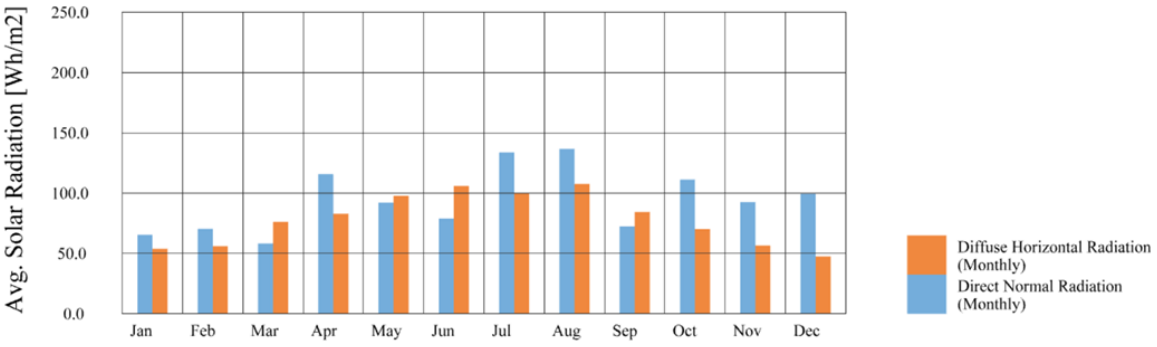
(graphs by the thesis author, unpublished)



LONDON/GATWICK_GBR



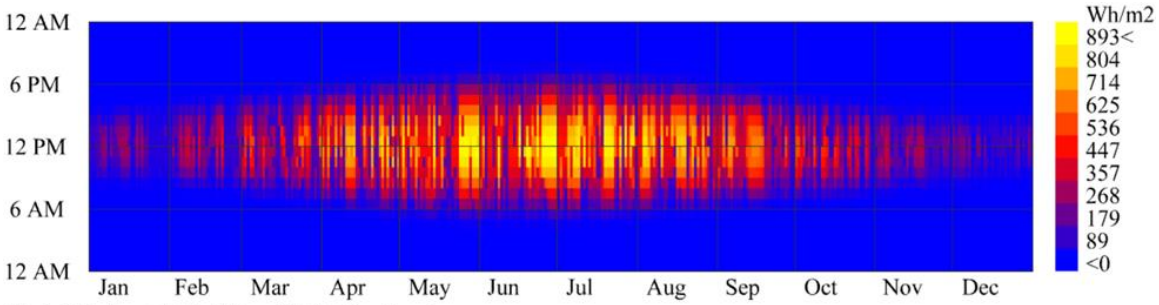
BARCELONA_ESP



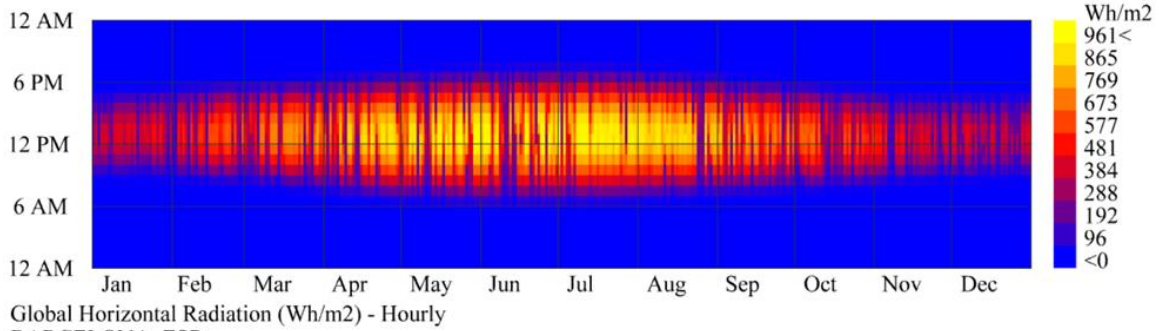
SHANGHAI_CHN

Appendix B: Annual solar radiation graphs showing the hourly global horizontal radiation for London, Barcelona and Shanghai

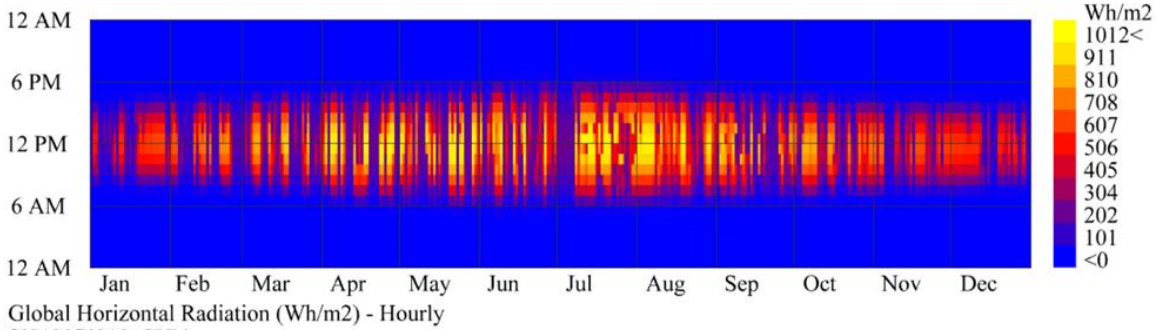
(graphs by the thesis author, unpublished)



Global Horizontal Radiation (Wh/m2) - Hourly
LONDON/GATWICK_GBR
1 JAN 1:00 - 31 DEC 24:00



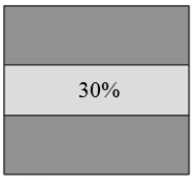
Global Horizontal Radiation (Wh/m2) - Hourly
BARCELONA_ESP
1 JAN 1:00 - 31 DEC 24:00



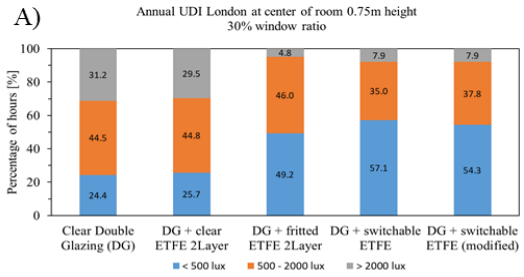
Global Horizontal Radiation (Wh/m2) - Hourly
SHANGHAI_CHN
1 JAN 1:00 - 31 DEC 24:00

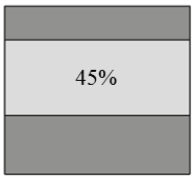
Appendix C: UDI bins London

(graphs by the thesis author, unpublished)

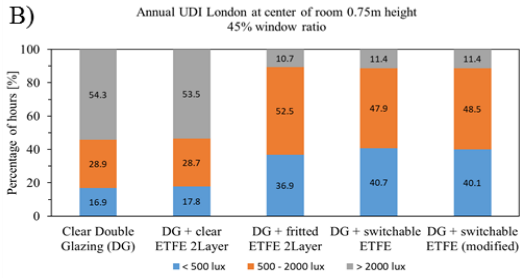


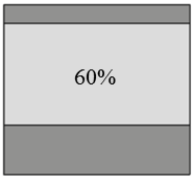
Window to Wall Ratio
30 / 70 %



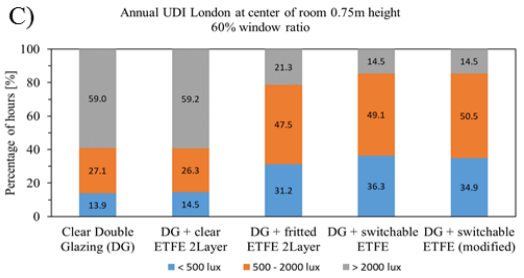


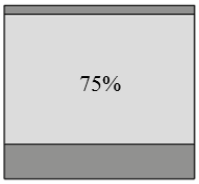
Window to Wall Ratio
45 / 55 %



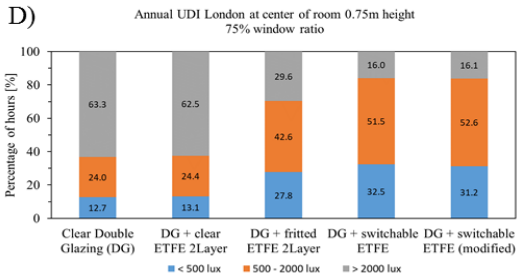


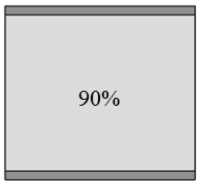
Window to Wall Ratio
60 / 40 %



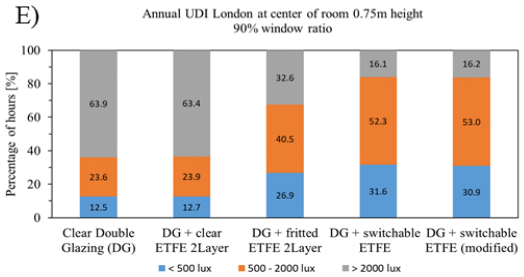


Window to Wall Ratio
75 / 25 %



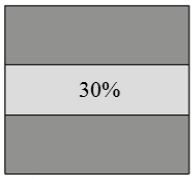


Window to Wall Ratio
90 / 10 %



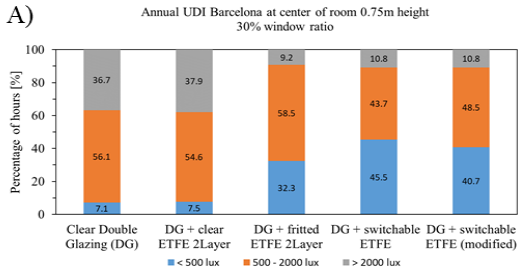
Appendix D: UDI bins Barcelona

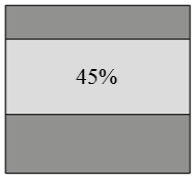
(graphs by the thesis author, unpublished)



Window to Wall Ratio
30 / 70 %

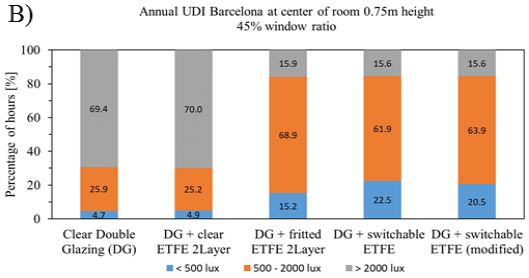
A)

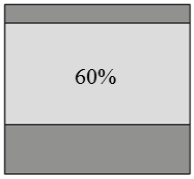




Window to Wall Ratio
45 / 55 %

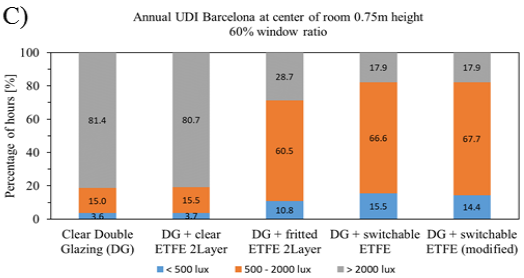
B)

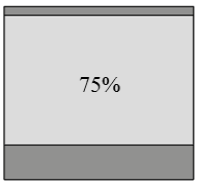




Window to Wall Ratio
60 / 40 %

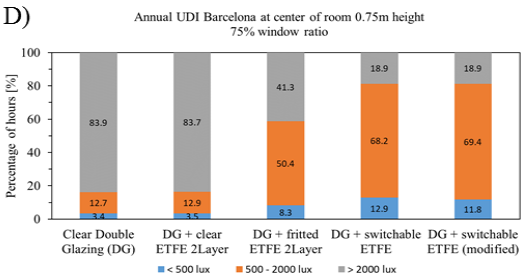
C)

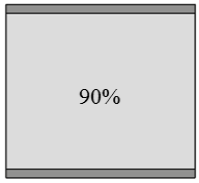




Window to Wall Ratio
75 / 25 %

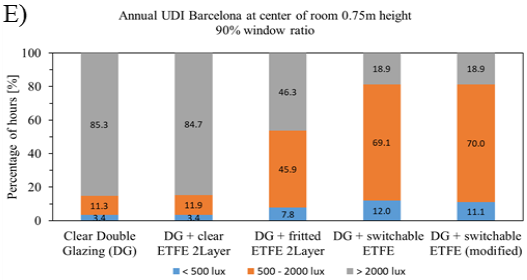
D)





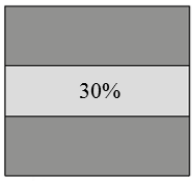
Window to Wall Ratio
90 / 10 %

E)

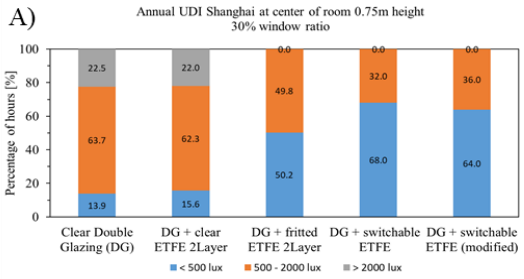


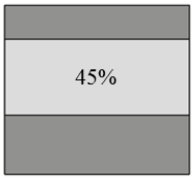
Appendix E: UDI bins Shanghai

(graphs by the thesis author, unpublished)

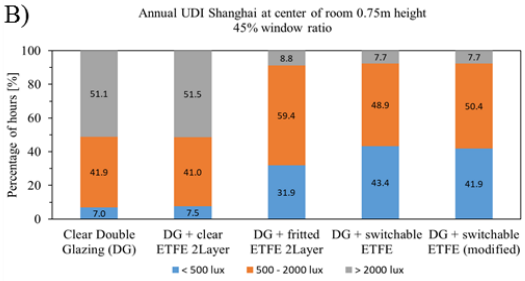


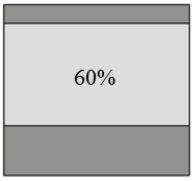
Window to Wall Ratio
30 / 70 %



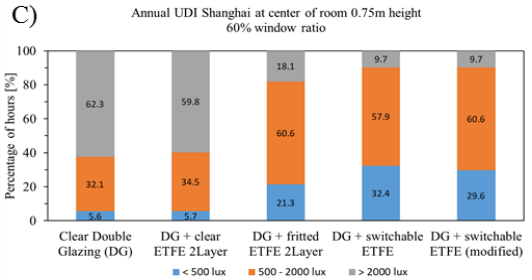


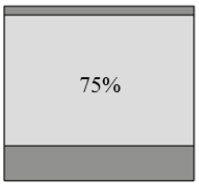
Window to Wall Ratio
45 / 55 %



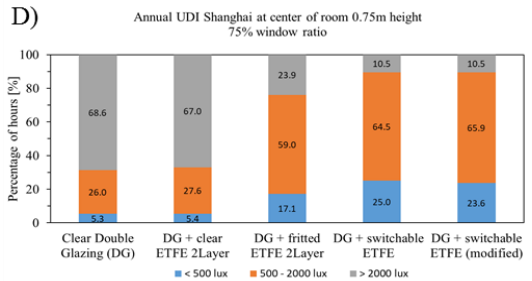


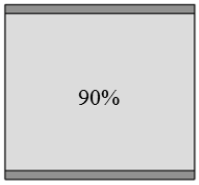
Window to Wall Ratio
60 / 40 %



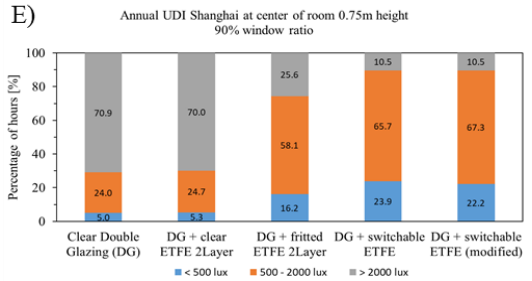


Window to Wall Ratio
75 / 25 %





Window to Wall Ratio
90 / 10 %



Appendix F: Virtual reality experiment questionnaire

(form by the thesis author, unpublished)

Questionnaire

Participant # : _____
VR Scene # : _____
VR Scene Type : _____
Date : _____

1. **Which outside objects can you distinguish from the following?**

Columns:	2	3	4
Trees:	2	3	4
Window shades:	5	10	20

2. **How clear is your outside view through the glazing?**

Not Clear 1 2 3 4 5 6 7 Very Clear

← continuous →

3. **How satisfied are you with the view from the window?**

Dissatisfied 1 2 3 4 5 6 7 Satisfied

← continuous →

4. **How satisfied are you with the amount of view?**

Dissatisfied 1 2 3 4 5 6 7 Satisfied

← continuous →

5. **How clear is the weather outside?**

Hazy* 1 2 3 4 5 6 7 Clear

← continuous →

6. **How sunny is the weather outdoor?**

Grey 1 2 3 4 5 6 7 Sunny

← continuous →

7. **How would you grade the vividness of the outside colours?**

Faded 1 2 3 4 5 6 7 Strong

← continuous →

For the following set of questions, rate your state in terms of how you feel about the space:

8. **How pleasant do you feel about the space?**

Unpleasant 1 2 3 4 5 6 7 Pleasant

← continuous →

9. **How energized or drowsy you feel due to the space?**

Drowsy 1 2 3 4 5 6 7 Energised

← continuous →

10. **How controlling versus controlled you feel due to the space?**

Submissive 1 2 3 4 5 6 7 Dominant

← continuous →

*Hazy: covered by something in the air that makes it difficult to see well.

Appendix G: Virtual reality experiment ethics approval

2018-19 academic year only

The University of Nottingham

Faculty of Engineering
Process for approval of research study involving human participants

Introduction

This document describes the process to be followed when planning and obtaining approval for studies involving human participants within the Faculty of Engineering. This process is based on one previously run within the School/Dept. M3. The process is administered by the Faculty Research Ethics Committee, and managed by the Chair of the Ethics Committee and the Faculty Research Ethics Officer. All queries regarding the process should be initially sent to ez-eng-ethics@nottingham.ac.uk

What is Ethics Approval?

When conducting any study or observation or collecting data about individuals, it is essential that full consideration is given to ethical issues and that steps are taken to ensure participant well-being throughout the study.

Participants involved in research studies have a right to:
- Know the goals of the study and who is funding the work
- Make an informed decision about whether or not they wish to participate
- Leave the study at any time if they do not wish to continue
- Know what will happen to them during the study and how long it will take
- Know if they may experience any discomfort
- Know what will happen to the findings
- Privacy of personal information
- Be treated courteously

The University of Nottingham and Faculty of Engineering have an ethics procedure that requires all staff and students to submit an application for ethical approval before conducting any research study involving human participants. Members of the Ethics Committee read through study proposals to check that the researcher has demonstrated that they have given full consideration to ethical issues and that they have provided participants with appropriate and sufficient information.

Who needs Ethics Approval?

ANY member of staff or registered student of the University of Nottingham involved in conducting any study or observation or collecting data about individuals **MUST** adhere to the University Code of Research Conduct and Research Ethics. Those affiliated with the Faculty of Engineering **MUST ALSO** comply with the Faculty ethical approval process before commencing their study.

Ethics application procedure

The attached document outlines the ethics approval process within the Faculty of Engineering. For all applications required to undergo formal review, applications must be submitted to the **Ethics Administrator**, APM Hub, L4-B03, Faculty of Engineering. The application will then be reviewed by the ethics committee. We aim to return a decision to applicants within two weeks but the procedure may be delayed if the ethics committee require further information. It is the applicant's responsibility to make sure that applications are submitted in good time.

THE STUDY MAY **NOT** START UNTIL ETHICAL APPROVAL HAS BEEN AWARDED

2018-19 academic year only

Information you should give to ALL participants

The following list describes the information that should be given to all participants. Normally this should be given in a participant information sheet at the beginning of the study, and participants should be required to confirm that they have understood the nature of the study, and that they are happy to participate.
The following information should be included:

- Details of who will be conducting the study.
- Details about who is sponsoring the study and what the terms of the sponsorship are (i.e. who will 'own' the data and how the data will be used).
- Details about the nature, purpose and duration of the study. (Participants whose first language is NOT English may need further explanation of what is involved as their understanding of some of the terminology may be limited).
- What kinds of procedures will be used and what participant will be asked to do.
- Details about any hazards, inconveniences and risks associated with the study.
- What procedures will be followed if a participant is injured. (only needed if risk of injury has been identified)
- What benefits (payments, expenses etc) are attached to the study.
- What they need to do in order to receive the payments described above.
- What procedures will be employed to maintain confidentiality and anonymity (e.g. removing personal details from data/reports, keeping data in locked files)
- What will happen to the data (how it will be used, how it will be stored, in what form it will be disseminated and if it is likely to be used for further analysis).
- How you will use photographs or video records (data analysis, illustration purposes, displayed to sponsors/ non-public academic audiences, printed in public domain documents etc).
- Details about who to contact if questions or problems arise.
- ALL participants must be told that any involvement in the study is voluntary and they are free to withdraw at any time. You should also explain any consequences for the participant of withdrawing from the study and indicate what will be done with the participant's data if they withdraw.

2018-19 academic year only

Faculty of Engineering
Application for approval of research study involving human participants

ALL applicants must provide the following information

The applicant must be the person who will conduct the investigations; each application must be made by one applicant:

- usually the student in the case of taught or research courses,
- usually the researcher (the member of university research or academic staff) who will conduct the study in the case of funded research projects,
- usually the principal investigator in the case of applications for ethics approval in advance of submission of a research proposal

If the applicant is an Undergraduate or Postgraduate taught or research student please complete the information below. The application must be approved by a Supervisor.

Name of student:	*Jan-Frederik Flor*	Student No:	*4268867*
Course of study:	*Architecture and Environmental Design*	Email address:	*jan.flor@nottingham.ac.uk*
Supervisor:	*Dr Yupeng Wu*	PGR [X]	PGT [ ]
		MSc [ ]	UG [ ]

If the applicant is a member of university research or academic staff, please complete the information below: For research staff, the application must be approved by the Principal Investigator

Name:		Principal Investigator (Budget Holder)	
Email address:		PI Signature:	

Title of investigation: *Evaluating Virtual Reality as an architectural presentation technique: a study into the visual parameters of virtual reality.*

Planned date for study to begin: *10/12/2018* Duration of Study: *1 month*

Please state whether this application is:

[ ] New [ ] Revised [ ] A renewal [X] For a continuation study

Selection of review process

Please indicate whether the application is required to go forward to the ethics committee for formal review, or, in the case of projects completed by ***taught undergraduate and postgraduate students only***, whether the application can be approved by the supervisor under the expedited review process*.

[X] Formal review, application will be submitted to ethics committee

[ ] Expedited review, application is approved by supervisor*
* This option can only be selected if the Supervisor is a member of the Faculty Ethics committee

Approval by supervisor: expedited review

I approve the application as supervisor of this project, under the expedited review procedure.

Name of supervisor..Yupeng Wu.. Signature..[signature].. Date..15/04/19

Office use only

Date form received: **Date decision returned to applicant:**

Passed to reviewers: 1. Name..... Date.....

(formal review only) 2. Name..... Date.....

2018-19 academic year only

Ethical Issues Checklist

The purpose of this Checklist is to facilitate the review process and to identify any ethical issues that may concern the Committee. It is meant to be an aid to both the researcher and the Committee. Listed below are areas which require some justification and attention on your part in specifying your study protocol. Please answer each question honestly, giving full details where required. Answering "YES" to any of the questions will not necessarily lead to a negative response to your application but it will draw issues to your attention and give the reviewers the opportunity to ensure appropriate steps are being taken. In expedited review, supervisors should ensure that for any questions where the answer "YES" has been given, appropriate measures have been taken to maintain ethical compliance.

Applicant's full name: *Christopher Alan Bennett*

You must complete ALL of this section before submitting your application

1 Who is the population to be studied?

Adult students and staff at the University of Nottingham. i.e. males and females over the age of 18.

2 Please give details of how the participants will be identified, approached and recruited. (Include any relationship between the investigator and participants e.g. instructor-student).

If they choose to, a time will be set to run through the questionnaire and study with them. The participants are volunteers without payment, and they will receive an appointment e-mail with a brief introduction of the experiment before the test.

3 Will the population studied include any vulnerable members of the public? **YES** ☐ **NO** ☒
Note: for the purpose of ethics approval this includes participants who are under 18, people who are disabled or in poor health, and also those who are non-English speakers and may not be able to understand the consent forms. (If YES, please give further details)

4 Will it be possible to associate specific information in your records with specific participants on the basis of name, position or other identifying information contained in your records? **YES** ☐ **NO** ☒

5 What steps have you taken to ensure confidentiality of personal information and anonymity of data both during the study and in the release of its findings?

Once data has been collected, participants are to be identified as a number only (ie. x number of males and x number of females). No data shall be released relating to name, age or any other personal details of the participant.

6 Describe what data will be stored, where, for what period of time, the measures that will be put in place to ensure security of the data, who will have access to the data, and the method and timing of disposal of the data.

Paper records should be stored in a locked filing cabinet. Digital data should be stored only on a password-protected computer and/or on a secure server. In accordance with the Data Protection Act, the data needs to be kept securely for seven years following publication kept securely for seven years following publication of results. After this time, electronic files will be deleted and any hard copies will be destroyed.

At the end of a student project, students are responsible for ensuring that all data from the study is passed on to their academic supervisor/s. The supervisors/s will then have responsibility for the storage of that data.

During the duration of the study, physical hard copy questionnaires completed will be kept in a locked filing cabinet in ETB at the University of Nottingham. This data will be scanned and data will be stored digitally on to the research computer in room B07, Energy Technology Building on Jubilee Campus. During the Study audio recordings of the task performance will be recorded and saved to the research computer in room B07, Energy Technology Building on Jubilee Campus. This data will be compiled and saved to the research computer in room B07, Energy Technology Building on Jubilee Campus. At the end of Christopher Bennett's Dissertation project, Christopher Bennett will pass along all data to the Academic Supervisor of the project, Dr Yupeng Wu. Dr Yupeng Wu will store the hard copies in his locked filing cabinet at ETB and store electronic data on his password protected university computer in ETB. In accordance with the

2018-19 academic year only

Data Protection Act, the data will be kept securely for seven years following publication of results. After this time, the hard copies will be shredded and the raw data electronic files will permanently be deleted by Dr Yupeng Wu.

		YES	NO
7	Will persons participating in the study be subjected to physical or psychological discomfort, pain or aversive stimuli which is more than expected from everyday life? (If YES, please give further details) *When using virtual reality headsets, there is a small risk that participants might experience "simulator sickness". It involves symptoms similar to those of motion-induced sickness, although simulator sickness tends to be less severe and to be of lower incidence. People who suffer from epilepsy, migraines, motion sickness, dizziness, sleep disorders or blurred vision are more likely to experience adverse effects, so participants are advised not take part in the study if they suffer from any of these conditions. If the participants experience any symptoms during the session, or any other discomfort, they are asked to alert the investigator, and the test will be stopped immediately. Alternatively, the participant can simply remove the headset themselves, like they would a pair of goggles.*	X	
8	Will participants engage in strenuous or unaccustomed physical activity? (If YES, please give further details)		X
9	Will the investigation use procedures designed to induce participants to act contrary to their wishes? (If YES, please give further details)		X
10	Will the investigation use procedures designed to induce embarrassment, humiliation, lowered self esteem, guilt, conflict, anger, discouragement or other emotional reactions? (If YES, please give further details)		X
11	Will participants be induced to disclose information of an intimate or otherwise sensitive nature? (If YES, please give further details)		X
12	Will participants be deceived or actively misled in any manner? (If YES, please give further details)		X
13	Will information be withheld from participants that they might reasonably expect to receive? (If YES, please give further details)		X
14	Will the research involve potentially sensitive topics? (If YES, please give further details)		X
15	Will data be collected which requires potentially invasive procedures (eg attaching electrodes to the skin) and/or other health-related information to be identified (eg heart rate). If yes please give details		X

If you require space for additional information, please add it here and identify the question to which it refers:

2018-19 academic year only

Checklist of information to include with your application:
Please tick the boxes below to confirm that you have included the following information with your submission. Failure to include the required information may result in your ethics application and approval for start of your research to be delayed.

☒ A brief description of the study design:
- number and type of participants
- number and duration of activities participants will be involved in
- equipment and procedures to be applied
- information about how participants will be recruited
- whether participants will be paid (state how this will be done)
- plans to ensure participant confidentiality and anonymity
- plans for storage and handling of data
- information about what will happen to the data after the study
- information about how any data and images may be used
- state whether it will be possible to identify any individuals.

☒ Copies of any information sheets to be given to participants (include recruitment information (e.g. adverts, posters, letters, etc)

☒ A copy of the participant consent form

☒ Copies of data collection sheets, questionnaires, etc

I confirm that all of the above is included in the application:

As the applicant I confirm that I have read and understand the Ethical requirements for my study and have read and complied with the University of Nottingham Code of Research Conduct and Research Ethics.

Signature of applicant ..... Date ...16/04/2019

As supervisor, I confirm that I have checked the details of this application.

Name of Supervisor Yupeng Wu **Signature** ..... **Date** 15/04/19

NB The signature of the supervisor on this part of the application DOES NOT indicate supervisor approval for expedited review. If supervisor approval is granted then the front page of the application MUST be signed for approval to be confirmed.

2018-19 academic year only

Ethics Committee Reviewer Decision

This form must be completed by each reviewer. Each application will be reviewed by two members of the ethics committee. Reviews may be completed electronically and sent to the Faculty ethics administrator (Donna Astill-Shipman) from a University of Nottingham email address, or may be completed in paper form and delivered to the APM Hub

Applicant full name ..... Jan-Frederik Flor .....

Reviewed by:

Name .....DE13.....

Signature (paper based only) .....

Date .....26 April 2019.....

☐ Approval awarded - no changes required

■ Approval awarded - subject to required changes (see comments below)

☐ Approval pending - further information & resubmission required (see comments)

☐ Approval declined – reasons given below

Comments:

Who is Christopher Alan Bennett and why does his name appear on the application form as the applicant?

The Planned date for study to begin is *10/12/2018*, has this study already commenced?

Assuming that these are errors and the study has not taken place, I am happy for this to proceed. This is not retrospective approval.

Please note:

1. The approval only covers the participants and trials specified on the form and further approval must be requested for any repetition or extension to the investigation.
2. The approval covers the ethical requirements for the techniques and procedures described in the protocol but does not replace a safety or risk assessment.
3. Approval is not intended to convey any judgement on the quality of the research, experimental design or techniques.
4. Normally, all queries raised by reviewers should be addressed. In the case of conflicting or incomplete views, the ethics committee chair will review the comments and relay these to the applicant via email. All email correspondence related to the application must be copied to the Faculty research ethics administrator.

Any problems which arise during the course of the investigation must be reported to the Faculty Research Ethics Committee

Appendix H: Virtual Reality consent form sample

PARTICIPANT CONSENT FORM

Project Title: Using VR to evaluate different visual environments

Researchers: Jan-Frederik Flor [jan.flor@nottingham.ac.uk], Fedaa Abd-AlHamid [laxfa10@nottingham.ac.uk] and Marina Aburas [ezxma17@ nottingham.ac.uk]

Supervisor: Dr Yupeng Wu [Yueng.Wu@nottingham.ac.uk]

I the undersigned as research participant confirmed that (please sign your initials as appropriate)

☐ I have read the Participant Information Sheet and the nature and purpose of the research project has been explained to me. I understand and agree to take part.

☐ I understand the purpose of the research project and my involvement in it.

☐ I do not suffer from any of the following: epilepsy, migraines, motion sickness, dizziness, sleep disorders or blurred vision.

☐ I understand that I may withdraw from the research project at any stage and that this will not affect my status now or in the future.

☐ I understand that while information gained during the study may be published, I will not be identified, and my personal results will remain confidential.

☐ I understand that the anonymised data are approved for use in secondary studies.

☐ I understand that data will be stored in a locked filing cabinet, digital data will be stored only on a password-protected computer and on a secure server. Only researchers and supervisors can get access to the data. At the end of the researcher student's project, all data from the study will be passed on to academic supervisor and the supervisors will then have responsibility for the storage of the data. In accordance with the Data Protection ACT, the data will be kept securely for seven years following the publication of results. After this time, electronic files will be deleted, and any hard copies will be destroyed.

☐ I understand that I may contact the researcher or supervisor if I require further information about the research.

Signed …… (Research participant)

Print name …… **Date** ……

Signed …… (Researcher)

Print name …… **Date** ……

POST STUDY PARTICIPANT CONSENT FORM

Project Title: Using VR to evaluate different visual environments

Researchers: Jan-Frederik Flor [jan.flor@nottingham.ac.uk], Fedaa Abd-AlHamid [laxfa10@nottingham.ac.uk] and Marina Aburas [ezxma17@ nottingham.ac.uk]

Supervisor: Dr Yupeng Wu [Yueng.Wu@nottingham.ac.uk]

I the undersigned as research participant confirmed that (please sign your initials as appropriate)

☐ Any feelings of discomfort I may have felt during the trials have subsided.

☐ I have been advised to wait for approximately 30 minutes between completing the simulator trial and driving

Signed …… (Research participant)

Print name …… **Date** ……

Signed …… (Researcher)

Print name …… **Date** ……

Appendix I: Title page of published paper (1)

FORM and FORCE

Proceedings of the IASS Annual Symposium 2019 – Structural Membranes 2019
Form and Force
7 – 10 October 2019, Barcelona, Spain
C. Lázaro, K.-U. Bletzinger, E. Oñate (eds.)

Switchable ETFE cushion: designing and building a model for experimental testing

Jan-Frederik FLOR*, Yanyi SUN, Paolo BECCARELLI, Yupeng WU, John CHILTON

* The University of Nottingham
Department of Architecture & Built Environment, University Park, Nottingham NG7 2RD, United Kingdom
jan.flor@nottingham.ac.uk , janflor@gmx.de

Abstract

Adaptive façade systems have the potential for saving energy and enhancing comfort conditions in buildings. Creating working models with materials, components and functions which embody the design idea of a responsive building envelope is an important part of the design process of these systems, because it allows the performance to be demonstrated and tested under realistic conditions and for difficulties to be detected in advance. This paper reports on the process of building and programming a functional model of a switchable ETFE cushion for preliminary performance tests. Different techniques of reverse engineering and prototyping were explored on a range of scales to build the membrane structure and its pneumatic control system. The study showcases the inter-link of advanced manufacturing techniques and parametric design software, the application of microcontrollers, actuators and sensors in combination with the building envelope. The paper further documents and theorizes the process from design to making and testing, outlining a practical workflow for the development and prototyping of adaptive building envelopes for energy efficient buildings.

Keywords: ETFE, Adaptive Building Envelope, Prototyping, Testing

1. Introduction: responsive control mechanisms for switchable ETFE cushions

Adaptive Architecture is thought of to perform beyond formal aesthetic and functional considerations and respond in an intelligent way to the changing conditions of the environment, improving the energy efficiency of buildings [1]. ETFE foil has been used as a building material for a variety of building typologies implementing adaptive design features [2]. Reflective frit prints, multilayer constructions and adaptive systems, which switch from one state to the other, have been developed to enhance the energy and lighting performance of buildings covered with inflated ETFE cushions [3]. The specific function of the switching mechanisms presented here is to control the light transmission of a triple layer ETFE foil cushion, allowing it to respond to variations of solar radiation, using sensors and actuators that interact following the logic of an algorithm, which defines the responsive behavior and automates the shading mechanism of the foil construction (Fig. 1). While performance of static ETFE foil construction has been investigated thoroughly, information about switchable systems is currently lacking. One reason for this is that the system has been implemented only in relatively few buildings in recent years (Adelaide University Learning Hub, Adelaide, 2011; St. Bartholomew's Hospital, London, 2013; IIT Innovation Center, Illinois, 2018) and post-occupancy data is not publicly available yet. Another reason relates to the challenging and costly computational task of conducting whole building simulations with switchable systems. Therefore, the resulting aim of this research was to build a physical model, which could deliver quick feedback under realistic conditions, with the purpose of validating numerical models and improving the system performance through experimentation. However, the information presented here is limited solely to the designing and building of the testing models.

Copyright © 2019 by Jan-Frederik Flor, Yanyi Sun, Paolo Beccarelli, Yupeng Wu, John Chilton
Published by the International Association for Shell and Spatial Structures (IASS) with permission.

Appendix J: Co-authors contribution declaration (paper 1)

Authors contribution to the joint paper:

Switchable ETFE cushion: designing and building a model for experimental testing

The PhD applicant Jan-Frederik is the first author of this publication and has made a significant intellectual contribution to this work. Jan designed and built the initial demonstration models, including the responsive control mechanism, and coordinated the design and manufacturing of the testing rig as well as the cushion samples in collaboration with the industry partner. Also, Jan was responsible for drafting the paper manuscript, editing and coordinating the publishing process. The co-authors have provided valuable contribution as follows:

- Yupeng Wu (Jack), is the principal supervisor who supervised all stages of this research paper, from designing to publishing. also provided valuable comments and suggestions to enhance the manuscript to be of a high-quality.
- Yanyi Sun, contributed to the publication of this paper with comments and suggestions at various stages of the project.
- Paolo Beccarelli, the second supervisor who supervised the work in this paper, advised the applicant with establishing the relationship with the industry partners and provided technical knowledge on ETFE construction and manufacturing to the applicant.
- John Chilton, the advisor, mentor and former supervisor of the applicant rigorously examined the work in this paper and helped with valuable comments and suggestions to improve the paper manuscript. John also proofread the paper before publication.

Appendix K: Title page of published paper (2)

9th edition of the international SOLARIS conference IOP Publishing
IOP Conf. Series: Materials Science and Engineering **556** (2019) 012004 doi:10.1088/1757-899X/556/1/012004

Experimental study on the thermal performance of ethylene-tetrafluoroethylene (ETFE) foil cushions

J-F Flor[1], Y Sun[1], P Beccarelli[1], C Rowell[2], J Chilton[1] and Y Wu[1]
[1]University of Nottingham, Faculty of Engineering, Department of Architecture and Built Environment, Nottingham, United Kingdom
[2] Architen Landrell, Station Road, Chepstow, United Kingdom

E-mail: jan.flor@nottingham.ac.uk, Yupeng.Wu@nottingham.ac.uk

Abstract. ETFE pneumatic foil constructions are used increasingly by designers and builders as an alternative to glass in state of the art building envelopes. Low weight, high transparency, mechanical resistance and self-cleaning properties of ETFE may contribute to the overall performance. However, reliable information on the thermal performance of ETFE cushions in building envelopes is scarce, limiting the performance prediction in energy simulations. The present study aims to investigate the thermal performance of air-inflated ETFE foil cushions and evaluates parameters of material properties and design which might affect the thermal transmittance. The paper reports on the experiments conducted to quantify the thermal performance using a climate chamber and full-size mock-ups. Based on available standards, tests were designed to compare the thermal performance of three different ETFE cushion designs, under changing climate conditions. The design variations, including frit prints and switchable shading mechanisms, were tested and compared at hot, temperate and cold weather scenarios. The test series provided detailed results on the thermal performance of ETFE cushions which may be of use for the comparison with the performance of other building components and materials, serve as input for energy simulations and provide a theoretical basis for future developments of novel building envelopes.

Keywords: solar radiation; energy, ETFE, thermal performance, building envelope

1. Introduction

Building light and flexible is a common approach in contemporary architecture. Benefits of saving energy and material while achieving attractive shapes and design features are made achievable with tensioned membrane structures. Pneumatic ETFE foil cushions are now considered state of the art for wide span canopy covers but are also increasingly applied in facades or conceived as a continuous enclosing building envelope. This development calls for new approaches of anticipating the thermal performance of the building envelope in order to meet the evermore demanding needs of reducing the energy consumption of buildings.

ETFE (ethylene-tetrafluoroethylene) is a material with outstanding characteristics of mechanical resistance, light transmittance and environmental performance. Buildings incorporating ETFE have achieved now, after four decades of successful implementation in permanent buildings, a high standard of building excellence and have allowed innovative design solutions to become reality. ETFE has been applied in a large number and variety of building types on a global scale and virtually matches any design brief with great flexibility. An example of a typical ETFE project mastering the complex site requirements for the modernization of a historical building can be seen in figure 1.

Content from this work may be used under the terms of the Creative Commons Attribution 3.0 licence. Any further distribution of this work must maintain attribution to the author(s) and the title of the work, journal citation and DOI.
Published under licence by IOP Publishing Ltd

Appendix L: Co-authors contribution declaration (paper 2)

Authors contribution to the joint paper:

Experimental study on the thermal performance of ethylene-tetrafluoroethylene (ETFE) foil cushions

The PhD applicant Jan-Frederik is the first author of this publication has made the most significant intellectual contribution to this work, in terms of finding the study aim, designing the testing mock-up and study's method, coordinating the sample and instruments acquisition, conducting the experiments in the climate chamber, acquiring, processing, analysing and discussing the data, drawing conclusions and writing the manuscript in paper format to be published. The coordination of communication between co-authors and the following up of reviewers' comments until publishing was also done by the applicant. The co-authors have provided valuable contribution as follows:

- Yupeng Wu (Jack), is the principal supervisor who supervised all stages of this research paper, from designing to publishing. Jack helped to organise the applicants technical training and access to the climate chamber. Also, Jack provided valuable comments and suggestions to enhance the manuscript to be of a high-quality.

- Yanyi Sun, helped during the experimental work in the climate chamber with technical support and theoretical background knowledge on thermal performance testing of complex fenestrations. Yanyi also contributed to the interpretation and discussion of the data and advised with comments and suggestions to during the editing of the manuscript.

- Paolo Beccarelli, the second supervisor who supervised the work in this paper, advised the applicant with establishing the relation with the industry partners and facilitated the acquisition of measuring devices.

- John Chilton, the advisor, mentor and former supervisor of the applicant rigorously examined the work in this paper and helped with valuable comments and suggestions to improve the paper manuscript. John also proofread the paper before publication.

- Christopher Rowell, CEO of Architen Landrell, and industry partner of the applicant facilitated the fabrication of a testing rig, provided material and cushion samples, advised on technical matters and contributed with specialist information from an industry perspective.

Appendix M: Title page of published paper (3)

Available online at www.sciencedirect.com

ScienceDirect

Energy Procedia 158 (2019) 3191–3195

Energy Procedia

www.elsevier.com/locate/procedia

10th International Conference on Applied Energy (ICAE2018), 22-25 August 2018, Hong Kong, China

Numerical investigations on the thermal performance of adaptive ETFE foil cushions

Haomin Wang, Jan-Frederik Flor, Yanyi Sun and Yupeng Wu*

Department of Architecture and Built Environment, The University of Nottingham, University Park, Nottingham, NG7 2RD, UK

Abstract

It has become increasingly popular among designers and engineers to use ETFE pneumatic foil constructions as an alternative to glass in state of the art building envelopes, due to the low weight, high transparency, mechanical resistance and self-cleaning features of ETFE. However, it is still unclear how the thermal performance of the ETFE cushions can be assessed comprehensively and what are the effects on building thermal performance. This study investigated the thermal performance of a developed prototype ETFE cushion through both experimental measurement and numerical simulation. The numerical model has been validated by results from experimental tests using a large climatic chamber. The thermal resistance of the developed ETFE cushion at various environmental conditions (different indoor and outdoor temperature conditions) and also different inclination angles were studied. Empirical correlations generated based on simulations could be used for future building energy simulation.

© 2019 The Authors. Published by Elsevier Ltd.
This is an open access article under the CC BY-NC-ND license (http://creativecommons.org/licenses/by-nc-nd/4.0/)
Peer-review under responsibility of the scientific committee of ICAE2018 – The 10th International Conference on Applied Energy.

Keywords: ETFE; Thermal Performance; Numerical simulation.

1. Introduction

The pneumatic ethylene tetrafluoroethylene (ETFE) foil cushion has been widely applied into building facades and atrium in recent years, due to its lightweight, high transparency, mechanical resistance, self-cleaning properties, etc.. Many landmark buildings adopted the ETFE cushion as their façade such as National Aquatics Center and

* Corresponding author. Tel.: +44 115 74 84011; fax: +44 115 95 13159.
E-mail address: Yupeng.Wu@nottingham.ac.uk.

1876-6102 © 2019 The Authors. Published by Elsevier Ltd.
This is an open access article under the CC BY-NC-ND license (http://creativecommons.org/licenses/by-nc-nd/4.0/)
Peer-review under responsibility of the scientific committee of ICAE2018 – The 10th International Conference on Applied Energy.
10.1016/j.egypro.2019.01.1012

Appendix N: Co-authors contribution declaration (paper 3)

Authors contribution to the joint paper:

Numerical investigations on the thermal performance of adaptive ETFE foil cushions

The PhD applicant Jan-Frederik is the second author of this joint paper and has made a significant intellectual contribution to this work. Jan designed the testing mock-up and experimental method, coordinated the sample and instruments acquisition, conducting the experiments in the climate chamber, acquired, processed, analysed and formatted the experimental data to be used in the numerical calculations and simulations, and provided suggestions and comments for the analysis of the results. The co-authors have provided valuable contribution as follows:

- Yupeng Wu (Jack), is the principal supervisor who supervised all stages of this research paper, from designing to publishing. Jack helped to organise the technical training and access to the climate chamber and guided the numerical calculations and CFD simulations. Jack also provided valuable comments and suggestions to enhance the manuscript to be of a high-quality.

- Yanyi Sun, helped during the experimental work in the climate chamber with technical support and theoretical background knowledge on thermal performance testing of complex fenestrations. Yanyi also contributed to the interpretation and discussion of both the experimental and numerical results and advised with comments and suggestions at various stages of the project

- Haomin Wang, fellow PhD colleague of the applicant, was the principal author of this study, who planned the study, conducted the numerical calculations and simulations, analysed and discussed the results, and formulated the conclusions to this work. Haomin was also responsible for drafting the manuscript and coordinating the publication process.

Appendix O: Title page of published paper (4)

Applied Energy 229 (2018) 335–351

Contents lists available at ScienceDirect

Applied Energy

journal homepage: www.elsevier.com/locate/apenergy

Optical aspects and energy performance of switchable ethylene-tetrafluoroethylene (ETFE) foil cushions

Jan-Frederik Flor*, Dingming Liu, Yanyi Sun, Paolo Beccarelli, John Chilton, Yupeng Wu*

Department of Architecture and Built Environment, Faculty of Engineering, The University of Nottingham, University Park, Nottingham NG7 2RD, UK

HIGHLIGHTS

- Switchable ETFE cushions has been employed in building envelope for daylight and solar heat control.
- Ray-tracing techniques were used to investigate the effects of various design aspects of the ETFE.
- A parametric study was carried out investigating the optical performance of switchable ETFE.
- The impact of switchable ETFE cushions on building performance were studied.

ARTICLE INFO

Keywords:
Ethylene-tetrafluoroethylene (ETFE) foil
Ray-tracing
Transmittance
Reflectance
Building simulation

ABSTRACT

A pneumatic multilayer foil construction with a kinetic shading mechanism has the potential to be an effective response to dynamic climatic factors, such as solar radiation, and therefore moderate the energy consumption of buildings. A parametric study was carried out on a switchable ethylene-tetrafluoroethylene (ETFE) foil cushion with the purpose of investigating the optical performance of an adaptive building envelope and its impact on building energy performance regarding heating, cooling and lighting. Ray-tracing techniques were used to investigate the effects of surface curvature, frit layout and frit properties, on the optical performance of the cushion in open and closed mode. A range of incidence angles for solar radiation were simulated. The results of the simulation showed an angle dependent optical behaviour for both modes. The influence of the dynamic shading mechanism on building energy performance was further evaluated by integrating the optical data obtained for the ETFE foil cushions in a comprehensive energy simulation of a generic atrium building using EnergyPlus. Results suggested that switchable ETFE foil cushions have a higher potential to reduce cooling and heating loads in different climatic regions, compared to conventional glazing solutions (i.e. uncoated double-glazing and reflective double-glazing), while providing good conditions of natural daylighting. Annual energy savings of up to 44.9% were predicted for the switchable ETFE foil cushion in comparison to reflective double glazing. As such, this study provides additional insight into the optical behaviour of multilayer foil constructions and the factors of design and environment that potentially have a major impact on buildings energy performance.

1. Introduction

The building sector currently consumes one third of the global final energy [1–4]. Increasing energy demands for commercial and residential building with an expected growth of up to 1.9%/year [5], raises the necessity for further improvement of the energy performance of buildings. Most of the energy consumed in buildings during their operation and maintenance is for space conditioning (approx. 50%) and lighting (approx. 25%) [6]. The building envelope, which is the interface between the external and internal environment, is, therefore, a crucial element of the building unit [7–9]. It has huge potential to impact the indoor comfort conditions and to improve the overall energy performance of the building by up to 40%, considering only savings in heating and cooling [10–13]. Much attention has been paid, over recent decades, to passive strategies, which aim to maximize the thermal damping effects of the building mass, while increasing insulation of walls and windows, and reducing thermal bridging of building elements [14–16]. However, the general tendency in architectural design moves towards light and transparent structures, such as membrane and foil structures, which offer high flexibility in form and function [17]. Although challenging in terms of energy efficient design, this solution is often adopted for widespan canopies because of its reduced weight and

* Corresponding author.
E-mail addresses: jan.flor@nottingham.ac.uk, janflor@gmx.de (J.-F. Flor), Yupeng.Wu@nottingham.ac.uk, Jackwuyp@googlemail.com (Y. Wu).

https://doi.org/10.1016/j.apenergy.2018.07.046
Received 25 April 2018; Received in revised form 3 July 2018; Accepted 12 July 2018
Available online 07 August 2018
0306-2619/ © 2018 Elsevier Ltd. All rights reserved.

Appendix P: Co-authors contribution declaration (paper 4)

Authors contribution to the joint paper:

Optical aspects and energy performance of switchable ethylene-tetrafluorethylene (ETFE) foil cushion

The PhD applicant Jan-Frederik is the first author of this publication has made the most significant intellectual contribution to this work, in terms of finding the study aim, designing the study's method, conducting the optical simulations, processing, analysing and discussing the data, drawing conclusions and writing the manuscript in paper format to be published, coordinate communication between co-authors and follow up reviewers' comments until publishing. The co-authors have provided valuable contribution as follows:

- Yupeng Wu (Jack), is the main supervisor who supervised all stages of this research paper, from designing to publishing. Jack helped to organise the software training of the applicant provided valuable comments and suggestions to enhance the manuscript to be of a high-quality.

- Dingming Liu is the second author of this paper. Dingming modelled the virtual building and conducted the energy simulation. Dingming was also responsible for processing and anaylsing the results of the energy simulation and redacted the corresponding sections for the paper manuscript.

- Yanyi Sun, helped during the energy simulations by providing technical support and insider knowledge to issues with dynamic simulation procedures in EnergyPlus. Yanyi also contributed to the interpretation and discussion of the data and advised with comments and suggestions during the final stage of the manuscript editing.

- Paolo Beccarelli, the second supervisor who supervised the work in this paper, provided valuable comments and suggestions to enhance the manuscript.

- John Chilton, the advisor, mentor and former supervisor of the applicant rigorously examined the work in this paper and helped with valuable comments and suggestions to improve the paper manuscript. John also proofread the paper at several stages before publication.

Appendix Q: Title page of published paper (5)

E3S Web of Conferences **22**, 00048 (2017) DOI: 10.1051/e3sconf/20172200048
ASEE17

Dynamic environmental control mechanisms for pneumatic foil constructions

Jan-Frederik Flor[1,*], *Yupeng* Wu[1], *Paolo* Beccarelli[1], and *John* Chilton[1]

[1]University of Nottingham, Department of Architecture and Built Environment, United Kingdom

Abstract. Membrane and foil structures have become over the last decades an attractive alternative to conventional materials and building systems with increasing implementation in different typologies and scale. The development of transparent, light, flexible and resistant materials like Ethylene Tetrafluoroethylene (ETFE) has triggered a rethinking of the building envelope in the building industry towards lightweight systems. ETFE foil cushions have proven to fulfil the design requirements in terms of structural efficiency and aesthetic values. But the strategies to satisfy increasing demands of energy efficiency and comfort conditions are still under development. The prediction and manipulation of the thermo-optical behaviour of ETFE foil cushion structures currently remain as one of the main challenges for designers and manufacturers. This paper reviews ongoing research regarding the control of the thermo-optical performance of ETFE cushion structures and highlights challenges and possible improvements. An overview of different dynamic and responsive environmental control mechanisms for multilayer foil constructions is provided and the state of the art in building application outlined by the discussion of case studies.

1 Introduction

The energy performance of the building envelope is becoming increasingly important since the building sector is held responsible for more than one-third of the worldwide energy consumption, according to the International Energy Agency. Dynamic environmental control mechanisms in building envelopes are a common strategy to balance between the reduction of solar heat gains and achieving good natural illumination while reducing energy consumption for cooling and artificial lighting at the same time. The integration and automatization of these mechanisms into complex fenestration systems and high-tech building facades has become a reality and opens possibilities for further optimisation of the energy performance and improvement of comfort conditions in the built environment. Responsive building envelopes can adapt to changing environmental conditions, or user demanded requirements and enhance the performance of the building. The developments in mechatronics, sensors and computer technology during the last decades, have made possible miniaturisation, mass production and successive cost reduction, which have

* Corresponding author: jan.flor@nottingham.ac.uk, janflor@gmx.de

© The Authors, published by EDP Sciences. This is an open access article distributed under the terms of the Creative Commons Attribution License 4.0 (http://creativecommons.org/licenses/by/4.0/).

Appendix R: Co-authors contribution declaration (paper 5)

Authors contribution to the joint paper:

Dynamic environmental control mechanisms for pneumatic foil constructions

The PhD applicant Jan-Frederik is the first author to this publication and contributed the most significant intellectual and practical work, in terms of finding the study aim, conducting the literature review, seeking permission for the image copyrights, communication and coordination among co-authors, drawing conclusions and writing the manuscript in paper format to be published, and follow up reviewers and editor comments. The co-authors have provided valuable contribution as follows:

- Yupeng Wu (Jack), is the main supervisor who supervised all stages of this review paper, from systemising information to publishing. Jack provided valuable comments and suggestions to enhance the manuscript to be of a high-quality and helped in directing the literature review and discussing the findings.

- Paolo Beccarelli, the second supervisor who supervised the work in this paper, provided industry contacts, essential sources of information and advice with valuable comments and suggestions to enhance the manuscript.

- John Chilton, mentor, advisor, and former supervisor rigorously examined the work in this paper and guided throughout the different phases of the literature review, providing background and insider information of the investigated topic. Besides, John helped in the preparation of the paper manuscript by providing valuable comments and suggestions and proofreading the final version of the paper.

Appendix S: Title page of published paper (paper 6)

Energy & Buildings 231 (2021) 110554

Contents lists available at ScienceDirect

Energy & Buildings

journal homepage: www.elsevier.com/locate/enb

Virtual reality as a tool for evaluating user acceptance of view clarity through ETFE double-skin façades

Jan-F. Flor [a,*], Marina Aburas [a,b], Fedaa Abd-AlHamid [a,c], Yupeng Wu [a,*]

[a] Department of Architecture and Built Environment, Faculty of Engineering, University of Nottingham, University Park, Nottingham NG7 2RD, United Kingdom
[b] School of Architecture and Built Environment, University of Adelaide, Adelaide, South Australia 5005, Australia
[c] Department of Architecture, Faculty of Architecture and Design, Al-Zaytoonah University of Jordan, Amman, Jordan

ARTICLE INFO

Article history:
Received 6 September 2020
Revised 4 October 2020
Accepted 10 October 2020
Available online 15 October 2020

Keywords:
View perception
Virtual reality
ETFE
Double-skin Façades

ABSTRACT

Equipping building envelopes with an additional layer is an effective measure for improving the overall thermal and daylighting performance and reducing the energy consumption of buildings. This study investigated the user acceptance of energy-saving retrofitting measures in office buildings, reporting on the view perception and emotional response towards ETFE double-skin façades (DSF). Virtual Reality (VR) and physics-based imaging techniques were used to evaluate the user experience of a window view in an office space equipped with a pneumatic ETFE cushion as a second building skin. Three DSF scenarios with different ETFE cushions, including a clear, fritted and switchable sample, were evaluated and compared to the original single-skin façade with double-glazed windows. The physical and luminous conditions of the office space were replicated in a virtual environment with a validated physically-based imaging technique and presented to a group of volunteers (N = 22) using a virtual reality headset. While immersed in the virtual environment, participants responded to a questionnaire enquiring into their view perception and emotional states. The results revealed a preference for view clarity of clear ETFE in double-skin façades (M_{dn} = 5) and less satisfaction for fritted (M_{dn} = 4) and switchable foil cushions (M_{dn} = 1.75), yet double glazing was preferred in all measured parameters (M_{dn} = 6). Statistical significance was found for fritted in comparison to switchable ETFE in terms of spatial pleasure and control. The highest ratings were given to clear glazing across all investigated parameters of view perception and emotional response. The lowest ranking in all questions was given to the sample with the switchable ETFE cushion. The study concluded that view clarity is a major aspect for the user acceptance of ETFE double-skin façades. Overall, this study provides a better understanding of the visual and emotional implications of viewing through ETFE foil and contributes to forming criteria for the design of next-generation ETFE building envelopes.
© 2020 The Authors. Published by Elsevier B.V. This is an open access article under the CC BY license (http://creativecommons.org/licenses/by/4.0/).

1. Introduction and background

Buildings currently consume over 40% of primary energy in developed countries and contribute significantly to the global greenhouse gas emissions responsible for climate change. According to the World Energy Outlook 2019 by the International Energy Agency, buildings account for one-quarter of the total CO_2 emissions and consume one half of the globally consumed electric energy [1]. While the goal of the Paris agreement is to limit global temperature rise below an average of 1.5–2 °C [2], the latest International Energy Outlook by the U.S. Energy Information Administration shows that energy consumption in the building sector is rising by a rate of 1.3% per year [3], a trend moving in the opposite direction to what is needed to reach global climate goals. Building energy consumption in developing countries is projected to grow even faster, with 2% annual increase due to economic growth and changing lifestyles. To close the gap between climate goal projections and realities of the built environment, building adaptation and retrofitting measures are necessary to address the twofold challenge of reducing CO_2 emission and responding to extreme weather in a changing climate [4,5]. Building concepts and standards such as the Passive House, nearly Zero Energy Building (nZEB) and Plus Energy Building (PEB) [6–9] target the building envelope as a crucial element to improve indoor comfort conditions and save or even generate energy at the same time [10]. A technical solution to achieve this objective is equipping buildings with climate adaptive and energy-saving building envelopes,

* Corresponding authors.
E-mail addresses: janflor@gmx.de (J.-F. Flor), yupeng.wu@nottingham.ac.uk (Y. Wu).

https://doi.org/10.1016/j.enbuild.2020.110554
0378-7788/© 2020 The Authors. Published by Elsevier B.V.
This is an open access article under the CC BY license (http://creativecommons.org/licenses/by/4.0/).

Appendix T: Co-authors contribution declaration (paper 6)

Authors contribution to the joint paper:

Virtual reality as a tool for evaluating user acceptance of view clarity through ETFE double-skin façades

The PhD applicant, Jan-Frederik Flor, is the first author of this publication and has made a significant intellectual contribution to this work. The applicant had the initial idea for the research study, wrote the original draft of the article and was responsible for administrating the project. Jan was deeply engaged in the design of the experimental methodology and applying the experimental procedures in practice. During the investigation the applicant was also involved in curating and analysing the experimental data, editing the manuscript and coordinating the publishing process.

- Marina Aburas, second author, and fellow PhD colleague of the applicant, provided very valuable, intellectual and practical, contributions to the investigation. Marina was deeply involved with the development of the methodology, data curation and formal analysis of the results. She also helped with writing, reviewing and editing the paper manuscript giving valuable comments and suggestions to enhance the manuscript. and proofreading the final version of the paper.

- Fedaa Abd-AlHamid, third author, and fellow PhD colleague of the applicant, provided technical skills and software know-how for creating the virtual environments used in the study. Fedaa contributed with background and insider knowledge of the investigated topic of view clarity which led to important improvements of the methodology. She was deeply involved in the processing of image data and validating scenarios for the application in experiments. Besides, Fedaa helped in the preparation of the paper manuscript with writing and editing, as well as contributing with technical aspects on virtual reality and view quality.

- Yupeng Wu (Jack), is the main supervisor of the applicant and fourth author of the paper. Jack supervised all stages of the study reported in this paper, from the research idea to publishing. Jack provided technical resources and acquired funding for the realisation of the research study. He provided valuable comments and suggestions to enhance the methodology, helped with reviewing and editing the manuscript, and contributed to the discussion and interpretation of the result.